Spine: 5.5 mm

Volume 75 • Issue 1 • January-March 2026

Journal of The Anatomical Society of India • Volume 75 • Issue 1 • January-March 2026 • Pages 1-118

ISSN : 0003-2778

Scopus® Indexed

JASI

# JOURNAL OF THE ANATOMICAL SOCIETY OF INDIA

An International Journal

An Official Publication of Anatomical Society of India

Full text online at https://journals.lww.com/joai
Submit articles online at https://review.jow.medknow.com/jasi

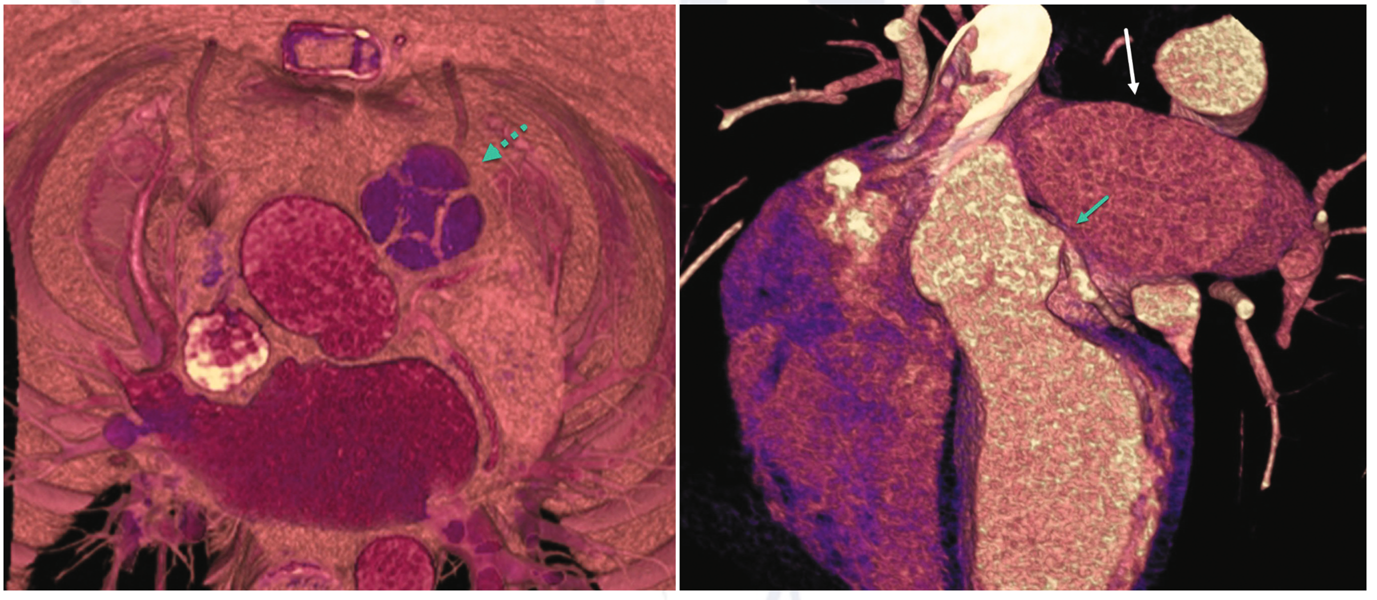

Jasi_204_25- Quadricuspid Pulmonary Valve

*Editor-in-Chief*
**Prof. C. S. Ramesh Babu**

Wolters Kluwer

Medknow

# Journal of the Anatomical Society of India

Print ISSN: 0003-2778

## GENERAL INFORMATION

**About the Journal**

Journal of the Anatomical Society of India (ISSN: Print 0003-2778) is peer-reviewed journal. The journal is owned and run by Anatomical Society of India. The journal publishes research articles related to all aspects of Anatomy and allied medical/surgical sciences. Pre-Publication Peer Review and Post-Publication Peer Review Online Manuscript Submission System Selection of articles on the basis of MRS system Eminent academicians across the globe as the Editorial board members Electronic Table of Contents alerts Available in both online and print form. The journal is published quarterly in the months of January, April, July and October.

**Scope of the Journal**

The aim of the *Journal of the Anatomical Society of India* is to enhance and upgrade the research work in the field of anatomy and allied clinical subjects. It provides an integrative forum for anatomists across the globe to exchange their knowledge and views. It also helps to promote communication among fellow academicians and researchers worldwide. The Journal is devoted to publish recent original research work and recent advances in the field of Anatomical Sciences and allied clinical subjects. It provides an opportunity to academicians to disseminate their knowledge that is directly relevant to all domains of health sciences.

The Editorial Board comprises of academicians across the globe.

JASI is indexed in Scopus, available in Science Direct.

**Abstracting and Indexing Information**

The journal is registered with the following abstracting partners:

Baidu Scholar, CNKI (China National Knowledge Infrastructure), EBSCO Publishing's Electronic Databases, Ex Libris – Primo Central, Google Scholar, Hinari, Infotrieve, Netherlands ISSN center, ProQuest, TdNet, Wanfang Data

The journal is indexed with, or included in, the following:

SCOPUS, Science Citation Index Expanded, IndMed, MedInd, Scimago Journal Ranking, Emerging Sources Citation Index.

Impact Factor® as reported in the 2024 Journal Citation Reports® (Clarivate Analytics, 2025): 0.2

**Information for Authors**

Article processing and publication charges will be communicated by the editorial office. All manuscripts must be submitted online at https://review.jow.medknow.com/jasi.

**Subscription Information**

A subscription to JASI comprises 4 regular issues. Prices include postage. Subscription rates for Supplementary and / or Special Issue are separate as given below

**Annual Subscription Rate for Non-members**

| | **India** | **Outside India** |
|---|---|---|
| Institutional ( for regular issues) | INR 15,000 | USD 1200 |
| Institutional (for Supplementary /Special Issues) | INR 4000 each | USD 300 each |
| Individual (for regular issues) | INR 7,500 | USD 800 |
| Individual (for Supplementary / Special Issues) | INR 2000 each | USD 200 each |

*The Journal of Anatomical Society of India (ISSN: 0003-2778)* is published quarterly **Subscriptions** are accepted on a prepaid basis only and are entered on a calendar year basis. Issues are sent by standard mail Priority rates are available upon request. The Journal intends to release Supplementary and / or Special Issues (on a specific subcategory of Anatomy) as and when necessary and it shall be announced in the last issue of the Journal every year. Subscribers can raise an invoice for regular and / or supplementary issues as required.

**Information to Members/Subscribers**

All members and existing subscribers of the Anatomical Society of India are requested to send their membership/existing subscription fee for the current year to the Treasurer of the Society on the following address: Prof (Dr.) Punita Manik, Treasurer, ASI, Department of Anatomy, KGMU, Lucknow - 226003. Email: treasurerasi@yahoo.com. All payments should be made through an account payee bank draft drawn in favor of the **Treasurer, Anatomical Society of India,** payable at **Lucknow** only, Payment bank details: (for online payment) A/C name: Treasurer, Anatomical Society of India, A/C NO: 20229838126, IFSC Code: IDIB000K656, Bank name-Indian Bank KGMC Branch Lucknow**.** Outstation cheques/drafts must include INR 70 extra as bank collection charges.

All complaints regarding non-receipt of journal issues should be addressed to the Editor-in-Chief, JASI at editorjasi@gmail.com. The new subscribers may, please contact wkhlrpmedknow_subscriptions@wolterskluwer.com.

For mode of payment and other details, please visit www.medknow.com/subscribe.asp

Claims for missing issues will be serviced at no charge if received within 60 days of the cover date for domestic subscribers, and 3 months for subscribers outside India. Duplicate copies cannot be sent to replace issues not delivered because of failure to notify publisher of change of address. The journal is published and distributed by Wolters Kluwer India Pvt. Ltd. Copies are sent to subscribers directly from the publisher's address. It is illegal to acquire copies from any other source. If a copy is received for personal use as a member of the association/society, one cannot resale or give-away the copy for commercial or library use.

The copies of the journal to the subscribers are sent by ordinary post. The editorial board, association or publisher will not be responsible for non receipt of copies. If any subscriber wishes to receive the copies by registered post or courier, kindly contact the publisher's office. If a copy returns due to incomplete, incorrect or changed address of a subscriber on two consecutive occasions, the names of such subscribers will be deleted from the mailing list of the journal. Providing complete, correct and up-to-date address is the responsibility of the subscriber.

*Nonmembers*: Please send change of address information to subscriptions@medknow.com.

**Advertising Policies**

The journal accepts display and classified advertising. Frequency discounts and special positions are available. Inquiries about advertising should be sent to Wolters Kluwer India Pvt. Ltd, advertise@medknow. com.

The journal reserves the right to reject any advertisement considered unsuitable according to the set policies of the journal.

The appearance of advertising or product information in the various sections in the journal does not constitute an endorsement or approval by the journal and/or its publisher of the quality or value of the said product or of claims made for it by its manufacturer.



**Permissions**

For information on how to request permissions to reproduce articles/information from this journal, please visit https://journals.lww.com/joai.

**Disclaimer**

The information and opinions presented in the Journal reflect the views of the authors and not of the Journal or its Editorial Board or the Publisher. Publication does not constitute endorsement by the journal. Neither the JASI nor its publishers nor anyone else involved in creating, producing or delivering the JASI or the materials contained therein, assumes any liability or responsibility for the accuracy, completeness, or usefulness of any information provided in the JASI, nor shall they be liable for any direct, indirect, incidental, special, consequential or punitive damages arising out of the use of the JASI. The JASI, nor its publishers, nor any other party involved in the preparation of material contained in the JASI represents or warrants that the information contained herein is in every respect accurate or complete, and they are not responsible for any errors or omissions or for the results obtained from the use of such material. Readers are encouraged to confirm the information contained herein with other sources.

**Addresses**

*Editorial Office*

Prof. C .S. Ramesh Babu, Editor-in-Chief, JASI,
309, Block-B, Canopy Calyx Apartment, Coffee Board Layout, Hebbal-Kempapura,
Bengaluru-560 024, India.
Email: editorjasi@gmail.com

*Published by*

Wolters Kluwer India Pvt. Ltd. (Medknow),
Smartworks, Marisoft, Wing-C, Wadgaon Sheri,
Kalyani Nagar Annex, Pune - 411 014,
Maharashtra, India.
Website: www.medknow.com

*Printed at*

Nikeda Art Printers Pvt. Ltd.,
Building No. C/3 - 14,15,16, Shree Balaji Complex, Vehele Road,
Village Bhatale, Taluka Bhiwandi, District Thane - 421302, India.

# Journal of the Anatomical Society of India

Print ISSN: 0003-2778

# Journal of the Anatomical Society of India

Volume 75 | Issue 1 | January-March 2026

## CONTENTS

# Developmental Anomalies of Arterial Semilunar Valves

Semilunar valves, the aortic and pulmonary, guard the origins of ascending aorta and pulmonary trunk arising from the left and right ventricles, respectively. These valves have three cusps (tricuspid/trileaflet) each and exhibit a semilunar margin attached to the arterial wall (hinge), a more or less straight but curved free margin with a thickening in the center (Nodule of Arantius), junction of free margins of adjacent cusps attached to the arterial wall (Commissure), and two surfaces convex facing the ventricular cavity and concave facing the arterial wall. Sinuses (of Valsalva) are depressions between the arterial wall and the concave surface of the cusps and are larger in the ascending aorta. The valve leaflets and the sinuses are similarly named. Two of the aortic sinuses give origin to coronary arteries, hence named, respectively, as the right coronary sinus and left coronary sinus, and the third noncoronary sinus is named as nonadjacent sinus, which is right posterior anatomically. The sinuses and cusps of the pulmonary trunk are smaller and named right adjacent, left adjacent, and nonadjacent leaflets. A portion of the wall of the great arteries proximal to the attached margin of the cusps and between the cusps is named the intercalated triangle. At the base of these triangles lie the transition zone between smooth muscles of arterial walls (positive for smooth muscle ∞ actin) and myocardium (negative for smooth muscle ∞ actin) of the outflow portions of the ventricles.

The arterial semilunar valves have a common origin from endocardial cushions and are closely related to septation of the outflow tract (OFT), the truncus arteriosus, regulated by cardiac neural crest cells (NCC). Congenital malformations affecting the semilunar valves include variability in the number of leaflets/cusps (bicuspid, quadricuspid, and unicuspid) and size and shape (dysplastic/aplastic). Bicuspid aortic valve (BAV) is the most common congenital cardiac anomaly affecting 1%–2% of the general population. In this issue, an article by Akturk *et al*.[1] observed a statistically significant increase in the diameter of the aorta between patients with BAV and normal age-matched patients with a tricuspid valve. Nearly 45% of BAV subjects exhibit calcific aortic valve disease requiring surgical replacement of the malformed BAV. They also suggested that the thickness of the epicardial adipose tissue may serve as a marker for aortopathy induced by BAV.

A second article by Tekinhatun *et al*.[2] describe what they claim to be the first case report of compression of the left main coronary artery caused by the aneurysm of the main pulmonary artery secondary to the presence of quadricuspid pulmonary valve. The 37-year-old female patient had undergone surgical closure of atrial septal defect about two decades before. So the authors claimed that the abnormal valve leaflets caused pulmonary hypertension, leading to aneurysmal dilatation of the main pulmonary artery and subsequent coronary artery compression. Pulmonary hypertension, due to reasons other than the presence of quadricuspid pulmonary valve, can lead to aneurysmal enlargement of pulmonary artery (more than 40 mm dia), which can displace or compress the origin of the left main coronary artery.[3]

The cardiac OFT, formed by the progenitor cells derived from secondary heart field and immigrant NCC, was divided into proximal (conus cordis), middle, and distal (truncus) segments. The primitive heart tube consists of inner endocardium and an outer myocardium separated by an extracellular matrix substance called cardiac jelly. Proliferation of two types of cells in the cardiac jelly at the middle part of OFT lead to formation of two endocardial cushions. Endocardial cells covering the cushion undergo endothelial–mesenchymal transition regulated by bone morphogenetic protein, transforming growth factor beta, NOTCH signaling, and migrant NCC populate the endocardial cushions. In the distal OFT, two spirally arranged cushions develop, the parietal and the septal regulated by NCC cells. The parietal OFT cushion contributes to the left leaflets of aortic and pulmonary valves, while the septal OFT leaflet contributes to right leaflets. Anterior nonadjacent leaflet of the pulmonary valve and the posterior noncoronary, nonadjacent leaflet of the aortic valve develop from intercalated leaflet valve swellings, which are formed at the junction of SHF-derived myocardium proximally and SHF-derived smooth muscle cells distally.[4-6]

The bulky endocardial cushions slowly undergo a process of sculpting during prenatal period. The extracellular matrix forms a three-layered arrangement, lamina fibrosa made up of Collagen I and III on the aortic side, middle lamina spongiosa containing proteoglycans and glycosaminoglycans, and the thinnest ventricularis made up of elastin fibers. Scant literature is available on the maturation of the arterial valves and changes occurring in the composition of extracellular matrix during the late prenatal period.[4]

Congenitally diseased semilunar valves lead to valvular stenosis and/or insufficiency, arterial wall dilatation, and act as a substrate for infection, thrombus formation, arrhythmias, and even sudden death.[5] Most common congenital semilunar valve anomaly is BAV with an incidence of up to 2% in general population. Incidence of unicuspid aortic valve is 0.02% and quadricuspid aortic valve is 0.013%–0.043%. The quadricuspid pulmonic valve is 9 times more common than the quadricuspid aortic valve, with an incidence of 0.02%–0.41%, with a male preponderance.[7] Rarely, both aortic and pulmonary valve anomalies may coexist.[8]

 

**C. S. Ramesh Babu**

*Editor-in-Chief, Journal of Anatomical Society of India, Professor Emeritus, Anatomy Department, Muzaffarnagar Medical College, Muzaffarnagar, Uttar Pradesh, India*

***Address for correspondence:*** *Prof. C. S. Ramesh Babu, Professor Emeritus, Department of Anatomy, Muzaffarnagar Medical College, Muzaffarnagar, Uttar Pradesh, India.*
*E-mail: csrameshb@gmail.com*

## References

1. Akturk Y, Durmus I, Kavak RP, Ozdemir M. Bicuspid aortic valve in adult patients: Accompanying cardiovascular pathology and variations. J Anat Soc India 2026;75:33-40.
2. Tekinhatun M, Cihan F, Emre H, Deniz MA. Quadricuspid pulmonary valve with main pulmonary artery aneurysm causing ostial left main coronary artery compression: A coronary computed tomography angiography case report. J Anat Soc India 2026;75:107-9.
3. Choi YJ, Kim U, Lee JS, Park WJ, Lee SH, Park JS, *et al*. A case of extrinsic compression of the left main coronary artery secondary to pulmonary artery dilatation. J Korean Med Sci 2013;28:1543-8.
4. Wu B, Wang Y, Xiao F, Butcher JT, Yutzey KE, Zhou B. Developmental mechanisms of aortic valve malformation and disease. Annu Rev Physiol 2017;79:21-41.
5. Stephens EH, Kearney DL, Grande-Allen KJ. Insight into pathologic abnormalities in congenital semilunar valve disease based on advances in understanding normal valve microstructure and extracellular matrix. Cardiovasc Pathol 2012;21:46-58.
6. Henderson DJ, Eley L, Turner JE, Chaudhry B. Development of the human arterial valves: Understanding bicuspid aortic valve. Front Cardiovasc Med 2021;8:802930.
7. Saith S, Saith S, Murthy A. Quadricuspid aortic valve: An introduction for clinicians. Cardiol Res 2022;13:2-10.
8. Gupta A, Tomar M, Tomar HS. Coexistence of bicuspid aortic and pulmonary valves in patients with normally related great vessels: Our experience. IHJ Cardiovasc Case Reports (CVCR) 2021;5:67-70.



**Article Info**

**Received:** 17 March 2026
**Revised:** 23 March 2026
**Accepted:** 24 March 2026
**Available online:** 27 March 2026

**Access this article online**

**Quick Response Code:**

**Website:** https://journals.lww.com/joai

**DOI:** 10.4103/jasi.jasi_50_26

**How to cite this article:** Babu CS. Developmental anomalies of arterial semilunar valves. J Anat Soc India 2026;75:1-2.

Original Article

# Prevalence and Morphological Variations of Ponticulus Posticus among North Karnataka Population: A Digital Lateral Cephalometric Study


## Abstract

**Aims and Objectives:** The present study aimed to investigate the prevalence and type of ponticulus posticus (PP) in patients of the North Karnataka population who reported for dental treatment to an institution. **Materials and Methods:** A total of 1000 digital lateral cephalographs were assessed for the presence, type of PP, gender predominance, and prevalence of each type of PP in either gender. Data obtained were tabulated and subjected to descriptive analysis. **Results:** PP had a prevalence rate of 27.3%, among which Grade II PP were observed in 60 (17.1%) males and 114 (17.6%) females, Grade III in 13 (3.7%) males and 30 (4.6%) females, and Grade IV in 22 (6.3%) in males and 34 (5.2%) females. While estimating the predominant gender in each grade, females displayed a higher incidence of Grade III (4.6%) compared to males (3.7%), and males displayed a higher incidence of Grade IV (6.3%) compared to females (5.2%). No statistically significant difference between males and females was found in the prevalence of PP or in the grading of its ossification ($P = 0.823$). **Conclusion:** Among the North Karnataka population, PP was found to be a relatively common anomaly and the trivial form of PP (Grade II) was found to be more prevalent as per our study. A thorough knowledge about the impact of the occurrence of PP is very crucial for an oral healthcare professional to facilitate a better treatment or appropriate referral for the patient.


**Keywords:** *Arcuate foramen, atlas, cervical vertebrae, migraine, ponticulus posticus*

**Veena B. Pujari, Kirty R. Nandimath, Venkatesh G. Naikmasur, Raju R. Naik**

*Department of Oral Medicine and Radiology, SDM College of Dental Sciences and Hospital, Shri Dharmasthala Manjunatheshwara University, Dharwad, Karnataka, India*

## Introduction

In human anatomy, among the seven cervical vertebrae, the superior-most and the widest cervical vertebra (C 1) is the "Atlas" which is a ring-like structure having no body or spinous process. It is so named due to its unique position, where it supports the skull and the spinal cord and gives attachment to the muscles of the neck. Anatomic variations of the atlas include retrotransverse foramen, the arcuate foramen, the unclosed transverse foramen and posterior atlas arch defects. The arcuate foramen's other anatomical names are Ponticulus posticus (PP), Pons posticus, Kimmerle anomaly, and Retroarticular superior foramen.[1] PP was first reported in 1879[2] and is derived from a Latin term meaning "the little posterior bridge,"[3] it consists of a complete or partial malformed bony bridge from the posterior portion of the superior articular process to the lateral portion of the upper margin of the posterior arch of atlas and surrounding all or part of the vertebral artery.[4] Across literature, presence of PP has been linked to various clinical symptoms such as migraines without aura, severe headache particularly tension-type, pain in the cervical region, onset of acute hearing loss, shoulder and arm pain, lacrimation, vertigo, vertebral artery stenosis and orofacialpain, Barre-Lieou syndrome and chronic upper cervical syndrome,[5,6] hence recognition of the anomaly by a healthcare professional is of utmost importance. Very few studies on digital lateral cephalographs have been reported on the prevalence of PP in the Asian population, especially the Indian population.[7,8] Literature search revealed only one previous study done in 2013 on the North Karnataka population for assessing the prevalence of PP.[9] The aim of this study was to determine the prevalence and type of PP in the North Karnataka population using data obtained from the institutional radiological archives.

## Materials and Methods

This cross-sectional study was conducted in the Department of Oral Medicine and Radiology of a Dental Institute, Dharwad, India.



**How to cite this article:** Pujari VB, Nandimath KR, Naikmasur VG, Naik RR. Prevalence and morphological variations of ponticulus posticus among North Karnataka population: A digital lateral cephalometric study. J Anat Soc India 2026;75:3-7.

**Article Info**

**Received:** 03 December 2025
**Revised:** 25 January 2026
**Accepted:** 30 January 2026
**Available online:** 27 March 2026

***Address for correspondence:***
*Dr. Veena B. Pujari, Department of Oral Medicine and Radiology, SDM College of Dental Sciences and Hospital, Shri Dharmasthala Manjunatheshwara University, Dharwad, Karnataka, India.*
*E-mail: pujariveena20@gmail.com*

**Access this article online**

**Website:** https://journals.lww.com/joai

**DOI:** 10.4103/jasi.jasi_191_25

**Quick Response Code:**

**Ethics statement**

The study was reviewed and approved by the Institutional Biomedical Ethics and Research Committee (SDMCDS IEC.No. 2025/S/OM/97), and the study was conducted in accordance with the ethical standards of the institutional committee and the principles of the Declaration of Helsinki. Since this was a retrospective observational study based on unidentified archived radiological data from the institution, the necessity of informed consent was waived off by the ethics committee.

**Study design**

A cross-sectional study was conducted where we reviewed 1000 digital lateral cephalographs from the radiology archives. The imaging was indicated on clinical grounds for the diagnosis and treatment of the patients and not specifically taken for our study. The radiographs obtained as samples were captured by an experienced technician on “CARESTREAM DENTAL CS9600” machine with unit’s patient size presets and appropriate imaging mode (exposure parameters included tube voltage 78–82 kV, tube current 8–10 mA, and exposure time 4.3s) were selected based on patient size and image quality requirements. All the digital lateral cephalographs of patients of 13–60 years of age in a 1 year time period from January to December 2024 were included in the study and radiographs with poor visualization of the posterior arch of the atlas due to overlapping of the occipital or mastoid process, Congenital deformities and syndromic conditions, history of trauma or surgeries of the craniofacial region, low diagnostic quality scans and presence of radiographic artifacts and radiographs of <13 years of age were excluded from the study. Sample selection was done using a consecutive sampling method, wherein all cephalographs meeting the inclusion criteria in the study time period were selected until the desired sample size was achieved.

Since we analyzed digital lateral cephalographs, we had an advantage of manipulating the contrast, brightness, and magnification of images in the area of interest for better assessment of the anatomy. Evaluation of the presence of PP was done by the principal investigator on radiographs that were visualized using CS imaging Version 8.0.33 software, Carestream Atlanta, GA USA on a flat LCD monitor under ambient lighting conditions. We followed the classification by Cederberg *et al*.[10] which is simple and clinically relevant.

- Grade I (Normal) – No calcification [Figure 1]. No degree of this anomaly can be detected; including exaggerated grooving of the fossa arterialis with no distinct spicule
- Grade 2 (Trivial) – Less than half calcified [Figure 2]. Partly developed foramen ranging from a minute but distinct spicule to a developing bridge that encases <50% of the circumference of the vertebral artery
- Grade 3 (Partial, well-developed) – At least half calcified [Figure 3]. Well-developed foramen encases at least the majority (>50%) of the vertebral artery’s circumference
- Grade 4 (Complete) – Complete calcification [Figure 4]. The vertebral artery is completely encased by bone.

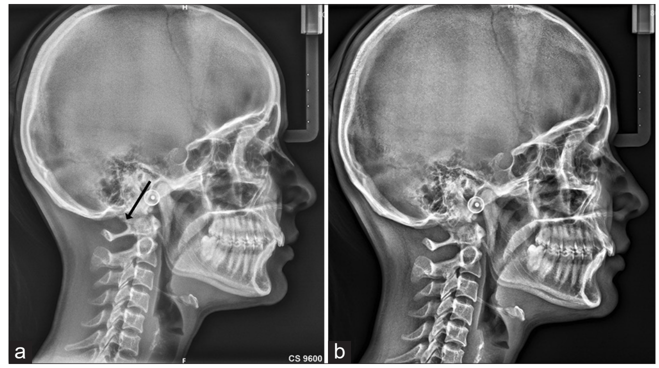


**Figure 1: Lateral cephalograph demonstrating Grade I ponticulus posticus (no degree of calcification detected). The arrow indicates the region of the posterior arch of the atlas where ponticulus posticus is typically observed. (a) Original image without digital enhancement, (b) Image after digital enhancement of contrast and brightness to facilitate improved visualization and more accurate assessment of the anatomical structures**

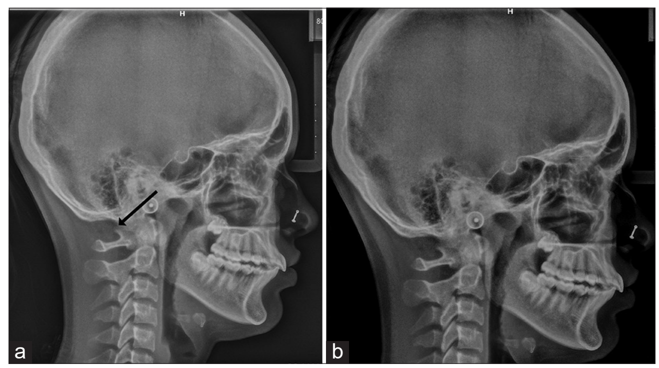


**Figure 2: Lateral cephalograph demonstrating Grade II ponticulus posticus. The arrow indicates less than half calcified bony bridge over the posterior arch of the atlas. (a) Original image without digital enhancement, (b) Image after digital enhancement of contrast and brightness to facilitate improved visualization and more accurate assessment of the anatomical structures**

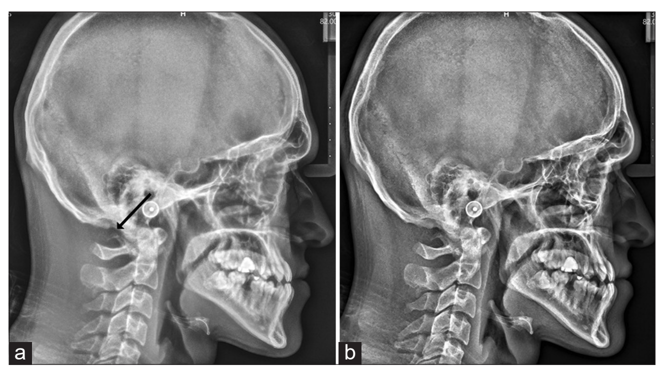


**Figure 3: Lateral cephalograph demonstrating Grade III ponticulus posticus. The arrow indicates at least half calcified bony bridge over the posterior arch of the atlas. (a) Original image without digital enhancement, (b) Image after digital enhancement of contrast and brightness to facilitate improved visualization and more accurate assessment of the anatomical structures**

Data obtained were entered into a Microsoft Excel sheet and subjected to statistical analysis.

The primary observer reassessed 15% of the sample population after a 3-month interval to evaluate intraobserver reliability. The observer was blinded to the initial assessment during the second assessment. Agreement between the two evaluations for the grading of PP was assessed using Cohen's weighted Kappa test.

**Sample size estimation**

The sample size was estimated using the formula:

$$\text{Sample size} = \frac{Z^2 \times P\,(1 - P)}{E^2}$$

$P = 0.50$ (50% based on previous research[7]) $E$ = margin of error = 5%.

The estimated minimum sample size was 385, since we had a huge dataset of lateral cephalographs, we analysed 1000 digital radiographs.

**Statistical analysis**

The data were tabulated and subjected to Statistical Package for the Social Sciences (SPSS), Version 20.0.software. Frequencies and percentages were calculated, and statistical significance was set at $P \leq 0.05$. Chi-square test was used to find the association and prevalence difference between categorical variables and to compare the mean, independent parametric, and nonparametric tests were used. The significance level was considered as <0.05% or 5%.

## Results

A total of 1000 digital lateral cephalographs were randomly selected and assessed in which 351 were males (35.1%) and 649 (64.9%) were females, of which 273 cases exhibited the presence of PP, giving an overall prevalence rate of 27.3% in the study population. The mean age of our study sample was 36.5 years (range 13–60 years). In the total study sample, both males (27.1%) and females (27.4%) demonstrated nearly equal occurrence of PP. No statistically significant association was observed between gender and the presence or grading of ossification, as determined by Fisher's exact test ($P > 0.05$). 95 (27.1%) out of 351 males and 178 (27.4%) out of 649 females showed the presence of ossification of PP. The distribution of grading of PP among the sample in our study is listed in Table 1. Among these, the Grade II (trivial or partial variant) was the most prevalent type, followed by Grade IV (complete calcification), while Grade III (well-developed partial variant) was the least observed. No gender predominance was found in our study. Table 2 summarizes the distribution of each of the grades of calcification of PP in males and females. Females exhibited a slightly higher incidence of Grade III PP (4.6%), whereas males showed a higher incidence of Grade IV PP (6.3%). However, these differences were not statistically significant ($P = 0.903$). The intra-observer reliability for the evaluation and grading of PP demonstrated a very good strength of agreement, with a weighted Cohen's Kappa value of 0.90. The 95% confidence interval for the kappa value ranged from 0.84 to 0.97, indicating excellent consistency and good reproducibility of the observations ($P < 0.001$, Kendall's Tau). MedCalc software was used for the intrarater agreement calculation.

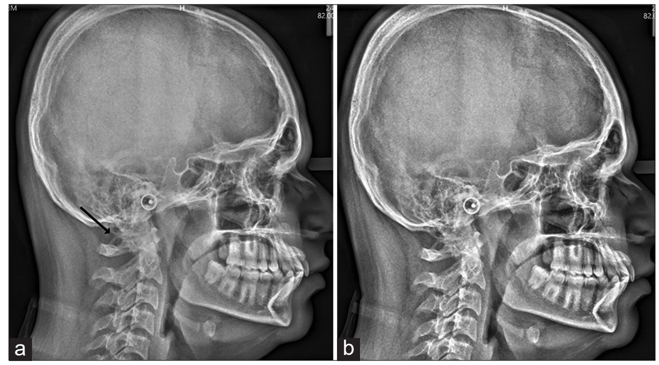


**Figure 4: Lateral cephalograph demonstrating Grade IV ponticulus posticus. The arrow indicates the completely ossified bony bridge over the posterior arch of the atlas. (a) Original image without digital enhancement, (b) Image after digital enhancement of contrast and brightness to facilitate improved visualization and more accurate assessment of the anatomical structures**

**Table 1: Distribution of grading of ponticulus posticus**

| Grading of PP | Total sample (%) |
|---|---|
| Grade I | 727 (72.7) |
| Grade II | 174 (17.4) |
| Grade III | 43 (4.3) |
| Grade IV | 56 (5.6) |
| Total | 1000 (100) |

PP: Ponticulus posticus

**Table 2: Distribution of each of the grades of ponticulus posticus in males and females**

| Grading of PP | Males (%) | Females (%) |
|---|---|---|
| Grade I | 256 (72.9) | 471 (72.6) |
| Grade II | 60 (17.1) | 114 (17.6) |
| Grade III | 13 (3.7) | 30 (4.6) |
| Grade IV | 22 (6.3) | 34 (5.2) |
| Total | 351 | 649 |

PP: Ponticulus posticus

## Discussion

In general, the vertebral artery runs a straight course superiorly through the foramen transversarium of C6–C2 vertebrae to the axis vertebra and enters through the foramen transversarium of the atlas. Later, it turns medially and posteriorly behind the lateral masses to reach the groove on the superior surface of the posterior arch of the atlas, and it enters the vertebral canal by crossing under the posterior atlantooccipital membrane. At times, calcification of the posterior atlantooccipital membrane in varying degrees is seen forming a partial or complete ring over the vertebral groove, clinically termed "PP". This simple anatomical variation may cause compression of the neurovascular bundle passing through it, resulting in symptoms of vertebrobasilar insufficiency, including migraine and headache without aura, tinnitus, weakness and paralysis of the upper extremities.[11]

In the domain of neurosurgery, PP is of utmost importance where spinal stabilization is achieved by insertion of screws into the lateral masses of the first and second vertebrae. Intraoperatively, a completely calcified PP can give a false impression and may mislead the surgeon to consider the anomaly as a wider posterior arch of the atlas. This error may lead to surgical drilling through the vertebral artery enclosed within, resulting in significant bleeding, stroke, or postoperative neurological deficits.[12] The presence of PP can cause Bow-Hunter's stroke during rotational neck movements, wherein the impingement and compression of the vertebral artery may form thrombi and subsequent embolism, causing life-threatening cerebellar infarction.

Literature reports relatively common occurrence of PP in cases of dental agenesis,[13] palatally displaced canines, maxillary jaw malformations, temperomandibular joint (TMJ) dysfunction, occlusal discrepancies, alterations in craniofacial morphology, deep bite, vertical craniofacial anomalies and mandibular condyle deformations.[14] Hence, it is undeniable that the mere presence of PP itself may be perilous to a patient and also correlated with significant challenges in the dentofacial complex.

Our study represents the first of its kind digital lateral cephalograph study in the North Karnataka population, wherein the presence of PP was found in 273 out of 1000 patients, with a total prevalence of 27.3%. Out of the 273 patients with PP, a significantly higher incidence of Grade II-17.4% (partial variant), followed by Grade IV-5.6%(complete calcification) and Grade III-4.3% (partial - at least half calcified) was found in our study. Partial variant of PP (Grade III) occurred the least, aligning to a study by Giri *et al*.[15] where the partial variant of PP prevalence was 3.9%. Our study was in contrast to a study done by Gibelli *et al*.[16] on 221 lateral cephalographs, which reported a higher occurrence of partial variant (9%) than the complete variant (7.7%) of PP.

Most of the studies reveal an ambiguous response to the prevalence of PP among either gender. Our study data analyzation reports no significant correlation between ossification grade and gender according to the Pearson Chi square test, confirming that both males and females had almost the same occurrence of PP (Males 27.1% and females 27.4%), suggesting that ossification of PP is independent of gender, confirming the observation by Tripodi *et al*.[4] that presence of PP cannot be considered a gender exclusive process of calcification. However, in contrast to our results, a higher prevalence of PP in males compared to females has been reported in studies conducted by Kim *et al*.[17], Miki *et al*.[18], Adisen and Misirlioglu[19] and Chitroda *et al*.[9]

### Strength of the study

Our study was conducted on a large sample size of 1000 digital cephalographs selected using strict inclusion and exclusion criteria, enhancing the statistical power, reducing bias and increasing uniformity of the sample. Use of noninvasive, routinely acquired imaging modality such as digital lateral cephalographs minimizes ethical concerns and helps in clear visualization of the atlas anomaly, facilitating reliable identification and assessment of PP. Our study provides strong prevalence data on PP, contributing valuable baseline epidemiological evidence for future clinical and radiographic studies.

### Limitations of the study

As the present study was cross-sectional, it is limited by the lack of clinical correlation to the presence of PP. Since our study was on a two-dimensional image, unilateral and bilateral presence of PP could not be distinguished. A limitation of the present study is the reliance on a single observer of the samples. Future studies with multiple observers or a panel of experts could mitigate this limitation.

### Future prospects of the study

Our study on cephalograms was to merely establish the prevalence of the PP in our population. A study on three-dimensional imaging, such as cone beam computed tomography with a much larger sample size, will be effective in detecting small ossifications that go unnoticed in the lateral cephalograms.

## Conclusion

PP is a relatively common anatomical variation in the North Karnataka population, as per our study. However, a conclusive statement with high-quality literature evidence on the clinical importance is yet to be derived. A thorough knowledge about the impact of the occurrence of PP in terms of orofacial signs and symptoms and its radiological findings is very crucial for a maxillofacial physician and radiologist to thoroughly assess the cephalographs of patients of any age for better identification and documentation of the anomaly and in turn facilitate a better treatment or appropriate referral for the patient. Here we report a study assessing the prevalence of this anomaly in Dharwad, North Karnataka population. We hope to have documented this potentially significant anomaly in our population in the hopes that further studies with a larger sample will provide the much-needed answers for better health and management of patients.

### Acknowledgments

The authors gratefully acknowledge and thank Dr. Ravi V Shirahatti for his expertise and meticulous support in conducting the statistical analysis. His contributions were instrumental in interpreting the data accurately.

**Financial support and sponsorship**

Nil.

**Conflicts of interest**

There are no conflicts of interest.

## References

1. Sanchis-Gimeno JA, Llido S, Perez-Bermejo M, Nalla S. Prevalence of anatomic variations of the atlas vertebra. Spine J 2018;18:2102-11.
2. Cossu G, Terrier LM, Destrieux C, Velut S, François P, Zemmoura I, *et al.* Arcuate foramen: "Anatomical variation shape or adaptation legacy?". Surg Radiol Anat 2019;41:583-8.
3. Sukhija P, Kamath G, Srivathsa SH, Medha B. Prevalence of ponticulus posticus (PP): A cross-sectional study using digitized lateral cephalograms. J Dent Sci 2022;7:1-8.
4. Tripodi D, Tieri M, Demartis P, Però G, Marzo G, D'Ercole S. Ponticulus posticus: Clinical and CBCT analysis in a young Italian population. Eur J Paediatr Dent 2019;20:219-23.
5. Simsek S, Yigitkanli K, Comert A, Acar HI, Seckin H, Er U, *et al.* Posterior osseous bridging of C1. J Clin Neurosci 2008;15:686-8.
6. Cakmak O, Gurdal E, Ekinci G, Yildiz E, Cavdar S. Arcuate foramen and its clinical significance. Saudi Med J 2005;26:1409-13.
7. Mudit G, Srinivas K, Satheesha R. Retrospective analysis of ponticulus posticus in Indian orthodontic patients-a lateral cephalometric study. Ethiop J Health Sci 2014;24:285-90.
8. Sharma V, Chaudhary D, Mitra R. Prevalence of ponticulus posticus in Indian orthodontic patients. Dentomaxillofac Radiol 2010;39:277-83.
9. Chitroda PK, Katti G, Baba IA, Najmudin M, Ghali SR, Kalmath B, *et al.* Ponticulus posticus on the posterior arch of atlas, prevalence analysis in symptomatic and asymptomatic patients of gulbarga population. J Clin Diagn Res 2013;7:3044-7.
10. Cederberg RA, Benson BW, Nunn M, English JD. Arcuate foramen: prevalence by age, gender, and degree of calcification. Clinical Orthodontics and Research 2000;3:162-67.
11. Mokhtari N, Ashtari F, Razavi M, Ghaffari R. Prevalence and characteristics of ponticulus posticus and its association with cervicogenic headache and migraine: A lateral cephalometric study. J Res Med Sci 2022;27:61.
12. Young JP, Young PH, Ackermann MJ, Anderson PA, Riew KD. The ponticulus posticus: Implications for screw insertion into the first cervical lateral mass. J Bone Joint Surg Am 2005;87:2495-8.
13. Putrino A, Leonardi RM, Barbato E, Galluccio G. The association between ponticulus posticus and dental agenesis: A retrospective study. Open Dent J 2018;12:510-9.
14. Leonardi R, Barbato E, Vichi M, Caltabiano M. Skeletal anomalies and normal variants in patients with palatally displaced canines. Angle Orthod 2009;79:727-32.
15. Giri J, Pokharel PR, Gyawali R. How common is ponticulus posticus on lateral cephalograms? BMC Res Notes 2017;10:172.
16. Gibelli D, Cappella A, Cerutti E, Spagnoli L, Dolci C, Sforza C. Prevalence of ponticulus posticus in a Northern Italian orthodontic population: A lateral cephalometric study. Surg Radiol Anat 2016;38:309-12.
17. Kim KH, Park KW, Manh TH, Yeom JS, Chang BS, Lee CK. Prevalence and morphologic features of ponticulus posticus in Koreans: Analysis of 312 radiographs and 225 three-dimensional CT scans. Asian Spine J 2007;1:27-31.
18. Miki T, Ohshima M, Uemura H, Hasegawa E, Takahashi S, Ito S. Ponticulus posticus: its clinical significance. Acta Med Kinki Univ 1979;4:427-30.
19. Adisen MZ, Misirlioglu M. Prevalence of ponticulus posticus among patients with different dental malocclusions by digital lateral cephalogram: A comparative study. Surg Radiol Anat 2017;39:293-7.

Original Article

# OEIS Complex: A Rare Fetal Autopsy Case Series with its Embryological Annotations

**Shubhi Saini,**
**Geeta,**
**Babita Pangtey,**
**Sabita Mishra**

*Department of Anatomy, Maulana Azad Medical College, New Delhi, India*

## Abstract

**Background:** OEIS Complex is a rare form of ventral body wall defect affecting 1 in 200,000–400,000 pregnancies and consists of a cluster of multiple congenital anomalies such as omphalocele, exstrophy of cloaca/bladder, imperforate anus, and spinal defects. It results from the defect of mesodermal migration during the primitive streak period leading to failure of ventral body wall closure. **Aims and Objectives:** In the present study, we aimed to study autopsy findings of cases, exhibiting varying spectrum of OEIS complex. **Materials and Methods:** The study was conducted on cases of foetal autopsies, referred from the department of Obstetrics and Gynaecology, to the department of Anatomy. Anthropometric measurements were done to assess the gestational age. The foetuses were then examined and dissected for findings related to OEIS complex. **Results:** On autopsy, three cases were observed with OEIS complex with cloacal exstrophy while one case with bladder exstrophy. All the cases of OEIS were associated with undifferentiated gonads and the absence of external genitalia. The other defects observed were great toe brachymetatarsia, serinomelia, and diaphragmatic defect. **Conclusion:** The fetal autopsy delineating detailed knowledge of all the OEIS components and associated other congenital defects can play a significant role in better understanding of the defect in diagnosis, prognosis evaluation, and management.

**Keywords:** *Autopsy, cloacal exstrophy, OEIS, omphalocele, spinal defect*

## Introduction

Omphalocele, Exstrophy bladder / cloaca, Imperforate anus, Spinal defects Complex (OEIS Complex) is a rare and severe developmental birth defect. It includes the cluster of multisystemic defects such as omphalocele, cloacal/bladder exstrophy, imperforate anus, and spinal defects.[1]

It is often associated with spina bifida, genital abnormalities, renal malformations, symphysis pubis diastasis, epispadias, and limb abnormalities. It is a rare defect affecting 1 in 200, 000–400, 000 pregnancies.[1] It is more common in females (2:1) than males.[2] Some authors use OEIS complex and cloacal exstrophy synonymously.[3]

The etiology of OEIS is multifactorial involving genetic and environmental factors. It results from a defect in mesodermal migration, during the 4th week of gestation leading to failure of closure of ventral body wall. There is also a failure of cephalocaudal and lateral folding with associated defects of cloaca and urorectal septum.[4]

Most cases of OEIS are sporadic; however, in some cases, genetic factors are considered. OEIS presents with a normal karyotype, but there are few cases of OEIS complex that presented with chromosomal abnormalities. A higher incidence of OEIS has been reported in monozygotic twins, supporting a possible genetic predisposition.[5]

The present study is a case series of fetal autopsy findings of three OEIS complex cases with illustration of spectrum of OEIS complex. Fetal autopsy can provide significant data knowledge of spectrum of OEIS and aid in better diagnosis.

## Materials and Methods

Three fetuses were referred for autopsy from the department of obstetrics and gynecology. The antenatal history was noted. All the three cases had no history of folic acid or iron supplementation. There was no history of any maternal medical disorders and congenital malformations in the previous pregnancies. The fetuses were examined externally and anthropometric measurements were taken [Table 1]. After measuring all the



**How to cite this article:** Saini S, Geeta, Pangtey B, Mishra S. OEIS complex: A rare fetal autopsy case series with its embryological annotations. J Anat Soc India 2026;75:8-11.

**Article Info**
**Received:** 01 October 2024
**Revised:** 20 August 2025
**Accepted:** 16 January 2026
**Available online:** 27 March 2026

***Address for correspondence:***
*Dr. Babita Pangtey, Department of Anatomy, Maulana Azad Medical College, New Delhi, India.*
*E-mail: drbabitapangtey@gmail.com*

**Access this article online**
**Website:** https://journals.lww.com/joai
**DOI:** 10.4103/jasi.jasi_158_24
**Quick Response Code:**

growth parameters, the gestational age was calculated and autopsy was performed.

### Case 1

An 18 weeks fetus of a 25-year-old second gravida was referred for fetal autopsy. Antenatal ultrasound described an acutely flexed spine and a multiseptated cystic lesion along with herniation of liver. On autopsy, a large midline abdominal wall defect (10 cm × 5 cm) with herniation of abdominal contents containing entire liver, coils of small, and large intestine were observed. These contents were covered by the thin layer of the membrane [Figure 1a and b]. A midline infraumbilical defect was also observed with herniation of urinary bladder, cecum, and proximal colon. Urinary bladder was divided into two halves and the caecum was observed to be situated between the halves of the bladder. The anal canal was not patent. Gonads were undifferentiated and no external genitalia was seen. Thus, exstrophy of cloaca was observed [Figure 2a].

A large midline cystic swelling [Figure 3a] was observed in the lumbosacral region. The swelling was dissected and observed to contain meninges and rudimentary neural tissue protruding through a vertebral arch defect [Figure 3b] and diagnosed as spina bifida (meningomyelocele). The first left metatarsal was observed to be shorter (great toe brachymetatarsia) [Figure 2b].

**Table 1: Measurements of the fetuses**

| Parameters (cm) | Case 1 | Case 2 | Case 3 |
|---|---|---|---|
| Crown rump length | 21 | 16 | 10.3 |
| Crown heel length | 29 | 25 | 14.5 |
| Biparietal diameter | 5 | 4.3 | 3.5 |
| Head circumference | 17.1 | 17 | 20 |
| Chest circumference | 12.4 | 13.5 | 9.4 |
| Abdomen circumference | 20.5 | 15 | 11.6 |
| Foot length | | | |
| Right | 3.6 | 3.2 | Fused |
| Left | 3.6 | 3.1 | |

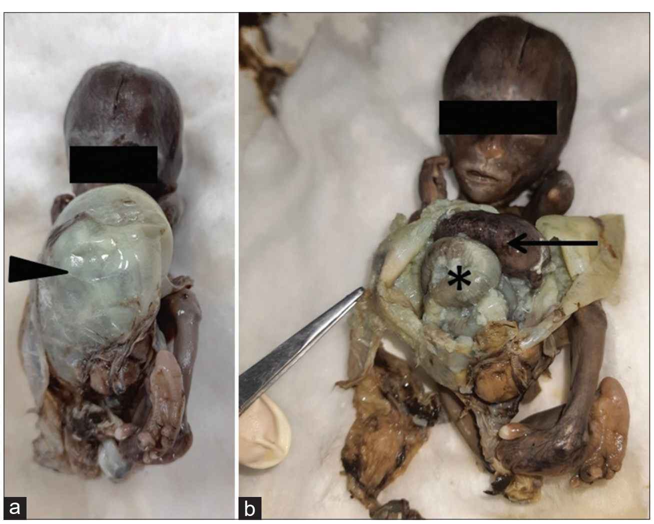


**Figure 1: Autopsy findings of Case 1 (anterior view). (a) A midline defect, Omphalocele, covered by a thin membrane (arrowhead), (b) Evisceration of liver (arrow), coils of small, and large intestine (*)**

### Case 2

Antenatal scans of a 19-week-old fetus showed anterior abdominal wall defect with herniation of liver and gastric bubble. On autopsy, a large midline ventral abdominal wall defect (8 cm × 3.6 cm) at the level of umbilicus was observed extending to pelvis with evisceration of liver, stomach, spleen, coils of small intestines, large intestine, along with right gonad, and right kidney. Urinary bladder exstrophy was observed through the infraumbilical wall defect [Figure 4a]. The external genitalia were not observed along with imperforate anus and scoliosis. An associated hypoplastic left lower limb was also observed [Figure 4b].

### Case 3

A dead fetus of $17^{+2}$ weeks was autopsied. In antenatal investigation, omphalocele along with spinal deformity was observed. On autopsy, an extensive median anterior abdominal wall defect was observed involving the entire ventral body wall extending from thoracic to abdominal and pelvic wall. There was evisceration of abdominopelvic contents as liver, stomach, small intestines, proximal part of large intestines [Figure 5], primitive cloaca was observed with continuous anorectal canal and urogenital sinus (cloacal exstrophy). Absence of external genitalia with undifferentiated gonads, imperforate anus, and kyphosis was also observed [Figure 6b].

A small oval anterior diaphragmatic defect (1 cm × 0.5 cm) was observed through which lower parts of the heart and right lung protruded into abdominal cavity. An inferior sternum defect was also observed with protrusion of upper

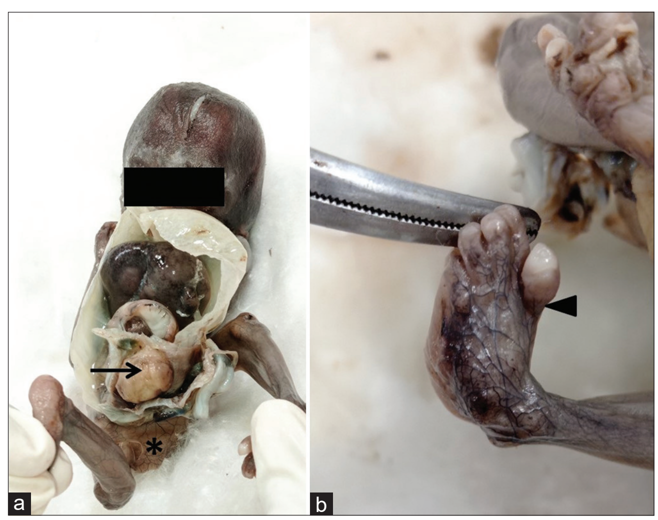


**Figure 2: Autopsy findings of Case 1. (a) Dissected infraumbilical ventral body wall defect in the lower part of anterior abdominal and pelvic wall with exposure of urinary bladder and a portion of gut, exstrophy of cloaca (arrow) with imperforate anus, and absence of external genitalia (*), (b) shortened left first metatarsal, great toe brachymetatarsia (arrowhead)**

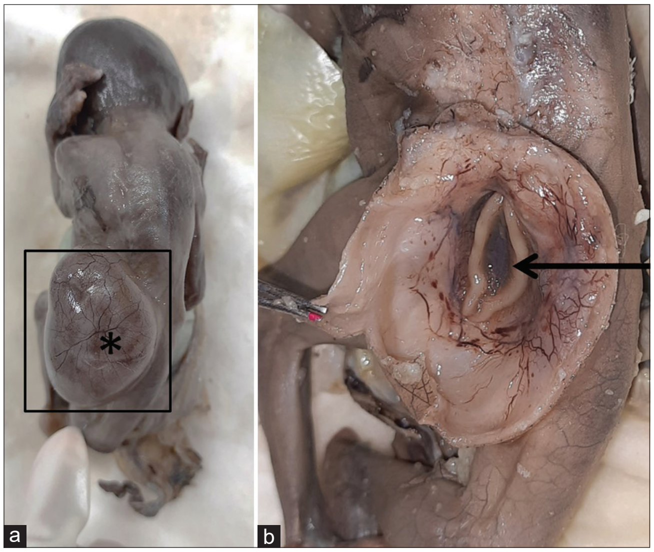


**Figure 3: Autopsy findings of Case 1 (posterior view). (a) A round cystic swelling (inset marked) in lumbosacral region, (b) On dissection of cystic swelling, a vertebral arch defect with meninges and rudimentary neural tissue protruding through the defect was observed-Meningomyelocele) (arrow)**


**Figure 5: Autopsy findings of Case 3: Showing a midline ventral body wall defect with herniated abdominal structures liver (L), stomach (S), coils of small intestines (I), proximal part of large intestines covered by a thin layer of membrane (*). Associated with kyphosis (arrowhead) and fusion of lower limbs (arrow) with single femur, tibia, fibula, and foot**

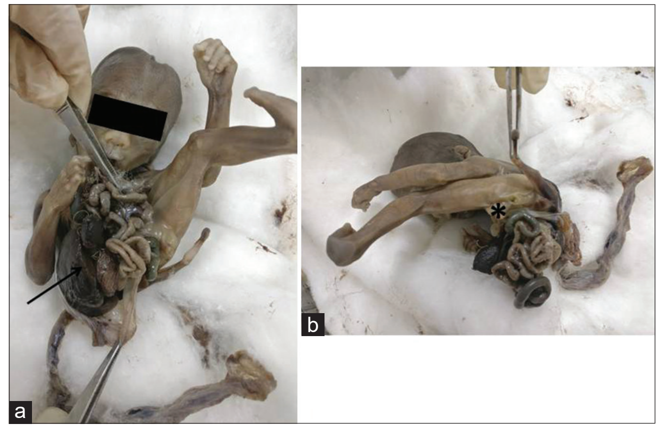


**Figure 4: Autopsy findings of Case 2. (a) Anterior view of fetus showing Omphalocele (arrow) and exstrophy of the bladder, (b) Lateral view of fetus showing imperforate anus (*), spinal defect and hypoplastic left lower limb (arrowhead)**


**Figure 6: Autopsy findings of Case 3. (a) dissected ventral body wall defect showing diaphragmatic hernia (arrow) with herniation of lower parts of the heart (*) and right lung (arrowhead) through the defect, (b) An inferior view showing the infra umbilical defect with exposure of urinary bladder and a portion of gut (exstrophy of cloaca) (arrow)**

portion of the heart (ectopia cordis) [Figure 6a]. In addition, fusion of lower limbs with single femur, tibia, fibula, and foot (serinomelia) was observed [Figure 5].

## Discussion

OEIS was first described by Littre in 1709, however, the term OEIS was first used by Carey in 1978. The etiology of OEIS is multifactorial with genetic and environmental factors.[6] The migratory failure of the lateral mesodermal folds prevents the normal mesodermal ingrowth to the cloacal membrane which results in premature rupture of the membrane.[7] The rupture of cloacal membrane prior to fusion with urorectal septum results in cloacal exstrophy, while late rupture sometime, after fusion gives rise to the less severe condition as bladder exstrophy.[8]

The present case series represents the varying spectrum of OEIS complex. Infraumbilical wall defect was observed in all three cases with two cases of cloacal exstrophy and one bladder exstrophy. Exstrophy in OEIS can be explained due to migratory failure of lateral mesodermal folds preventing the normal mesodermal ingrowth to cloacal membrane which results in premature rupture of membrane.[9] Thus, rupture of cloacal membrane prior to fusion with urorectal septum resulted in cloacal exstrophy.

A round cystic swelling was observed in Case 1 in the lumbosacral region. This cystic swelling was diagnosed with sacrococcygeal teratoma in ultrasonography. However, autopsy confirmed it as spina bifida (meningomyelocele) with meninges and rudimentary neural tissue protruding through the vertebral arch defect. Fetal autopsy corrected the prenatal assesment. Hence, the present study reinforces that radiological evaluation of such cases must be supplemented with autopsy for validation of diagnosis and further management.

Genetics has a major role in etiology of OEIS. There are several reports where siblings are affected.[8] The association of with twinning also supports genetic correlation.[5] OEIS complex has been reported with chromosomal abnormalities such as Trisomy 18, 21, mosaic Turner, unbalanced translocation between chromosome 9 and Y chromosome, deletion 3 (q12.2–q13.2) and deletion 1p36.[6] Homeobox genes defects (HLXB9) with mutations, can result in presacral teratoma, spine and anorectal abnormalities but there has not been an ascertained causal gene as yet. Existing genetic research with identification of definitive gene responsible for OEIS is still inconclusive. Genetic investigations like karyotyoing may be done for associated chromosomal disorders. Microarray analysis and next generation sequencing might be beneficial with advanced genetic studies.[9]

There are reported association of maternal exposure to diazepam, smoking, maternal obesity, uterine fibroids, gonococcal infection in early pregnancy, and fetal alcohol exposure throughout the pregnancy.[10]

Differential diagnosis of OEIS complex includes Pentalogy of Cantrell, Limb-body wall complex, and Exstrophy-epispadias complex.[11] Pentalogy of Cantrell is associated with omphalocele and may be suspected with thoracic defect with ectopia cordis, but absence of spinal defects differentiates it from OEIS. In Case 3, we observed OEIS with additional findings as sternal cleft, ectopia cordis, and anterior diaphragmatic hernia, which were suggestive of Pentalogy of Cantrell. Therefore, combined features of both Pentalogy of Cantrell and OEIS were observed in case 3**.** Limb body wall complex is a defect with similar abnormalities along with cranial, facial, and limb defects. Exstrophy-epispadias complex involves abdominal wall, genitourinary system, musculoskeletal, pelvis, pelvic floor, and spine. Its severity ranges from the mildest forms of epispadias to bladder and cloacal exstrophy.[12]

## Conclusion

OIES complex needs a multidisciplinary team involving early ultrasonographic detections, maternal screening, surgical management in less severe cases and fetal autopsy. Detailed fetal autopsy findings of OEIS complex case series in the present study will be significant for establishing spectrum of OEIS and assisting radiologists, obstetrician, and surgeons for better evaluation and management.

**Financial support and sponsorship**

Nil.

**Conflicts of interest**

There are no conflicts of interest.

## References

1. Carey JC, Greenbaum B, Hall BD. The OEIS complex (omphalocele, exstrophy, imperforate anus, spinal defects). Birth Defects Orig Artic Ser 1978;14:253-63.
2. Källén K, Castilla EE, Robert E, Mastroiacovo P, Källén B. OEIS complex – A population study. Am J Med Genet 2000;92:62-8.
3. Bohring A. OEIS complex, VATER, and the ongoing difficulties in terminology and delineation. Am J Med Genet 2002;107:72-6.
4. Mamatha K, Yelikar BR, Deshpande VR, Disha BS. A rare case of genital malformation with omphalocele, exstrophy of bladder, imperforate anus and spinal defect complex-autopsy findings. J Clin Diagn Res 2017;11:D37-8.
5. Lee DH, Cottrell JR, Sanders RC, Meyers CM, Wulfsberg EA, Sun CC. OEIS complex (omphalocele-exstrophy-imperforate anus-spinal defects) in monozygotic twins. Am J Med Genet 1999;84:29-33.
6. Mildenberger H, Kluth D, Dziuba M. Embryology of bladder exstrophy. J Pediatr Surg 1988;23:166-70.
7. Woo LL, Thomas JC, Brock JW. Cloacal exstrophy: A comprehensive review of an uncommon problem. J Pediatr Urol 2010;6:102-11.
8. Sadler TW. Langman's medical embryology. 15th. Edn. Wolters Kluver. 2023.
9. Akalın M, Demirci O, Dizdaroğulları GE, Çiftçi E, Karaman A. Contribution of chromosomal microarray analysis and next-generation sequencing to genetic diagnosis in fetuses with normal karyotype. J Obstet Gynaecol Res 2023;49:519-29.
10. Noack F, Sayk F, Gembruch U. Omphalocoele-exstrophy-imperforate anus-spinal defects complex in dizygotic twins. Fetal Diagn Ther 2005;20:346-8.
11. Vasudevan PC, Cohen MC, Whitby EH, Anumba DO, Quarrell OW. The OEIS complex: Two case reports that illustrate the spectrum of abnormalities and a review of the literature. Prenat Diagn 2006;26:267-72.
12. El-Hattab AW, Skorupski JC, Hsieh MH, Breman AM, Patel A, Cheung SW, *et al*. OEIS complex associated with chromosome 1p36 deletion: A case report and review. Am J Med Genet A 2010;152A: 504-11.

Original Article

# Peer-assisted Learning in Embryology: Enhancing Knowledge Retention through Three-dimensional Model-making and Jigsaw Teaching


## Abstract

**Introduction**: Embryology, a complex and three-dimensional (3D) field of anatomy, requires a multifaceted approach to learning. Traditional lectures often result in short-term retention, while visual aids such as videos can improve recall. However, creating models of embryological concepts and congenital anomalies facilitates a deeper understanding of the material. Building on this, the current study investigates the impact of combining two innovative methods – 3D model-making and jigsaw peer teaching – on both short-term and long-term knowledge retention in learning embryology. By engaging students actively and promoting peer-to-peer learning, this approach aims to enhance the learning experience and improve comprehension of this intricate subject. **Materials and Methods:** Sixty-two 1st-year MBBS students learned systemic embryology topics and participated in a model-making competition, followed by jigsaw grouping. Short-term retention was assessed through pre- and posttests, analyzed using paired *t*-tests. Long-term retention was evaluated by correlating posttest scores with performance in the Common Internal Assessment Test (CIAT). Student feedback was also collected after the model-making and jigsaw activities. **Results:** The intervention yielded a significant 14.2-point increase in mean test scores ($P < 0.001$). Posttest scores strongly correlated with scores in the CIAT ($r = 0.68$) and embryology ($r = 0.62$). Regression analysis confirmed a significant independent association between posttest scores and IA/embryology scores, controlling for confounding variables. **Conclusion:** Students found model-making and jigsaw learning to be valuable, time-consuming but effective methods for retaining long-term memory and learning embryology. Both approaches, being student-centered, fostered a dynamic learning environment, promoting teamwork, communication, leadership, and motivation, beyond just academic knowledge.


**Keywords:** *Embryology learning, embryology model-making, jigsaw learning*


**Saranya Ragavan, Vijaykishan Bheemavarapu, Vidya Gunasegaran[1], Ramachandran Thiruvengadam[2]**

*Department of Anatomy, JIPMER, Karaikal, [1]Department of Anatomy, JIPMER, Puducherry, [2]BRIC-Translational Health Science and Technology Institute, Faridabad, Haryana, India*


## Introduction

Anatomical knowledge, particularly embryology, involves three-dimensional (3D) learning and the capacity to interpret with time. Chinese philosopher and reformer Confucius (551 BC to 479 BC) stated, "I hear and I forget. I see and I remember. I do and I understand." This illustrates that students often forget what they hear in lectures and merely remember what they see in videos; however, when they engage in the hands-on practice of creating embryological models, they truly understand the complex concepts.[1,2] A number of authors have adopted techniques that promote the learning of embryology through visual and kinesthetic means.[3-6] Like model-making, another way of actively engaging the students to enhance their learning is peer teaching. As we know "To teach is to learn twice," peer teaching has a good educational value.[7] In either of the methods, i.e., model-making or peer teaching, improved short-term retention of memory has been proven by several studies. Though, ideally, the understanding should also aid the long-term memory retention. The current study aims to test the effect of combined 3D model-making and jigsaw peer teaching in learning embryology in terms of both short-term and long-term retention of memory.

## Materials and Methods

To enhance teaching and learning outcomes in embryology for 1st-year MBBS students, the department of anatomy faculty engaged in a focus group discussion (FGD).[8] This 40-min brainstorming session aimed to identify innovative solutions to



**How to cite this article:** Ragavan S, Bheemavarapu V, Gunasegaran V, Thiruvengadam R. Peer-assisted learning in embryology: Enhancing knowledge retention through three-dimensional model-making and jigsaw teaching. J Anat Soc India 2026;75:12-8.

**Article Info**

**Received:** 20 May 2025
**Revised:** 11 February 2026
**Accepted:** 11 February 2026
**Available online:** 27 March 2026

***Address for correspondence:***
*Dr. Saranya Ragavan, Department of Anatomy, Academic Building, Jawaharlal Institute of Post Graduate Medical Education and Research, Puducherry, India. E-mail: drsaranya05@gmail.com*

**Access this article online**

**Website:** https://journals.lww.com/joai

**DOI:** 10.4103/jasi.jasi_93_25

**Quick Response Code:**

overcome the complexities of embryology. We ensured a collaborative participation among faculty, designated a note-taker for minute-taking, and did coding and thematic analysis of discussions. Our main consensus was to pilot a novel pedagogical approach combining 3D model-making and jigsaw peer teaching, assessing the efficacy of this integrated method in improving embryology learning outcomes.

The study was conducted among all 62 1st-year MBBS students at our institute. To implement this intervention, the standard curriculum for the gastrointestinal and excretory systems was restructured to emphasize active learning. Typically, the curriculum allocates 8 h to these systems, comprising 5 h of didactic lectures (3 h for gastrointestinal and 2 h for the excretory system) and 3 h of practical chart demonstrations. In the current study, the didactic teaching was condensed into 3 h (2 h for the gastrointestinal system and 1 h for the excretory system). Following these initial lectures, an announcement was made regarding the upcoming model-making competition and jigsaw peer-learning sessions.

The students were then given a 2-week period of self-directed learning to construct their models outside of formal class hours. They were instructed to minimize the use of nonrecyclable materials. During this time, five distinct model categories were constructed, corresponding to the following topics: the development of peritoneal folds and cavities and the development and associated anomalies of the foregut, midgut, hindgut, and the urinary system [Figure 1].

After obtaining written informed consent, a dedicated 2-h model-making competition was held, which included the exhibition, judging, and viva voce. In the following week, the remaining 5 h of the original curricular time (repurposed from the standard lecture/practical schedule) were utilized for the jigsaw peer-learning sessions. To execute the jigsaw learning, the number of topics, number of groups, and number of time slots used for the discussion must be the same [Figure 2]. Twelve students were allotted for each topic, which forms the main group. Each main group of 12 students was divided into 5 subgroups (e.g., A, B, C, D, and E) and each subgroup had two students. The addition of a third student to any subgroup was decided based on the academic performance of the remaining two students. Hence, wherever there was a poor learner in any subgroup, this addition was done. In this way, sampling bias was reduced.

The subgroups were redistributed to form a doublet of five jigsaw groups of 6–7 students each. Ultimately, every jigsaw group/cluster had at least one student from each main group. The students shared a scheduled chart displaying the topic and time slot for discussion at each workstation, where the prepared models and the key points to be learnt at the end of the session are displayed. Hence, the jigsaw groups were given timed rotations to learn all the five topics chosen for model-making competition with adequate breaks in between. Hence, after the jigsaw method of peer learning, every subgroup was able to thoroughly learn about all the topics in an active manner. Each workstation was moderated by one faculty to ensure active participation of all the students, to clarify their doubts, and to lead the discussion in a focused manner.

To assess the short-term retention of memory, pretest and posttest in the form of multiple-choice questions [Supplementary File] were conducted ensuing the jigsaw peer discussion, whose results were compared using paired *t*-tests. The students' long-term retention of memory was tested by correlating posttest scores and performance in embryology questions in the Common Internal Assessment Test (CIAT) by correlation and regression analysis. The


**Figure 1: Student-made three-dimensional models illustrating the embryonic development of the gastrointestinal and excretory tracts**

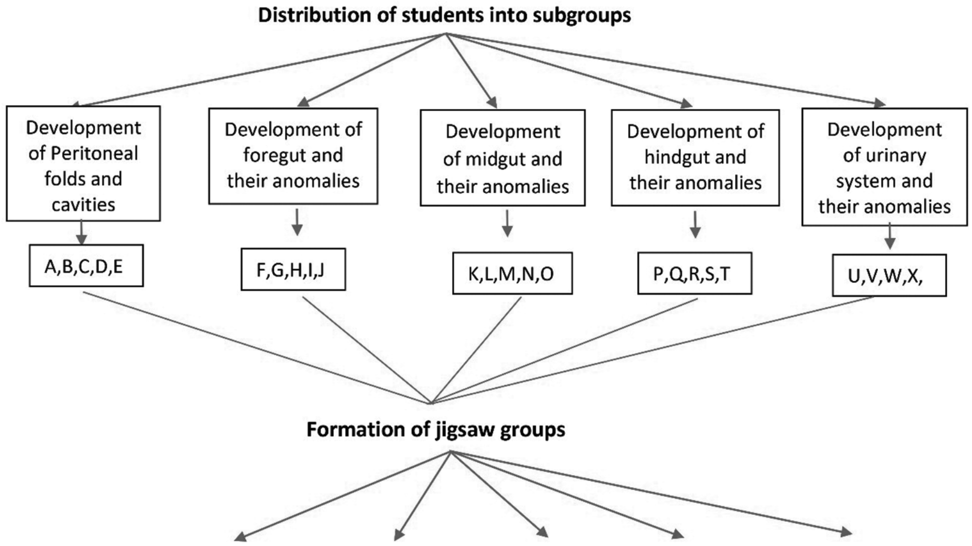


| Day | Topic & Timing | Development of peritoneal folds and cavities | Development of foregut and their anomalies | Development of midgut and their anomalies | Development of hindgut and their anomalies | Development of urinary system and their anomalies |
|---|---|---|---|---|---|---|
| Day 1 | Hour 1 | A,F,K,P,U | B,G,L,Q,V | C,H,M,R,W | D,I,N,S,X | E,J,O,T,Y |
| | Hour 2 | B,G,L,Q,V | C,H,M,R,W | D,I,N,S,X | E,J,O,T,Y | A,F,K,P,U |
| | Hour 3 | C,H,M,R,W | D,I,N,S,X | E,J,O,T,Y | A,F,K,P,U | B,G,L,Q,V |
| Day 2 | Hour 4 | D,I,N,S,X | E,J,O,T,Y | A,F,K,P,U | B,G,L,Q,V | C,H,M,R,W |
| | Hour 5 | E,J,O,T,Y | A,F,K,P,U | B,G,L,Q,V | C,H,M,R,W | D,I,N,S,X |

**Figure 2: Study design for jigsaw grouping**

CIAT is a standardized institutional examination comprising a total of 100 marks. Within this assessment, a specific subset of questions, accounting for 15 marks, was dedicated to the embryology topics covered in the study intervention. An independent association between posttest scores and CIAT and embryology scores was found by doing an adjusted analysis against the potential confounders (vide infra). Hence, the effectiveness was drawn by statistically comparing the scores of students who participated in this active learning versus their performance on those specific embryology questions in the CIAT. Feedback was also obtained from the students after the model-making and jigsaw learning.

## Results

The FGD was conducted as a brainstorming session. Content analysis and coding of discussions were done, from which themes were identified [Figure 3]. Consequently, the current study was intended to test the effect of combined 3D model-making and jigsaw peer teaching in learning Embryology in terms of both short-term and long-term retention of memory. Following the model-making and jigsaw learning, feedback was also obtained from the students.

### Objective 1: Short-term retention of memory

Total number of participants in the study: 62

- Number of students who responded to the pretest: 57
- Number of students who responded to the posttest: 50
- Number of students who responded to both the tests: 45.

In order to test the short-term retention of memory, the scores of pretest, that was given between model-making competition and jigsaw discussion and posttest conducted following the jigsaw discussion, were compared by paired *t*-test. The mean pretest score was 14.1 (SD: 4.2), and the mean posttest score was 28.6 (SD: 7.3) upon 50 marks. The difference in mean posttest score compared to mean pretest score was 14.2 marks, which is a statistically significant increase ($P < 0.001$).

After the model-making exercise and jigsaw discussion, 74% (37/50) scored at least 50% in the posttest, with the maximum score being 39/50.

### Objective 2: Long-term retention of memory

To investigate whether the combined effect of model-making and jigsaw peer teaching improved long-term retention of embryology knowledge, we analyzed the students' performance in the CIAT conducted 2 months after the intervention.

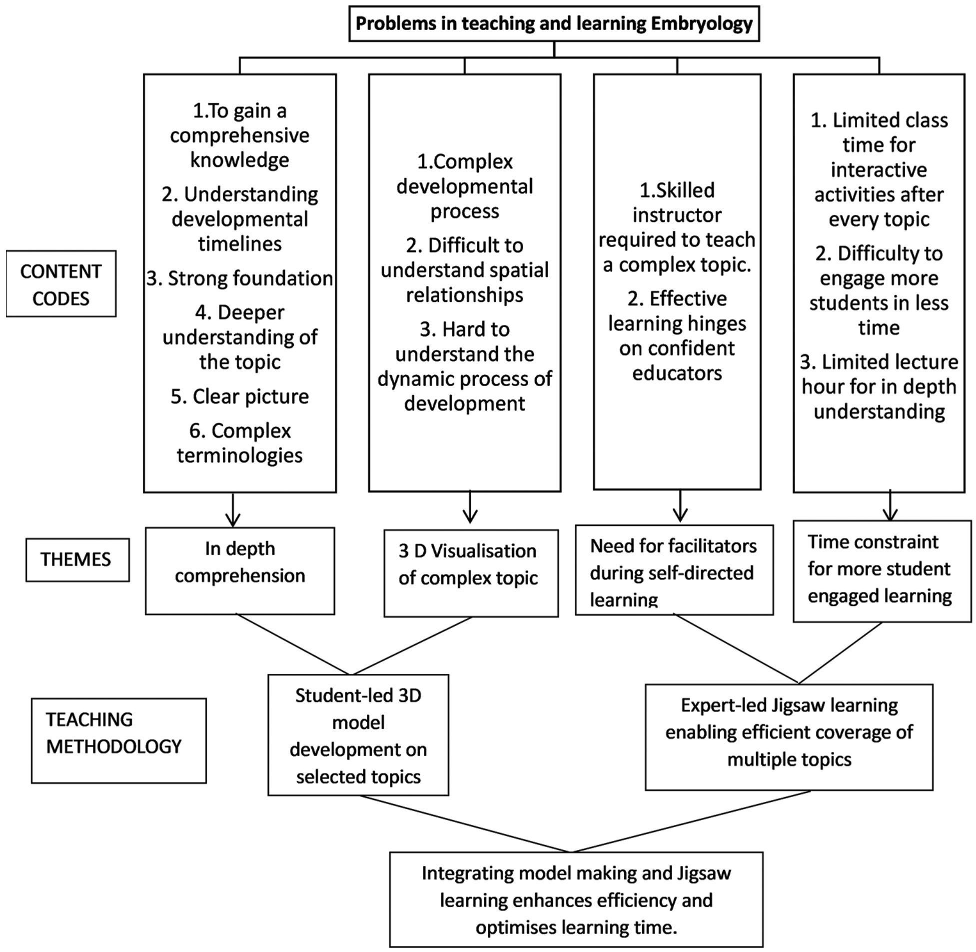


**Figure 3: Results of focus group discussion showing a synergistic effect of three-dimensional model-making and jigsaw peer teaching**

*Methods*

- We calculated Pearson's correlation coefficients to examine the relationships between posttest scores and
- Overall performance in CIAT (A)
- Performance in embryology questions in CIAT (B)
- We also conducted an adjusted analysis (C) to control for potential confounders, including age, NEET score, nonnativity, and difficulty understanding English.

*Results*

- All 62 students took the CIAT, with a mean total score of 50.1/100 (SD: 13.5) and a mean embryology score of 7.4/15 (SD: 3.1)
- 59.7% of students scored at least 50% in embryology questions, compared to 54.8% in the total score
- Posttest scores showed strong correlations with CIAT scores ($r$ = 0.68) and embryology scores ($r$ = 0.62)
- After adjusting for confounders, the posttest score remained independently associated with CIAT score and embryology score [Figure 4]
- For every mark increase in posttest score, there was a 1% increase in CIAT total score ($P$ < 0.001) and a 1.1% increase in embryology score ($P$ = 0.005).

### Objective 3: Feedback obtained from the students

Both model-making and jigsaw learning were found very useful by the students, and on a Likert scale of 10, the average score given was 8.9 for the model-making and 8.5 for the jigsaw learning. Table 1 reveals some of the repetitive feedback given by the students.

### Summary of results

The difference in mean pre- and posttest scores showed a mean of 14.2 marks increase that was statistically significant ($P$ < 0.001). The mean score in embryology questions in IA was 7.4/15 (SD: 3.1). Posttest scores were highly correlated with CIAT score (Pearson's correlation coefficient: 0.68) and embryology score (Pearson's correlation coefficient: 0.62). Multivariable regression analysis also showed a statistically significant independent association of the posttest scores with IA and embryology scores amid the variable confounding factors.

The students' perception about model-making and jigsaw learning showed that though it consumed more time, the model-making competition was a very useful exercise and it gave them a good long-term memory. The jigsaw method

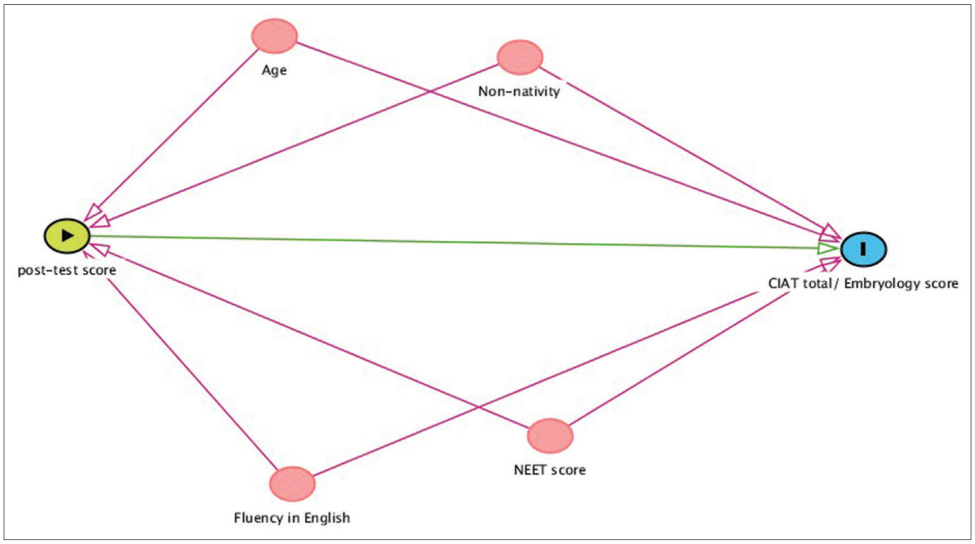


**Figure 4: Causal diagram depicting the relationship between various confounders with the exposure and outcome**

**Table 1: Students' feedback on model-making and jigsaw learning**

| Event | Facilitating factors/advantages | Hindering factors/disadvantages |
|---|---|---|
| Model-making | Team work | More members in the group |
| | Communication skills | Too much time to make the models |
| | Competitive spirit | All the group members were not equally contributing |
| | Faculty's guidance was useful | |
| | We learned the subject in a more practical manner | |
| | Motivated to read and learn about the topic from the model | |
| | Leadership quality | |
| | More creativity | |
| | Precision in making something | |
| Jigsaw learning | When our classmates taught the concepts, we didn't hesitate to ask doubts and clarify many times | It requires a student with good knowledge for each model |
| | When I myself had to explain the concepts, it gave me a deeper understanding | Since our friends were teaching, more time was required |
| | Learning from our classmates makes it more understandable | Everyone was not actively involved |
| | | I learned more thoroughly through model-making than the jigsaw method |

was yet another useful way of learning for the students, as it gave them the opportunity to learn about all the rest of the embryology models within a stipulated time period. Since both the methods were student-centered, the learning process was dynamic, and apart from studies, they had exposure to other qualities of professionalism, such as team building, communication skills, and leadership quality and also gained motivation toward learning the subject.

## Discussion

Among the different fields of anatomy, embryology is a hard area for many students where didactic lectures alone would not be sufficient for an effective learning of embryology. To implement self-directed learning and to make the subject more interesting, several innovative tools such as clay modeling, animated teaching, and video-based teaching have been practised across the world.

Aversi-Ferreira *et al*. used model construction in topics such as organogenesis, embryo folding, and neurogenesis and found that nearly 41% of the students evaluated that the construction of the models caught their attention the most, and 95% of them stated that it improved their learning.[1] Kamkhedkar S *et al*. used 3D embryology models and evaluated the cognitive domain scores of the 1st-year MBBS students before and after model-based teaching and found significant differences in their pre- and posttests.[6] A randomized controlled trial using animated teaching in embryology topics of gastrulation and neurulation conducted among 1st-year health science students showed a positive impact on knowledge gain both quantitatively and qualitatively.[5] Another study conducted in North France showed that in the method of video-based learning, the students obtained the best scores with a mean rate of success of 30% only in questions related to video content, and those not related to the video content had the success rate of approximately 9%.[4]

There are different types of learning styles for a student: auditory, visual, verbal, logical and mathematical and kinesthetic. Several authors have employed such techniques that facilitated the learning of embryology by the visual and kinesthetic way of learning.[1,3-6,9,10] The current study is combining the model-making and jigsaw learning, wherein all the five types of learners are benefitted. When a student is involved in the construction process, i.e. model-making using clay/recyclable material, it promotes metacognition that facilitates better understanding.[1,2] In the current study, in selected topics in systemic embryology, lecture classes were taken in a brief manner followed by a model-making competition. Since it is nearly time-consuming to allow the students to prepare models after every embryology topic, we assigned multiple topics to different groups of students so that each group became an expert in the particular topic. However, in order to ensure equality of learning among all the students in a short span about all the topics assigned, a jigsaw method of peer discussion was added on to it, expecting a good learning outcome.

Jigsaw technique is an active form of cooperative learning that builds a relationship among students through five elements: positive interdependence, individual accountability, interpersonal skills, face-to-face promotive interaction, and group processing.[7] Several authors have employed the jigsaw technique and found statistically significant results that promote student-centered and active learning of concepts.[11-13] Considering the student expert as tutor, peer–peer tutoring has contributed to higher examination scores.[12] In a study conducted by Oakes *et al*., this method was applied among students to teach abdominal anatomy, and it was found that though there was a gain in student performance with better motivation, the short-term knowledge gain was effective compared to end-semester performance.[7] Soundariya *et al*. applied this technique in physiology and found that most of the students accepted that the jigsaw method generated interest, enabled in-depth understanding, enhanced the communication skills, and considered it an effective way of learning.[14] The feedback was almost similar to the current study [Table 1], However, only 30% of their students preferred this method in future learning and only 13.3% of the students expressed easy adaptability to the jigsaw technique, whereas in the current study, nearly 82% of the students gave a Likert score of more than 7, and there was no obvious difficulty in adapting to the technique by sharing the jigsaw plan prior with the students. Haviz and Lufri introduced a subject jigsaw model for the embryology course and found that it effectively improved cooperative skills along with subject efficiency.[11]

In our exercise of combined model-making and jigsaw learning, Kirkpatrick's model of training evaluation could be applied as follows.[15]

**Level 1**

"Reaction" of the students after the training program was obtained through feedback following model-making and jigsaw learning. The feedback revealed that apart from active learning of embryology, the students could gain team spirit, leadership qualities, creativity, and good interpersonal communication skills among the peers. Jigsaw learning in particular could help the students learn rapidly about all the topics; however the in-depth learning on a particular topic was better achieved through model-making [Table 1].

**Level 2**

In the combined tool of model-making cum jigsaw learning exercise, "Learning transfer" (level 2) was tested by comparing the pretest with posttest performance. The mean difference by using a paired *t*-test between the pre- and posttest performance was 14.2, which was statistically significant ($P < 0.0001$). This elucidates about the immediate learning effect or good short-term retention of memory.

**Level 3**

"Impact or behavior" of this combined teaching method was tested by their performance in CIAT. The significance of CIAT is that the test is conducted in common for our students as well as the students of another campus of the same institute, wherein the question paper setting is done by an external subject expert, and evaluation is also made common to both the campuses. This absolutely rules out the bias in evaluation. Posttest performance was highly correlated with CIAT score (Pearson's correlation coefficient: 0.68) and embryology score (Pearson's correlation coefficient: 0.62). The correlation between the posttest score and CIAT or its embryology score was proved independent by multivariable regression analysis [Figure 4].

Hence, the combined model-making and jigsaw approach proved efficacious in resolving themes that emerged from FGD, namely, enhancing comprehension, visualizing complex concepts, facilitating self-directed learning, and optimizing time for student engagement.

**Ethical consideration**

As this study involved a low-risk observational design, incorporating model-making and jigsaw learning, it was exempted from formal ethical review.

**Limitations and future plan**

A larger sample size and comparison of scores with a control group would have added more value to the results. The department intends to implement this hybrid pedagogical model over the next three academic cycles to validate the consistency of these outcomes and assess the impact on subsequent university examination results.

## Conclusion

The exercise of model-making benefitted only a small group of students who gained expertise in their own topics. However, this model-making experience motivated and facilitated their active contribution to peer discussion, and the combined effect has ultimately proven good long-term retention of memory in embryology. Neither model-making nor jigsaw teaching independently would have proven the same long-term retention effect in the whole study population. Hence, the study results suggest that the "model-making exercise followed by peer-group discussion" is an innovative teaching tool that improves the long-term retention of embryology knowledge and helps to score better in the assessment examination.

In conclusion, the model-making and jigsaw learning methods have proven to be highly effective and engaging approaches to learning embryology. Despite the time-consuming nature of these methods, students have benefited significantly from them, developing not only a deeper understanding and long-term retention of the subject matter but also essential professional skills such as teamwork, communication, leadership, and motivation. By incorporating these student-centered approaches into the curriculum, we can foster a more dynamic and holistic learning environment that prepares students for success in their future careers.

### Acknowledgment

We would like to thank the faculty and staff of the department of anatomy and the MBBS students of JIPMER Karaikal for their co-operation in the conduct of this study.

### Financial support and sponsorship

Nil.

### Conflicts of interest

There are no conflicts of interest.

## References

1. Aversi-Ferreira TA, Aversi-Ferreira RA, do Nascimento GN, Nyamdavaa E, Araujo MF, Ribeiro PP, *et al*. Teaching embryology using models construction in practical classes. Int J Morphol 2012;30:188-95.
2. Correia JC, Baatjes KJ, Meyer I. Student-perceived value on the use of clay modelling in undergraduate clinical anatomy. Adv Exp Med Biol 2022;1388:153-70.
3. Kiecker C, Clarke J, Bell E. Teaching embryology through science fiction and role-play. Med Educ 2019;53:519.
4. Koscinski I, El Alaoui-Lasmaili K, Di Patrizio P, Kohler C. Videos for embryology teaching, power and weakness of an innovative tool. Morphologie 2019;103:72-9.
5. O'Connor C, Jordan K, Vagg T, Murphy CE, Barry DS, Toulouse A, *et al.* Animated teaching improves student learning of human gastrulation and neurulation. Ann Anat 2023;247:152057.
6. Kamkhedkar SG, Malgaonkar AA, Kartikeyan S. Three-dimensional embryology models as teaching aids for first-year medical students. Int J Biomed Res 2017;8:177-81.
7. Oakes DJ, Hegedus EM, Ollerenshaw SL, Drury H, Ritchie HE. Using the Jigsaw method to teach abdominal anatomy. Anat Sci Educ 2019;12:272-83.
8. Wong LP. Focus group discussion: A tool for health and medical research. Singapore Med J 2008;49:256-60.
9. Moraes SG, Pereira LA. A multimedia approach for teaching human embryology: Development and evaluation of a methodology. Ann Anat 2010;192:388-95.
10. Popovici R, Pristavu A, Sava A. Three dimensional ultrasound and hdlive technology as possible tools in teaching embryology. Clin Anat 2017;30:953-7.
11. Haviz M, Lufri L. Implementing of subject jigsaw learning model and its impact on students' achievement in Embryology course. Indones J Biol Educ 2019;5:435-42.
12. Shenoy A, Petersen KH. Peer tutoring in preclinical medical education: A review of the literature. Med Sci Educ 2020;30:537-44.
13. Walker S, Olvet DM, Chandran L. The jigsaw technique of peer teaching and learning: An efficient and enjoyable teaching strategy in medicine. MedEdPublish 2015;6:14.
14. Soundariya K, Senthilvelou M, Teli SS, Deepika V, Senthamil Selvi K, Mangani Mangalavalli S. Jigsaw technique as an active learning strategy in physiology for I MBBS students. Biomedicine (India) 2021;41:654-9.
15. Muraleedharan A, Ragavan S, Bage NN, Devi R. Perceptions of medical undergraduate students on curricular changes in anatomy: An embedded design mixed method study. J Adv Med Educ Prof 2022;10:22-9. [doi: 10.30476/JAMP.2021.92149.1472].

# Anatomical Variations of the Circle of Willis on Noncontrast Time-of-flight Magnetic Resonance Angiography in Ischemic Stroke Patients

**Jatla Jyothi Swaroop, Bonthu Anuradha[1]**

*Department of Radiodiagnosis, NIMRA Institute of Medical Sciences, Vijayawada, [1]Department of Radiodiagnosis, Rangaraya Medical College, Kakinada, Andhra Pradesh, India*

## Abstract

**Background:** The circle of Willis (CoW) is the principal intracranial collateral arterial network. Variations in its configuration may influence cerebral perfusion and stroke distribution. Data correlating CoW variants with ischemic stroke patterns in large Indian cohorts remain limited. **Aim:** The aim of this study was to evaluate anatomical variations of the CoW using noncontrast three-dimensional (3D) time-of-flight (TOF) magnetic resonance (MR) angiography in ischemic stroke patients and assess their clinical relevance in relation to stroke distribution. **Materials and Methods:** This prospective cross-sectional study with retrospective image analysis included 2000 adult patients with magnetic resonance imaging-confirmed ischemic stroke (January 2022–June 2025). Noncontrast 3D-TOF MR angiography was performed on a 1.5 T scanner. CoW configurations were classified using standardized criteria. Vessel diameters were measured on source images. Stroke territories were categorized as anterior or posterior circulation infarcts. Statistical analysis included Chi-square and Mann–Whitney *U* tests. **Results:** A complete CoW was observed in 54% of patients, while 46% demonstrated partially complete and incomplete configurations. Posterior circulation incompleteness (43%) was significantly associated with posterior circulation infarcts ($P = 0.02$). The mean vessel diameter was significantly greater in complete CoW configurations (1.20 ± 0.3 mm) compared to incomplete configurations (0.81 ± 0.2 mm; $P < 0.001$). **Conclusion:** Incomplete posterior CoW configurations are significantly associated with posterior circulation infarcts and reduced vessel caliber, highlighting their hemodynamic and clinical relevance in ischemic stroke. Routine reporting of CoW anatomy may improve risk stratification and management planning.

**Keywords:** *Anatomical variations, circle of Willis, collateral circulation, ischemic stroke, time-of-flight magnetic resonance angiography*

## Introduction

The circle of Willis (CoW), first described by Thomas Willis in 1664, is a polygonal arterial anastomotic network located at the base of the brain within the interpeduncular cistern. It connects the anterior circulation (internal carotid arteries) and posterior circulation (vertebrobasilar system), serving as the primary intracranial collateral pathway during arterial occlusion or hemodynamic compromise.[1,2]

A classical complete and symmetrical CoW is present in only 30%–60% of individuals.[3] Variations commonly involve hypoplasia or absence of the anterior communicating artery (AComA), A1 segment, posterior communicating artery (PComA), or the first segment of the posterior cerebral artery (P1). These anatomical differences influence collateral capacity, infarct evolution, and stroke severity.[4]

Several studies have demonstrated that incomplete CoW configurations are associated with reduced collateral efficiency, larger infarct volumes, and poorer functional outcomes in selected stroke subtypes.[5] Posterior circulation strokes are highly dependent on PCoA and P1 integrity due to limited alternative collateral pathways.

Although previous anatomical and radiological studies have described the prevalence of CoW variants, most investigations have been limited by small sample sizes. Moreover, in the Indian population, few large studies have systematically correlated CoW morphology with stroke territory, laterality, and vessel caliber using standardized noncontrast three-dimensional (3D) time-of-flight (TOF) magnetic resonance (MR) angiography.[6] This



**How to cite this article:** Swaroop JJ, Anuradha B. Anatomical variations of the circle of Willis on noncontrast time-of-flight magnetic resonance angiography in ischemic stroke patients. J Anat Soc India 2026;75:19-24.

**Article Info**

**Received:** 20 October 2025
**Revised:** 27 January 2026
**Accepted:** 23 February 2026
**Available online:** 27 March 2026

***Address for correspondence:***
*Dr. Jatla Jyothi Swaroop, Department of Radiodiagnosis, NIMRA Institute of Medical Sciences, Ibrahimpatnam, Vijayawada - 521 456, Andhra Pradesh, India.*
*E-mail: haijatle@gmail.com*

**Access this article online**

**Website:** https://journals.lww.com/joai

**DOI:** 10.4103/jasi.jasi_165_25

**Quick Response Code:**

gap in the literature underscores the need for a large-scale, magnetic resonance imaging (MRI)-based evaluation of CoW variants in ischemic stroke patients. Understanding the prevalence and functional implications of anatomical variants is clinically relevant, as it can inform risk stratification, predict stroke distribution, and guide interventional planning. The present study was therefore designed to evaluate the anatomical variations of the CoW in a large cohort of Indian stroke patients and assess their association with stroke distribution patterns, laterality, and vessel caliber.

### Aims and objectives

The objectives of the present study were to evaluate the anatomical variations of the CoW in patients with ischemic stroke using noncontrast TOF MR angiography (MRA) and to assess their association with stroke distribution patterns. The study further aimed to determine the prevalence of complete and incomplete CoW configurations, classify anterior and posterior circulation variants using standardized criteria, correlate these variants with anterior versus posterior circulation stroke patterns, and compare vessel diameters between complete and incomplete configurations to assess potential hemodynamic implications.

## Materials and Methods

### Study design

This was a prospective cross-sectional study with retrospective image analysis.

### Study population

This study enrolled 2000 consecutive adult patients (1120 males, 880 females; age 45–82 years) with MRI-confirmed ischemic stroke between January 2022 and June 2025.

### Inclusion criteria

- Acute or subacute ischemic stroke confirmed on diffusion-weighted imaging (DWI)
- Adequate coverage of CoW on MRA.

### Exclusion criteria

- Prior intracranial surgery
- Known vascular malformations
- Poor-quality MRA.

The study was approved by the Institutional Ethics Committee (Approval No.: RMC/ETC/016 dated 03.01.2022). Written informed consent was obtained from all participants prior to inclusion in the study.

### Imaging protocol

All examinations were performed on a 1.5 T MRI scanner (GE Healthcare) using an 8-channel head coil. The institutional acute stroke protocol included the following sequences: axial sections of the brain in T1, T2, fluid-attenuated inversion recovery, gradient sequence, coronal T2, sagittal T1, and diffusion-weighted imaging (DWI)–apparent diffusion coefficient maps.

Intracranial MRA was performed using a 3D-TOF sequence with the following acquisition parameters: repetition time 20–40 ms, echo time 3–7 ms, and flip angle 18°–25°. Images were obtained in the axial plane with a slice thickness of 0.6–0.8 mm, matrix size of 256 × 256, and field of view ranging from 180 to 220 mm. An inferior saturation band was applied to suppress venous inflow and enhance arterial visualization.

Image reconstruction included maximum intensity projection images, multiplanar and 3D reformations, and detailed evaluation of source images. Vessel diameter measurements were performed on source images to minimize flow-related overestimation. This sequence was primarily used for assessment of CoW anatomy and detection of intracranial large-vessel occlusion.

The standard noncontrast stroke MRI protocol had an average acquisition time of approximately 18–25 min. Inclusion of the 3D-TOF MRA sequence required an additional 5–7 min. Therefore, the total imaging acquisition time for the complete stroke MRI protocol, including intracranial angiography, was approximately 25–30 min. The average cost of an MRI brain with MRA in most centers ranges between ₹5000 and 8000, whereas a computed tomography (CT) brain with angiography study typically costs ₹3500–4500. MRI offers the advantages of being radiation-free and having superior sensitivity for early detection of acute ischemic stroke compared to CT. However, as our institution is a government-supported tertiary care center, both MRI and CT services are provided free of cost to all patients. This facilitates greater utilization of MRI in the acute stroke setting during hospital admission. CT brain in stroke patients is primarily reserved for patients with head trauma, suspected hypertensive stroke to rule out acute hemorrhage, or those with poor compliance and contraindications to MRI.

### Classification criteria

- Complete CoW: All segments ≥1 mm
- Incomplete CoW: Absence or hypoplasia (<1 mm or <50% contralateral)
- Fetal posterior cerebral artery (PCA): PCA supplied predominantly via PCoA with hypoplastic/absent P1.

### Statistical analysis

Statistical analysis was performed using the IBM Corp. Released 2025. IBM SPSS Statistics for Windows, Version 29.0. Armonk, NY: IBM Corp. Categorical variables were analyzed using the Pearson's Chi-square test to assess associations between CoW configurations and stroke distribution patterns. Continuous variables, including vessel diameters, were compared between complete and incomplete configurations using the Mann–Whitney *U* test. $P < 0.05$ was considered statistically significant.

## Results

Among the 2000 stroke patients evaluated, a complete CoW configuration was observed in 1080 patients (54%), while 720 patients (36%) demonstrated a partially complete configuration, and 200 patients (10%) had an incomplete CoW. Segmental analysis revealed that the anterior circulation was complete in 1680 patients (84%), whereas posterior circulation completeness was observed in 1140 patients (57%). These findings indicate that posterior circulation variations were considerably more frequent than anterior circulation variations in the present cohort.

The observed patterns of anterior and posterior circulation variants of the CoW are summarized in Table 1.

Analysis of stroke distribution demonstrated a statistically significant association between posterior CoW status and stroke territory ($P = 0.02$). Among patients with a complete posterior CoW ($n = 1140$), 210 (18.4%) developed posterior circulation strokes, whereas 930 (81.6%) had anterior circulation strokes. In contrast, among those with an incomplete posterior CoW ($n = 860$), posterior circulation strokes were observed in 280 patients (32.6%), while 580 (67.4%) had anterior circulation strokes.

The mean vessel diameter in patients with a complete CoW was $1.20 \pm 0.3$ mm, whereas in those with an incomplete configuration, it was $0.81 \pm 0.2$ mm. The difference was statistically significant ($P < 0.001$) [Table 2].

Bilateral infarcts were proportionally more frequent in patients with absent AComA (12/70; 17%) compared to those with a complete anterior CoW (100/1320; 7.6%), indicating reduced cross-flow compensation in variant anatomy. Unilateral A1 hypoplasia demonstrated an asymmetric infarct distribution, reflecting increased ipsilateral vulnerability [Table 3]. The differences in categorical distribution were statistically significant on Chi-square analysis ($P < 0.05$).

Occipital infarcts were proportionally more frequent in patients with unilateral fetal PCA (150/220; 68%) compared to those with a normal PCA configuration (56%). A similar predominance of occipital involvement was observed in bilateral fetal PCA variants [Table 4]. These findings suggest anterior-to-posterior hemodynamic dependency in fetal-type PCA configurations, wherein posterior cerebral territories rely predominantly on anterior circulation flow, influencing the pattern of infarction.

**Table 1: The frequency distribution of anterior and posterior circulation variants of the circle of Willis in the study population (%)**

| Anterior circulation variant | Frequency (%) | Posterior circulation variant | Frequency (%) |
|---|---|---|---|
| Typical type A | 80 | Bilateral PCoA hypoplasia | 28 |
| Unilateral A1 hypoplasia | 8 | Unilateral f-PCA | 9 |
| Absent AComA | 4 | Bilateral f-PCA | 2 |
| AComA duplication | 5 | Hypoplastic P1 | 6 |
| AComA triplication | 1 | Aplastic PCoA | 4 |

AComA: Anterior communicating artery, PCoA: Posterior communicating artery, P1: First segment of posterior cerebral artery, PCA: Posterior cerebral artery, f-PCA: Fetal-PCA

**Table 2: Comparison of mean vessel diameter between complete and incomplete circle of Willis configurations**

| Configuration | Mean diameter (mm) | *P* |
|---|---|---|
| Complete CoW | 1.20±0.3 | <0.001 |
| Incomplete CoW | 0.81±0.2 | |

CoW: Circle of Willis

**Table 3: Anterior circulation variants and stroke laterality (*n*=1510)**

| Anterior variant | Right ACI | Left ACI | Bilateral ACI | Total ACI |
|---|---|---|---|---|
| Complete anterior CoW (*n*=1680) | 620 | 600 | 100 | 1320 |
| Unilateral A1 hypoplasia (*n*=160) | 60 | 45 | 15 | 120 |
| Absent AComA (*n*=80) | 30 | 28 | 12 | 70 |
| Total | 710 | 673 | 127 | 1510 |

CoW: Circle of Willis, AComA: Anterior communicating artery, ACI: Anterior circulation infarct

**Table 4: Fetal-type posterior cerebral artery and posterior stroke distribution (*n*=490)**

| PCA configuration | Occipital stroke | Brainstem stroke | Total PCI |
|---|---|---|---|
| Normal PCA (*n*=178 posterior strokes in this group) | 100 | 78 | 178 |
| Unilateral f-PCA (*n*=220 posterior strokes in this group) | 150 | 70 | 220 |
| Bilateral f-PCA (*n*=92 posterior strokes in this group) | 55 | 37 | 92 |
| Total | 305 | 185 | 490 |

PCA: Posterior cerebral artery, f-PCA: Fetal-PCA, PCI: Posterior circulation infarct

## Discussion

The CoW constitutes the principal intracranial arterial collateral network, enabling compensatory redistribution of cerebral blood flow during arterial stenosis or occlusion. Its anatomical configuration determines the efficiency of primary collateral pathways and plays a pivotal role in cerebral perfusion reserve, infarct evolution, and vulnerability to territorial ischemia.[4,5] Figure 1 depicts the MR TOF angiography of a typical complete CoW.

Increasing evidence suggests that CoW integrity influences not only stroke distribution but also functional outcome and recovery following reperfusion therapies.[7]

In this large cohort of 2000 MRI-confirmed ischemic stroke patients, we systematically evaluated CoW morphology using noncontrast 3D TOF MRA and correlated anatomical variants with stroke territory and vessel caliber, thereby addressing a significant gap in Indian stroke literature.

**Prevalence and structural asymmetry of the circle of Willis**

A complete CoW configuration was identified in 54% of patients, while 46% demonstrated partial or incomplete configurations. This prevalence aligns with previously reported anatomical and radiological studies (30%–60%),[2,3,8] confirming that classical textbook symmetry represents only a subset of the population. Indian studies have reported complete CoW prevalence between 32% and 62%,[6,9,10] supporting the external validity of our findings.

Notably, anterior circulation completeness (84%) was substantially higher than posterior circulation completeness (57%). This posterior predominance of variation is consistent with developmental embryology of the vertebrobasilar system, where P1 segments and PCoAs demonstrate greater variability in caliber and patency.[11]

The structural asymmetry observed in our cohort suggests that posterior circulation collateral pathways may be inherently less robust, potentially predisposing patients to vertebrobasilar ischemia.

**Anterior circulation variants and hemodynamic implications**

The typical type A anterior configuration was present in 80% of cases, indicating relative stability of the anterior segment. However, unilateral A1 hypoplasia (8%), absent AComA (4%), and AComA duplication (6%) were observed.

From a hemodynamic perspective, unilateral A1 hypoplasia is clinically significant. During internal carotid artery (ICA) occlusion, collateral cross-flow via the contralateral A1 segment and AComA becomes critical. Studies have demonstrated that a well-developed contralateral A1 segment facilitates anterior cross-filling and is associated with improved collateral grading and smaller infarct volumes in ICA and carotid-T occlusions.[12,13]

Figure 2 demonstrates the same clinical scenario of unilateral ICA occlusion with preserved intracranial flow bilaterally.

Conversely, hypoplastic or absent A1 segments may restrict compensatory flow, increasing the risk of extensive anterior circulation infarction. Although infarct volume was not directly quantified in this study, the anatomical prevalence of A1 hypoplasia highlights its potential prognostic relevance. Figure 3 demonstrates a clinical case scenario of a 50-year-old female presenting with acute confusion with bilateral anterior cerebral artery territory infarcts and associated anterior circulation CoW abnormalities.

**Posterior circulation variants and stroke vulnerability**

Posterior circulation variants were more frequent and demonstrated stronger clinical associations. Bilateral PCoA hypoplasia or absence (28%) represented the most common posterior alteration. Unilateral fetal-type PCA fetal posterior cerebral artery (f-PCA) was observed in 9%, bilateral f-PCA in 2%, hypoplastic P1 segments in 6%, and aplastic PCoA in 4%.

Posterior circulation strokes are particularly dependent on anterior-to-posterior collateral flow via the PCoA. When bilateral PCoA segments are hypoplastic or absent, compensatory redistribution during vertebrobasilar compromise becomes limited.[14]

This anatomical limitation likely explains the statistically significant association observed between incomplete posterior CoW configurations and posterior circulation infarcts in our cohort ($P$ = 0.020). Patients with incomplete posterior CoW demonstrated a higher frequency of posterior strokes (280 vs. 210), underscoring the functional consequences of anatomical insufficiency. Figure 4 demonstrates the high-definition 3D-TOF MR angiographic

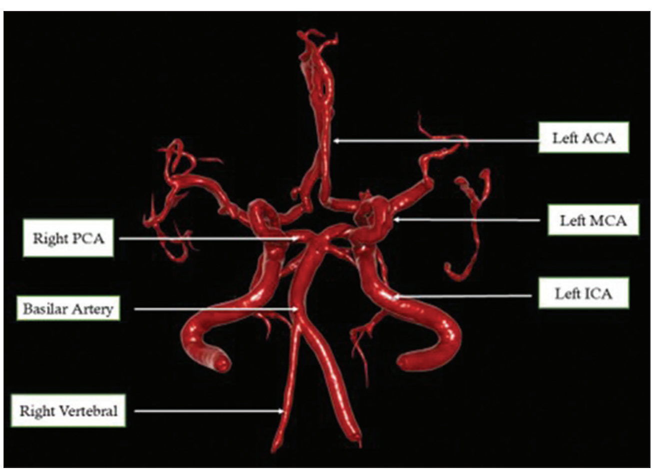


**Figure 1: Three-dimensional time-of-flight magnetic resonance angiography of a complete circle of Willis configuration. Labeled vessels: Left anterior cerebral artery, anterior communicating artery, left middle cerebral artery, left internal carotid artery, right posterior cerebral artery, basilar artery, and right vertebral artery. PCA: Posterior cerebral artery, ACA: Anterior cerebral artery, MCA: Middle cerebral artery, ICA: Internal carotid artery**

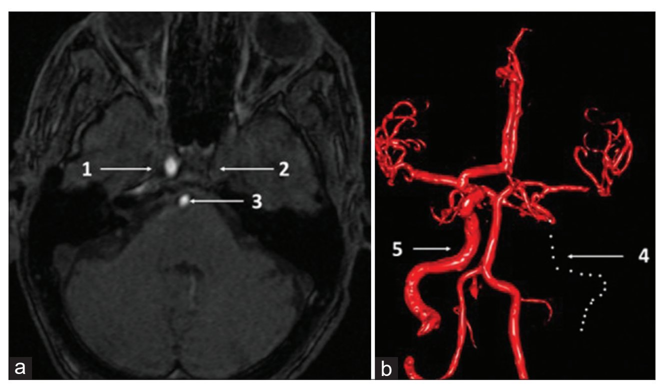


**Figure 2: Axial source image and three-dimensional (3D) time-of-flight (TOF) magnetic resonance (MR) angiography in a patient with unilateral internal carotid artery (ICA) occlusion: (a) Axial source image at the level of the cavernous sinus shows preserved signal in the right ICA (1), absent signal in the left ICA (2), and patent flow in the basilar artery (3). (b) 3D-TOF MR angiography confirms the absence of flow along the expected course of the left ICA (4), with opacification of the bilateral anterior cerebral artery, middle cerebral artery, and posterior cerebral artery via collateral flow from the right ICA (5)**

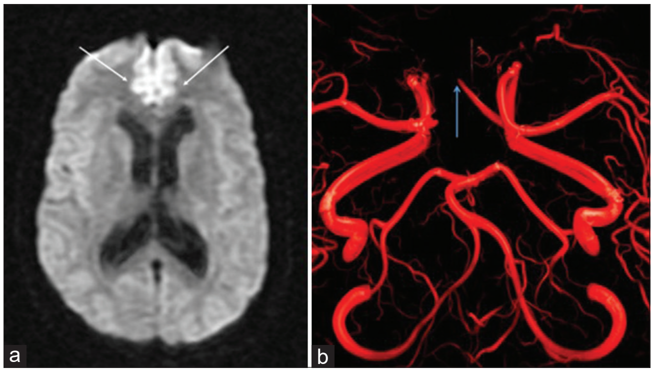


**Figure 3: Clinical case of a 50-year-old female with acute confusion and bilateral anterior cerebral artery (ACA) territory infarcts: (a) Diffusion-weighted image shows bilateral ACA territory infarcts (white arrows). (b) Corresponding high-definition magnetic resonance angiography shows absent right A1 segment of ACA and distal left ACA occlusion (blue arrows), resulting in bilateral ACA territory infarcts**


**Figure 4: High-definition three-dimensional time-of-flight magnetic resonance angiography in a patient with left occipital lobe infarct demonstrating anterior and posterior circle of Willis variants: (1) Absent left anterior cerebral artery (ACA) A1 segment; left ACA supplied by right ACA via anterior communicating artery ("complete collateralization"), (2) Left internal carotid artery forms left middle cerebral artery but not left ACA ("absent A1"), (3) Left vertebral artery continues as basilar artery; right vertebral artery aplastic ("unilateral vertebral artery dominance")**

image of a patient with vertigo and left occipital lobe infarct, demonstrating associated anomalies of both the anterior and posterior circulation components of the CoW.

Fetal-type PCA reflects the persistence of embryonic carotid dominance of the PCA. While it may enhance anterior-to-posterior collateralization in vertebrobasilar insufficiency, it simultaneously renders occipital territories vulnerable during ICA pathology. Thus, fetal PCA represents a double-edged hemodynamic configuration depending on the site of arterial compromise.[4,15]

### Correlation with stroke distribution

The significant association between incomplete posterior CoW and posterior circulation infarcts emphasizes that CoW variants are not merely anatomical curiosities but functionally relevant determinants of stroke territory distribution. Posterior circulation lacks the extensive leptomeningeal collateral redundancy observed in anterior territories.[12,16] Consequently, primary communicating arteries (PCoA and P1) assume critical importance in maintaining perfusion during arterial compromise.

The absence of a statistically significant association between anterior completeness and anterior stroke distribution may reflect the compensatory capacity of secondary leptomeningeal collaterals in the anterior circulation, which can partially offset primary communicating artery hypoplasia. This distinction reinforces the differential physiological vulnerability of anterior versus posterior circulation.

### Vessel diameter and collateral efficiency

A particularly important finding of this study was the significant difference in mean arterial diameter between complete (1.20 ± 0.3 mm) and incomplete (0.81 ± 0.2 mm) configurations ($P < 0.001$). Vessel caliber is a critical determinant of flow capacity; according to the Poiseuille's law, blood flow is proportional to the fourth power of vessel radius. Even modest reductions in diameter may therefore lead to disproportionately large reductions in flow reserve.

Reduced vessel diameter in incomplete configurations suggests impaired primary collateral efficiency and diminished hemodynamic compensation during acute occlusion. Prior hemodynamic studies have shown that incomplete collateral configurations are associated with reduced cerebrovascular reactivity and impaired flow augmentation during carotid compression testing.[14,17] Our morphometric findings provide structural corroboration of these functional observations.

### Impact of circle of Willis variants on functional outcomes

Beyond stroke distribution, growing literature supports the prognostic significance of CoW integrity. Systematic reviews and cohort studies have demonstrated that preserved communicating arteries are associated with better collateral grading, smaller infarct core, and improved functional outcomes in selected large-vessel occlusions.[7,13]

Patients with intact AComA and contralateral A1 segments have shown improved outcomes following mechanical thrombectomy in carotid-T lesions.[18] Conversely, incomplete CoW configurations have been associated with lower odds of favorable discharge outcomes and trends toward increased mortality in some cohorts.[19]

Although functional outcome scores (e.g., modified Rankin Scale) were not directly evaluated in our study, the demonstrated association between anatomical incompleteness and posterior stroke distribution, combined with reduced vessel caliber, supports the broader evidence that CoW morphology influences stroke pathophysiology and potentially clinical recovery.

### Clinical and diagnostic implications

The findings of this study reinforce the clinical importance of systematic evaluation of CoW anatomy in stroke imaging protocols. Identification of incomplete posterior circulation may:

1. Indicate increased vulnerability to vertebrobasilar ischemia
2. Provide insight into infarct pattern and territorial distribution
3. Assist in planning carotid and posterior circulation interventions
4. Offer indirect information regarding collateral reserve.

Noncontrast 3D-TOF MRA remains a reliable, radiation-free modality for evaluating CoW anatomy, particularly in patients with contraindications to iodinated contrast. Routine reporting of CoW configuration may enhance risk stratification and improve individualized therapeutic decision-making.

This study has certain limitations. Comparative evaluation with CT angiography or digital subtraction angiography was not performed, which could have provided additional validation of vascular anatomy and occlusion status. Furthermore, 3D TOF MRA is susceptible to flow-related artifacts, which may influence visualization and accurate assessment of vessel caliber, particularly in cases of slow or turbulent flow.

## Conclusion

The CoW demonstrates substantial anatomical variability in patients with ischemic stroke, with posterior circulation variants occurring more frequently than anterior variants. In this large MRI-based cohort, incomplete posterior configurations were significantly associated with posterior circulation infarcts, highlighting the functional importance of primary communicating arteries in maintaining collateral perfusion.

Reduced vessel caliber in incomplete configurations further supports impaired hemodynamic reserve and diminished collateral efficiency. These findings emphasize that CoW morphology is not merely an anatomical variant but a clinically relevant determinant of stroke distribution and potential vulnerability. Routine assessment of CoW configuration using noncontrast 3D-TOF MRA may therefore enhance stroke risk stratification, prognostic evaluation, and endovascular planning, particularly in posterior circulation ischemia.

### Financial support and sponsorship

Nil.

### Conflicts of interest

There are no conflicts of interest.

## References

1. Standring S, editors. Circle of Willis. In: Gray's Anatomy: The Anatomical Basis of Clinical Practice. 42nd ed. London: Elsevier; 2021.
2. Krabbe-Hartkamp MJ, van der Grond J, de Leeuw FE, de Groot JC, Algra A, Hillen B, *et al.* Circle of Willis: Morphologic variation on three-dimensional time-of-flight MR angiograms. Radiology 1998;207:103-11.
3. Alpers BJ, Berry RG, Paddison RM. Anatomical studies of the circle of Willis in normal brain. AMA Arch Neurol Psychiatry 1959;81:409-18.
4. van Raamt AF, Mali WP, van Laar PJ, van der Graaf Y. The fetal variant of the circle of Willis and its influence on the cerebral collateral circulation. Cerebrovasc Dis 2006;22:217-24.
5. van Seeters T, Hendrikse J, Biessels GJ, Velthuis BK, Mali WP, Kappelle LJ, van der Graaf Y; SMART Study Group. Completeness of the circle of Willis and risk of ischemic stroke in patients without cerebrovascular disease. Neuroradiology 2015;57:1247-51. Available from: https://pubmed.ncbi.nlm.nih.gov/26358136/. [Last accessed on 2026 Mar 13].
6. Ravikanth R, Philip B. Magnetic resonance angiography determined variations in the circle of Willis: Analysis of a large series from a single center. Tzu Chi Med J 2019;31:52-9. Available from: https://journals.lww.com/tcmj/fulltext/2019/31010/magnetic_resonance_angiography_determined.10.aspx. [Last accessed on 2026 Mar 13].
7. Bang OY, Saver JL, Buck BH, Alger JR, Starkman S, Ovbiagele B, *et al.* Impact of collateral flow on tissue fate in acute ischaemic stroke. J Neurol Neurosurg Psychiatry 2008;79:625-9.
8. Enyedi M, Scheau C, Baz RO, Didilescu AC. Circle of Willis: Anatomical variations of configuration. A magnetic resonance angiography study. Folia Morphol (Warsz) 2023;82:24-9.
9. Rajan ML. Study of variations in the posterior part of the circle of Willis using magnetic resonance angiography in an Indian population. Indian J Clin Anat Physiol 2021;8:11-4.
10. Rathod T, Joish UK. Variations of Circle of Willis in Indian Population. Asian J Med Radiol Res 2018;6:5-8. Available from: https://aijournals.com/index.php/ajmrr/article/view/288/250. [Last accessed on 2026 Mar 13].
11. Padget DH. The development of the cranial arteries in the human embryo. Contrib Embryol 1948;32:205-61.
12. Shuaib A, Butcher K, Mohammad AA, Saqqur M, Liebeskind DS. Collateral blood vessels in acute ischaemic stroke: A potential therapeutic target. Lancet Neurol 2011;10:909-21.
13. Maas MB, Lev MH, Ay H, Singhal AB, Greer DM, Smith WS, *et al.* Collateral vessels on CT angiography predict outcome in acute ischemic stroke. Stroke 2009;40:3001-5.
14. Hartkamp MJ, van Der Grond J, van Everdingen KJ, Hillen B, Mali WP. Circle of Willis collateral flow investigated by magnetic resonance angiography. Stroke 1999;30:2671-8.
15. Kapoor K, Singh B, Dewan LI. Variations in the configuration of the circle of Willis. Anat Sci Int 2008;83:96-106.
16. Liebeskind DS. Collateral circulation. Stroke 2003;34:2279-84.
17. Hoksbergen AW, Legemate DA, Ubbink DT, de Vos HJ, Jacobs NJ. Influence of the collateral function of the circle of Willis on hemispherical perfusion during carotid occlusion as assessed by transcranial colour-coded duplex ultrasonography. Eur J Vasc Endovasc Surg 1999;17:486-92.
18. Širvinskas A, Lengvenis G, Ledas G, Mosenko V, Lukoševičius S. Circle of Willis configuration and thrombus localization impact on ischemic stroke patient outcomes: A systematic review. Medicina (Kaunas) 2023;59:2115.
19. Lin E, Kamel H, Gupta A, RoyChoudhury A, Girgis P, Glodzik L. Incomplete circle of Willis variants and stroke outcome. Eur J Radiol 2022;153:110383.

Original Article

# Anatomical Variations of the Major Duodenal Papilla in a Select Adult Population


## Abstract

**Background:** The appearance of the major duodenal papilla (MDP) has ethnic variations that determine the ease of cannulation during endoscopic retrograde cholangiopancreatography. Understanding its variant anatomy may help ensure safety during surgical procedures around the duodenum. **Materials and Methods:** This observational cross-sectional study examined 140 adult specimens with intact MDP obtained from nairobi funeral home, university of nairobi-chiromo funeral parlour, and kenyatta national hospital farewell home following ethical approval granted by the institutional ethics and research committee. The morphology of the MDP was classified as protruded, flat, and depressed, and its distance from the pylorus, transverse diameter, and the protruded papilla's longitudinal measurements were taken. Data were analyzed using SPSS (Version 27.0). Means and standard deviations were calculated. Results were represented with tables. **Results:** The morphology of the MDP was identified as protruded (69.29%), flat (19.29%), and depressed (11.43%). Among protruded papilla, small protrusion was (17%), regular protrusion (80%), and large protrusion (3%). The mean distance from the pylorus was 90.23 ± 23.39 mm. The mean transverse diameter of the papillae was 6.88 ± 3.13 mm, and the mean longitudinal protrusion length of the protruded papillae was 5.93 ± 2.84 mm. The One-way ANOVA statistical test found that older individuals (59 + years) had a statistically significant shorter distance of the MDP from the pylorus ($P = 0.018$). **Conclusion:** Since the anatomic location, morphology, and morphometry of the MDP showed inter-individual and inter-population variation, we recommend that endoscopists operating in the region of the MDP thoroughly investigate the papilla and use its morphology as a guide for the technique of canulation.


**Keywords:** *Anatomy, major duodenal papilla, morphology, morphometry, variations*

**Oliver Munene Kinoti, Paul Ochieng Odula, Pamela Mandela Idenya, Bernard Ndung'u**

*Department of Human Anatomy and Medical Physiology, Faculty of Health Sciences, University of Nairobi, Nairobi, Kenya*

## Introduction

The major duodenal papilla (MDP) constitutes the junction of the biliary, pancreatic, and digestive tracts, surrounded by the sphincter of Oddi. The junction traverses the duodenal wall, terminating at the mucosa-covered MDP.[1] It is the primary access point to the liver and pancreas via the duodenum and is crucial for various diagnostic techniques, such as endoscopic retrograde cholangiopancreatography (ERCP), sphincterotomy, and other peri-duodenal procedures. Variations in its morphology, including the papilla's size, shape, and orientation, are reported in different populations.[2-7] There are several main classification systems used in the clinical setting, but the most common, easiest to understand, and most reproducible identifies the papilla as protruded, flat, and depressed papillae/diverticular type.[2,6,8,9] The protruded papillae are further divided into large, regular, or small protrusions.[10] The dimensions and positioning, including the length of protrusion of the papilla, transverse diameter, location on the intestinal wall, and distance of the MDP from the pylorus, also vary.[4,7]

ERCP is essential in diagnosing and treating biliopancreatic diseases, and the approach to biliary cannulation integrates technical and cognitive strategies based on papillary morphology. This is because the variant morphology predicts the ease and success of cannulation during ERCP and post-ERCP complication rates, such as life-threatening post-ERCP pancreatitis (PEP).[11-13] Despite advancements in technology and training, biliary cannulation in ERCP can still be unsuccessful in 20% of patients, even in the hands of experienced endoscopists.[14] Some morphologies are more challenging to cannulate and, therefore, prone to



**How to cite this article:** Kinoti OM, Odula PO, Idenya PM, Ndung'u B. Anatomical variations of the major duodenal papilla in a select adult population. J Anat Soc India 2026;75:25-32.

**Article Info**

**Received:** 14 January 2026
**Revised:** 04 February 2026
**Accepted:** 09 February 2026
**Available online:** 27 March 2026

***Address for correspondence:***
*Mr. Oliver Munene Kinoti, Department of Human Anatomy and Medical Physiology, Faculty of Health Sciences, University of Nairobi, Nairobi, Kenya.*
*E-mail: olivermunene39@gmail.com*

**Access this article online**

**Website:** https://journals.lww.com/joai

**DOI:** 10.4103/jasi.jasi_9_26

**Quick Response Code:**

complications and the need for rescue procedures.[15,16] The large protruded papilla is difficult to cannulate due to its relaxed and unstable nature, making it prone to inadvertent main pancreatic duct (MPD) cannulation, that can lead to PEP.[16] The flat papilla increases the time and attempts of cannulation because its small diameter impedes the smooth insertion of the cannula into the CBD.[6] The depressed papilla presents difficulties in localizing and intubating it as it is found at the margin or the floor of the depression or concealed by wide duodenal folds.[17] Excessively altered positioning in the duodenum or extremely large sizes of the MDP make it difficult for operators to maintain a good axis when approaching it, impeding its adequate visualization, thus resulting in a longer time to search for the papilla and making canulation more challenging. A more distal or proximal MDP, located in the third portion of the duodenum, may make it difficult to reach and hinder maneuverability, necessitating multiple maneuvers, which increases the difficulty of cannulation and the risk of intestinal perforations. There is no published data on the variant anatomy of the MDP in the Kenya's populace, despite its importance in determining the ease of cannulation and occurrence of complications during ERCP.

Understanding the MDP's morphologies is essential for enhancing procedural training, managing operational methods, reducing adverse events, improving patient outcomes in peri-duodenal procedures, and increasing patient safety locally. Special focus on difficult-to-cannulate papillae can reduce risks linked to excessive manipulation during cannulation attempts. Knowledge of papilla morphology can facilitate quick adaptation and informed decision-making during procedures, guiding the selection of suitable tools and techniques. It may also aid in surgical planning for patients at higher risk of developing PEP because of different papilla morphologies. We aimed to identify MDP anatomical variants within Kenya's population, to contribute to safer and more effective endoscopic procedures by expanding our understanding of MDP's variant anatomy.

### Study objective

The objective of the study was to determine the anatomical variations of the MDP in a select adult population.

## Materials and Methods

This observational cross-sectional study using postmortem specimens was conducted in the Department of Human Anatomy at the University of Nairobi, with ethical approval granted by the institutional ethics and research committee. We obtained adult postmortem specimens from nairobi funeral home, University of Nairobi-Chiromo funeral parlour, and kenyatta national hospital farewell home, with approved consent from the next of kin. We excluded cases with pathological processes restricted to the duodenum, pancreas, or papilla, such as papillary cancer, gastrointestinal tuberculosis, Sphincter of Oddi dysfunction, ectopic ampulla or ampullae, as well as those that could not be classified due to mucosal swelling, deformity, ulcers, or surgically altered anatomy. We applied the convenience sampling method. We applied the convenience sampling method where participants were enrolled to the study based on availability and accessibility. The sample size was calculated using the formula described by Jung,[18] where the estimated prevalence (P) of the most frequent variant of the MDP segmental position was taken as 91%, based on findings from a previous study by Sulochana *et al*.[19] Substituting these values into the formula yielded a minimum required sample size of 126. This was subsequently rounded up to 150 to account for potential missing or incomplete data.

### Procedure for accessing the major duodenal papilla

The peritoneal cavity was opened via a midline incision, and the duodenum was incised along the convex margin. The major papilla was identified, and a photograph of the undisturbed papilla was taken using a 12-megapixel camera to document its gross morphological features. The segmental location and position on the wall were noted, and the size was measured by recording the papilla's transverse (p-trans) and longitudinal (p-long) dimensions. The shape of the papilla was noted as protruded, flat, or depressed. The protruded papilla was subclassified based on its level of protrusion into small, regular, or large protrusion using a ratio of its length to its transverse diameter. The orifice morphology was recorded as either slit, rounded, or with two holes. The distance to the pylorus was also measured using a digital Vernier caliper version CVU 200 m (precision of 0.01 mm). The dissections were carried out by the principal investigator of the study, together with two research assistants (senior medical students) who participated in taking photographs and documentation. All measurements were taken twice by two researchers to minimize errors. The same digital Vernier caliper and protractor were utilized for all the measurements. Box plots, histograms, and the Kolmogorov–Smirnov test were used to check the normality of the data. The anatomical characteristics were presented as photomacrographs, and their frequency distribution was noted. We used the Independent *t*-test to compare p-longitudinal, p-transverse, and distance from the pylorus measurements between sexes (male and female), and one-way ANOVA for the analysis of these measurements between the age groups (18–38, 39–58, 59+).

## Results

### Study demographics

We identified 150 specimens for inclusion in the study and selected 140 specimens for the final analysis. Of the 10 excluded cases, 4 had duodenal ulceration, 3 had lodged gallstones, 2 had gastrointestinal malignancy, and 1 had a surgically altered anatomy. Specimens were obtained from 81 (59%) males and 59 (41%) females. The mean age of the participants was 39.7 (±14.1) years, ranging from 18 to 88 years. The mean age for males was 38.9 (±10.4) years and 40.9 (±11.2) years for females. The Independent *t*-test did not find the age or sex distribution differences to be statistically significant ($P$ = 0.444 and $P$ = 0.501, respectively).

### Anatomical characteristics of the major duodenal papilla

We characterized the anatomical features as types of papillae, by the level of protrusion of the papilla, the positioning of the papilla, and the orifice type, and assessed the distribution by age and sex.

### Types of papillae

We observed three types of papillae, whereby the protruded type was the most frequent in 97/140 (69.29%) of cases (55/140 [39.29%] males and 42/140 [30.00%] females), followed by flat in 27/140 (19.29%) of cases (14/140 [10.00%] males and 13/140 [9.29%] females) and depressed papillae in 16/140 (11.43%) of cases (12/140 [8.6%] males and 4/140 [2.9%] females) [Figure 1]. The distribution of the types of papillae by the overall mean age (years) was 47.3 ± 5.7 (protruded type), 48.3 ± 7.0 (flat type), and 45.3 ± 6.5 (depressed type), respectively. The Fisher's Exact Test did not show a statistically significant difference in the type of papilla between age groups ($\chi^2$ = 2.676, $P$ = 0.654, df = 4) and by sex ($\chi^2$ = 2.381, $P$ = 0.307, df = 2) [Table 1].

### Levels of papillae protrusion

We observed three protruded papillae types, whereby the regularly protruded papilla was the most frequent in 78/97 (80.4%) of cases (45/97 [46.4%] males and 33/97 [34.0%] females), followed by the small protrusion in 16/140 (16.5%) of cases among (9/97 [9.3% males] and 7/97 [7.2%] females), and the large protrusion in 3/97 (3.1%) of cases in (1/97 [1.0%] males and 2/97 [2.1%] females) [Figure 2]. The Fisher's Exact Test did not find a statistically significant difference in the papilla protrusion level between age groups ($\chi^2$ = 2.642, $P$ = 0.702, df = 4) and by sex ($\chi^2$ = 0.700, $P$ = 0.816, df = 2) [Table 2].

### Positioning of the papilla

There were three locations of papillae in the C-loop of the duodenum [Figure 3], whereby the MDP was commonly found in the 2nd part in 116/140 (87%) of cases in the C-loop of the duodenum, especially on the posteromedial wall in 91/140 (65%) of cases. In 2 (1.4%) cases, both females, the MDP was at the junction between the 1st and 2nd parts of the duodenum. In 16/140 (11.5%) cases (12/140 [8.6%] males, and 4/140 [2.9%] females), the papilla was located at the junction between the 2nd and 3rd parts of the duodenum. In 2 (1.4%) cases of the males, the papilla was found on the posterior wall of the 2nd part of the duodenum [Table 3].

### Orifice type

The three types of papillae orifices were observed as rounded papilla orifice in 117/140 (83.6%) cases (69/140 [49.3%] males and 48/140 [34.3%] females), the slit type in 21/140 (15.0%) cases (11/140 [7.9%] males

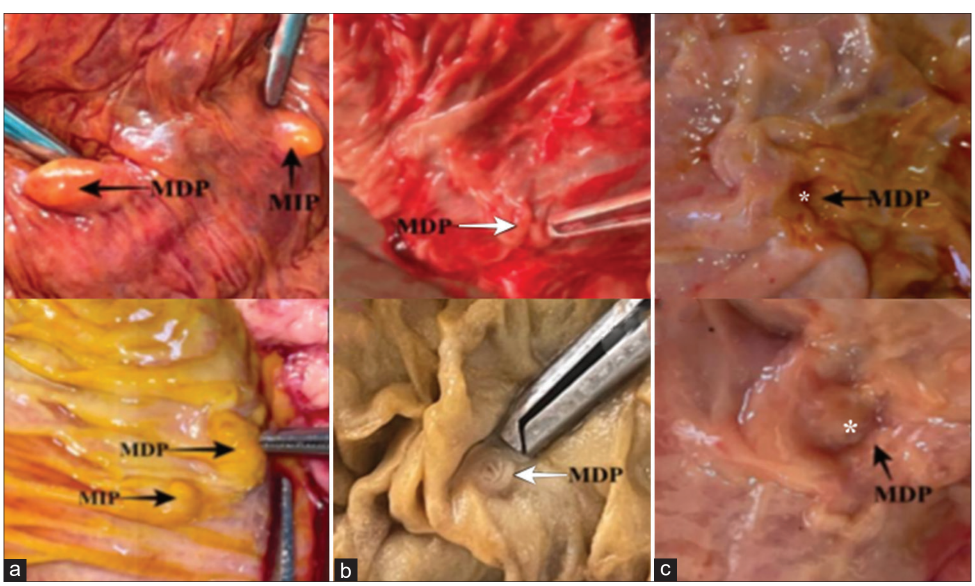


**Figure 1: Photomacrographs displaying the different types of papillae: Minor papilla, major duodenal papilla. The protruded papilla (a, both upper and lower left panels) projects above the surrounding duodenal mucosa membrane. Note the mucosal bump (black arrowhead). The flat papilla (b, both upper and lower middle panels) is level with the surrounding duodenal mucosa (white arrowhead). The depressed papilla (c, both upper and lower right panels) presents a visible orifice (*) surrounded by irregular ridges of the duodenal mucosa membrane. MDP: Major duodenal papilla, MIP: Minor papilla**

**Table 1: Distribution of the types of papillae by age groups**

| Type of papilla | Sex | Age (years) 18–38, *n* (mean±SD) | 39–58, *n* (mean±SD) | 59+, *n* (mean±SD) |
|---|---|---|---|---|
| Protruded | Male | 32 (30.34±6.12) | 15 (45.93±5.91) | 8 (65.25±6.82) |
| | Female | 19 (30.11±5.78) | 19 (47.37±5.26) | 4 (64.25±2.50) |
| | Total | 51 (30.3±5.9) | 34 (46.7±5.5) | 12 (64.9±5.6) |
| Flat | Male | 9 (27.56±4.80) | 2 (43.00±5.66) | 3 (75.67±10.97) |
| | Female | 7 (31.43±5.97) | 4 (45.00±5.66) | 2 (64.50±6.36) |
| | Total | 16 (29.3±5.5) | 6 (44.30±5.20) | 5 (71.20±10.4) |
| Depressed | Male | 8 (28.00±7.27) | 4 (46.00±6.63) | - |
| | Female | 2 (24.50±7.78) | 1 (45.00) | 1 (63.0) |
| | Total | 10 (27.1±7.1) | 5 (45.80±5.80) | 1 (63.0) |

Fisher's exact test (type of papilla vs. sex), $\chi^2$=2.381, *P*=0.307, df=2; Fisher's exact test (type of papilla vs. age groups) $\chi^2$=2.676, *P*=0.654, df=4. SD: Standard deviation

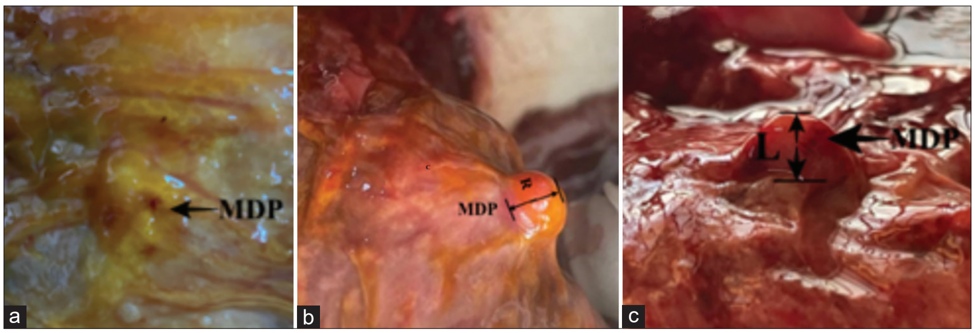


**Figure 2: Photomacrographs displaying the levels of protrusion observed: Major duodenal papilla, regular protrusion (r), large protrusion (l). The small protruded papilla (a) has a ratio of its length to diameter of <0.5. The regularly protruded papilla (b) has a length-to-diameter ratio of 0.5–2. The large protruded papilla (c) has a ratio of its length to height of more than 2. MDP: Major duodenal papilla**

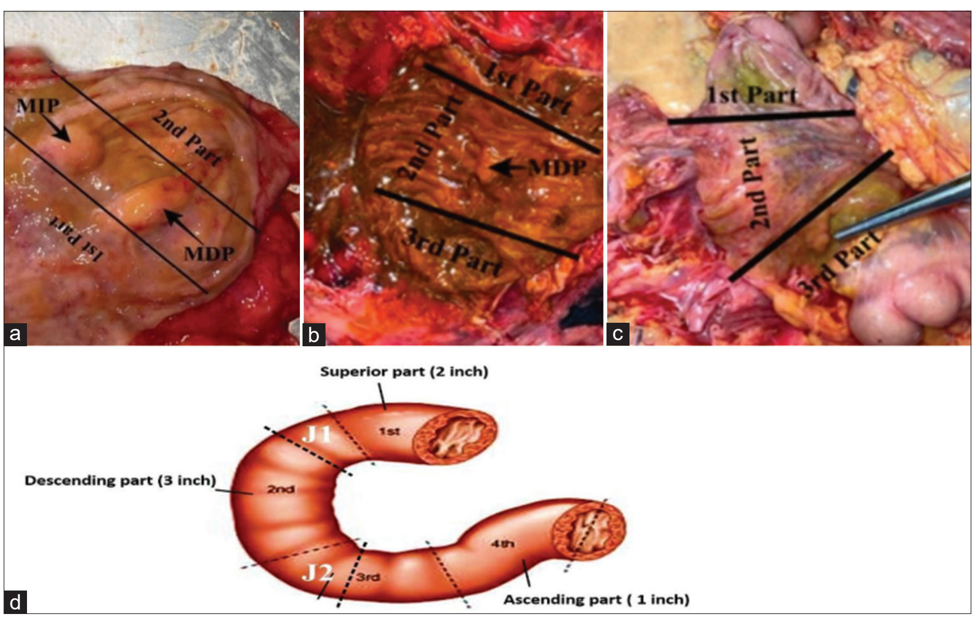


**Figure 3: Photomacrographs displaying the different locations of the major duodenal papilla (MDP) in the duodenum, observed: MDP, minor papilla. The papilla is at the junction of the 1st and 2nd parts of the duodenum (a). The papilla is on the 2nd part of the duodenum (b). The papilla is on the junction between the 2nd and 3rd part of the duodenum (c) (probed by forceps). The locations of the junctions (J1 and J2) are shown in a diagrammatic representation (d). MDP: Major duodenal papilla, MIP: Minor papilla**

and 10/140 [7.1%] females), and the two-hole orifice papillae in 2/140 (1.4%) cases (1/140 [0.7%] male and 1/140 [0.7%] female). The rounded orifice was more commonly found amongst the protruded papillae. The protruded papillae were found to have a rounded orifice in 78/97 (80%) of the participants. The slit-type orifice was

**Table 2: Distribution of papilla levels by sex and age groups**

| Papilla protrusion type | Sex | Age (years) | | |
|---|---|---|---|---|
| | | 18–38, *n* (mean±SD) | 39–58, *n* (mean±SD) | 59+, *n* (mean±SD) |
| Protrusion S | Male | 5 (30.80±6.54) | 3 (49.67±8.02) | 1 (61.00) |
| | Female | 2 (30.50±10.61) | 5 (46.20±7.43) | - |
| | Total | 7 (30.70±6.9) | 8 (47.50±7.3) | 1 (61.00) |
| Protrusion R | Male | 26 (30.04±6.18) | 12 (45.00±5.29) | 7 (65.86±7.13) |
| | Female | 16 (30.38±5.55) | 13 (48.08±4.59) | 4 (64.25±2.50) |
| | Total | 42 (30.20±5.) | 25 (46.60±5.1) | 11 (61.00±5.7) |
| Protrusion L | Male | 1 (36.00) | - | - |
| | Female | 1 (25) | 1 (44.00) | - |
| | Total | 2 (30.50±7.8) | 1 (44.00) | - |

Fisher's exact test (papilla protusion type vs. sex) $\chi^2$=0.700, *P*=0.816, df=2; Fisher's exact test (papilla protusion type vs. age groups) $\chi^2$=2.642, *P*=0.702, df=4. SD: Standard deviation

**Table 3: Positioning of the papilla on the C-loop of the duodenum by sex and mean age**

| Papilla position | Male | Mean age - male (years) | Female | Mean age - female (years) |
|---|---|---|---|---|
| Posteromedial | 52 (37.1) | 39.06 | 39 (28.9) | 40.92 |
| Medial | 26 (18.6) | 39.54 | 20 (14.3) | 40.95 |
| Posterior | 2 (1.4) | 30.67 | 0 | - |
| Junction of 1st and 2nd parts | 0 | - | 2 (1.4) | 24.00 |
| 2nd part | 61 (43.6) | 39.54 | 55 (39.3) | 41.58 |
| Junction of 2nd and 3rd parts | 12 (8.6) | 35.25 | 4 (2.9) | 40.75 |

Table 3 shows the positions of the papilla on the C-loop of the duodenum by total number (*n*), percentage (%), and mean age of males and females

found in 18/97 (19%) of cases with protruded papillae, and the two separate hole orifices in 1/140 (1%) of cases with protruded papillae. Figure 4 shows the orifice types observed.

### Morphometry of the major duodenal papilla

The morphometric analysis included measures of the papilla dimensions and the distance of the papillae from the pylorus, distributed by age and sex. The overall average length of papilla protrusion (p-longitudinal) was 5.93 ± 2.84 mm (5.98 ± 2.43 mm in males, 5.87 ± 3.32 mm in females, 6.28 ± 2.51 mm in the 18–38 age group, 5.53 ± 2.64 mm in the 39–58 age group, and 5.60 ± 2.30 mm in the 59 + age group). The average diameter of the papilla (p-transverse) was 6.88 ± 3.13 mm (7.30 ± 3.35 mm in males, 6.31 ± 2.74 mm in females, 7.08 ± 2.82 mm in the 18–38 age group, 7.00 ± 3.14 mm in the 39–58 age group, and 5.73 ± 2.64 mm in the 59 + age group). The average distance of the MDP from the pylorus [Table 4] was 90.32 ± 25.39 mm (91.89 ± 26.47 mm in males, 88.16 ± 23.86 mm in females, 93.53 ± 22.32 mm in the 18–38 age group, 90.96 ± 27.39 mm in the 39–58 age group, and 74.93 ± 22.31 mm in the 59+ age group). The statistical test revealed a statistically significant shorter distance to the pylorus among older individuals (59+ years) compared to middle-aged (39–58) and younger individuals (18–38) (*P* = 0.018). However, the dimensions of the papilla did not show a statistically significant difference between sexes [Table 4].

## Discussion

### Anatomical characteristics

The observed prevalence of the protruded papilla (69.29%) was lower than that observed in the Peruvians (79.2%), Canadians (82.8%), Portuguese (75.3%), Taiwanese (90.3%), Scandinavians (87%), and Indians (96%).[2,6,11,19-21] The lowest prevalence of the protruded papilla was observed among Americans (54%).[9,22] The prevalence of the flat papilla (19.3%) was similar to that of the Peruvians (20%), Romanians (18.9%), and Americans (22%).[9,20,22,23] Some studies did not report depressed papillae because their classifications did not include this normal variant, but instead categorized it as "distorted."[5,10] Nonetheless, there has been a recent call for modifying older classification systems or developing new ones that include the depressed papilla to increase uniformity in reporting.[24,25] The difference in papilla morphology amongst populations may be due to the significant discrepancy in the study sample sizes, or underlying population genetics, as hypothesized by Fukuda *et al*.,[4] the differing methodologies, and the myriad complexities of the classifications. Several of these complexities have been highlighted in the literature. For example, due to the variability in the appearance of the papilla, several systems, such as Haraldsson *et al*.'s classification,[5] don't comprehensively capture the full spectrum of papillary morphologies, subsequently leading to the development of more detailed classifications, such as the Vianna Classification,[2] which provides a more exhaustive morphological framework. However, it is

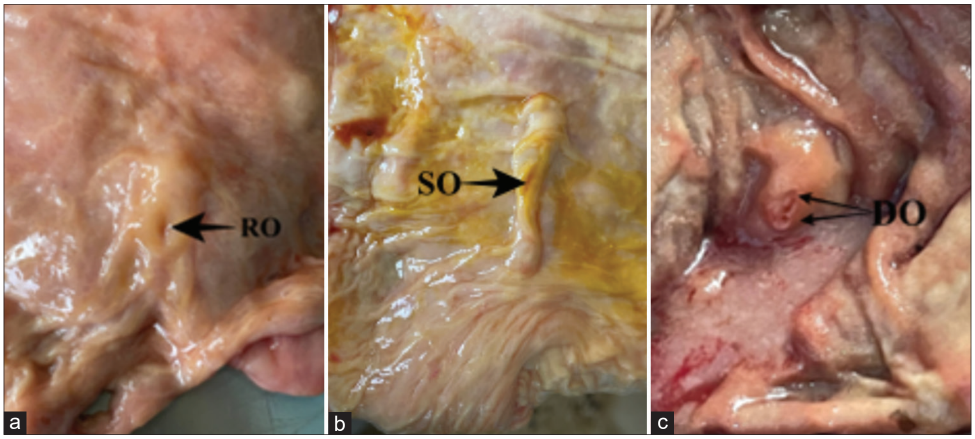


**Figure 4: Photomacrographs displaying the orifice types observed: Round orifice, slit orifice, and double orifices. The rounded orifice papilla (a) has an oblong to circular orifice. The slit-type orifice papilla (b) has an orifice that is longer than it is wide. The 2-holed orifice papilla (c) has 2 orifice openings. RO: Round Orifice, SO: Slit Orifice, DO: Double Orifice**

**Table 4: Papilla dimension comparisons between sex and age groups**

| Variable | Sex | *n* | Range | Mean±SD | *P* (differences between sexes) | Age groups (years) | Mean±SD (males) | Mean±SD (females) | Mean±SD (total) | *P* (differences between age groups) |
|---|---|---|---|---|---|---|---|---|---|---|
| Length of protruded papilla (*P*-longitudinal) (mm) | Male | 55 | 0.89–18.00 | 5.98±2.43 | 0.342 | 18–38 | 6.43±2.65 | 6.04±2.21 | 6.28±2.51 | 0.448 |
| | Female | 42 | | 5.87±3.32 | | 39–58 | 5.57±2.33 | 5.51±2.88 | 5.53±2.64 | |
| | | | | | | 59+ | 4.98±2.05 | 6.84±2.55 | 5.60±2.30 | |
| Transverse diameter of the papilla (*P*-transverse) (mm) | Male | 81 | 0.20–18.27 | 7.30±3.35 | 0.311 | 18–38 | 7.65±3.21 | 6.10±2.35 | 7.08±2.82 | 0.246 |
| | Female | 59 | | 6.31±2.74 | | 39–58 | 7.38±3.13 | 6.67±3.15 | 7.00±3.14 | |
| | | | | | | 59+ | 5.61±2.85 | 5.92±2.48 | 5.73±2.64 | |
| Distance from pylorus (mm) | Male | 81 | 33.50–167.90 | 91.89±26.47 | 0.388 | 18–38 | 94.62±24.10 | 91.65±20.55 | 93.53±22.32 | 0.018* |
| | Female | 59 | | 88.16±23.86 | | 39–58 | 94.61±28.45 | 87.76±26.32 | 90.96±27.39 | |
| | | | | | | 59+ | 74.54±20.87 | 75.55±23.75 | 74.93±22.31 | |

*Indicates statistical significance at $p < 0.05$. Independent sample *t*-test, significant $P<0.05$, One-way ANOVA, significant $P<0.05$. SD: Standard deviation

reportedly complex, particularly for novice endoscopists. Classifications like those used by Watanabe *et al*.[10] and Lopes *et al*.,[26] though easier to understand, lack inter- and intraobserver validation, which may limit their reproducibility.

On average, in the present study, males presented with the depressed papilla category more than females. Age does not seem to be associated with the appearance of the papilla (Fisher's Exact Test $\chi^2 = 2.676$, $P = 0.654$, df = 4). This differs from findings reported by Haraldsson *et al*.,[21] where the protruded papilla was more prevalent in younger individuals. The regular protrusion level was most common (80%), showing similarity to the 77.9% reported by Watanabe *et al*.[10] in the Japanese population. The large protrusion papilla (Protrusion L) observed in 3.1% of the current study's population contrasts with the 10.4% reported in the Japanese population by Watanabe *et al*.[10]

In approximately 1 in every 100 people, the papilla is located at the junction of the first and second parts of the duodenum, with a predominance of this abnormality observed in females. In 11.5%, the MDP was at the junction between the second and third parts of the duodenum. This is similar to findings by Berry *et al*.,[14] who reported 15% and Keddie *et al*.,[27] who reported 11% of papilla being located at the junction between the second and third parts of the duodenum in their studies. No papilla was found on the third part of the duodenum despite this position being described in previous literature.[27,28] The diversity observed in the measurements and location of the papilla may be due to genetic and environmental differences associated with ethnicity and region, or congenital abnormalities.[4,29,30]

### Morphometric dimensions of the major duodenal papilla

The mean distance of the MDP from the pylorus from the current study was similar to that reported by Khalil *et al*.,[31] who recorded a mean distance of 9.8 cm. The mean distance in the present study was considerably larger than that obtained in the Argentinian and South Indian populations.[19,30] The significantly shorter mean distance of MDP from pylorus ($P$ = 0.018) seen in the older age group (59+ years) compared to young individuals (18–38 years) and Middle-aged individuals (39–57 years) was an interesting finding, as to the best of our knowledge, our study is the first study to describe this finding. Further investigations should determine the exact mechanism that leads to this apparent decrease in the distance of the MDP from the pylorus in older individuals because it could influence the ease and success of canulation for individuals in this age group.

The mean transverse diameter of the papilla (6.88 mm) was similar to that of the Indian population (7.2 mm) by Sulochana *et al*.[19] and 6.8 mm in the Americans by Sterling.[9] This differed from the findings of Komorowski[32] and Avisse *et al*.,[33] with average diameters of about 5 mm. The protrusion length of 6 mm for the elevated papillae falls in the 5–10 mm range described by Avisse *et al*.[33] The values in the study were greater than those stated by Sulochana *et al*.[19] for the Indian population of 3.0 mm. The values are in agreement with those of endoscopic findings of the protruded papilla's length, generally averaging at about 4 mm.[34] The values are <12 mm presented by Komorowski[32] and 14 mm by Sterling.[9] There were no extreme values of >3 cm for papilla dimensions as presented by Poppel and Jacobson.[35]

This study has some limitations: The population was specifically from Kenya, offering valuable population-specific anatomical data in this demographic, but may limit the external validity of the results, as the anatomy of the MDP may differ across ethnic and geographic populations; therefore, our findings may not be directly generalizable to Non Kenyan. Future multicenter studies incorporating participants from different counties and regions would improve population representativeness and reduce potential bias. Secondly, as much as a key strength of our study is the use of postmortem specimens instead of cadaveric specimens, which avoids the inaccuracies associated with tissue fixation and foreshortening, postmortem changes may still introduce a degree of measurement imprecision; however, these changes are likely to result in minor underestimation of morphometric measurements rather than systematic overestimation. The magnitude of this bias is expected to be small but should be acknowledged. Future studies should consider using imaging techniques such as ERCP on live patients which would yield more real-time, accurate results and would corroborate our findings and provide valuable insights into the practical implications of variant MDP anatomy in a clinical setting.

## Conclusion

Since the anatomic location, morphology, and morphometry of the MDP showed inter-individual and interpopulation variation, we recommend that endoscopists operating in the region of the MDP thoroughly investigate the papilla and use its morphology as a guide for the technique of canulation.

**Financial support and sponsorship**

Nil.

**Conflicts of interest**

There are no conflicts of interest.

## References

1. Horiguchi S, Kamisawa T. Major duodenal papilla and its normal anatomy. Dig Surg 2010;27:90-3.
2. Canena J, Lopes L, Fernandes J, Costa P, Arvanitakis M, Koch AD, *et al.* Influence of a novel classification of the papilla of Vater on the outcome of needle-knife fistulotomy for biliary cannulation. BMC Gastroenterol 2021;21:147.
3. Dusunceli Atman E, Erden A, Ustuner E, Uzun C, Bektas M. MRI findings of intrinsic and extrinsic duodenal abnormalities and variations. Korean J Radiol 2015;16:1240-52.
4. Fukuda A, Kawaguchi Y, Furuyama K, Kodama S, Kuhara T, Horiguchi M, *et al.* Loss of the major duodenal papilla results in brown pigment biliary stone formation in pdx1 null mice. Gastroenterology 2006;130:855-67.
5. Haraldsson E, Lundell L, Swahn F, Enochsson L, Löhr JM, Arnelo U, *et al.* Endoscopic classification of the papilla of Vater. Results of an inter- and intraobserver agreement study. United European Gastroenterol J 2017;5:504-10.
6. Mohamed R, Lethebe BC, Gonzalez-Moreno E, Kayal A, Bass S, Cole M, *et al.* Morphology of the major papilla predicts ERCP procedural outcomes and adverse events. Surg Endosc 2021;35:6455-65.
7. Wood M. Anomalous location of the papilla of Vater. Am J Surg 1966;111:265-8.
8. Lee TH, Bang BW, Park SH, Jeong S, Lee DH, Kim SJ. Precut fistulotomy for difficult biliary cannulation: Is it a risky preference in relation to the experience of an endoscopist? Dig Dis Sci 2011;56:1896-903.
9. Sterling JA. Significant facts concerning the papilla of Vater. Am J Dig Dis 1953;20:124-6.
10. Watanabe M, Okuwaki K, Kida M, Imaizumi H, Yamauchi H, Kaneko T, *et al.* Transpapillary biliary cannulation is difficult in cases with large oral protrusion of the duodenal papilla. Dig Dis Sci 2019;64:2291-9.
11. Chen PH, Tung CF, Peng YC, Yeh HZ, Chang CS, Chen CC. Duodenal major papilla morphology can affect biliary cannulation and complications during ERCP, an observational study. BMC Gastroenterol 2020;20:310.
12. Katsinelos P, Gkagkalis S, Chatzimavroudis G, Beltsis A, Terzoudis S, Zavos C, *et al.* Comparison of three types of precut technique to achieve common bile duct cannulation: A retrospective analysis of 274 cases. Dig Dis Sci 2012;57:3286-92.
13. Miyaguchi K, Mizuide M, Tanisaka Y, Fujita A, Jinushi R, Hiromune K, *et al.* Distinguishing the papilla of Vater during biliary cannulation using texture and color enhancement imaging: A pilot study. DEN Open 2023;3:e125.

14. Berry R, Han JY, Tabibian JH. Difficult biliary cannulation: Historical perspective, practical updates, and guide for the endoscopist. World J Gastrointest Endosc 2019;11:5-21.
15. Matsushita M, Uchida K, Nishio A, Takakuwa H, Okazaki K. Small papilla: Another risk factor for post-sphincterotomy perforation. Endoscopy 2008;40:875-6.
16. Testoni PA, Testoni S, Giussani A. Difficult biliary cannulation during ERCP: How to facilitate biliary access and minimize the risk of post-ERCP pancreatitis. Dig Liver Dis 2011;43:596-603.
17. Phillip J, Koch H, Classen M. Variations and anomalies of the papilla of vater, the pancreas and the biliary duct system. Endoscopy 1976;6:70-7.
18. Jung SH. Stratified fisher's exact test and its sample size calculation. Biom J 2014;56:129-40.
19. Sulochana S, Sasikala P, Sivakami T. Gross morphology of major and minor duodenal papilla: A cadaveric study. Natl J Clin Anat 2013;2:61.
20. Estela EL, Tovar NR, Maldonado FA, Tisoc LM, Goicochea-Lugo S, Rossell MC. Association between type of major duodenal papilla and difficult biliary cannulation at first ERCP in adults: A cross-sectional study with bootstrap method. Ann Gastroenterol 2023;36:216-22.
21. Haraldsson E, Kylänpää L, Grönroos J, Saarela A, Toth E, Qvigstad G, *et al.* Macroscopic appearance of the major duodenal papilla influences bile duct cannulation: A prospective multicenter study by the Scandinavian association for digestive endoscopy study group for ERCP. Gastrointest Endosc 2019;90:957-63.
22. Sterling JA. The Biliary Tract With Special Reference to the Common Bile Duct. Baltimore: Williams & Wilkins; 1955.
23. Balan GG, Arya M, Catinean A, Sandru V, Moscalu M, Constantinescu G, *et al.* Anatomy of major duodenal papilla influences ERCP outcomes and complication rates: A single center prospective study. J Clin Med 2020;9:1637.
24. Adler DG. Response. Gastrointest Endosc 2020;91:960-1.
25. Adler DG. ERCP biliary cannulation difficulty as a function of papillary subtypes: A tale of shapes and Shar-Pei dogs. Gastrointest Endosc 2019;90:964-5.
26. Lopes L, Canena J, Fernandes J, Moreira M, Costa I, Gomes-Fonseca J, *et al.* Should we use papilla morphology to estimate the size of the terminal common bile duct during endoscopic retrograde cholangiopancreatography? Eur J Gastroenterol Hepatol 2020;32:181-6.
27. Keddie NC, Taylor AW, Sykes PA. The termination of the common bile duct. Br J Surg 1974;61:623-5.
28. Schwartz A, Birnbaum D. Roentgenologic study of the topography of the choledocho-duodenal junction. Am J Roentgenol Radium Ther Nucl Med 1962;87:772-6.
29. Paraskevas G, Papaziogas B, Natsis K, Katsinelos P, Gigis P, Atmatzidis K. Abnormal location of papilla of Vater: A cadaveric study. Folia Morphol (Warsz) 2005;64:51-3.
30. Pina L, Abramson L, Samoilovich FS, Rodriguez A, Knaus DC, Tartaglia ML, *et al.* The pancreatic ductal system and biliopancreatic union: A study of 50 cases. Eur J Anat 2013;17:193-201.
31. Khalil MM, Islam MN, Khalil MM, Khan ZI, Adiluzzaman AA, Hossain MI. Topography and morphometry of the common bile duct and major duodenal papilla of man and principal domesticated animals. Mymensingh Med J 2005;14:6-12.
32. Komorowski RA. Anatomy and histopathology of the human sphincter of Oddi. Gastrointest Endosc Clin N Am 1993;3:1-11.
33. Avisse C, Flament JB, Delattre JF. Ampulla of Vater. Anatomic, embryologic, and surgical aspects. Surg Clin North Am 2000;80:201-12.
34. Zhang QS, Xu JH, Dong ZQ, Gao P, Shen YC. Success and safety of needle knife papillotomy and fistulotomy based on papillary anatomy: A prospective controlled trial. Dig Dis Sci 2022;67:1901-9.
35. Poppel MH, Jacobson HG. Roentgen aspects of the papilla of Vater. Am J Dig Dis 1956;1:49-58.

Original Article

# Bicuspid Aortic Valve in Adult Patients: Accompanying Cardiovascular Pathology and Variations

**Yeliz Akturk, Irfan Durmus[1], Rasime Pelin Kavak, Meltem Ozdemir**

*Department of Radiology, Etlik City Hospital, Ankara, [1]Department of Radiology, Gumushane State Hospital, Gumushane, Turkey*

## Abstract

**Introduction:** This study aimed to investigate the prevalence of aortic valve calcification, aortic dilatation, and coronary artery disease (CAD) in patients with bicuspid aortic valve (BAV) identified incidentally through coronary computed tomography angiography (CCTA) and to compare epicardial adipose tissue (EAT) thickness between BAV and tricuspid aortic valve (TAV) patients. **Materials and Methods:** Thirty-five BAV patients aged 42–67 and 75 TAV patients aged 31–66 were included in the study. Aortic diameters were measured at the sinus of Valsalva, sinotubular junction, and ascending and descending aorta. Agatston calcium scores and CAD–Reporting and Data System were used to assess coronary artery calcification and atherosclerosis severity. EAT thickness was measured volumetrically, and its relationship with clinical and imaging parameters was evaluated. **Results:** In patients with BAV, the aortic diameters at the Valsalva sinus, sinotubular junction, and ascending aorta were larger compared to patients with TAV. The difference was statistically significant ($P < 0.001$). Aortic valve calcification was present in 45.7% of BAV patients, with an average Agatston score of 349.06 ± 413.22, while no calcification was detected in TAV patients. Although no significant difference in EAT thickness or CAD prevalence was observed between BAV and TAV groups, EAT thickness was positively correlated with aortic dilatation, coronary artery calcification, and aortic valve calcification. **Conclusions:** BAV patients exhibit distinct vascular and valvular characteristics, with aortic dilatation and aortic valve calcification being prominent. EAT may serve as a marker for these complications. Further prospective studies are needed to elucidate the pathophysiology of BAV and optimize early intervention strategies.

**Keywords:** *Bicuspid aortic valve, coronary artery, coronary artery disease, computed tomography angiography, epicardial adipose tissue*

## Introduction

Bicuspid aortic valve (BAV) is the most prevalent congenital cardiac anomaly, with a reported prevalence of 0.8%–1.5% in the general population.[1,2] Its pathogenesis is attributed to defects arising during early embryonic development.[1] Individuals with BAV are predisposed to valvular pathologies, such as thoracic aortopathy and aortic stenosis (AS), supporting the classification of BAV as a valvuloaortopathy.[3] Notably, both valvular dysfunction and aortic abnormalities demonstrate significant interindividual variability in terms of associated complications and clinical outcomes.[2]

AS and coronary artery disease (CAD) are complex conditions that share overlapping pathophysiological mechanisms and common cardiovascular risk factors, including hypertension, hypercholesterolemia, smoking, advanced age, and male sex.[4,5] Although patients with BAV have a higher risk of AS, several studies have shown that the prevalence of CAD is significantly lower compared to individuals with tricuspid aortic valve (TAV).[6,7] Furthermore, some reports suggest that patients with BAV have reduced calcification and fewer atherosclerotic plaques in their thoracic aortas, hypothesizing that they may have a lower burden of atherosclerotic disease compared to individuals with TAV.[4] However, the literature remains inconclusive, as other studies have suggested an elevated risk of atherosclerosis in BAV patients.[8]

Aortic dilatation is among the most common complications in individuals over 60 years of age with BAV. However, the pattern of aortic dilatation observed in BAV patients, along with its molecular and clinical characteristics, exhibits significant heterogeneity.[9] Previous studies have

**Article Info**

**Received:** 05 June 2025
**Revised:** 05 February 2026
**Accepted:** 09 February 2026
**Available online:** 27 March 2026

***Address for correspondence:***
*Dr. Yeliz Akturk, Department of Radiology, Etlik City Hospital, Halil Sezai Erkut Street, Etlik, Ankara 06170, Turkey.*
*E-mail: yelizakturk@yahoo.com*

**Access this article online**

**Website:** https://journals.lww.com/joai

**DOI:** 10.4103/jasi.jasi_99_25

**Quick Response Code:**



**How to cite this article:** Akturk Y, Durmus I, Kavak RP, Ozdemir M. Bicuspid aortic valve in adult patients: Accompanying cardiovascular pathology and variations. J Anat Soc India 2026;75:33-40.

highlighted the role of defective vascular smooth muscle cell differentiation and alterations in extracellular matrix composition in the pathogenesis of aortopathy associated with BAV.[10] The precise etiology underlying thoracic aortic wall pathology in BAV remains elusive. Most investigations suggest a distinct mechanism for aneurysm formation in BAV patients, one that diverges from the atherosclerotic processes commonly observed in individuals with TAV and involves minimal or no atherosclerotic involvement.[11]

Epicardial adipose tissue (EAT), located between the myocardium and the visceral pericardium, is a type of adipose tissue known to secrete bioactive molecules referred to as adipokines that exert various exocrine and paracrine effects.[12] Recent studies suggest that, due to its proximity to coronary arteries, EAT may contribute to the progression of coronary atherosclerosis, although the exact underlying mechanisms remain incompletely understood. An association between EAT thickness and valvular heart disease has also been identified. Notably, increased EAT thickness has been observed in patients with calcific AS.[13] Moreover, studies have proposed that elevated EAT, through local or systemic effects, acts as an independent risk factor for ascending aortic dilatation in hypertensive patients.[14] However, all of these studies have focused exclusively on TAV cases. To date, no studies have investigated the relationship between EAT thickness and BAV.

This study aims to investigate the presence of aortic valve calcification, aortic dilatation, and coexisting CAD in adult patients with incidentally detected BAV during coronary computed tomography angiography (CCTA) performed for chest pain evaluation. In addition, it seeks to compare EAT thickness in BAV patients with that of the TAV population.

## Materials and Methods

### Study population

Following the acquisition of necessary ethical approvals, radiological images of patients aged 18 years and older who underwent CCTA in our clinic between May 2023 and June 2024 were retrospectively reviewed. Patients diagnosed with BAV were included in the study. Those under the age of 18 and patients whose CCTA studies were inadequate for evaluation (e.g., inappropriate imaging phase and motion artifacts) were excluded. A control group was formed from patients with TAV who had similar demographic characteristics.

For all included patients, body mass index (BMI) was calculated. The presence of diabetes mellitus (DM), hypertension (HT), hypercholesterolemia, and smoking history were recorded.

### Evaluation of computed tomography angiography images

All CCTA scans were acquired using either a dual-energy 128-slice CT scanner (GE Revolution Frontier, Milwaukee, USA) or a 1024-slice (512 × 2) CT scanner (GE Revolution Apex Pxtream, Milwaukee, USA). Scans were performed with electrocardiogram (ECG)-gating. Initially, a noncontrast scan was conducted to assess calcified plaques, followed by intravenous administration of a nonionic contrast agent at a rate of 5 mL/s through an automatic injector, using the bolus tracking method. Depending on the patient's baseline heart rate (BPM), prospective ECG-gated scanning was used for patients with a BPM ≤80, while retrospective ECG-gated scanning was employed for those with a BPM >80.

All CCTA images included in the study were retrospectively reviewed by two radiologists, one of whom was experienced in cardiothoracic imaging, using multiplanar and curved planar reconstructions on a dedicated workstation (AWS 4.6, GE, Milwaukee, USA). The aortic diameters were measured in millimeters at the levels of the sinus of Valsalva, sinotubular junction, ascending aorta, and descending aorta. The diameter of the sinus of Valsalva and the sinotubular junction was measured at its widest point using coronal reformatted imaging. The diameter of the ascending aorta was measured from axial sections passing through the pulmonary trunk level, and the diameter of the descending aorta was measured from axial sections passing through the T6 vertebral plane.

The presence of vascular anomalies in the coronary arteries (including anomalies in origin and course) and CAD was evaluated. For patients with detected CAD, calcified plaques were quantified using the Agatston total calcium score. Both calcified and noncalcified plaques were assessed for the degree of atherosclerotic stenosis and scored using the CAD–Reporting and Data System (CAD-RADS). Atherosclerotic wall calcifications in the ascending and descending aorta were also documented. In cases where aortic valve calcification was observed, the extent of calcification was quantitatively measured using the Agatston scoring method. EAT thickness was measured on noncontrast ECG-gated axial cardiac CTA images with a slice thickness of 2.5 mm. Manual delineation of EAT was performed on each slice using a threshold range of − 195 to − 45 Hounsfield Units. The total EAT volume was calculated in cubic millimeters ($mm^3$) as a volumetric measurement.

### Statistical analysis

Descriptive statistics for continuous variables were presented as mean ± standard deviation, median, and interquartile range, whereas categorical variables were summarized as frequencies and percentages. The Shapiro–Wilk test was used to assess the normality of distribution for continuous variables. Comparisons between BAV and TAV groups were performed using the independent samples *t*-test for normally distributed continuous variables and the Mann–Whitney *U*-test for nonnormally distributed continuous variables. For categorical variables, the Chi-square test was applied in cross-tabulations. The relationships between EAT values and continuous variables were analyzed using Spearman's correlation coefficient. Multivariate linear regression analysis was conducted to identify factors influencing EAT values. All statistical analyses were performed using IBM SPSS for Windows, version 20.0 (SPSS Inc., Chicago, IL, USA), with a significance threshold set at $P < 0.05$.

## Results

Thirty-five BAV patients aged between 42 and 67 (mean age 52), 17 of whom were women (48.5%), and 75 TAV patients aged between 31 and 66 (mean age 54), 30 of whom were women (40%), were included in the study. While 2 (5.7%) of the BAV cases were two-sinus BAV subtype, the other BAV cases (94.3%) were right–left (R-L) fusion subtype [Figure 1].

There were no statistically significant differences between the BAV and TAV groups in terms of age, BMI, gender distribution, prevalence of DM, HT, or smoking history ($P > 0.05$). However, the prevalence of hyperlipidemia was significantly higher in the BAV group compared to the TAV group ($P < 0.01$). No significant differences were observed between the BAV and TAV groups regarding the presence of atherosclerotic wall calcifications in the ascending and descending aorta, Agatston scores derived from coronary arteries, CAD-RADS values, or the prevalence of coronary artery anomalies ($P > 0.05$). Aortic diameters measured at the levels of the coronary sinus of Valsalva, sinotubular junction, and ascending aorta were significantly larger in BAV patients compared to TAV patients ($P < 0.001$). However, no significant difference was found in descending aortic diameter between the two groups ($P > 0.05$). Aortic valve calcification was present in 16 (45.7%) BAV patients. The mean Agatston calcium score for the aortic valve was 349.06 ± 413.22. No valve calcification was detected in the control group. A comparative evaluation of BAV and TAV patients is provided in Table 1.

No statistically significant difference was found in EAT thickness between BAV and TAV patients ($P > 0.05$). Consequently, statistical analyses were conducted by pooling BAV and TAV patients to identify factors influencing EAT. A positive correlation was observed between patient age and EAT thickness (r = 0.331, $P < 0.001$). In addition, EAT thickness positively correlated with aortic diameter and CAD-RADS scores in coronary arteries. Correlations between EAT thickness and other clinical parameters are summarized in Table 2. From a clinical perspective, patients with DM, HT, and hyperlipidemia had significantly higher EAT thickness compared to those without these conditions ($P < 0.01$). Furthermore, patients with coronary artery Agatston scores >0 and those with aortic valve calcification exhibited significantly higher EAT thickness ($P < 0.001$ and $P < 0.05$, respectively). No significant differences in EAT thickness were noted based on sex, smoking status, or the presence of coronary artery anomalies in origin and course ($P > 0.05$). A comparison of EAT thickness across patient characteristics is detailed in Table 3. In the univariate analysis, variables that showed significant associations with EAT thickness – DM, HT, hyperlipidemia, aortic valve calcification, coronary artery Agatston score, age, aortic diameter, and CAD-RADS – were included in a multivariate linear regression model. Using the stepwise method, the final model identified DM, CAD-RADS, and descending aortic diameter as independent predictors of EAT thickness ($R^2 = 0.349$, $F = 18.941$, $P < 0.001$). DM was associated with an increase in EAT thickness by 20.171 $mm^3$ ($P < 0.05$), while a one-point increase in CAD-RADS resulted in an 18.105 $mm^3$ increase in EAT thickness ($P < 0.001$). In addition, a 1-mm increase in descending aortic diameter was linked to a 2.598 $mm^3$ rise in EAT thickness ($P < 0.05$) [Table 4].

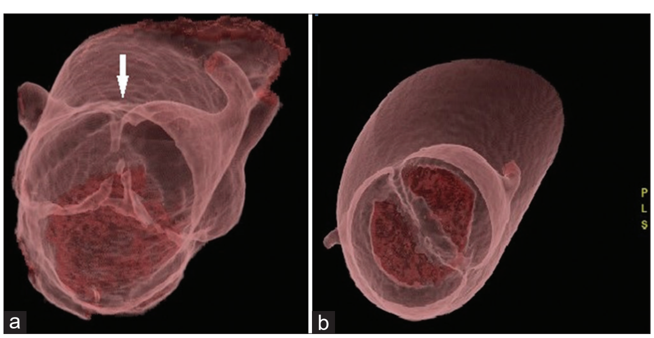

**Figure 1: Reformat images of bicuspid aortic valve cases. Right–left (R-L) fusion subtype with raphe (white arrow) (a); two-sinus subtype (b)**

Findings by gender in BAV cases are summarized in Table 5.

## Discussion

Aortopathy associated with BAV is a complex clinical condition that requires thorough radiological evaluation. Key aspects include measuring aortic diameters, assessing the progression rate of aortic dilatation, and evaluating valve function. Comprehensive patient management necessitates consideration of individual patient characteristics, familial predisposition, and genetic history. This underscores the need for a multidisciplinary approach.[15]

According to the 2020 ACC/AHA guidelines for the management of valvular heart diseases, transthoracic echocardiography (TTE) is the first-line imaging modality for diagnosing BAV and assessing aortic valve anatomy, with an accuracy rate of 80%–90% in most cases.[2,16] The primary objectives of TTE include evaluating valve phenotype and function, measuring thoracic aortic diameters, assessing for other aortic malformations, and ruling out potential complications such as infective endocarditis and aortic dissection.[2] However, TTE has certain limitations, including poor acoustic windows, heavy

**Table 1: Comparisons of patients with bicuspid aortic valve and tricuspid aortic valve**

| | BAV, *n* (%) | TAV, *n* (%) | *P* |
|---|---|---|---|
| Age (mean±SD) | 48.97±10.56 | 49.64±8.06 | 0.716[b] |
| BMI (kg/m$^2$), mean±SD | 29.83±3.65 | 30.73±4.82 | 0.386[b] |
| Gender | | | |
| Female | 14 (40.0) | 32 (42.7) | 0.792[c] |
| Male | 21 (60.0) | 43 (57.3) | |
| DM | | | |
| None | 22 (62.9) | 53 (70.7) | 0.413[c] |
| Yes | 13 (37.1) | 22 (29.3) | |
| HT | | | |
| None | 17 (48.6) | 49 (65.3) | 0.095[c] |
| Yes | 18 (51.4) | 26 (34.7) | |
| Hypercholesterolemia (%) | | | |
| None | 16 (45.7) | 54 (72.0) | 0.008[c] |
| Yes | 19 (54.3) | 21 (28.0) | |
| Current smoking | | | |
| None | 19 (54.3) | 41 (54.7) | 0.970[c] |
| Yes | 16 (45.7) | 34 (45.3) | |
| Atherosclerotic wall calcifications in the aorta | | | |
| None | 30 (85.7) | 64 (85.3) | 0.958[c] |
| Yes | 5 (14.3) | 11 (14.7) | |
| Agatston score of the coronary artery | | | |
| None | 22 (62.9) | 46 (61.3) | 0.878[c] |
| Yes | 13 (37.1) | 29 (38.7) | |
| EAT | | | |
| Mean±SD | 120.14±41.02 | 111.80±47.92 | 0.305[d] |
| Median (minimum–maximum) | 108.55 (46.44–204.98) | 106.98 (43.70–261.53) | |
| Aortic diameter at the level of the coronary sinus (mm) | | | |
| Mean±SD | 37.97±4.63 | 33.85±4.05 | <0.001[d] |
| Median (minimum–maximum) | 39 (26–46) | 34 (21–43) | |
| Sinotubular junction diameter (mm) | | | |
| Mean±SD | 30.83±4.85 | 26.12±3.34 | <0.001[d] |
| Median (minimum–maximum) | 32 (21–41) | 25 (18–37) | |
| Ascending aorta diameter (mm) | | | |
| Mean±SD | 39.77±4.90 | 34.63±5.27 | <0.001[d] |
| Median (minimum–maximum) | 40 (27–47) | 34 (25–45) | |
| Descending aorta diameter (mm) | | | |
| Mean±SD | 24.63±2.40 | 24.61±3.29 | 0.618[d] |
| Median (minimum–maximum) | 24 (18–30) | 25 (18–33) | |
| CAD-RADS | | | |
| Mean±SD | 1.49±1.09 | 1.17±1.09 | 0.159[d] |
| Median (minimum–maximum) | 1 (0–4) | 1 (0–4) | |
| Aortic valve calsification (*n*=16) | | | |
| Mean±SD | 349.06±413.22 | - | |
| Median (minimum–maximum) | 143 (2–1234) | - | |
| Coronary artery anomalies | | | |
| None | 28 (80.0) | 58 (77.3) | 0.752[c] |
| Yes | 7 (20.0) | 17 (22.7) | |

[b]Independent samples *t*-test, [c]Chi-square test, [d]Mann–Whitney *U*-test. SD: Standard deviation, BAV: Bicuspid aortic valve, TAV: Tricuspid aortic valve, EAT: Epicardial adipose tissue, CAD-RADS: Coronary artery disease reporting and data system, BMI: Body mass index, DM: Diabetes mellitus, HT: Hypertension

valve calcifications, small cusps, difficulty in assessing the distal ascending aorta, and its operator-dependent nature.[17,18] Valve calcification can result in shadowing and artifacts in echocardiographic images, complicating the evaluation of valve morphology and the determination of stenosis severity.[15] Despite these challenges, TTE offers advantages such as the absence of ionizing radiation and the lack of need for intravenous contrast agents. TEE is also useful for detecting BAV, although it is semi-invasive and has limitations in visualizing the upper ascending aorta and proximal arch.[2] Several studies have demonstrated that ECG-gated CCTA provides high specificity and sensitivity in distinguishing BAV from TAV.[15,16,18] Additionally, CCTA allows for the quantitative assessment of aortic valve calcification using the Agatston scoring method.[19] The use of multimodality imaging is crucial for the comprehensive management of this congenital condition, particularly in evaluating the need for surgical intervention and in postoperative follow-up.[2]

**Table 2: Correlations between epicardial adipose tissue thickness and other clinical parameters**

| | EAT | |
|---|---|---|
| | ***r**** | ***P*** |
| Age | 0.331 | <0.001 |
| BMI (kg/m$^2$) | 0.110 | 0.254 |
| Aortic diameter at the level of the sinus of Valsalva diameter (mm) | 0.237 | 0.013 |
| Sinotubular junction diameter (mm) | 0.282 | 0.003 |
| Ascending aorta diameter (mm) | 0.372 | <0.001 |
| Descending aorta diameter (mm) | 0.320 | <0.001 |
| CAD-RADS | 0.484 | <0.001 |

*Spearman's correlation coefficient. CAD-RADS: Coronary artery disease reporting and data system, EAT: Epicardial adipose tissue, BMI: Body mass index

BAV is a heterogeneous congenital heart anomaly with two primary morphological subtypes. These include the fused BAV, characterized by the presence of three aortic sinuses with dissimilar cusps, and the two-sinus BAV, which features relatively symmetrical cusps and two aortic sinuses.[15] The fused type is the most common, accounting for 90%–95% of cases. This subtype typically displays a congenital fibrous ridge, known as a "raphe," between the fused cusps.[20] The most prevalent BAV phenotype is the right–left (R-L) fusion, observed in approximately 75% of cases. This is followed by the right–noncoronary (R-N) fusion, present in 20%–25% of cases, and the left–noncoronary (L-N) fusion, which occurs in <3% of cases. The two-sinus BAV subtype is rare, comprising about 5%–7% of cases.[2] In our study, the R-L fusion phenotype was also the most frequently observed BAV subtype.

Although aortic dissection or rupture is rare, aortic dilatation has been reported in 20%–40% of patients with BAV.[16] Studies have demonstrated that the intimal layer in adult BAV patients is significantly thinner than in those with TAV. Unlike in TAV, the maturation of the vascular wall in BAV occurs prenatally. Postnatally, the intimal layer of the aorta in BAV patients exhibits minimal thickening, which impairs the vessel's ability to respond to

**Table 3: Comparison of epicardial fat tissue thickness with patient characteristics**

| | ***n*** | EAT | | ***P*** |
|---|---|---|---|---|
| | | **Mean±SD** | **Median (minimum–maximum)** | |
| Gender | | | | |
| Female | 46 | 114.86±52.57 | 102.66 (43.70–261.53) | 0.557[d] |
| Male | 64 | 114.16±40.71 | 112.22 (46.01–204.98) | |
| DM | | | | |
| None | 75 | 104.39±42.57 | 101.23 (43.70–261.53) | 0.001[d] |
| Yes | 35 | 136.01±45.63 | 125.25 (49.51–228.09) | |
| HT | | | | |
| None | 66 | 107.43±47.04 | 100.43 (43.70–261.53) | 0.033[d] |
| Yes | 44 | 124.99±42.26 | 112.72 (60.24–228.09) | |
| Hypercholesterolemia (%) | | | | |
| None | 70 | 107.65±45.24 | 102.09 (43.70–261.53) | 0.029[d] |
| Yes | 40 | 126.36±44.91 | 113.44 (46.44–228.09) | |
| Current smoking | | | | |
| None | 60 | 113.56±40.76 | 110.13 (43.70–228.09) | 0.859[d] |
| Yes | 50 | 115.53±51.64 | 107.76 (46.21–261.53) | |
| Aortic valve classification | | | | |
| None | 94 | 109.20±41.10 | 107.61 (43.70–204.98) | 0.037[d] |
| Yes | 16 | 145.33±59.90 | 124.02 (69.04–261.53) | |
| Agatston score of the coronary artery | | | | |
| None | 68 | 100.72±39.46 | 97.87 (43.70–200.82) | <0.001[d] |
| Yes | 42 | 136.69±47.08 | 124.24 (66.33–261.53) | |
| Coronary artery anomalies | | | | |
| None | 86 | 118.35±46.34 | 109.77 (46.01–261.53) | 0.138[d] |
| Yes | 24 | 100.49±41.83 | 101.60 (43.70–195.54) | |

[d]Mann–Whitney *U*-test. DM: Diabetes mellitus, HT: Hypertension, SD: Standard deviation, EAT: Epicardial adipose tissue

potential vascular injury. In BAV, vascular smooth muscle cells fail to differentiate properly, leading to increased extracellular matrix degeneration under hypoxic conditions. This contributes to the weakening of the ascending aortic wall and elevates the risk of aortopathy.[21] Furthermore, the medial layer in BAV patients is found to be significantly thicker than that in TAV patients, despite a similar number of lamellae. Increased spacing between lamellae facilitates the accumulation of mucoid extracellular matrix, which plays a crucial role in the pathogenesis of aortic dilatation.[21-23] Our findings align with these observations, as aortic diameters at the levels of the sinuses of Valsalva, sinotubular junction, and ascending aorta were significantly greater in the BAV group compared to the TAV group, corroborating the existing literature.

AS typically appears after age 70 in TAV patients but develops earlier (under 65) in those with BAV.[5,24] Key contributing factors include lipid buildup, inflammation, and calcification.[5] Age-related cardiovascular changes, mechanical stress, and valve calcification drive this process.[1] Shared risk factors for CAD and AS include age, smoking, HT, and dyslipidemia.[5] This multifactorial process, recognized as atherosclerotic, also underlies CAD.[1] However, the link between BAV and CAD remains unclear. In BAV patients, AS may result more from hemodynamic alterations due to valve morphology than from classic CAD risk factors.[5] These flow disturbances increase mechanical stress on the valve and ascending aorta. Still, current findings are inconsistent, warranting further study.[25] In our study, 45.7% of BAV patients had aortic valve calcification, while none was observed in the TAV group. However, CAD prevalence did not differ significantly between groups.

In a study assessing the coronary artery atherosclerotic burden in BAV patients with AS requiring aortic valve replacement, coronary artery calcium scores were significantly lower in BAV patients compared to TAV patients.[11] This finding is inconsistent with our results. Nevertheless, the incidence of atherosclerosis in BAV individuals, the underlying molecular pathophysiology, and the prognostic significance of BAV-associated atherosclerosis remain unclear. Furthermore, some data in the literature on this topic remain controversial.[24]

CCTA, unlike echocardiography and cardiac magnetic resonance, enables precise measurement of EAT thickness while simultaneously evaluating coronary arteries. Under normal conditions, EAT functions as a protective layer, shielding coronary arteries from arterial pulse waves and cardiac contractions. In addition, it provides an immunological barrier by surrounding underlying cardiac structures, thus offering protection against pathogens.[12] However, EAT is also known to play a

**Table 4: Multivariate linear regression analysis**

| Parameters | *B* | SE | 95% CI | *P* |
|---|---|---|---|---|
| DM | 20.171 | 7.893 | 4.523–35.819 | 0.012 |
| CAD-RADS | 18.105 | 3.439 | 11.287–24.923 | <0.001 |
| Descending aorta diameter | 2.598 | 1.239 | 0.141–5.054 | 0.038 |

CAD-RADS: Coronary artery disease reporting and data system, CI: Confidence ınterval, SE: Standard error, DM: Diabetes mellitus

**Table 5: Gender-based findings in bicuspid aortic valve cases**

| | Male (*n*=21) | Female (*n*=14) | *P* |
|---|---|---|---|
| Atherosclerotic wall calcifications in the aorta, *n* (%) | | | |
| None | 19 (90.5) | 11 (78.6) | 0.366 |
| Yes | 2 (9.5) | 3 (21.4) | |
| EAT | | | |
| Mean±SD | 116.72±40.32 | 125.29±43.04 | 0.49 |
| Median (minimum–maximum) | 108.55 (46.44–204.98) | 109.80 (73.25–201.24) | |
| Aortic diameter at the level of the coronary sinus (mm) | | | |
| Mean±SD | 39.71±3.41 | 35.36±5.11 | 0.011 |
| Median (minimum–maximum) | 40.0 (33–46) | 37.0 (26–42) | |
| Sinotubular junction diameter (mm) | | | |
| Mean±SD | 31.67±4.76 | 29.57±4.89 | 0.294 |
| Median (minimum–maximum) | 32.0 (21–41) | 31.0 (22–36) | |
| Ascending aorta diameter (mm) | | | |
| Mean±SD | 40.19±5.67 | 39.14±4.13 | 0.34 |
| Median (minimum–maximum) | 40 (27–47) | 40 (32–46) | |
| Descending aorta diameter (mm) | | | |
| Mean±SD | 24.57±2.14 | 24.21±3.07 | 0.74 |
| Median (minimum–maximum) | 25 (21–9) | 24 (18–30) | |
| Aortic valve calcification (*n*=16), *n* (%) | | | |
| Present | 9/21 (42.9) | 7/14 (50.0) | 0.945 |
| Absent | 12/21 (57.1) | 7/14 (50.0) | |

SD: Standard deviation, EAT: Epicardial adipose tissue detrimental role in cardiac health. It serves as a source of several pro-inflammatory and proatherogenic cytokines, which can exert biological effects on the myocardium and epicardial coronary arteries through paracrine or vasocrine mechanisms. EAT has been identified as a specific marker of visceral adiposity, which is strongly associated with the presence and severity of CAD.[26] EAT has been shown to release inflammatory mediators such as interleukin (IL)-1 β, IL-6, and tumor necrosis factor, which are known to contribute to the pathogenesis of calcific AS.[13] The literature reports a significant correlation between EAT thickness, pro-inflammatory cytokine levels, and calcific AS, highlighting a strong relationship between EAT and AS.[26] In this context, the findings of our study are consistent with the existing literature.

In addition, some studies in the literature suggest that EAT may play a significant role in ascending aortic dilatation. Argan *et al*. found that increased EAT thickness and BMI are independent predictors of ascending aortic dilatation in hypertensive patients. They reported that elevated EAT could contribute to the progression of aortic dilatation through local or systemic effects.[14] In our study, we also identified a positive correlation between aortic dilatation and EAT thickness. However, no significant difference was observed between BAV and TAV patients in this regard. To the best of our knowledge, no other study in the literature has specifically examined the relationship between BAV and EAT. In our study, EAT thickness showed a significant difference between patients with and without aortic valve calcification. In the subgroup of 16 patients with calcified BAV, EAT thickness was significantly higher compared to other patients with non-calcified valves. However, due to the small number of patients, this positive correlation could not be highlighted as a conclusive result.

In our study, when comparing the findings between genders in BAV cases, the aortic diameter at the level of the coronary sinus was found to be higher in men. This result too may be due to the low number of patients. Given our limited sample size, further studies with larger cohorts are needed to explore this association.

Our study has some limitations. Due to its retrospective design, the study was conducted on patients who presented to our hospital with chest pain and underwent CCTA, and thus does not represent the general population. In addition, some patients were referred to our clinic for CCTA from other centers, making it impossible to access their TTE and TEE results. Consequently, echocardiographic findings and cardiovascular examination data could not be included in the study. Due to the small number of patients, data from calcified and non-calcified BAV were combined. This may have led to the impression that there was no significant difference in EAT thickness between the BAV and TAV patient subgroups. In our study, the thickness of the intima layer was not measured, and therefore, intergroup differences and its relationship with aortic dilation could not be evaluated. Therefore, further studies with larger patient cohorts are needed to better investigate these aspects.

## Conclusions

BAV is a complex congenital anomaly requiring comprehensive evaluation and lifelong follow-up due to its association with complications such as aortic dilatation and valve calcification. In our study, BAV patients exhibited significantly larger aortic diameters at the sinus of Valsalva, sinotubular junction, and ascending aorta, along with a 45.7% prevalence of valve calcification, compared to no calcification in TAV patients. A positive correlation between EAT thickness and aortic dilatation suggests that EAT may serve as a marker for vascular changes. Although EAT thickness was associated with aortic valve calcification and coronary artery calcium scores, no significant differences in CAD prevalence or EAT thickness were observed between BAV and TAV groups, indicating a predominant role of hemodynamic stress in BAV-related complications. These findings underscore the need for further large-scale studies to better understand BAV pathophysiology and optimize early intervention strategies to improve clinical outcomes.

**Financial support and sponsorship**

Nil.

**Conflicts of interest**

There are no conflicts of interest.

## References

1. Dolmaci OB, Hilhorst TL, Malekzadeh A, Mertens BJ, Klautz RJ, Poelmann RE, *et al*. The prevalence of coronary artery disease in bicuspid aortic valve patients: An overview of the literature. Aorta (Stamford) 2023;11:191-7.
2. Evangelista Masip A, Galian-Gay L, Guala A, Lopez-Sainz A, Teixido-Turà G, Ruiz Muñoz A, *et al*. Unraveling bicuspid aortic valve enigmas by multimodality imaging: Clinical implications. J Clin Med 2022;11:456.
3. Grewal N, Gittenberger-de Groot AC, Lindeman JH, Klautz A, Driessen A, Klautz RJ, *et al*. Normal and abnormal development of the aortic valve and ascending aortic wall: A comprehensive overview of the embryology and pathology of the bicuspid aortic valve. Ann Cardiothorac Surg 2022;11:380-8.
4. Michelena HI, Della Corte A, Evangelista A, Maleszewski JJ, Edwards WD, Roman MJ, *et al*. International consensus statement on nomenclature and classification of the congenital bicuspid aortic valve and its aortopathy, for clinical, surgical, interventional and research purposes. J Thorac Cardiovasc Surg 2021;162:e383-414.
5. Dolmaci OB, Legué J, Lindeman JH, Driessen AH, Klautz RJ, Van Brakel TJ, *et al*. Extent of coronary artery disease in patients with stenotic bicuspid versus tricuspid aortic valves. J Am Heart Assoc 2021;10:e020080.
6. Brown ML, Burkhart HM, Connolly HM, Dearani JA, Cetta F, Li Z, *et al*. Coarctation of the aorta: Lifelong surveillance is mandatory following surgical repair. J Am Coll Cardiol 2013;62:1020-5.

7. Fuchs MM, Attenhofer Jost C, Babovic-Vuksanovic D, Connolly HM, Egbe A. Long-term outcomes in patients with turner syndrome: A 68-year follow-up. J Am Heart Assoc 2019;8:e011501.
8. Michelena HI, Katan O, Suri RM, Baddour LM, Enriquez-Sarano M. Incidence of infective endocarditis in patients with bicuspid aortic valves in the community. Mayo Clin Proc 2016;91:122-3.
9. Barker AJ, Markl M, Bürk J, Lorenz R, Bock J, Bauer S, *et al*. Bicuspid aortic valve is associated with altered wall shear stress in the ascending aorta. Circ Cardiovasc Imaging 2012;5:457-66.
10. Andreassi MG, Della Corte A. Genetics of bicuspid aortic valve aortopathy. Curr Opin Cardiol 2016;31:585-92.
11. Dolmaci OB, Driessen AH, Klautz RJ, Poelmann R, Lindeman JH, Grewal N. Comparative evaluation of coronary disease burden: Bicuspid valve disease is not atheroprotective. Open Heart 2021;8:e001772.
12. Guglielmo M, Lin A, Dey D, Baggiano A, Fusini L, Muscogiuri G, *et al*. Epicardial fat and coronary artery disease: Role of cardiac imaging. Atherosclerosis 2021;321:30-8.
13. Ertaş G, Ekmekçi A, Şahin S, Murat A, Bakhshaliyev N, Erer HB, *et al*. Epicardial fat thickness assessment by multi-slice computed tomography for predicting cardiac outcomes in patients undergoing transcatheter aortic valve implantation. Cardiovasc J Afr 2022;33:108-11.
14. Argan O, Avci E, Yildirim T, Safak O. Epicardial adipose tissue is a predictor of ascending aortic dilatation in hypertensive patients, but not paracardial adipose tissue. BMC Cardiovasc Disord 2020;20:142.
15. Choo KS. The advantage of cardiac CT in the evaluation of the bicuspid aortic valve compared to transthoracic echocardiography. J Korean Soc Radiol 2023;84:1337-8.
16. Kim J, Kim SM, Ahn J, Kim J, Choe YH. Diagnostic performance of cardiac CT and transthoracic echocardiography for detection of surgically confirmed bicuspid aortic valve: Effect of calcium extent and valve subtypes. J Korean Soc Radiol 2023;84:1324-36.
17. Alkadhi H, Leschka S, Trindade PT, Feuchtner G, Stolzmann P, Plass A, *et al*. Cardiac CT for the differentiation of bicuspid and tricuspid aortic valves: Comparison with echocardiography and surgery. Am J Roentgenol 2010;195:900-8.
18. Tanaka R, Yoshioka K, Niinuma H, Ohsawa S, Okabayashi H, Ehara S. Diagnostic value of cardiac CT in the evaluation of bicuspid aortic stenosis: Comparison with echocardiography and operative findings. Am J Roentgenol 2010;195:895-9.
19. Pawade T, Sheth T, Guzzetti E, Dweck MR, Clavel MA. Why and how to measure aortic valve calcification in patients with aortic stenosis. JACC Cardiovasc Imaging 2019;12:1835-48.
20. Michelena HI, Della Corte A, Evangelista A, Maleszewski JJ, Enriquez-Sarano M, Bax JJ, *et al*. Speaking a common language: Introduction to a standard terminology for the bicuspid aortic valve and its aortopathy. Prog Cardiovasc Dis 2020;63:419-24.
21. Grewal N, Gittenberger-de Groot AC, Thusen JV, Wisse LJ, Bartelings MM, DeRuiter MC, *et al*. The development of the ascending aortic wall in tricuspid and bicuspid aortic valve: A process from maturation to degeneration. J Clin Med 2020;9:908.
22. Grewal N, Gittenberger-de Groot AC, Poelmann RE, Klautz RJ, Lindeman JH, Goumans MJ, *et al*. Ascending aorta dilation in association with bicuspid aortic valve: A maturation defect of the aortic wall. J Thorac Cardiovasc Surg 2014;148:1583-90.
23. Mimler T, Nebert C, Eichmair E, Winter B, Aschacher T, Stelzmueller ME, *et al*. Extracellular matrix in ascending aortic aneurysms and dissections – What we learn from decellularization and scanning electron microscopy. PLoS One 2019;14:e0213794.
24. Magni P. Bicuspid aortic valve, atherosclerosis and changes of lipid metabolism: Are there pathological molecular links? J Mol Cell Cardiol 2019;129:231-5.
25. Poggio P, Cavallotti L, Songia P, Di Minno A, Ambrosino P, Mammana L, *et al*. Impact of valve morphology on the prevalence of coronary artery disease: A systematic review and meta-analysis. J Am Heart Assoc 2016;5:e003200.
26. Parisi V, Rengo G, Pagano G, D'Esposito V, Passaretti F, Caruso A, *et al*. Epicardial adipose tissue has an increased thickness and is a source of inflammatory mediators in patients with calcific aortic stenosis. Int J Cardiol 2015;186:167-9.

Original Article

# Anatomical and Morphological Variations of Menisci with Relation to the Anterior Cruciate Ligament Tibial Insertion and its Clinical Significance: A Human Cadaveric Study

**Waad Mohammed Assiri, Ahmed Fathalla El Fouhil, Muhammad Atteya, Khaleel I. Alyahya**

*Department of Anatomy, Clinical Anatomy Lab, College of Medicine, King Saud University, Riyadh, Saudi Arabia*

## Abstract

**Background:** The knee joint is highly prone to injury, particularly involving the anterior cruciate ligament (ACL) and menisci. Anatomical variations in meniscal morphology and their relationship to the ACL tibial insertion (ACLTI) and tibial plateau may influence injury patterns and surgical outcomes. This study aimed to evaluate the morphological and morphometric variations of the menisci in relation to the ACLTI and tibial plateau surface area and to highlight their clinical significance. **Materials and Methods:** Thirty-four lower limbs from formalin-fixed adult cadavers (68 menisci and 34 ACLTIs) were dissected. Meniscal dimensions, horn attachment sites, ACL measurements, and tibial plateau surface areas were measured using digital calipers. Meniscal shape types were recorded. Statistical analysis was performed using Student's *t*-test and ANOVA, with significance set at $P < 0.05$. **Results:** Five meniscal morphological types were identified: Crescent semilunar, C-shaped, U-shaped, sickle, and V-shaped. The medial meniscus showed significantly greater dimensions than the lateral meniscus (LM). The medial tibial plateau was significantly longer than the lateral plateau ($P < 0.05$). Distances between the ACLTI and the medial meniscal horns were significantly greater than those of the LM ($P < 0.05$). **Conclusion:** The findings demonstrate a close anatomical and morphometric relationship between meniscal horn attachments and the ACLTI. Awareness of these anatomical variations is important for accurate surgical planning and outcomes in procedures such as ACL reconstruction and meniscal allograft transplantation.

**Keywords:** *Anterior cruciate ligament, lateral meniscus, medial meniscus, meniscal horns, morphology, tibial plateau*

## Introduction

The menisci and anterior cruciate ligament (ACL) are essential for knee joint stability, load transmission, and mobility. Anatomical variations in these structures influence injury patterns and surgical outcomes. Anatomically, the medial meniscus (MM) is described as crescentic and the lateral meniscus (LM) as more circular,[1] although considerable morphological variability has been reported.[2-5] Differences in meniscal width and thickness are clinically relevant, as these parameters affect joint biomechanics and resistance to injury.[6,7] ACL injuries are more frequently associated with LM tears, particularly involving the posterior horn (PH),[8] and the anterior horn (AH) of the LM serves as an important landmark during ACL reconstruction.[9]

Accurate assessment of meniscal morphology, horn insertions, and tibial plateau congruence is critical for successful meniscal allograft transplantation.[10,11] Despite this, few studies have quantified the morphometric relationships between meniscal morphology, the ACL tibial insertion (ACLTI), and the tibial plateau. The present study aimed to characterize the morphological variants and morphometric parameters of the medial and lateral menisci in relation to the ACLTI and tibial plateau anatomy to provide anatomically relevant data with clinical significance.

## Materials and Methods

### Data collecting

This study was performed on 34 adult cadaveric lower limbs (17 right, 17 left), including 68 menisci and 34 ACLTIs. Pathologically altered specimens were excluded. No demographic data were recorded. Ethical committee approval was exempt under the institutional guidelines of the College of Medicine Research Center



**How to cite this article:** Assiri WM, El Fouhil AF, Atteya M, Alyahya KI. Anatomical and morphological variations of menisci with relation to the anterior cruciate ligament tibial insertion and its clinical significance: A human cadaveric study. J Anat Soc India 2026;75:41-7.

**Article Info**

**Received:** 18 October 2025
**Revised:** 24 January 2026
**Accepted:** 30 January 2026
**Available online:** 27 March 2026

***Address for correspondence:***
*Dr. Waad Mohammed Assiri, Department of Anatomy, College of Medicine, King Saud University, Riyadh 11461, Saudi Arabia.*
*E-mail: waad.assiri@gmail.com*

**Access this article online**

**Website:** https://journals.lww.com/joai

**DOI:** 10.4103/jasi.jasi_163_25

**Quick Response Code:**

at King Saud University (Approval No. E-22-7320; Date: November 15, 2022).

### Morphological assessment

Various shapes of menisci were identified according to previous classifications in the literature.[12] The variants included crescentic, C-shaped, sickle-shaped, and sided V/U shapes. The shape distributions of the MM and LM were compared.

### Morphometric analysis

All the following parameters were measured manually at selected points, as shown in Figures 1 and 2, using a digital Vernier caliper with an accuracy of 0.05. The meniscus size measurements were taken as previously reported in the literature.[13] Measurements were captured through the principal individual at three different periods for every attribute. The average of three readings was then taken as a representative value to avoid variation. The mean values were recorded.

*Meniscal body dimensions*

- Inner and outer circumferences: Measured with a silk thread
- Anterior–PH distance
- Thickness and width at AH, body, and PH.

*Meniscal horn measurements*

- Distance from AH/PH to medial/lateral tibial eminences (MTE/LTE)
- Distance from AH/PH to ACLTI anterior margin
- Distance from AH to the tibial tuberosity (TT).

*Anterior cruciate ligament and tibial plateau dimensions*

- ACL width at midsubstance and insertion
- Distances from ACLTI center to MTE and LTE
- Medial/lateral tibial plateau widths and lengths.

### Statistical analysis

Independent *t*-tests and ANOVA were performed Via the program of SPSS Statistics version 17.0 (SPSS Inc., Chicago, IL, USA) (or specific software), with $P < 0.05$ considered statistically significant.

## Results

### Morphological results

Of the 68 menisci (34 medial and 34 lateral), five distinct morphological shapes were observed: Crescentic (semilunar), C-shaped, sickle-shaped, sided U-shaped, and sided V-shaped [Figure 3]. The crescent shape was most prevalent in the MM (76.50%), whereas the LM predominantly exhibited a C shape (70.58%). The LM crescentic shape was the least common, with only 2 (5.89%), and equal numbers of MM sickle and sided V-shaped ($n$ = 4; 5.88%, each). No discoid menisci were identified [Table 1 and Figure 4]. The incidence of shape differed between the left and right knees. The LM C and U shapes, and the MM crescentic variant, were more common on the left side of the knee [Table 2].

### Morphometric results

Compared with LMs, MMs presented significantly greater outer and inner circumferences and greater anterior–PH distances ($P < 0.05$). The MM anterior and PHs were also

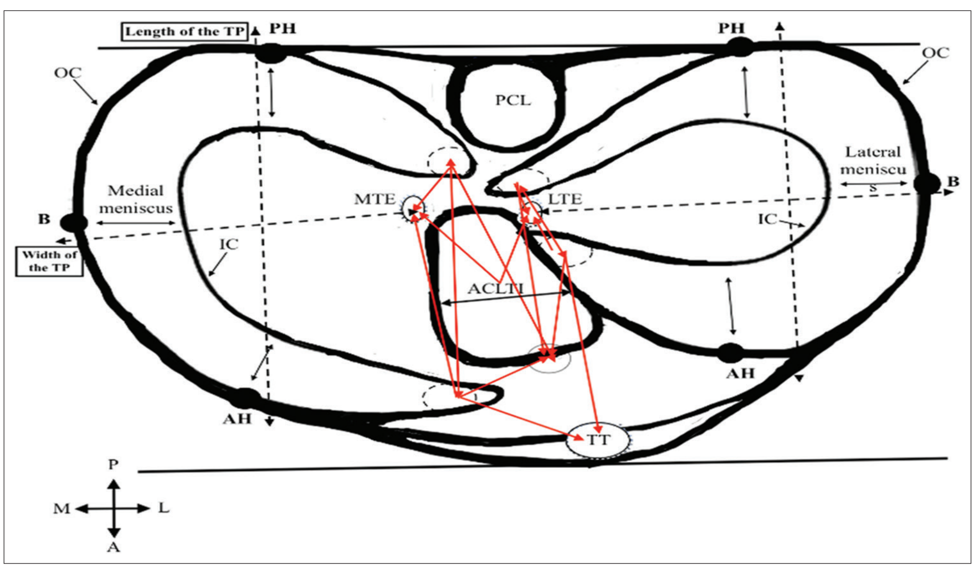


**Figure 1: Parameters used to measure cadaver specimens of the meniscus. Including outer and inner circumference, width, and thickness measurements of the anterior (AH); body (b); and posterior horns (PH); the distance between the apex horns (PH, AH); tibial tuberosity; anterior border, medial and lateral tibial eminence (MTE and LTE); anterior margin of the anterior cruciate ligament (ACL) tibial insertion fibers; (ACL) width at the mid-substance and tibial insertion site; tibial plateau width and length; distance from (ACL tibial insertion) center to (LTE) and (MTE). PH: Posterior horn, MTE: Medial tibial eminence, LTE: Lateral tibial eminence, ACL: Anterior cruciate ligament, ACLTI: ACL tibial insertion, IC: Inner circumference, OC: Outer circumference, TT: Tibial tuberosity, AH: Anterior horn, PCL: Posterior cruciate ligament**

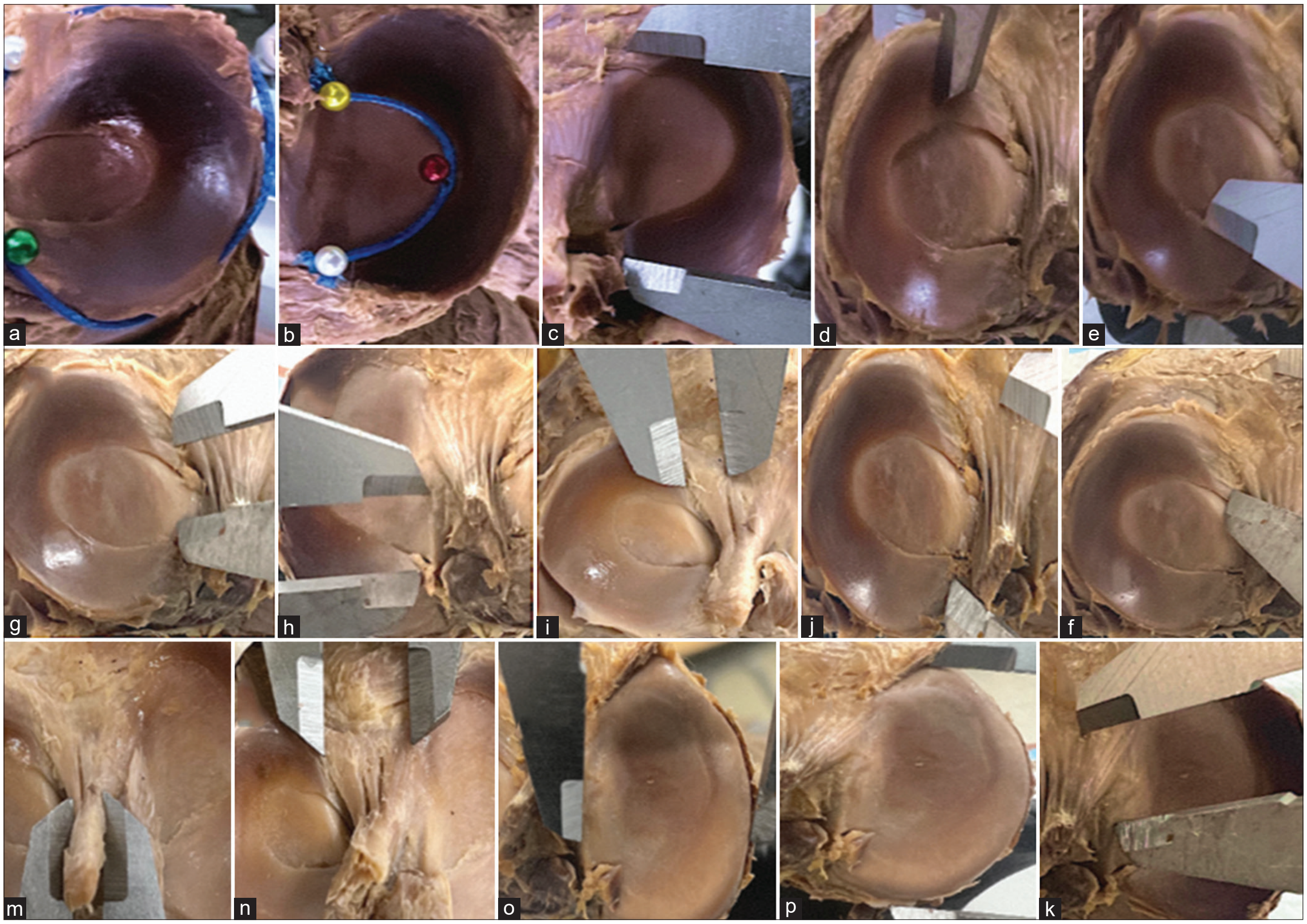


**Figure 2: The morphometric analysis of menisci and the anterior cruciate ligament (ACL) using a vernier caliper. (a) Measurement of the outer circumference, (b) measurement of the inner circumference, and (c) distance between meniscus horns. (d) Measurement of meniscal thickness, (e) measurement of meniscal width, (g) distance from the anterior horn to the corresponding tibial eminence. (h) Distance from the posterior horn to the corresponding tibial eminence, (i) distance from the anterior horn to the anterior margin of the ACL tibial insertion fibers, (j) distance from the posterior horn to the anterior margin of the ACL tibial insertion fibers, (f) distance from the anterior horn to the anterior border of the tibial tuberosity, (m) measurement of the anterior cruciate ligament width at the mid-substance area, (n) measurement of the anterior cruciate ligament tibial insertion site width, (o) measurement of the tibial plateau width, (p) measurement of the tibial plateau length, and (k) distance from the center of the ACL tibial insertion site to the tibial eminence**

**Table 1: Number and percentage distribution of the shape variants of the lateral meniscus and the medial meniscus (*n*=68 menisci)**

| Shape | LM, *n* (%) | MM, *n* (%) | Total, *n* (%) |
|---|---|---|---|
| Crescentic | 2 (5.89) | 26 (76.50) | 28 (41.17) |
| C-shape | 24 (70.58) | 0 | 24 (35.30) |
| Sickle shape | 0 | 4 (11.76) | 4 (5.88) |
| Sided U-shaped | 8 (23.53) | 0 | 8 (11.76) |
| Sided V-shaped | 0 | 4 (11.70) | 4 (5.88) |
| Complete discoid | 0 | 0 | 0 |
| Incomplete discoid | 0 | 0 | 0 |

LM: Lateral meniscus, MM: Medial meniscus

thicker, whereas the LM AH and body were significantly wider ($P < 0.05$) [Table 3].

Distances from the anterior and posterior meniscal horns to ACLTI and other tibial landmarks revealed key spatial differences. The MM horn distances to ACLTI and MTE were significantly greater than those to LM ($P < 0.05$) [Table 4].

The medial tibial plateau length was significantly longer than the lateral plateau length ($P < 0.05$), although the widths were comparable. The ACL was considerably wider at the insertion position than at the mid-substance position, and there was no statistically significant difference ($P > 0.05$) between the distance from the center of ACLTI to MTE and LTE [Table 5].

## Discussion

The knee joint is highly susceptible to injuries, especially to the meniscus and ACL. The menisci originate from vascular mesenchymal tissue within the developing knee joint during fetal life, gradually assuming their characteristic C-shaped configuration before maturing into fibrocartilaginous structures with reduced vascularity in adulthood.[14,15] This developmental process contributes to their morphological characteristic in shape, size, thickness, and tibial insertion patterns, which are important for load transmission and overall knee biomechanics and may

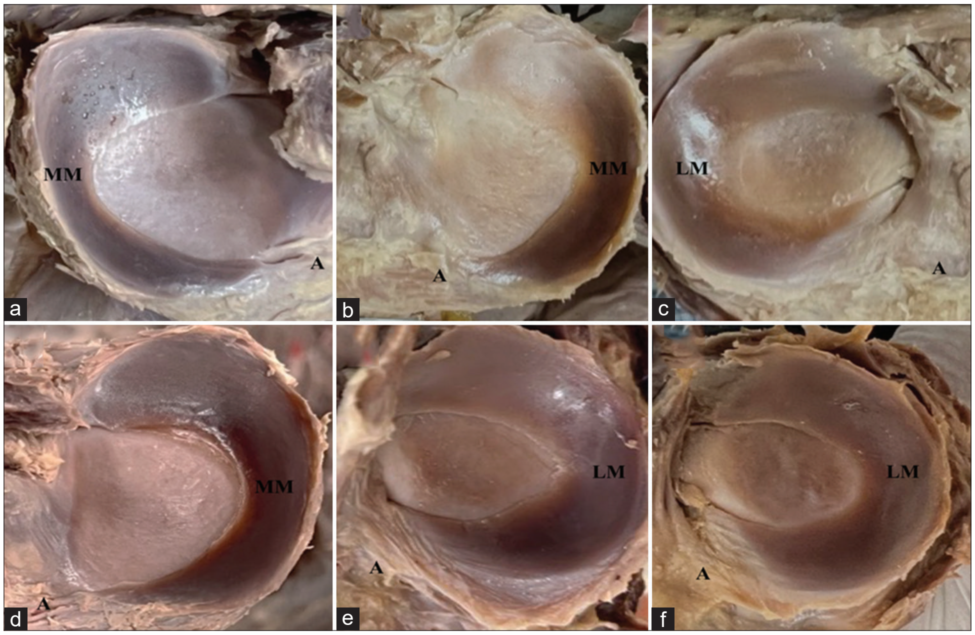


**Figure 3: The different meniscus shapes, (a) medial meniscus (MM) crescentic (semilunar) shape, (b) MM V-shaped, (c) lateral meniscus (LM) C-shaped, (d) MM C-sickle-shaped, (e) LM crescentic (semilunar) shape, (f) LM sided U-shaped. A: Anterior horn, LM: Lateral meniscus, MM: Medial meniscus**

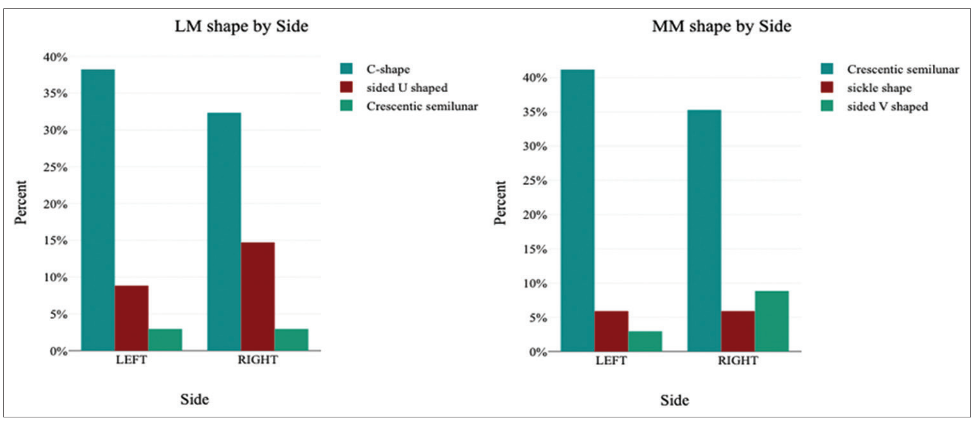


**Figure 4: Graphic representation of different shapes of lateral menisci (LM) and Medial meniscus (MM) on the left and right sides**

**Table 2: Shape incidence of menisci in the side knee joint (*n*=34 for each lateral meniscus and medial meniscus)**

| | Left, *n* (%) | Right, *n* (%) | Total, *n* (%) |
|---|---|---|---|
| LM shapes | | | |
| C-shape | 13 (38.24) | 11 (32.35) | 24 (70.59) |
| U-shape | 3 (8.82) | 5 (14.71) | 8 (23.53) |
| Crescentic | 1 (2.94) | 1 (2.94) | 2 (5.88) |
| MM shapes | | | |
| Crescentic | 14 (41.18) | 12 (35.29) | 26 (76.47) |
| Sickle shape | 2 (5.88) | 2 (5.88) | 4 (11.76) |
| V-shape | 1 (2.94) | 3 (8.82) | 4 (11.76) |

LM: Lateral meniscus, MM: Medial meniscus

affect susceptibility to injury.[16,17] Clinically, meniscal tears are frequently associated with ACL ruptures, occurring in approximately 16%–82% of acute cases and in up to 96% of chronic ACL-deficient knees.[18,19] Accordingly, the present study aimed to analyze the morphological and morphometric features of the menisci and their relationship to the ACLTI. Understanding the anatomical variations of the menisci is essential for accurate diagnosis, surgical planning, and the development of prosthetic designs and meniscal allografts.

It was reported that the MM of the human knee joint is consistently crescentic in shape, whereas the LM is approximately circular.[1] Many studies have supported this observation,[2,3] while others have reported morphological variations in both menisci.[4,5]

In the present study, five distinct meniscal shapes were identified: Crescentic, C-shaped, sickle-shaped, sided U-shaped, and sided V-shaped. Morphologically, the predominance of the crescentic shape in the MM (76.50%) and the C shape in the LM (70.58%) corroborates classical anatomical descriptions emphasizing the

**Table 3: Comparison of meniscal body dimensions (*n*=68)**

| Parameter (mm) | MM | LM | *P* |
|---|---|---|---|
| Outer circumference* | 88.15±10.97 | 81.29±8.73 | 0.006* |
| Inner circumference* | 50.21±8.38 | 43.22±8.46 | 0.001* |
| PH-AH distance* | 28.71±2.91 | 14.64±2.84 | <0.001* |
| Thickness - AH* | 6.35±1.4 | 3.81±0.79 | <0.001* |
| Thickness - Body | 5.81±1.08 | 5.35±0.93 | 0.068 |
| Thickness - PH* | 6.11±1.53 | 5.31±0.74 | 0.008* |
| Width -AH* | 7.89±1.33 | 9.98±1.75 | <0.001* |
| Width - Body* | 8.01±0.77 | 10.56±1.33 | <0.001* |
| Width - PH* | 13.65±2.93 | 9.77±1.65 | <0.001* |

*Statistically significant at *P*<0.05. Values are mean±SD.
SD: Standard deviation, PH: Posterior horn, AH: Anterior horn, LM: Lateral meniscus, MM: Medial meniscus

**Table 4: Distance from menisci horns to tibial landmarks (*n*=68)**

| Parameters (mm) | MM | LM | *P* |
|---|---|---|---|
| AH to TT | 16.76±3.64 | 18.22±4.4 | 0.14 |
| AH to respective tibial eminence* | 21.88±2.71 | 12.98±2.14 | <0.001* |
| PH to the respective tibial eminence | 10.8±2.62 | 9.57±3.09 | 0.082 |
| AH to ACLTI* | 15.6±3.69 | 9.45±2.63 | <0.001* |
| PH to ACLTI* | 24.81±3.06 | 20.55±2.68 | <0.001* |

*Statistical significance *P*<0.05. Values are mean±SD.
LM: Lateral meniscus, MM: Medial meniscus, AH: Anterior horn, PH: Posterior horn, ACLTI: Anterior cruciate ligament tibial insertion, TT: Tibial tuberosity, SD: Standard deviation

**Table 5: Anterior cruciate ligament and tibial plateau dimensions (*n*=34)**

| Parameters (mm) | (Mean ± SD) |
|---|---|
| Tibial plateau length - Medial* | 45.76±4.55 |
| Tibial plateau length - Lateral* | 39.98±5.08 |
| Tibial plateau width - Medial | 33.48±4.44 |
| Tibial plateau width - Lateral | 32.13±3.53 |
| ACLTI to MTE | 12.63±2.79 |
| ACLTI to LTE | 13.4±1.98 |
| ACL width - Mid-substance* | 6.47±2.15 |
| ACL width - Insertion* | 13.55±1.5 |

*Statistical significance *P*<0.05. Values are mean±SD.
MTE: Medial tibial eminence, LTE: Lateral tibial eminence, ACL: Anterior cruciate ligament, ACLTI: ACL tibial insertion, SD: Standard deviation

semilunar configuration of the MM and the more circular configuration of the LM.[20]

This observation is consistent with,[5] who reported that the most common shape of the MM was crescentic, whereas the V-shaped and U-shaped types were the least common. For the LM, the C-shaped configuration was most frequent, whereas the U-shaped type was the least common. They also described an incomplete discoid shape of the LM.

The discoid meniscus is considered an anomalous shape characterized by a thicker-than-usual, more prominent crescent configuration, with a reported incidence of 0.4%–17% for the LM.[21] According to Silverman *et al*. study,[22] the prevalence of discoid MM ranges from 0.1% to 0.3%. Unlike some radiological studies reporting variable incidences of discoid menisci, particularly in pediatric populations,[23] no discoid menisci were identified in the present study. This finding aligns with anatomical studies conducted in populations in which discoid variants are rare.[24]

The observed side-dependent variation in meniscal shapes – specifically, the higher prevalence of crescent-shaped MM and C-shaped LM on the left side – introduces a novel aspect of anatomical variability, as previous imaging and surgical studies have rarely stratified meniscal morphology by side. However, several morphological studies have reported variations between the right and left knee joints.[25,26]

Morphometrically, the significantly greater outer and inner circumferences and the increased anterior–PH distances observed in the MM reflect its broader functional role in load transmission and joint stabilization. These findings are supported by cadaveric and magnetic resonance imaging (MRI)-based studies by Erbagci *et al*. and Bloecker *et al*.[27,28] and by Chaware *et al*.,[3] who reported that the MM has a greater distance between its horns than the LM. However, the present results contradict those of Chaware *et al*.[3] who stated that the mean lengths of the outer and inner circumferences are greater in the LM than in the MM.

Differences in meniscal size, including thickness and width, can influence both susceptibility to injury and the location of meniscal tears.[29] Furthermore, meniscal allograft sizing depends on the dimensions of the host meniscus, which remains an unresolved challenge in clinical practice.[30] These dimensional variations arise from structural characteristics unique to each meniscus type.[20] According to Battistelli *et al.*'s study,[5] the MM is thicker than the LM in all three regions – the AH, body (B), and PH.

In the present study, the AH of the MM was the narrowest region, whereas the PH was significantly wider. In addition, the MM was thicker in the anterior and PHs compared to the LM. Statistical analysis revealed no significant difference in body thickness between the MM and LM. These findings are consistent with the MRI-based study by Erbagci *et al*.,[27] which reported that the PH of the MM is the widest region, while the AH, mid-body, and PH of the LM exhibit comparable widths. Previous studies have reported that the PH of the MM is significantly thicker than the AH.[31,32] In contrast, the present study found no significant differences in thickness among the three regions of the MM. These discrepancies may be attributed to differences in sample size, specimen age, measurement techniques, or the specific areas analyzed.

According to Park *et al*. and Cui *et al*.'s study,[33,34] narrower menisci experience less femoral condylar movement and are therefore less prone to rupture than wider menisci. In agreement with these findings, the wider PH of the MM observed in this study may explain its higher susceptibility to injury in cases of chronic ACL deficiency.[19] No major right–left differences were identified, except for a slightly wider AH of the LM on the right side,[35] emphasized that defining meniscal dimensions in relation to tibial and ACL landmarks can improve diagnostic accuracy and treatment strategies for both orthopedic surgeons and radiologists. The spatial relationships between meniscal horns, tibial landmarks, and the ACLTI site further enhance biomechanical understanding and have direct surgical implications. In the present study, the distances of the medial meniscal horns from the anterior tibial margin (ACLTI) were significantly greater than those of the LM. Conversely, no significant differences were observed in the distances between the posterior meniscal horns and their respective tibial eminences.

In addition, the distance from the anterior border of the TT to the AH of the MM was slightly shorter than that to the AH of the LM. These findings are consistent with MRI-based measurements reported in recent radiological studies,[36] underscoring the importance of accurate meniscal horn positioning for functional restoration. While[37] described the relationship between meniscal and ACL attachments, they did not compare medial and lateral meniscal variations or include distances to the ACL anterior margin and TT, as performed in the present study. Incorporating these anatomical references may improve ACLTI localization and enhance diagnostic accuracy and surgical planning.

The LM covers approximately 70% of the tibial plateau, whereas the MM covers about 50%, making accurate meniscal sizing essential to prevent increased joint pressure and the development of osteoarthritis following implantation.[11-14] In the present study, no significant difference was found in tibial plateau width between the medial and lateral sides; however, the medial tibial plateau was significantly longer. This finding is consistent with morphometric data from both anatomical dissections and imaging studies.[38,39] These results highlight the importance of preoperative assessment of tibial plateau dimensions to avoid under-or oversizing of meniscal grafts.

The observation of a wider ACL insertion site relative to its mid-substance and the significantly shorter distance from the ACLTI center to the MTE compared to the LTE is consistent with the findings of Oka *et al*.,[40] who reported the presence of specialized ACL fibers connected to the MTE but not to the LTE. These findings reinforce the importance of restoring native ACL anatomy during reconstruction while avoiding damage to the menisci at critical insertion sites. Further investigation into the relationship between meniscal horn morphology, the ACL, and tibial plateau anatomy is needed to provide surgeons with additional anatomical reference points and tools for arthroscopic ACL reconstruction. Such knowledge may help prevent iatrogenic meniscal injury and improve the accuracy of ACL assessment.

The limitations of the present study include: (i) the lack of donated cadaveric information, such as age and sex; (ii) a relatively small sample size due to medical education requirements; and (iii) the possibility that cadaveric tissues may not fully represent the architecture of living tissues. Future studies involving larger and more diverse samples are required to validate and extend these findings.

## Conclusion

Understanding the anatomical differences between the medial and lateral menisci in relation to the ACL and tibial plateau is crucial for accurate diagnosis and effective management of meniscal injuries. Our findings indicate that the MM exhibits greater morphometric parameters than the LM, which may explain the region-specific injury patterns observed. These observations underscore the close relationship between meniscal horn attachments and the ACL, highlighting the importance of considering anatomical variability during imaging interpretation and surgical planning.

**Financial support and sponsorship**

Nil.

**Conflicts of interest**

There are no conflicts of interest.

## References

1. Parson HG. The external semilunar cartilage of the knee in the primates. J Anat 1900;34:32.
2. Clark CR, Ogden JA. Development of the menisci of the human nee joint. Morphological changes and their potential role in childhood meniscal injury. J Bone Joint Surg Am 1983;65:538-47.
3. Chaware P, Kumar B, Patil S, Surya V, Rathinam B, Gandhi K, *et al*. A cadaveric study to define morphology and morphometry of human knee menisci in the region of Central India. Cureus 2023;15:e41174.
4. Battistelli M, Favero M, Burini D, Trisolino G, Dallari D, De Franceschi L, *et al*. Morphological and ultrastructural analysis of normal, injured and osteoarthritic human knee menisci. Eur J Histochem 2019;63:2998.
5. Gupta GK, Kumar P, Rani S, Kumari A. Morphological study of the menisci of the knee joint in human cadaver in Jharkhand population. J Family Med Prim Care 2022;11:4723-9.
6. Mameri ES, Dasari SP, Fortier LM, Verdejo FG, Gursoy S, Yanke AB, *et al*. Review of meniscus anatomy and biomechanics. Current Reviews in Musculoskeletal Medicine 2022;15:323-35. doi: 10.1007/s12178-022-09768-1.

7. Bradley PX, Thomas KN, Kratzer AL, Robinson AC, Wittstein JR, DeFrate LE, *et al*. The interplay of biomechanical and biological changes following meniscus injury. Curr Rheumatol Rep 2023;25:35-46.
8. Venkataraman S, Ethiraj P, Shanthappa AH, Vellingiri K. Association of meniscus injuries in patients with anterior cruciate ligament injuries. Cureus 2022;14:e25878.
9. Kassam AM, Schranz, PJ, Mandalia VI. Anatomic anterior cruciate ligament reconstruction: The use of the anterior horn of the lateral meniscus as a guide to tibial tunnel placement. Arthroscopy Techniques 2016;5:e809-e814. doi: 10.1016/j.eats.2016.03.008.
10. Pereira H, Fatih Cengiz I, Gomes S, Espregueira-Mendes J, Ripoll PL, Monllau JC, *et al.* Meniscal allograft transplants and new scaffolding techniques. EFORT Open Rev 2019;4:279-95.
11. Haut Donahue TL, Hull ML, Rashid MM, Jacobs CR. The sensitivity of tibiofemoral contact pressure to the size and shape of the lateral and medial menisci. J Orthop Res 2004;22:807-14.
12. Murlimanju BV, Nair N, Pai MM, Krishnamurthy A, Chandra Philip X. Morphology of the medial meniscus of the knee in human fetuses. Rom J Morphol Embryol 2010;51:347-51.
13. Almeida SK, Demoraes AS, Tashiro T, Neves SE, Toscano AE, Deabreu RR. Morphometric study of menisci of the knee joint. Int J Morphol 2004;22:181-4.
14. Fox AJ, Bedi A, Rodeo SA. The basic science of human knee menisci: Structure, composition, and function. Sports Health 2012;4:340-51.
15. Arnoczky SP, Warren RF. Microvasculature of the human meniscus. Am J Sports Med 1982;10:90-5.
16. Paton R. Basic orthopaedic sciences: The Stanmore guide. Ann R Coll Surg Engl 2008;90:358.
17. Guilak F. Biomechanical factors in osteoarthritis. Best Pract Res Clin Rheumatol 2011;25:815-23.
18. Ahn JH, Bae TS, Kang KS, Kang SY, Lee SH. Longitudinal tear of the medial meniscus posterior horn in the anterior cruciate ligament-deficient knee significantly influences anterior stability. Am J Sports Med 2011;39:2187-93.
19. Bellabarba C, Bush-Joseph CA, Bach JB. Patterns of meniscal injury in the anterior cruciate-deficient knee: a review of the literature. American Journal of Orthopedics (Belle Mead, NJ) 1997;26:18-23.
20. Fox AJ, Wanivenhaus F, Burge AJ, Warren RF, Rodeo SA. The human meniscus: A review of anatomy, function, injury, and advances in treatment. Clin Anat 2015;28:269-87.
21. Trisolino G, Stallone S, Grassi A, Olivotto E, Battistelli M, Zarantonello P, *et al*. The discoid lateral meniscus in children: A narrative review of pathology, diagnosis and treatment. Ann Jt 2022;7:38.
22. Silverman JM, Mink JH, Deutsch AL. Discoid menisci of the knee: MR imaging appearance. Radiology 1989;173:351-4.
23. Accadbled F, Sygacz O, Rassi J, Herdea A. Pediatric medial discoid meniscus: Case series and postoperative outcomes. Children (Basel) 2025;12:646.
24. Dickason JM, Del Pizzo W, Blazina ME, Fox JM, Friedman MJ, Snyder SJ. A series of ten discoid medial menisci. Clinical Orthopaedics and Related Research 1982. p. 75-79.
25. Asseln M, Hänisch C, Schick F, Radermacher K. Gender differences in knee morphology and the prospects for implant design in total knee replacement. Knee 2018;25:545-58.
26. Olewnik Ł, Gonera B, Kurtys K, Podgórski M, Polguj M, Topol M. A proposal for a new classification of the fibular (lateral) collateral ligament based on morphological variations. Ann Anat 2019;222:1-11.
27. Erbagci H, Gumusburun E, Bayram M, Karakurum G, Sirikci A. The normal menisci: *In vivo* MRI measurements. Surg Radiol Anat 2003;25:404-9.
28. Bloecker K, Wirth W, Hudelmaier M, Burgkart R, Frobell R, Eckstein F. Morphometric differences between the medial and lateral meniscus in healthy men – A three-dimensional analysis using magnetic resonance imaging. Cells Tissues Organs 2012;195:353-64.
29. Bayer S, Meredith SJ, Wilson KW, de Sa D, Pauyo T, Byrne K, *et al*. Knee morphological risk factors for anterior cruciate ligament injury: A systematic review. J Bone Joint Surg Am 2020;102:703-18.
30. Haen TX, Boisrenoult P, Steltzlen C, Pujol N. Meniscal sizing before allograft: Comparison of three imaging techniques. Knee 2018;25:841-8.
31. Bedoya MA, Barrera CA, Chauvin NA, Delgado J, Jaramillo D, Ho-Fung VM. Normal meniscal dimensions at different patient ages-MRI evaluation. Skeletal Radiol 2019;48:595-603.
32. Liu Y, Du G, Liu J. Meniscal anterior and posterior horn heights are associated with MRI-defined knee structural abnormalities in middle-aged and elderly patients with symptomatic knee osteoarthritis. BMC Musculoskelet Disord 2022;23:218.
33. Park JY, Kim BH, Ro DH, Lee MC, Han HS. Characteristic location and rapid progression of medial femoral condylar chondral lesions accompanying medial meniscus posterior root tear. Knee 2019;26:673-8.
34. Cui JC, Wu WT, Xin L, Chen ZW, Lei PF. Efficacy of arthroscopic treatment for concurrent medial meniscus posterior horn and lateral meniscus anterior horn injury: A retrospective single center study. Orthop Surg 2021;13:45-52.
35. Banovetz MT, Roethke LC, Rodriguez AN, LaPrade RF. Meniscal root tears: A decade of research on their relevant anatomy, biomechanics, diagnosis, and treatment. Arch Bone Jt Surg 2022;10:366-80.
36. Choi NH, Yoo SY, Victoroff BN. Position of the bony bridge of lateral meniscal transplants can affect meniscal extrusion. Am J Sports Med 2011;39:1955-9.
37. LaPrade CM, Ellman MB, Rasmussen MT, James EW, Wijdicks CA, Engebretsen L, *et al*. Anatomy of the anterior root attachments of the medial and lateral menisci: A quantitative analysis. Am J Sports Med 2014;42:2386-92.
38. Fukazawa I, Hatta T, Uchio Y, Otani H. Development of the meniscus of the knee joint in human fetuses. Congenit Anom (Kyoto) 2009;49:27-32.
39. Eboh DE. Morphometric anatomy of the tibia plateau in Nigerians. Ethiop J Health Sci 2022;32:155-60.
40. Oka S, Schuhmacher P, Brehmer A, Traut U, Kirsch J, Siebold R. Histological analysis of the tibial anterior cruciate ligament insertion. Knee Surg Sports Traumatol Arthrosc 2016;24:747-53.

Original Article

# Computed Tomographic Investigation of the Upper Segmental Renal Artery and its Relation with the Major Calyx among Renal Donors: A Radiological Study and Review


## Abstract

**Introduction:** Understanding the correlation between the upper segmental renal artery and the collecting system is crucial when approaching the upper pole of the kidney. This study was done to analyze the anatomical variations in the upper segmental artery and its relationship with the major calyx. **Materials and Methods:** Multidetector computed tomography renal angiogram reports of 99 renal donors who underwent preoperative renal angiograms at a scan center in Chennai, India were included in this study. **Results:** Upper segmental branch was classified into four types based on their origin. Type 1 was the most common type and was seen in 65.65% on the right side and 50.5% on the left side. Type 2 pattern was seen in 7.07% on the right side and 21.21% on the left side. Type 3 pattern was seen in 14.14% on the right side and 18.18% on the left side. Type 4 pattern was seen in 11.11% on the right side and 8.08% on the left side. Other undefined types were seen in 2.02% on both sides. **Conclusion:** A thorough understanding of calyceal and intrarenal patterns empowers surgeons to approach renal disorders with precision, minimizing risks and maximizing the chances of successful outcomes in patients.


**Keywords:** *Computed tomography, donors, renal artery, upper segmental artery*

**Kumaresan Munusamy, Sangeetha Achuthan[1], Jayakumar Saikarthik[2], Ilango Saraswathi[3,4]**

*Department of Anatomy, Rajalakshmi Medical College and Research Institute, Rajalakshmi Health City, Pennalur, Sriperumbudur, [1]Department of Physiology, Sri Ramachandra Medical College and Research Institute, Sri Ramachandra Institute of Higher Education, Chennai, [3]Department of Physiology, Mauli Medical College and Hospital, Buldhana, [4]Department of Business Administration, Manipal Academy of Higher Education, Manipal, India, [2]Department of Maxillofacial Surgery and Diagnostic Sciences, College of Dentistry, Majmaah University, Al Majmaah, Saudi Arabia*

**Article Info**

**Received:** 17 September 2025
**Revised:** 14 February 2026
**Accepted:** 18 February 2026
**Available online:** 27 March 2026

***Address for correspondence:***
*Dr. Jayakumar Saikarthik, Department of Maxillofacial Surgery and Diagnostic Sciences, College of Dentistry, Majmaah University, AI Majmaah, Saudi Arabia.*
*E-mail: s.jaya@mu.edu.sa*

**Access this article online**

**Website:** https://journals.lww.com/joai

**DOI:** 10.4103/jasi.jasi_145_25

**Quick Response Code:**

## Introduction

The kidney, a vital organ of the urinary system, plays a central role in maintaining homeostasis by filtering blood, regulating electrolyte balance, and excreting metabolic waste products. Renal vascular segmentation was originally recognized by the anatomists Hunter 1794 and Brödel 1901.[1,2] Study by Graves FT in 1954 laid the foundation for the segmental pattern of intrarenal arterial distribution and its variation.[3] The renal artery divides into the anterior division and the posterior division. The anterior division of the renal artery gives origin to the apical segmental artery first and then to the upper, middle, and lower segmental arteries.[4]

Delineating renal vasculature with its numerous variations has been a challenge for scientists. As of now, a consensus on the lobar, zonal, and segmental organization of the kidney vasculature has not been reached among the scientific community. Partial nephrectomy is a promising treatment option for renal cell carcinoma, which caused a worldwide mortality of 179,368 deaths (115,600 men and 63,768 women), with a global age-standardized rate of 1.8/100,000 in 2022. An annual increase in 2% of incidence of renal cell carcinoma occurred both worldwide and in Europe in the past 20 years.[5] Partial nephrectomy is also advised in renal calculus and renal tuberculosis. Understanding the vascular pattern of the kidney significantly aids surgeons during renal surgical procedures; however, this knowledge is neither comprehensive nor easily accessible.

The arteries of the upper renal segment show large morphologic variability regarding origin and the supplied renal territory. Anatomical knowledge about the upper segmental artery of the human kidney is important for performing intrarenal surgeries, to avoid postoperative complications and injury to the adjacent parenchyma.[6] Although because of a smaller supplied territory, it may have a limited significance within the systematization of the renal blood supply. In certain situations, the upper pole of



**How to cite this article:** Munusamy K, Achuthan S, Saikarthik J, Saraswathi I. Computed tomographic investigation of the upper segmental renal artery and its relation with the major calyx among renal donors: A radiological study and review. J Anat Soc India 2026;75:48-53.

the kidney receives additional branches from the primary arterial trunk. However, the superior renal pole will receive 2–5 arteries that will increase the difficulty of a superior polar nephrectomy with multiple ligatures.[6]

A vascular plane is a fairly constant aspect of a kidney, and this hypo-vascular area is usually oriented 20°–30° from the sagittal plane. Puncturing these area results in reduced bleeding risk compared to puncturing other areas of kidney. Bleeding may occur during any aspect of percutaneous nephrolithotomy (PCN) injury to main renal vessels and also occurs during initial percutaneous access. Major bleeding during direct percutaneous access to renal pelvis is increased due to proximity of large renal hilar vessels.[7]

Knowledge of renal segmental artery variations is indispensable for surgical planning, risk assessment, preservation of renal function, patient safety, and medical education in the management of renal disorders and procedures. Anatomical comprehension of the upper segmental artery is vital for executing intrarenal procedures to mitigate postoperative complications. To reduce the risk of injury, surgeons must consider the spatial orientation of intra-renal vascularity. Renal collecting system complications, including abnormal hemodynamic parameters and reduced drainage of irrigation fluid during PCN, were reported in 46.9% of patients.[8]

Although several cadaveric and corrosion cast studies have described segmental renal artery patterns, there is limited radiological data correlating upper segmental arterial origin with its spatial relationship to the major calyx in living renal donors. Furthermore, most previous studies relied on postmortem techniques, and few have evaluated gender- and side-specific associations using multidetector computed tomography (MDCT) angiography in an Indian donor population. In our study, we utilized a 64-slice angiographic technique, aiming to delineate various upper segmental artery patterns and their associations with the calyceal system, which hold significant clinical implications.

## Materials and Methods

### Study design

An estimated 9834 live kidney donor renal transplantations were performed in 2022 in India.[9] Using Statcalc software with a 10% margin of error and a 95% confidence interval, the minimum required sample size for this study was determined to be 96 individuals. The current study focused on renal donors who underwent preoperative renal angiograms at a scan center in Chennai, India. The study spanned over a year, involving the computed tomography (CT) renal angiograms of 99 renal donors. Inclusion criteria included adults (age >18 years) without renal disease, devoid of pathological conditions likely to impact renal vasculature, and demonstrating adequate contrast media enhancement in the arterial phase (150 HU). The study adhered to the Declaration of Helsinki, and ethical approval was granted by the institutional Human Ethical Committee (001/09/2015/IEC/SU). Written consent was obtained from all the participants of the study.

### Multidetector computed tomography and postprocessing

All donors underwent a CT renal angiogram using a 64-slice MDCT scanner from GE systems. The scanning parameters included 120 kV, 240 mAs, and a slice thickness of 0.625 mm. The scan area covered from the diaphragm to the iliac crest, and images were captured at a rotational speed of 0.7 s. Employing a bolus tracker positioned in the abdominal aorta at the level of renal arteries, and with a delay of approximately 6–8 s, CT images were obtained during the arterial phase. A combined volume of 90 mL of nonionic contrast agent (omnipaqueTM), along with 20 mL of saline, was administered through the ante-cubital vein utilizing a pressure injector operating at a rate of 5 mL/s.

The serial thin-section images acquired were transferred to a specialized three-dimensional (3D) workstation, where they underwent reconstruction using minimum intensity projection (MIP), multiplanar reformation, and 3D volume rendering techniques for diagnostic assessment. These methodologies facilitated the identification of variant branching patterns of the renal artery and precise measurement of the renal arteries. All observations and measurements were conducted by a single observer, with meticulous details being documented.

### Statistical analysis

Descriptive statistics were performed for the obtained data. Chi-square test was used to compare the prevalence between gender and side. All statistical analysis was performed using SPSS version 21, IBM corporation, NY, USA. $P < 0.05$ was considered to be statistically significant.

## Results

There were 54 males and 45 females in the studied sample, and all the participants exhibited normal renal functions. The origin and calyceal relationship of the upper segmental artery exhibited considerable variability both among and within the individuals examined.

### Pattern of upper segmental artery

The upper segmental branch was classified into 4 types based on its origin. Type-1 arises from the anterior division. Type-2 arises with middle segmental artery. Type-3 arises with the apical segmental artery. Type-4 arises from the posterior division of renal artery. In this study, the majority of the upper segmental branches were found to be of type-1, and the upper segmental branch arises directly from the main renal artery in 2 cases (1%).

In the present study, the upper segmental branch shows the following variations. Type-1 is more frequent in the right (65 kidneys, 65.65%) than left (50 kidneys, 50.50%). On the right side, type-1 is more frequent in female (66.6%). On the left side, Type 1 is more frequent in male (52%). Type 2 is more frequent in the left (21 kidneys, 21.21%) than in the right (7 kidneys, 7.07%). On the right side, Type 2 is more frequent in males (9.6%), and on the left side, Type 2 is more frequent in females (31.1%). Type-3 is more frequent in the left (18 kidneys, 18.18%) than the right (14 kidneys, 14.14%). On the right side, Type 3 is more frequent in females (7 kidneys, 15.5%), and on the left side, Type 3 is more frequent in males (10 kidneys, 18.5%). Type 4 is more frequent in the right (11 kidneys, 11.11%) than in the left (10 kidneys, 10.1%). On the right side, Type 4 is more frequent in females (6 kidneys, 13.3%), and on the left side, Type 4 is more frequent in males (7 kidneys, 13%). Other patterns were also observed in 4 kidneys.

The distribution of the upper segmental branch between sides and gender is given in Table 1 in detail. Distributional patterns of the upper segmental branch on different sides are given in Figure 1.

**Relationship between upper segmental artery type with major calyx**

We observed variations in the relation between the collecting system and the upper segmental artery. These variations have been divided into two groups, namely upper segmental artery Group 1 (USAG 1) and USAG 2.[10] USAG-1 ran in front of upper major calyx and was seen in 76 kidneys on right side (76.77%) and 65 kidneys on left side (65.66%). USAG-2 ran upwards medial to the pelvis and upper major calyx, which was seen in 23 kidneys in right side (23.23%) and 34 kidneys on left side (34.34%). There was a significant association between the occurrence of USAG and USAT in the right side in females ($\chi^2$ = 14.217 $P$ = 0.03). The occurrence of upper segmental arterial pattern in association with group and their statistical value are given in Table 2. The different types of USAG and USAT are given in Figure 2a-f.

## Discussion

In an earlier study, we investigated the peri hilar branching pattern of renal artery and reported 8 cardinal branching pattern and 10 minor branching pattern. In the current study, Type 1 Upper segmental artery is observed in majority of the donors than other types which is similar to the study conducted by Mishra *et al*.[10] Type 3 is seen more than Type 2 in our study which is similar to study conducted by Fine *et al.*,[11] and contrary to study conducted by Mishra *et al*.[10,12] Type 4 was the least frequent in our study which was similar to previous studies by Mishra *et al*. and Dăescu *et al*.[10,13] We also observed a few undefined branching patterns in this study [Table 3].

In the present study, we found that out of the 4 types of upper segmental artery, type-1 arising from anterior division of renal artery was found to be more frequent which is similar to other studies. There was no association between the pattern of upper segmental branch of renal artery between right and left side ($\chi^2$ = 8.554; $P$ = 0.073). Each segmental artery supplies a distinct portion of the kidney with no collateral circulation between them. Thus, occlusion or injury to a segmental branch will cause segmental renal infarction.[12,17] The relationship of these

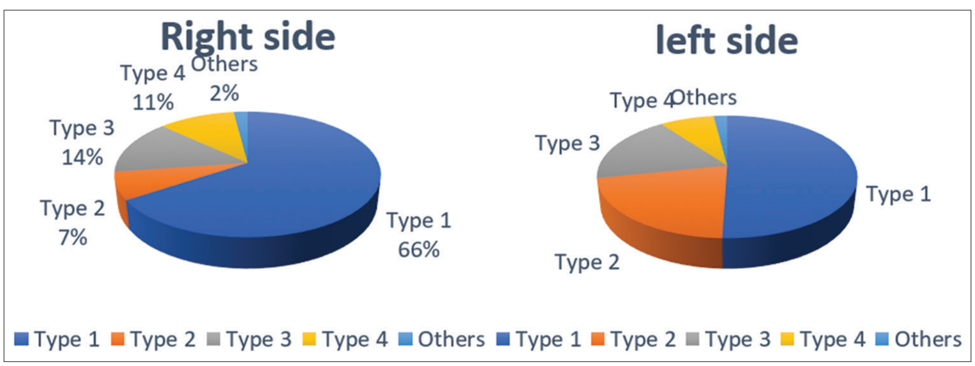


**Figure 1: Distribution pattern of upper segmental branch. There was no association between the pattern of upper segmental branch between right and left side**

**Table 1: Pattern of upper segmental branch of renal artery**

| Pattern | Right | | | Left | | |
|---|---|---|---|---|---|---|
| | Total ($n$=99), $n$ (%) | Male ($n$=54), $n$ (%) | Female ($n$=45), $n$ (%) | Total ($n$=99), $n$ (%) | Male ($n$=54), $n$ (%) | Female ($n$=45), $n$ (%) |
| Type 1 | 65 (65.65) | 35 (64.8) | 30 (66.6) | 50 (50.5) | 28 (52) | 22 (48.8) |
| Type 2 | 7 (7.07) | 5 (9.6) | 2 (4.4) | 21 (21.21) | 7 (13) | 14 (31.1) |
| Type 3 | 14 (14.14) | 7 (13) | 7 (15.5) | 18 (18.18) | 10 (18.5) | 8 (17.7) |
| Type 4 | 11 (11.11) | 5 (9.6) | 6 (13.3) | 8 (8.08) | 7 (13) | 1 (2.2) |
| Others | 2 (2.02) | 2 (2.02) | Nil | 2 (2.02) | 2 (2.02) | Nil |

segmental arteries is important because the posterior segmental branch passes posterior to the renal pelvis while the others pass anterior to the renal pelvis. Ureteropelvic junction obstruction caused by a crossing vessel can occur when the posterior segmental branch passes anterior to the ureter causing occlusion.[18] This division between the posterior and anterior segmental arteries has an additional surgical importance-between these circulations is an avascular plan. Knowledge of the segmental blood supply to the kidney is essential for proper performance of partial nephrectomy.[19] Midpolar partial nephrectomy may be useful in patients with segmental lesions that affect the superior or inferior branches of the anterior segmental renal artery. In upper pole partial nephrectomy, it is therefore possible to damage the main renal artery during tumor excision or occlude a segmental artery supplying the lower portion of the kidney during renography.[6,20]

**Table 2: Relationship of upper segmental artery type and upper segmental artery group**

| Gender | Side | USAT | USAG | | $\chi^2$ |
|---|---|---|---|---|---|
| | | | Group 1 | Group 2 | |
| Male | Right | 1 | 22 | 13 | $\chi^2$=2.078 *P*=0.721 |
| | | 2 | 4 | 1 | |
| | | 3 | 5 | 2 | |
| | | 4 | 4 | 1 | |
| | | Others | 2 | Nil | |
| Male | Left | 1 | 20 | 8 | $\chi^2$=7.958 *P*=0.093 |
| | | 2 | 6 | 1 | |
| | | 3 | 5 | 5 | |
| | | 4 | 2 | 5 | |
| | | Others | 2 | 0 | |
| Female | Right | 1 | 27 | 3 | $\chi^2$=14.217 *P*=0.03 |
| | | 2 | 0 | 2 | |
| | | 3 | 6 | 1 | |
| | | 4 | 6 | 0 | |
| | | Others | 0 | 0 | |
| Female | Left | 1 | 16 | 6 | $\chi^2$=2.864 *P*=0.413 |
| | | 2 | 7 | 7 | |
| | | 3 | 6 | 2 | |
| | | 4 | 1 | 0 | |
| | | Others | 0 | 0 | |

USAT: Upper segmental artery type, USAG: Upper segmental artery group

Knowledge of the arterial branching pattern is of therapeutic value in selective embolization of segmental arteries.[21,22] In terms of the relation between the collecting duct system and upper segmental artery, we found two types, with type 1 being more common than type 2 [Table 2]. USAG 1 was found in 141 (71.21%) kidneys, and USAG 2 was found in 57 (28.79%) kidneys. This is similar to a study by Mishra *et al*. who found USAG 1 in 80% of kidneys.[10] There was a significant association found on the right side in females between USAT and USAG [Table 2]. Successful embolization of segmental arteries has been reported in cases of paediatric renal hypertension, palliative surgeries in renal carcinoma, and postsurgical renal vascular injuries.[23-25] In cases where partial nephrectomy is indicated, such as for small renal masses, knowledge of calyceal and intrarenal patterns is essential for preserving as much healthy kidney tissue as possible while removing the diseased portion. Surgeons can tailor their approach based on the individual patient's anatomy to achieve optimal outcomes with minimal loss of renal function. Studies have shown that factors such as tumor size, location (upper pole), exophytic rate, and nearness to the collecting system significantly affect the decision-making process for surgical approach in laparoscopic partial nephrectomy.[26] The knowledge of relationship of USAT will greatly assist

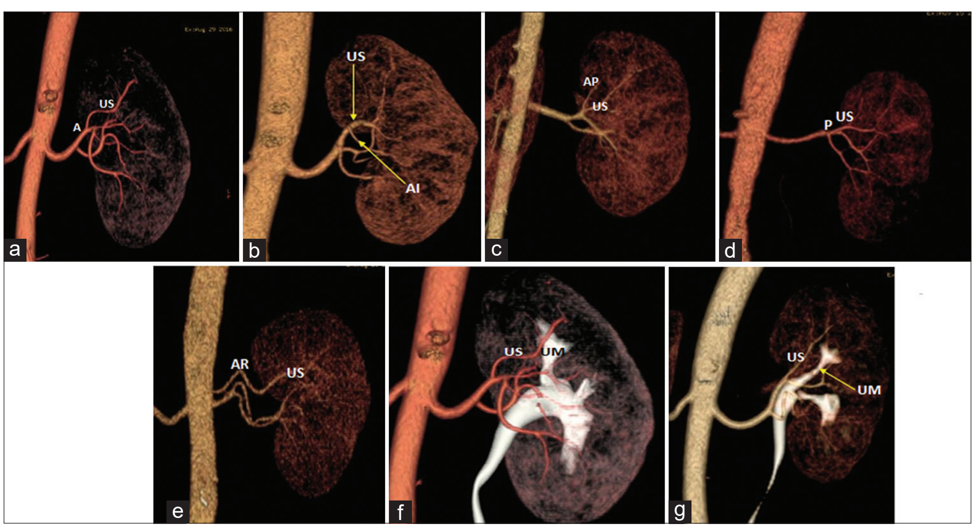


**Figure 2: (a) Upper segmental (US) artery type 1 left side. US artery arises from the anterior division of renal artery (a) given inside the kidney (intrarenal), (b) US artery type 2. US artery arises with anterior inferior segmental artery given at the level of hilum, (c) US type 3. US artery arises with apical segmental artery given inside the kidney (intrarenal), (d) US artery type 4. US artery arises from the posterior division (p) of renal artery given outside the kidney (extrarenal), (e) US artery arises from accessory renal artery, (f) US artery group 1 (passes in front of upper major calyx (UM) left side, (g) US artery group-2 (Runs upwards medial to pelvis and UM calyx)**

**Table 3: Comparison of upper segmental branch with previous studies**

| | Fine and Keen, 1966[14] | Bordei *et al.*, 2012[15] | Dăescu *et al.*, 2012[13] | Mishra *et al.*, 2015[10] | Rani *et al.*, 2014[16] | Present study 2024 |
|---|---|---|---|---|---|---|
| Method | Corrosion cast technique | Dissection, corrosion cast, MRI and CT angiography | Dissection method | Postmortem kidneys by corrosion cast method | Corrosion cast technique | CT angiography |
| Kidneys studied | 107 | 461 | 60 | 100 | 40 | 198 |
| Type I - From anterior division of renal artery (%) | 46.72 | 41.21 | 40 | 40 | - | 58.08 |
| Type II - With middle segmental artery (%) | 19.62 | - | 1.67 | 28 | - | 14.14 |
| Type III - With apical segmental artery (%) | 31.77 | - | 46.67 | 20 | 60 | 16.16 |
| Type IV - From posterior division of renal artery (%) | - | - | 1.67 | 10 | - | 9.59 |
| Others (%) | - | - | - | - | 40 | 2.02 |

CT: Computed tomography, MRI: Magnetic resonance imaging

the surgeon in planning surgical intervention carrying out intrarenal surgeries.[27,28] This study is novel in that it utilizes high-resolution 64-slice MDCT angiography to analyze both the origin pattern of the upper segmental artery and its spatial relationship with the major calyx in live renal donors, with statistical correlation between arterial type, side, and gender.

### Strengths and limitations

The present study was conducted on 99 renal donors and using CT angiogram of 198 kidneys to investigate variations in the upper segmental renal artery and its relationship with the collecting system. The study contributes to the existing body of literature on renal anatomy variations, filling gaps in knowledge and providing a basis for future research and clinical practice guidelines in the field of urology and renal surgery. Despite being derived from a specific population of renal donors, the inclusion of 99 individuals and 198 kidneys provides a substantial dataset for analysis, which can enhance the reliability of study's findings. However, the study's sample may not represent the broader population of individuals with renal anatomy variations, as it focuses specifically on renal donors potentially limiting the generalizability of the findings to larger populations or different demographic groups. While standardized CT angiography ensures consistent imaging and data acquisition, minimizing variability across participants, the interpretation of CT angiograms remains subject to observer bias.

## Conclusion

The present study found four types of variations in the branching pattern of the upper segmental artery in the CT angiograms of renal donors. The upper segmental artery arose from the anterior division in 58.08%, with middle segmental artery in 14.14%, with apical segmental artery in 16.16%, from posterior division in 9.59%, and other undefined sites in 2.02% of kidneys. There were also two distinct types of relationship between upper segmental artery and the collecting system with USAG 1 where the upper segmental artery running in front of the upper major calyx was common being found in 71.21% of kidneys.

A thorough understanding of calyceal and intrarenal patterns empowers surgeons to approach renal disorders with precision, minimizing risks and maximizing the chances of successful outcomes for their patients. A comprehensive understanding of this information can enhance partial-renal transplant surgeries involving the end-to-end anastomosis of the resected kidney segment. With this, the incidence of urological complications following partial nephrectomy would be significantly diminished. It is imperative to preserve every fragment of healthy, functional renal tissue to maintain normal urine excretion.

## Future Directions

Future prospective clinical correlation studies are needed to investigate the association between identified anatomical variations and specific renal pathologies, surgical outcomes, and postoperative complications. Replicating the study with larger and more diverse patient populations and collaborating with urological societies and expert panels to develop evidence-based guidelines and recommendations for surgical approaches and techniques tailored to different renal vascular anatomies could be beneficial.

### Acknowledgment

The authors would like to thank all the participants of this study.

### Declarations

The authors declare that there is no conflict of interest. The entire study was conducted as per the Declaration of Helsinki standards, and the study was approved by the institutional ethics committee. Written consent was obtained from all the study participants of this study.

**Data availability statement**

The data that support the findings of this study are not openly available due to reasons of sensitivity and privacy of the donors. It can be made available from the corresponding author (JS) upon reasonable request.

**Financial support and sponsorship**

Nil.

**Conflicts of interest**

There are no conflicts of interest.

## References

1. Hunter J. Vasculature of the body. Br J Surg. 1794;38:1-8.
2. Brödel M. The Intrinsic Blood-Vessels of the Kidney and Their Significance in Nephrotomy. Proc Assn Am Anat 1900;14:251-60.
3. Graves FT. The anatomy of the intrarenal arteries and its application to segmental resection of the kidney. Br J Surg 1954;42:132-9.
4. Kher G, Bhargava I, Makhni F. Intrarenal branching of the renal artery. Indian J Surg 1960;22:563-79.
5. Bukavina L, Bensalah K, Bray F, Carlo M, Challacombe B, Karam JA, *et al.* Epidemiology of renal cell carcinoma: 2022 update. Eur Urol 2022;82:529-42.
6. Macchi V, Crestani A, Porzionato A, Sfriso MM, Morra A, Rossanese M, *et al.* Anatomical study of renal arterial vasculature and its potential impact on partial nephrectomy. BJU Int 2017;120:83-91.
7. Mousavi-Bahar SH, Mehrabi S, Moslemi MK. Percutaneous nephrolithotomy complications in 671 consecutive patients: A single-center experience. Urol J 2011;8:271-6.
8. Asif M, Farooq K, Ullah MI, Azam A, Bibi R. Complications rate of conventional percutaneous nephrolithotomy (PCNL) in a tertiary care center. Pak J Med Health Sci 2023;17:111.
9. Perappadan BS. Organ Shortage Continues to Cost Lives. The Hindu; 2023. Available from: https://www.thehindu.com/sci-tech/health/indias-poor-organ-donation-record-continues-to-cost-lives/article67161978.ece. [Last accessed on 2023 Aug 07].
10. Mishra GP, Bhatnagar S, Singh B. Anatomical variations of upper segmental renal artery and clinical significance. J Clin Diagn Res 2015;9:C01-3.
11. Fine H, Keen EN. The arteries of the human kidney. J Anat 1966;100:881-94.
12. Bordei P, Şapte E, Iliescu D, Brânzaniuc K, Baz R, Matusz P, *et al.* Morphological assessments on the arteries of the superior renal segment. Surg Radiol Anat 2012;34:137-44.
13. Dăescu E, Zăhoi DE, Motoc A, Alexa A, Baderca F, Enache A. Morphological variability of the renal artery branching pattern: A brief review and an anatomical study. Rom J Morphol Embryol 2012;53:287-91.
14. Rani N, Singh S, Dhar P, Kumar R. Surgical importance of arterial segments of human kidneys: An angiography and corrosion cast study. J Clin Diagn Res 2014;8:1-3.
15. Kumaresan M, Saikarthik J, Sangeetha A, Saraswathi I, Senthil Kumar K, Roselin P. Peri-hilar branching pattern and variations of the renal artery among Indian kidney donors using pre-operative computed tomography angiography: An anatomical study and review. Folia Morphol (Warsz) 2022;81:971-82.
16. Silverberg D, Menes T, Rimon U, Salomon O, Halak M. Acute renal artery occlusion: Presentation, treatment, and outcome. J Vasc Surg 2016;64:1026-32.
17. Chu PL, Wei YF, Huang JW, Chen SI, Chu TS, Wu KD. Clinical characteristics of patients with segmental renal infarction. Nephrology (Carlton) 2006;11:336-40.
18. Ishii H, Aboumarzouk OM, Van Poppel H. Kidney and ureter anatomy. In: Aboumarzouk OM, editor.Blandy's Urology. 3rd ed. Hoboken, NJ:Wiley-Blackwell;2019.p.93-106.
19. Bouzouita A, Saadi A, Hermi A, Chakroun M, Bouchiba N, Allouche M, *et al.* Cadaveric study of arterial renal anatomy and its surgical implications in partial nephrectomy. Surg Radiol Anat 2021;43:1449-59.
20. Marconi L, Desai MM, Ficarra V, Porpiglia F, Van Poppel H. Renal preservation and partial nephrectomy: Patient and surgical factors. Eur Urol Focus 2016;2:589-600.
21. Dogra A, Chauhan R, Sharma S, Partap A, Diwan Y, Chawla K, *et al.* Variations of renal arteries on 64 slice multidetector computed tomography. J Anat Soc India 2017;66:20-5.
22. Trivedi S, Dixit A, Kotgiriwar S, Athavale S, Gupta V, Deopujari R. Variations in the branching pattern of renal artery and its clinical implications. J Anat Soc India 2012;61:229-33.
23. Fung KF, Wong SW, Chan EY, Cheng KK, Cho HY, Kan EY, *et al.* Embolisation of an aneurysmal high-flow renal arteriovenous fistula in a paediatric patient: Simultaneous arterial and venous approach. CVIR Endovasc 2022;5:24.
24. Antabak A, Papeš D, Bulić K, Sjekavica I, Jurca I, Perkov D, *et al*. Traumatic protracted hematuria and segmental renal artery pseudoaneurysm in a 16-year-old boy, treater with endovascular embolization. Lijec Vjesn 2021;143:108-12.
25. Fantoni M, Marcato C, Ciuni A, Pellegrino C, Russo U, Zannoni R, *et al.* Renal artery embolization of non-functioning graft: An effective treatment for graft intolerance syndrome. Radiol Med 2021;126:494-7.
26. Kazan O, Cakici MC, Kokurcan A, Ozenc G, Karakoyunlu N, Atis G, *et al.* Factors influencing the decision-making in laparoscopic partial nephrectomy for small renal masses. Urologia 2023;90:693-701.
27. Bretan PN Jr., Malone MJ. Complex renal reconstruction. Urol Clin North Am 1999;26:201-17, x.
28. Khamanarong K, Prachaney P, Utraravichien A, Tong-Un T, Sripaoraya K. Anatomy of renal arterial supply. Clin Anat 2004;17:334-6.

Original Article

# Anatomical, Morphometrical, and Clinical Relevance of Human Mandible Mental Foramen

**Rasha Mamdouh Salama**

*Department of Anatomy and Histology, College of Medicine, Qassim University, Buraydah, Saudi Arabia*

## Abstract

**Introduction:** The mental foramen (MF) serves as an important reference point in dental and maxillofacial surgeries. Identifying its anatomical, morphometrical, and clinical relevance is vital for surgical planning and implant placement. **Aim:** The aim of this study was to perform an anatomical and morphometrical analysis of the MF in dry human adult mandibles. **Materials and Methods:** The study was conducted on 58 dry adult human mandibles. On each mandible, the number and shape of the mental foramina were recorded, along with their distances to key mandibular landmarks. In addition, the vertical and horizontal diameters of the mental foramina were measured. **Results:** 62.1% exhibited a single MF on both sides, whereas 20.7% had a single foramen on the right side, with the left side lacking a foramen. Ten mandibles (17.2%) displayed a double MF on the right side and a single foramen on the left. Considering the 109 documented mental foramina, 89 were round in shape, whereas the remaining 20 were oval. The positions of the MF relative to key mandibular landmarks showed noticeable differences between the right and left sides. On the right side, the vertical diameter of the MF measured 3–5 mm, and the horizontal diameter measured 2.5–6.5 mm. On the left side, the vertical diameter measured 3–5.5 mm, and the horizontal diameter measured 2–6 mm. **Conclusion:** MF is a consistent anatomical foramen present on every mandible under study. It demonstrates marked variability in anatomical and morphometrical parameters. Recognizing these variations is vital for surgeons to protect the mental nerve from inadvertent injury.

**Keywords:** *Anatomical, mandible, mental foramen, mental nerve, morphometrical*

## Introduction

Mental foramen (MF) is an oval or circular aperture situated on the body of the mandible, typically positioned equidistant from its superior and inferior borders, marking the termination of the mandibular canal. Through this foramen pass the mental nerve, artery, and vein – terminal branches of the inferior alveolar neurovascular bundle. Functionally, the mental nerve is purely sensory and divides into three or four terminal branches that provide essential innervation to the lower face, including the mandibular teeth, lower lip, labial mucosa, and gingiva.[1] Because of its critical anatomical role, the mental nerve is vulnerable to injury during various surgical and dental procedures, and such damage may result in sensory disturbances that significantly affect a patient's quality of life.[2] Moreover, accurate localization of the MF is fundamental for performing effective mental nerve block anesthesia.[3]

The anatomical study of the MF holds considerable clinical relevance. Determining its precise position is crucial for dentists and surgeons involved in periodontal surgery,[4] surgical orthodontics,[5] endodontic treatments, implantology, and other maxillofacial interventions. As an important anatomical landmark, the MF must be carefully identified during osteotomy procedures, surgical approaches to the mandible, and nerve-block techniques to avoid neurovascular damage.[6] Furthermore, detailed knowledge of its anatomical variations is essential to preventing postoperative complications such as persistent paresthesia or dysesthesia.

Beyond its clinical implications, the anatomy and morphology of the MF are valuable for broader scientific and anthropological purposes. Its characteristics contribute to the assessment of mandibular symmetry, the analysis of bone remodeling patterns, and the study of microscopic and macroscopic variations across populations. These features also provide insights into evolutionary and paleoanthropological



**How to cite this article:** Salama RM. Anatomical, morphometrical, and clinical relevance of human mandible mental foramen. J Anat Soc India 2026;75:54-60.

**Article Info**

**Received:** 03 December 2025
**Revised:** 10 January 2026
**Accepted:** 14 January 2026
**Available online:** 27 March 2026

***Address for correspondence:***
*Dr. Rasha Mamdouh Salama, Department of Anatomy and Histology, College of Medicine, Qassim University, Buraydah, Saudi Arabia.*
*E-mail: r.salama@qu.edu.sa*

**Access this article online**

**Website:** https://journals.lww.com/joai

**DOI:** 10.4103/jasi.jasi_192_25

**Quick Response Code:**

differences in the facial skeleton.[7] In maxillofacial and anesthetic surgery, a lack of familiarity with the MF's potential variations can lead to inadvertent transection of the mental nerve, resulting in long-term sensory deficits in the perioral tissues.

The precise identification of the nerve's emergence point is therefore essential, especially when performing unilateral mental nerve blocks – commonly required for procedures involving the lower lip, chin, or gingiva – to ensure adequate anesthesia while minimizing complications. Mental nerve block anesthesia is generally preferred over infiltration techniques to reduce the risk of tissue damage and postoperative sequelae, particularly during wound repair.[8]

Given these considerations, this study aimed to conduct a comprehensive analysis of the MF by evaluating its anatomical location, incidence, number, and shape, as well as its spatial relationships to key mandibular landmarks. In addition, the study assessed both the vertical and horizontal diameters of the MF to provide detailed morphometric data that may enhance clinical safety and improve surgical and anesthetic planning.

## Materials and Methods

### Study design and setting

This comparative descriptive study was conducted over a 3-month period, from November 2025 to January 2026, in the Department of Anatomy. All dry adult human mandibles meeting the eligibility criteria were systematically examined. Each mandible was evaluated independently to define all anatomical landmarks prior to measurement. All measurements were performed professionally twice to ensure accuracy, reproducibility, and interobserver consistency.

### Inclusion criteria

Mandibles were included if they met the following conditions:

- Adult human dry mandibles of fully developed size and morphology
- Integrity of the mandible was preserved without evidence of fractures, deformities, or structural defects
- Well-preserved alveolar margins without signs of alveolar bone resorption or postmortem deterioration
- Clearly identifiable bony landmarks are required for measurement of the MF.

### Exclusion criteria

Mandibles were excluded from the study if they demonstrated:

- Damage affecting the body, ramus, or alveolar process, rendering measurements unreliable
- Partial or complete loss of anatomical landmarks relevant to the MF
- Severe post-mortem deterioration, warping, or erosion
- Evidence of pathological lesions or congenital abnormalities altering normal mandibular morphology
- Fragmentation or breakage preventing accurate assessment of foramen number or position.

### Sample description

A total of 58 dry adult mandibles satisfied the inclusion criteria and were included in the final analysis. All mandibles were fully edentulous or partially dentate without alveolar collapse severe enough to obscure anatomical references.

### Measurement tools

The following instruments were used for precise morphometric assessment:

- Double-pointed compass for marking reference points
- Graduated ruler and a tape measure for gross measurements
- Digital Vernier caliper (precision to 0.01 mm) for fine linear measurements, such as vertical and horizontal diameters of the MF.

All tools were calibrated before use to ensure measurement accuracy.

### Parameters assessed

For each mandible, the following anatomical and morphometric variables were assessed:

1. Number of mental foramina present on each side
2. Shape of the MF, categorized as round or oval
3. Position relative to the symphysis menti (expressed in millimeters)
4. Distance from the upper border of the mandibular body
5. Distance from the lower border of the mandibular body
6. Vertical and horizontal diameters of the mental foramina.

Both the shape as well as number of the foramina were identified through direct visual inspection. Linear distances and diameters were measured leveraging the Digital Vernier caliper, with all values recorded in millimeters (mm). Care was taken to ensure consistent orientation of each mandible during measurement.

### Data collection process

All measurements were recorded on a pre-established data collection form. The findings documented independently and cross-validated entries. Any discrepancies were remeasured and resolved to minimize interobserver variation.

Data were then transferred into an Excel spreadsheet for organization, tabulation, and preliminary numerical summarization.

### Classification of mandibles by foramen distribution

Based on the number and laterality of mental foramina among the 58 mandibles, three major patterns were identified:

1. Single MF on both sides ($n$ = 36): Each mandible

exhibited one foramen on the right and one on the left
2. Single MF on right side, absent on left (*n* = 12): Only one foramen was present on the right, with no corresponding left foramen
3. Double MF on right side and single on left (*n* = 10): Two foramina were identified on the right, with a single foramen on the left.

In total, 109 mental foramina were identified in the sample. These foramina were further classified by shape:
- Round foramina (*n* = 89)
- Oval foramina (*n* = 20).

Shape determination was based on the longest-to-shortest diameter ratio observed during inspection and caliper measurement.

### Ethical approval

All procedures adhered to the ethical guidelines of the Deanship of Graduate Studies and Scientific Research, Qassim University, Saudi Arabia. The study obtained ethical approval from the Committee of Research Ethics (Approval No. 26-6-7).

### Statistical analysis

Quantitative variables – including linear distances and diameters – were analyzed using descriptive statistics such as mean, standard deviation, and minimum and maximum values. Qualitative variables – including number, laterality, and shape categories – were summarized as frequencies and percentages.

Statistical analysis was performed using SPSS version 26.0 (IBM Corp., Armonk, NY, USA). Data entry and verification were conducted carefully to ensure accuracy and reproducibility. The analysis workflow ensured methodological rigor and allowed valid interpretation of the morphometric variations observed among the mandibles.

## Results

MF is a small but constant anatomical opening identified in all 58 mandibles examined in this study. It is situated on the anterolateral surface of the mandibular body, typically positioned at the level between the second premolar and first molar, and located approximately midway between the upper (alveolar) border – containing 16 dental sockets – and the lower border of the mandible [Figure 1].

Fifty-eight dry human mandibles were evaluated in this study for the number and laterality of mental foramina. It was found that thirty-six mandibles (62.1%) represented the majority of studied mandibles presented a single MF on the right side as well as on the left side [Figures 2, 3 and Table 1]. Twelve mandibles (20.7%) presented a single foramen on the right side only with absent foramen on the left side [Figures 3, 4 and Table 1]. Finally, 10 mandibles (17.2%) presented double mental foramina on the right side and a single foramen on the left side [Figures 3, 5 and Table 1].

The present study outlined 109 mental foramina out of the 58 mandibles studied. Based on the shape of these mental foramina. The series outlined 89 mental foramina (81.7%) were round in shape. However, the remaining 20 foramina (18.3%) were oval shaped [Figures 6, 7 and Table 2].

The position of the MF with respect to the symphysis menti and the upper and lower borders of the mandibular body was assessed, as illustrated in [Figure 8 and Table 3]:

I. Distance between MF and symphysis menti [Figure 8a]:
   - Right side: Measurements varied between 23 mm and 30 mm, with an average of 26.5 mm and a variability of 2.29 mm
   - Left side: Values extended from 20 mm to 28 mm, with a mean of 24 mm and a variability of 2.58 mm

II. Distance between MF and the upper border of the mandibular body [Figure 8b]:
   - Right side: Distances were measured at 12–14 mm, averaging 13 mm, with a variability of 0.82 mm

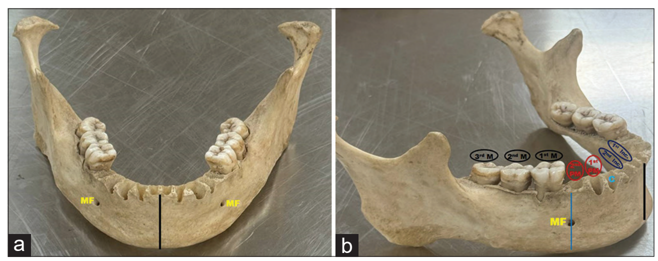


**Figure 1: Dry human mandible illustrating: (a) Anterior view of mandible showing MF on both sides of the mandible and symphysis menti, a vertical indistinct line along midline on body of mandible (black line). (b) Right side of the mandible showing the upper alveolar border of body of mandible bears eight sockets for permanent teeth as follow; first incisor (1st Inc.), second incisor (2nd Inc.), canine (C), first premolar (1st PM), second premolar (2nd PM), first molar (1st M), second molar (2nd M), and third molar (3rd M). Right MF located nearly at the level between the 2nd premolar and 1st molar (blue line), midway between the upper and lower borders of the mandible. Note; symphysis menti (black line) were also observed**

**Table 1: Allocation of mental foramen according to the number and laterality (*n*=58 mandibles)**

| Allocation of MF according to the number and laterality | Frequency (%) |
|---|---|
| Single MF on both sides | 36 (62.1) |
| Single MF on right side and absent on left side | 12 (20.7) |
| Double MF on right side and a single MF on left side | 10 (17.2) |

MF: Mental foramen

**Table 2: Distribution of mental foramen according to the shape (*n*=109 mental foramina)**

| Distribution of MF according to the shape | Frequency (%) |
|---|---|
| Round MF | 89 (81.7) |
| Oval MF | 20 (18.3) |

MF: Mental foramen

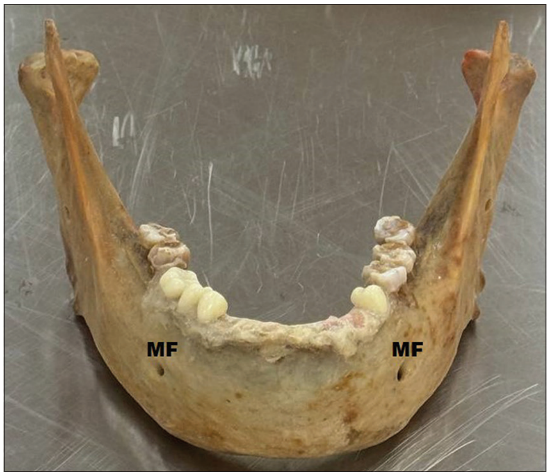


**Figure 2: Dry human mandible demonstrating a single MF on the right side as well as on the left side. MF: Mental foramen**


**Figure 4: Dry human mandible displaying a single MF on the right side with absent foramen on the left side. MF: Mental foramen**

**Figure 6: Dry human mandible revealing round MF on left side (blue) and oval MF on the right side (red)**

- Left side: Values ranged from 13 mm to 16 mm, with an average of 14.5 mm and a variability of 1.12 mm

III. Distance between MF and the lower border of the mandibular body [Figure 8b]:

- Right side: Measurements fell between 11 mm and 15 mm, with a mean of 13 mm and a variability of 1.41 mm
- Left side: Values extended from 12 mm to 16 mm, averaging 14 mm, with a variability of 1.41 mm.

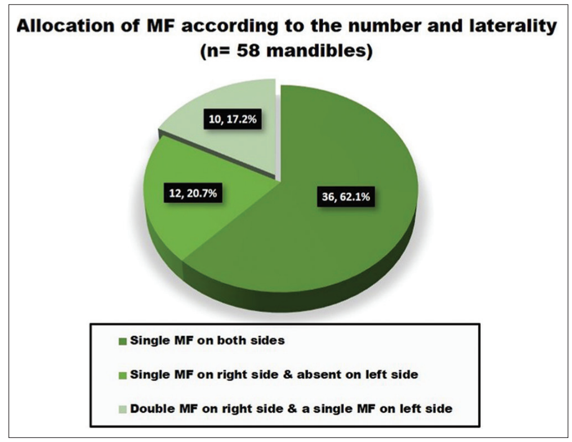


**Figure 3: Chart demonstrating allocation of MF according to the number and laterality (*n* = 58 mandibles). MF: Mental foramen**

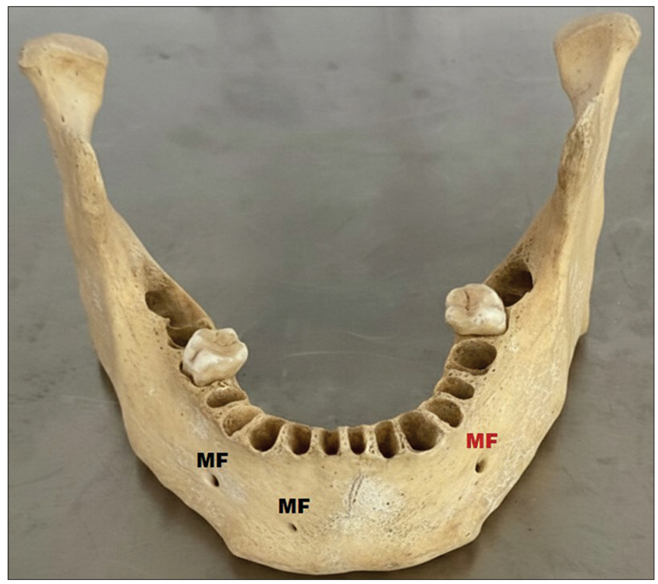


**Figure 5: Dry human mandible revealing double mental foramina on the right side and a single foramen on the left side. MF: Mental foramen**

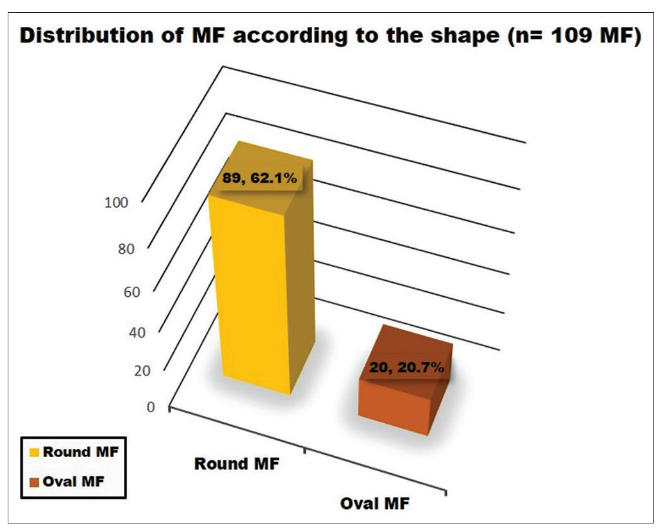


**Figure 7: Histogram revealing the distribution of MF according to the shape (*n*= 109 mental foramina). MF: Mental foramen**

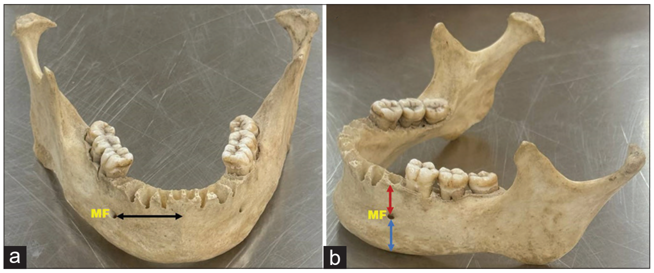


**Figure 8: (a) Location of the MF with respect to the symphysis menti (black arrow). (b) Location of the MF relative to the upper border of the mandibular body (red arrow) and the lower border of the mandibular body (blue arrow). MF: Mental foramen**

Finally, Table 4 demonstrating the vertical and horizontal diameters of MF: On the right side, the vertical diameter of the MF measured 3–5 mm, averaging 4 mm with a variability of 0.82 mm, whereas the horizontal diameter extended 2.5–6.5 mm, with a mean of 4.5 mm and a variability of 1.15 mm. On the left side, the vertical diameter measured 3–5.5 mm, with an average of 4.25 mm and a variability of 0.72 mm, and the horizontal diameter measured 2–6 mm, averaging 4 mm with a variability of 1.16 mm.

**Table 3: Descriptive statistics of the variations of the distance of mental foramen to symphysis menti, and the upper and lower borders of the body of the mandible**

| Variables (mm) | Range (minimum–maximum) | Mean±SD |
|---|---|---|
| Distance between MF and symphysis menti | A (23–30)<br>B (20–28) | A (26.5±2.29)<br>B (24±2.58) |
| Distance between MF and the upper border of the body of the mandible | A (12–14)<br>B (13–16) | A (13±0.82)<br>B (14.5±1.12) |
| Distance between MF and the lower border of the body of the mandible | A (11–15)<br>B (12–16) | A (13±1.41)<br>B (14±1.41) |

A: Right side, B: Left side, SD: Standard deviation, MF: Mental foramen

**Table 4: Descriptive statistics of the vertical and horizontal diameters of mental foramen**

| Diameters (mm) | Range (minimum–maximum) | Mean±SD |
|---|---|---|
| Vertical diameter of MF | A (3–5)<br>B (3–5.5) | A (4±0.82)<br>B (4.25±0.72) |
| Horizontal diameter of MF | A (2.5–6.5)<br>B (2–6) | A (4.5±1.15)<br>B (4±1.16) |

A: Right side, B: Left side, SD: Standard deviation, MF: Mental foramen

## Discussion

MF is a key anatomical landmark of the mandible and holds considerable clinical, surgical, and forensic significance. It serves as the exit point of the mental neurovascular bundle and is therefore critically important during maxillofacial diagnostics, local anesthesia administration, dental interventions, implant placement, and various esthetic or reconstructive procedures.[9] Because the MF is often difficult to palpate and lacks easily identifiable soft-tissue landmarks, numerous studies have focused on determining its precise position and morphological characteristics using dry mandibles, cadaveric dissections, and advanced radiographic modalities.[10,11] These variations are not only relevant for clinical practice but also have anthropological value in identifying skeletal remains and distinguishing population-specific patterns for forensic investigations. Thus, ensuring accurate knowledge of the MF's location, shape, number, and symmetry is essential to avoid neurovascular injury and to improve procedural success across different subpopulations.

The present study, therefore, aimed to provide detailed anatomical insights into the MF, including its incidence, shape, number, symmetry, distances from key mandibular landmarks, and its vertical and horizontal diameters. This comprehensive assessment contributes valuable reference data that may aid clinicians, surgeons, and anatomists in planning safe interventions.

All 58 mandibles examined in this study exhibited MF, confirming its presence as a constant anatomical structure. In most cases, the MF was located in the anterolateral region of the mandible, typically at the level between the second premolar and first molar and approximately midway between the superior and inferior borders of the mandibular body. These findings are consistent with those reported by Eboh and Oliseh,[12] who noted that MF position varies among populations but tends to lie near the region of the second premolar, with a slightly more posterior tendency in Black populations compared to White populations. A study on Tanzanian mandibles similarly documented predominant positioning below the second premolar or at the line between the second premolar and first molar, with asymmetry also frequently observed.[13]

Assessment of MF shape revealed that 81.7% of foramina were round, whereas 18.3% were oval. This contrasts with some previous reports – such as Eboh and Oliseh[13] and Udhaya *et al.*[14] – in which the oval shape was more common. The reasons for shape variation remain unclear, but embryological factors and population-specific feeding behaviors have been proposed as possible contributors.[15] These discrepancies underscore the importance of establishing region-specific anatomical databases.

Regarding the number and laterality of MF, the present study found that 62.1% of mandibles showed a single MF on both sides, wheras 20.7% exhibited a single MF on the right side with absence on the left, and 17.2% demonstrated double foramina on the right side and a single on the left. Duplication of the MF is the most frequently reported numerical variation, and although some studies – such as Ndiaye *et al.*[8] – identified only isolated cases of double foramina, others with larger samples (e.g., Udhaya *et al.*[14]) reported a greater number of supernumerary foramina. No cases of complete MF absence were observed in the present study, consistent with findings by Ndiaye *et al.*,[8] although rare reports of MF absence do exist.[16]

The morphometric assessments in our sample also demonstrated meaningful variability. The distance between the MF and the symphysis menti ranged from 23 to 30 mm on the right (mean 26.5 mm) and 20–28 mm on the left (mean 24 mm). These values align closely with the 25 mm average reported by Ndiaye *et al.*[8]

Similarly, the distance from the foramen to the superior border of the mandible ranged from 12 to 14 mm on the right and 13–16 mm on the left. The inferior border distances (mean 13 mm on the right and 14 mm on the left) were nearly identical to those documented by Ndiaye *et al.*[8] Such consistency reinforces the reliability of these measurements for clinical application.

With respect to MF diameters, this study found mean vertical diameters of 4 mm (right) and 4.25 mm (left), and mean horizontal diameters of 4.5 mm (right) and 4 mm (left). Ndiaye *et al.*[8] reported slightly smaller vertical diameters (3.3 mm right, 3.2 mm left), whereas Igbigbi and Lebona[17] observed even smaller dimensions, particularly vertically. Such differences may reflect population-specific structural variations, environmental influences, or measurement methodologies.

Overall, the findings of this study corroborate much of the existing literature while highlighting certain population-based variations. These differences emphasize the need for careful preoperative evaluation of the MF, especially when performing dental implants, periapical surgery, fracture fixation, or mental nerve blocks.

Misidentification of the MF position or diameter may lead to mental nerve injury, postoperative paresthesia, or inadequate anesthesia – complications that can have clinical, psychological, and even medicolegal repercussions.

## Conclusion

The anatomical variability of the MF documented in this study underscores the critical importance of population-specific morphometric knowledge. Accurate localization, awareness of potential asymmetry, and recognition of morphological variations are essential to ensuring safe surgical approaches, minimizing risks to the neurovascular bundle, and enhancing procedural success in dental and maxillofacial practice.

### Limitation of the study

1. Age, sex, and ethnic background of the examined mandibles were not available, which restricted the ability to evaluate morphological variations related to demographic or population-specific characteristics. Such information is crucial for determining whether observed anatomical differences are influenced by biological sex, age-related changes, or ethnic variability
2. The study relied exclusively on dry mandibles, which, although valuable for direct morphological assessment, do not allow evaluation of soft-tissue relationships that may influence the clinical palpation or radiographic appearance of the MF.

Future studies incorporating larger, well-documented samples and correlating dry bone measurements with radiographic imaging could provide more comprehensive insights.

### Acknowledgments

I have the pleasure to express my sincere appreciation to the Deanship of Higher Education and Research at Qassim University for their invaluable and continuous support throughout this project. Their commitment to advancing scholarly inquiry, coupled with the logistical, administrative, and institutional support they provided, played a pivotal role in ensuring the smooth execution and successful completion of this research. Their continual encouragement and dedication to advancing academic excellence are sincerely acknowledged and greatly appreciated.

### Financial support and sponsorship

Nil.

### Conflicts of interest

There are no conflicts of interest.

## References

1. Thomaidi ZM, Tsatsarelis C, Papadopoulos V. Accessory Mental Foramina in Dry Mandibles An Observational Study Along with Systematic Review and Meta-Analysis. Dent J 2025;13:94.
2. Pelé A, Berry PA, Evanno C, Jordana F. Evaluation of Mental Foramen with Cone Beam Computed Tomography A Systematic Review of Literature. Radiol Res Pract 2021;2021:8897275.
3. Sheikhi M, Kheir MK. CBCT Assessment of Mental Foramen Position Relative to Anatomical Landmarks. Int J Dent 2016;2016:5821048.
4. Gaudy FF, Cannas B, Gillo L, Gorce T. Atlas of Implant Anatomy. Issy-les-Moulineaux: Elsevier-Masson; c2011.
5. Von Arx T. [The mental foramen or "the crossroads of the mandible." An anatomic and clinical observation]. Schweiz Monatsschr Zahnmed 2013;123:205-25.
6. Kqiku L, Weiglein A, Kamberi B, Hoxha V, Meqa K, Städtler P. Position of the mental foramen in Kosovarian population. Coll Antropol 2013;37:545-549.
7. Voljevica A, Talovic E, Hasanovic A. Morphological and morphometric analysis of the shape, position, number and size of mental foramen on human mandibles. Acta Med Acad 2015;44:31-38.
8. Ndiaye MR, Mar NB, Yacouba Garba K, Ndoye JMN. Mental foramen of Human Mandible Morphometric Study. Int J Anat Res 2021;9:8109-8115.

9. Ravindranadh G, Rao SB, Kommanda RKS. Study of mental foramen in dry human mandibles of adult and its significance An anatomical study. Int J Health Sci 2022;6:2285-2292.
10. Currie CC, Meechan JG, Whitworth JM, Carr A, Corbett IP. Determination of the mental foramen position in dental radiographs in 18-30 year olds. Dentomaxillofac Radiol 2016;45:20150195.
11. Sankar DK, Bhanu SP, Susan PJ. Morphometrical and morphological study of mental foramen in dry dentulous mandibles of South Andhra population of India. Indian J Dent Res 2011;22:542-546.
12. Eboh DE, Oliseh EI. Analysis of mental foramen in dry human mandibles of adult Nigerians. Afr J Med Med Sci 2014;43:107-113.
13. Rajkohila J, Daniel P, Ambikaipakan S, Rabi S. Morphological and morphometric analysis of accessory mental foramen in dry human mandibles of south indian population. Indian J Dent Res 2018;29:56.
14. Udhaya K, Saraladevi KV, Sridar J. The morphometric analysis of the mental foramen in adult dry mandibles a study on the South Indian population. J Clin Diagn Res 2013;7:1547-1551.
15. Balakrishnan YA, Vikram S, Rao CP, Revankar SK. Position of mental foramen in dry human mandibles and its significance. Int J Anat Res 2018;6:5228-5232.
16. Hassan T, Fauzi M, Hasan D. Bilateral absence of mental foramen a rare variation. Int J Anat Var 2010;3:187-189.
17. Igbigbi PS, Lebona S. The position and dimensions of the mental foramen in adult Malawian mandibles. West Afri J Med 2005;24:184-189.

Original Article

# Cervical Intervertebral Disc Degeneration in Patients with Chronic Neck Pain: Role of Interleukin-1α, Interleukin-6, and Tumor Necrosis Factor-α as Biomarkers


## Abstract

**Background and Objectives:** Cervical intervertebral disc degeneration (CIDD) frequently leads to neck pain, yet its exact cause remains unclear. While inflammation is associated with degenerative disc disease, the precise function of cytokines in CIDD remains a mystery. The aim was to investigate the role of serum cytokines (interleukin [IL]-1α, IL-6, and tumor necrosis factor [TNF]-α) as biomarkers in patients with chronic neck pain having CIDD. **Subject and Methods:** The case–control study was carried out among 88 participants. Forty-four patients with chronic neck pain (pain lasting >3 months), exhibiting moderate or severe CIDD in lateral X-ray of the cervical spine, and age, sex, and body mass index matched 44 controls, were included in the study. Levels of IL-1, IL-6, and TNF-α in serum were measured using enzyme-linked immunosorbent assay. Pain intensity was assessed utilizing a Visual Analog Scale. **Results:** Out of 44 patients, 14 had severe, whereas 30 had moderate CIDD. The mean intensity of pain in patients was 72.25 ± 11.18. Serum levels of IL-1 (patients – 7.32 pg/mL, control – 2.98 pg/mL, $P = 0.021$), IL-6 (patients – 8.59 pg/mL, control – 2.98 pg/mL, $P = 0.023$), and TNF-α (patients – 19.29 pg/mL, control – 7.44 pg/mL, $P = 0.011$) were significantly elevated in patients compared to the controls. The pain intensity showed a positive correlation with the severity of CIDD ($P = 0.045$) and serum levels of IL-6 ($P = 0.034$) and TNF-α ($P = 0.041$). **Conclusions:** The serum levels of IL-1α, IL-6, and TNF-α cytokines are significantly elevated in patients with moderate or severe CIDD. There is a significant positive association between serum IL-6 and TNF-α, with the intensity of pain. Assessing the cytokine profiles of patients could provide valuable insights into managing CIDD and predicting their outcomes.


**Keywords:** *Biomarkers, cervical intervertebral disc degeneration, chronic neck pain, cytokines, enzyme-linked immunosorbent assay, intensity of pain*


**Thuduwage Chamalika Sujeewanie Weerakoon[1], Poruwalage Harsha Dissanayake[2], Thilini Nisansala[3,4], Manjula Manoji Weerasekera[4], Surangi Jayakody[5,6], Surangi Gayaneetha Yasawardene[2]**

*[1]Department of Anatomy, Faculty of Medicine, Sabaragamuva University of Sri Lanka, Batuhena, Ratnapura, Departments of [2]Anatomy, [4]Microbiology and [6]Community Medicine, Faculty of Medical Sciences, University of Sri Jayewardenepura, Gangodawila, Nugegoda, [3]Preclinical Department, Faculty of Veterinary Medicine, Universiti Malaysia Kelantan, Kota Baru, Kelatan, Malaysia, [5]Division of Health Sciences, Warwick Medical School, University of Warwick, United Kingdom*



**Article Info**

**Received:** 02 November 2024
**Accepted:** 18 August 2025
**Available online:** 27 March 2026



***Address for correspondence:***
*Dr. Thuduwage Chamalika Sujeewanie Weerakoon, Department of Anatomy, Faculty of Medicine, Sabaragamuwa University of Sri Lanka, Batuhena, Ratnapura, Sri Lanka. E-mail: tcsweerakoon@med.sab.ac.lk*



**Access this article online**

**Website:** https://journals.lww.com/joai

**DOI:** 10.4103/jasi.jasi_179_24

**Quick Response Code:**


## Introduction

Cervical intervertebral disc degeneration (CIDD) has long been considered to be a common cause of neck pain.[1] Diagnosis and treatment of CIDD are difficult as the pathology behind the disease is not yet fully understood.[2]

The cervical intervertebral disc consists of the nucleus pulposus (NP) and the surrounding annulus fibrosus (AF). Disc degeneration can result from the production of proinflammatory molecules secreted by NP and AF cells, as well as by macrophages, T cells, and neutrophils.[3,4] These cytokines trigger pathogenic reactions in disc cells, leading to autophagy and apoptosis.[4] CIDD is marked by structural changes and cell-mediated responses to disc composition alterations.[5]

Studies on the lumbar region have shown that interleukin (IL)-1, IL-6, and tumor necrosis factor (TNF)-α are linked to disc degeneration.[6] Earlier research found IL-1 produced in degenerated lumbar discs,[7] and later suggested both IL-1 and TNF-α play roles, with IL-1 being more significant for therapeutic targeting.[8] IL-6, IL-8, and prostaglandin E2 levels were measured in lumbar disc tissue from patients undergoing fusion surgery for discogenic pain, showing significant differences in IL-6 and IL-8 levels ($P < 0.05$).[9] Lumbar disc degeneration (LDD) involves elevated levels of inflammatory cytokines, including TNF-α, IL-1, IL-6, and others.[2,10]

Most studies carried out to assess the role of cytokines on the lumbar region using tissue samples of the intervertebral disc. Studies



**How to cite this article:** Weerakoon TC, Dissanayake PH, Nisansala T, Weerasekera MM, Jayakody S, Yasawardene SG. Cervical intervertebral disc degeneration in patients with chronic neck pain: Role of interleukin-1α, interleukin-6, and tumor necrosis factor-α as biomarkers. J Anat Soc India 2026;75:61-7.

using serum samples to investigate the levels of cytokines in patient populations are lacking[11] and further studies on the neck region are few. This study was designed to seek a possible association between the selected serum cytokines and CIDD in patients with chronic neck pain.

Studies conducted on LDD[6,12,13] demonstrated the association between LDD and the level of different cytokines. However, an association of inflammatory cytokines in cervical pathologies is lacking.[13] A better understanding of the role of cytokines in relation to CIDD will update the current knowledge on this subject to stimulate future research. As well as to focus on novel cytokine-centered therapeutic interventions for controlling this disease.

Our study aimed to detect the role of selected ILs (IL-1, IL-6), and TNF-α in chronic neck pain patients with CIDD. Furthermore, we studied the association of IL-1, IL-6, and TNF-α levels with the intensity of pain.

## Subject and Methods

### Study design, setting, and participants

A case–control study was conducted in Colombo, Sri Lanka, from March 2021 to March 2022, including 44 chronic neck pain patients (aged 40–69) with moderate or severe CIDD on lateral cervical spine X-rays. These patients were selected from 384 chronic neck pain patients (>3 months) attending the rheumatology clinic at Colombo South Teaching Hospital. CIDD was graded using the previously developed scoring system[14] and categorized as "none or mild" and "moderate or severe." Random sampling was used to select 44 patients from the 246 with moderate or severe CIDD.

Chronic neck pain was defined as "pain originating from musculoskeletal tissue in the region from the occiput to the first thoracic vertebrae" that lasted for more than 3 months.[15,16]

History of the surgical interventions of the cervical spine, trauma to the neck, diagnose patients of metabolic bone diseases (e.g., osteoporosis and osteomalacia), neoplasia (e.g., metastases, multiple myeloma), bone infections (e.g., osteomyelitis, abscess in the vertebral column, tuberculosis), chronic lumbar pain, LDD, inflammatory diseases, and autoimmune disease, who were on medications such as nonsteroidal anti-inflammatory drugs and pregnant mothers were excluded from the study. Age between 40–69 years and age (±5 years), sex, and body mass index (BMI) matched controls ($n$ = 44) were selected through an open notice. A person with any neck-related complaints or diagnosed inflammatory conditions, such as rheumatoid arthritis or any form of disease condition listed in the above exclusion criteria, was excluded from the control group too. Since we did not want to expose healthy individuals to unnecessary radiation, X-rays were not done for the control group.

This study obtained the ethical approval from the Ethics Review Committee of the University of Sri Jayewardenepura (Ref. No 45/20, Date: January 29, 2021). Written consent was obtained from all participants, following the ethical guidelines specified by the Declaration of Helsinki principles.

### Radiological assessments

The X-ray measurements, such as: height loss and size of anterior osteophytes on the lateral cervical X-ray were taken by the software "AutoCAD 2014" (computer-aided design is a powerful tool for automating graphical work) [Figure 1]. These X-ray features and endplate sclerosis [Figure 2] were assessed independently by two consultant radiologists, who were unaware of the patients' clinical information, and the average of their findings was obtained. Height loss and size of anterior osteophytes were graded, and CIDD was derived using the method previously developed[14] [Table 1].

### Data collection

Demographic and clinical data were collected through a pretested questionnaire. Pain intensity was assessed using the Visual Analog Scale (0–100) based on the average over the past seven days.[17] Pain intensity was categorized as mild (1–25), moderate (26–50), severe (51–75), and worst possible (76–100), following Jensen *et al*. with modifications.[18] Weight (SALTER scale) and height (Prestige Stadiometer) were measured with light

**Table 1: Scoring system to assess the degree of cervical intervertebral disc degeneration in lateral cervical**

| Grade | Score |
|---|---|
| Height loss of middle disc height compared to a normal middle disc height at an adjacent level | |
| 0% | 0 points |
| ≤25% | 1 point |
| >25%–≤50% | 2 points |
| >50%–≤75% | 3 points |
| >75% | 4 points |
| The length of anterior osteophytes with respect to the AP diameter of the corresponding vertebral body | |
| No osteophytes | 0 points |
| ≤1/8 AP diameter | 1 point |
| >1/8–≤1/4 AP diameter | 2 points |
| >1/4 AP diameter | 3 points |
| Endplate sclerosis | |
| No sclerosis | 0 point |
| Detectable | 1 point |
| Definite | 2 points |
| Overall degree of disc degeneration=1+2+3 | |
| 0 point (no degeneration) | |
| 1–3 points (mild degeneration) | |
| 4–6 points (moderate degeneration) | |
| 7–9 points (severe degeneration) | |

AP: Anterior posterior

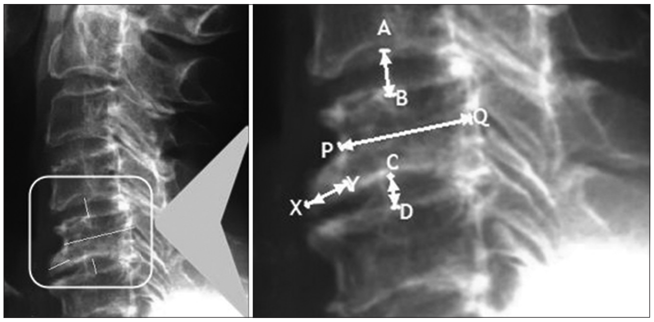


**Figure 1: Lateral X-ray of cervical spine shows height loss and size of anterior osteophytes, A-B: normal middle disc height at an adjacent level, C-D: middle disc height at the degenerated level, P-Q: anterior posterior diameter of the vertebral body, X-Y: length of anterior osteophytes, Height loss (CD/AB) and size of anterior osteophytes (XY/PQ)**

clothing and no shoes, rounded to the nearest 0.1 kg and 0.1 cm. BMI was calculated using Asia-Pacific cutoff points.[19]

### Specimen collection

Venous blood (3 mL) was collected between 8:00 a.m. and 9:00 a.m. to reduce any variability resulting from diurnal variations. The serum was separated and preserved at −80°C for cytokine studies.

### Detection of serum levels of cytokines

Serum levels of IL-1, IL-6, and TNF-α in patients and controls were measured using ELISA according to the manufacturer's guidelines [Supplementary Data Sheet 1]. Absorbance at 450 nm was corrected for background and analyzed in GraphPad Prism 6 to determine cytokine concentrations.

### Statistical analysis

Data were entered and checked for errors using SPSS version 25.0 (IMB SPSS, New York, USA). ELISA results were analyzed with GraphPad Prism version 7. Descriptive statistics were used for data presentation and population parameter estimation among CIDD patients, with a 95% confidence interval (CI). A significance level of 0.05 was chosen.

Normality was assessed using the Shapiro–Wilk test. Categorical variables were compared using the Pearson Chi-square test, whereas continuous variables were analyzed using either the Student's *t*-test or Mann–Whitney *U*-test, as appropriate. Spearman's correlation coefficient evaluated linear correlations. Receiver operating characteristic (ROC) curves for biomarkers were created in GraphPad Prism. Significance was set for $P < 0.05$ and area under the curve (AUC) >0.65, with a 95% CI for parameter estimation.

## Results

Among 384 chronic neck pain patients, 239 (62.2%) had moderate or severe height loss, and 130 (33.9%) had mild height loss. Of the total 384 patients, 258 (67.2%) had moderate or severe and 108 (28.1%) had mild size of anterior osteophytes. Of the patients, 238 out of 384 (62.0%) had detectable or definite endplate. Two hundred forty-six (246/384, 64.1%) had moderate or severe CIDD, and 130 (130/384, 33.9%) had mild CIDD.

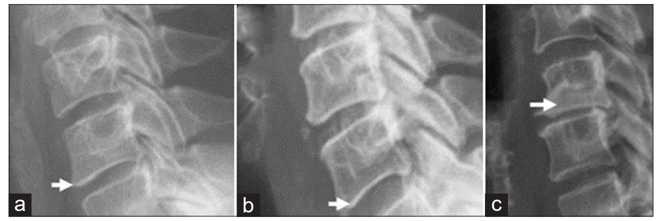


**Figure 2: Lateral X-ray of cervical spine shows Endplate sclerosis; (a) The arrow points to the endplate, which appear normal, indicating the absence of the feature being graded. (b) The arrow points to the endplate, where sclerosis is present but not definitively clear. (c) The arrow points to the endplate, where sclerosis is definitively present**

### Cervical intervertebral disc degeneration and serum level of cytokines

Out of the 44 patients with chronic neck pain having CIDD, 30 patients had moderate, and 14 patients had severe CIDD and were enrolled as the test group. Age (±5 years), sex, and BMI-matched 44 controls were included in the study. The demographic data and the clinical data of patients are summarized in Table 2.

A strong positive correlation was observed between the intensity of pain and the severity of CIDD ($r = 0.680$, $P = 0.045$). The median value of serum levels of IL-1, IL-6, and TNF-α in patients was significantly higher when compared with healthy individuals [Table 3 and Figure 3].

### Cytokines as biomarkers for cervical intervertebral disc degeneration

To assess the validity of cytokines and MMP3 as biomarkers for CIDD, ROC curve analysis was conducted [Figure 4]. IL-1, IL-6, and TNF-α demonstrated abilities of 86.7% (AUC = 0.867), 82.4% (AUC = 0.824), and 89.2% (AUC = 0.892), respectively, to differentiate chronic neck pain patients with moderate or severe CIDD from controls. Cutoff values were determined based on maximum specificity and sensitivity. According to Table 4, serum IL-1 with a cutoff >4.11 pg/mL showed 84.1% sensitivity and 68.2% specificity. For IL-6, a cutoff >3.76 pg/mL provided 84.1% sensitivity and 70.5% specificity, whereas for TNF-α, a cutoff >8.96 pg/mL resulted in 84.1% sensitivity and 93.2% specificity.

The ROC curves plot sensitivity against specificity for various cutoff points, with each point representing a sensitivity/specificity pair corresponding to a specific threshold. The AUC for the overall analysis was 0.674, with statistically significant results ($P = 0.022$).

**Table 2: Demographic and the clinical data of the patients with chronic neck pain having cervical intervertebral disc degeneration and controls**

| Variable | CIDD patients number (*n*=44) (%) | Controls number (*n*=44) (%) |
|---|---|---|
| Age (years), mean±SD | 56.42±10.14 | 53.53±08.22 |
| Gender | | |
| Male | 13 (29.54) | 13 (29.54) |
| Female | 31 (70.45) | 31 (70.45) |
| BMI | | |
| Mean±SD | 27.58±3.86 | 26.72±1.66 |
| Under weight | 0 | 0 |
| Normal | 8 (18.19) | 8 (18.18) |
| Overweight or obese | 36 (81.81) | 36 (81.81) |
| Intensity of pain, mean±SD | 72.25±11.18 | - |
| Pain duration (months), mean±SD | 30.19±36.93 | - |
| Radiation of pain into the arm | | |
| Yes | 35 (79.54) | - |
| No | 9 (20.46) | - |

CIDD: Cervical intervertebral disc degeneration, SD: Standard deviation

**Table 3: Serum concentrations of interleukin-1, interleukin-6, and tumor necrosis factor alpha in patients with chronic neck pain having cervical intervertebral disc degeneration and controls**

| | Range | | Median | | *P* (95% CI) |
|---|---|---|---|---|---|
| | CIDD patients (pg/ml) | Controls (pg/ml) | CIDD patients (pg/ml) | Controls (pg/ml) | |
| IL-1 | 3.01–10.98 | 1.71–8.45 | 7.32 | 2.98 | 0.021 |
| IL-6 | 1.55–34.96 | 1.05–13.83 | 8.59 | 2.98 | 0.023 |
| TNF-α | 5.13–75.94 | 4.15–11.63 | 19.29 | 7.44 | 0.011 |

CI: Confidence interval, TNF-α: Tumor necrosis factor alpha, IL: Interleukin, CIDD: Cervical intervertebral disc degeneration

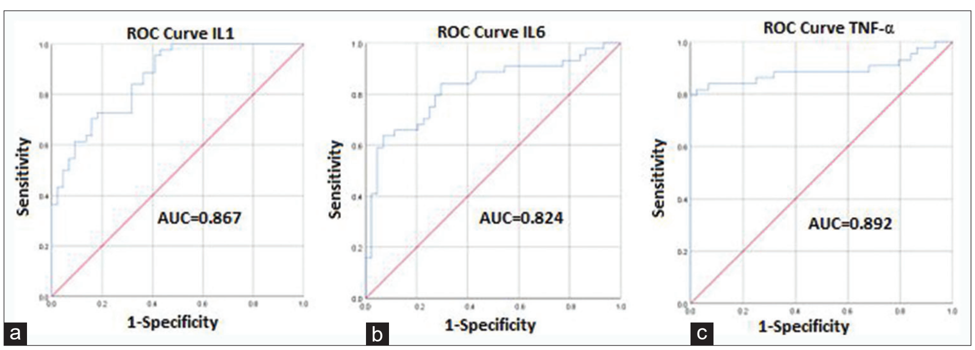


**Figure 3: Receiver operating characteristics curves: (a) ROC curve for interleukin-1 (IL-1), (b) ROC curve for interleukin-6 (IL-6), and (c) ROC curve for tumor necrosis factor-α (TNF-α). The AUC is the area under the curve of the receiver operating characteristics curve (ROC). AUC values more than 0.7, COV was calculated for significant AUC only**

### Cytokines and intensity of pain

Among the patients with chronic neck pain having CIDD, Spearman's rank correlation showed a significant moderate positive association of pain intensity with IL-6 ($r$ = 0.41, $P$ = 0.034) and TNF-α ($r$ = 0.30, $P$ = 0.041).

The association of serum cytokines (IL-1 α, IL6 and TNF- α) with age, sex and BMI in patients with chronic neck pain who had CIDD and in the control group were assessed and results are presented in Supplementary Data Sheet 2.

## Discussion

The present study investigated the relationship of the serum level of cytokines, IL-1α, IL-6, and TNF-α, with chronic neck pain due to CIDD and the association of these cytokines with the intensity of pain. We observed a higher serum level of cytokines in patients with chronic neck pain who had moderate or severe CIDD when compared to the control group. The intensity of pain in patients with chronic neck pain who had CIDD was positively associated with IL-6 and TNF-α but not with IL-1α. The relationship between IL-1α and intensity of pain, compared to IL-6 and TNF-α, can be complex. It is important to note that pain

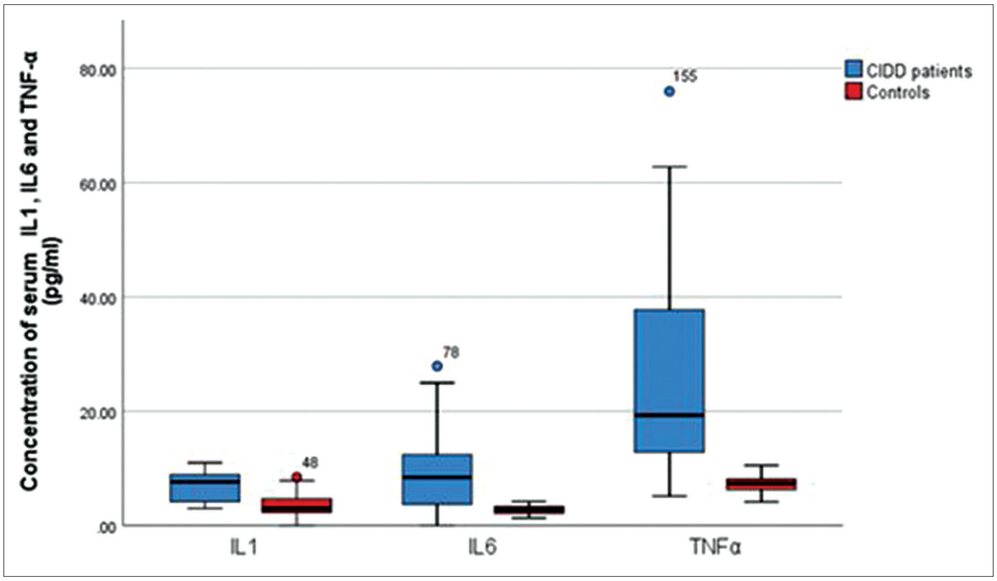


**Figure 4: Serum level of IL-1, IL-6, and TNF-α: serum level of IL-1, IL-6, and TNF-α o in chronic neck pain patients with CIDD were higher than the healthy control. TNF-α: Tumor necrosis factor alpha, IL: Interleukin, CIDD: Cervical intervertebral disc degeneration**

**Table 4: Discriminating ability of the serum cytokines**

| | Patients/control |
|---|---|
| IL-1 | |
| AUC | 0.867 |
| 95% CI for AUC | 0.795–0.938 |
| *P* | <0.001 |
| Cut off value | 4.1192 pg/ml |
| Sensitivity at COV | 84.1% |
| Specificity at COV | 68.2% |
| IL-6 | |
| AUC | 0.824 |
| 95% CI for AUC | 0.734–0.914 |
| *P* | <0.001 |
| Cut off value (COV) | 3.7673 pg/ml |
| Sensitivity at COV | 84.1% |
| Specificity at COV | 70.5% |
| TNF-α | |
| AUC | 0.892 |
| 95% CI for AUC | 0.841–0.932 |
| *P* | <0.001 |
| Cutoff value | 8.9635 pg/ml |
| Sensitivity at COV | 84.1% |
| Specificity at COV | 93.2% |

The AUC is the area under the curve of the ROC. CI is the CI, COV is the cut-off value, the significant value denoted for $P<0.05$ and AUC values more than 0.7, COV was calculated for significant AUC only. ROC: Receiver operating characteristics curve, COV: Cutoff value, AUC: Area under the curve, CI: Confidence interval

is a multifaceted experience influenced by various factors, including inflammation, tissue damage, and immune responses. According to our knowledge, there is a lack of evidence in this area, and therefore, it is recommended to conduct further research in this field.

The important role of ILs in the regulation of immune responses and inflammation, and its contribution to intervertebral disc degeneration, has been demonstrated.[20] Increased levels of proinflammatory cytokines such as IL-1α, IL-6, and TNF-α are characteristic of intervertebral disc degeneration, causing an imbalance between catabolic and anabolic processes.[21] This was also demonstrated in a study that found IL-1α is produced in human lumbar degenerate intervertebral disc tissue and revealed that IL-1α disturbs the normal metabolic reactions leading to further intervertebral disc degeneration. Another observation they made was the pivotal role of IL-1α in the intervertebral disc desease.[7] Plasma level of IL-6 showed a positive association with the severity of LDD,[22] whereas TNF-α was also found to play a significant role.[23]

The current study on patients with chronic neck pain who had CIDD revealed that there was a significant elevation in the serum levels of IL-1α, IL-6, and TNF-α when compared to the serum levels in the control group. We observed 2.5, 2.9, and 2.6-fold increment in the serum level of IL-1α, IL-6, and TNF-α of the patients when compared to the control group, respectively.

An animal study investigating the role of cytokines in CIDD induced by static and unbalanced dynamic forces in rats showed that serum IL-1 and TNF-α levels increased in parallel with disease progression at 1 and 3 months, whereas no significant changes in serum IL-6 levels were observed between test and control groups at any time point.[11]

According to our knowledge, the serum level of IL-1, IL-6, and TNF-α in patients with chronic neck pain having CIDD has not been investigated on human cervical discs.

The findings from lumbar disc disease and serum levels of cytokines are therefore used in this study to discuss our results.

A study conducted in Brazil has demonstrated 4.6-fold and 3.5-fold increment, respectively, in serum level of IL-6 and TNF-$\alpha$ in patients (mean age – 42.8 years) with herniated lumbar disc compared to the control. There was, however, no significant increase in IL-1 levels of the above patients.[24] Another study carried out using serum sample in China has shown a 4.1-fold increment in IL-1, a 8.3-fold in IL-6, and a 6.6-fold in TNF-$\alpha$ in patients (mean age – 44.1 years) with lumbar intervertebral disc protrusion when compared with the control group.[25]

Elevated levels of the cytokines are not only associated with disc degeneration but also with the severity of pain.[23] It decreases the threshold level for pain and increases the sensitivity of pain.[26] During intervertebral disc degeneration, IL-1, IL-6, and TNF-$\alpha$ secretions increase in the intervertebral disc tissue cells. The breakdown of the extracellular matrix and the reduction in the hydrophilic matrix create an imbalance between catabolic and anabolic processes, ultimately triggering the release of molecules associate with pain.[27] Proinflammatory molecules including IL-1, IL-6, and TNF-$\alpha$ were elevated in tissue of intervertebral disc degeneration and would cause pain in many conditions, suggesting an association between discogenic pain and elevation of proinflammatory molecules.[28]

Our study additionally revealed a statistically significant correlation of pain intensity with CIDD and the serum levels of IL-6 and TNF-$\alpha$. Pain radiating to the arm, either to the right, left, or both, was significantly associated with all three cytokines.

The use of cytokines as biomarkers in the diagnosis and management of CIDD patients would be further enhanced with a clearer understanding of the role of inflammatory markers in intervertebral disc degeneration and of the molecular basis of its pathophysiology. It can also be used for the monitoring of the disease process and the development of important novel therapeutic targets for preventing and controlling disc degeneration.[7] The few clinical studies published have shown the efficacy of anticytokine therapies and also its benefits in treating radicular pain.[10,29]

Our study was carried out using serum samples of patients with CIDD. Studies on lumbar regions reported used both disc tisue samples and serum levels with comparable results, although cytokine concentration in disc tissue is high.[30] The scarcity of cervical discectomies compared to the lumbar discectomies may be cause of the lack of studies on cervical disc tissues. Serum samples are, however, easy to obtain compared to disc tissues, and in clinical practice, the use of serum samples will be more feasible.

Although MRI is considered an advance technique for evaluating CIDD, in this study, CIDD was assessed only using X-ray of the cervical spine, which is an identified limitation. CIDD can be present without neck pain; however, in this study, we could not exclude those from healthy controls as we did not perform radiological assessment for the healthy control, mainly due to ethical considerations.

## Conclusion

The serum levels of IL1-$\alpha$, IL-6, and TNF-$\alpha$ cytokines are significantly elevated in patients with chronic neck pain diagnosed with severe or moderate CIDD. There is a significant positive association of intensity of pain with severity of CIDD and serum IL-6 and TNF-$\alpha$. The pain radiating to the arm (one arm or both arms) was significantly associated with IL-1, IL-6, and TNF-$\alpha$. IL-1, IL-6, and TNF-$\alpha$ in serum could be a useful therapeutic intervention for CIDD and pain related to CIDD in a Sri Lankan population.


### Acknowledgments

I would like to convey my profound and heartfelt appreciation to retired Prof. Shanti Goonewardene, previously from the Department of Anatomy at the Faculty of Medicine, University of Colombo, for her valuable guidance, especially in writing assistance and proofreading the article.

### Financial support and sponsorship

This research was supported by a Research Grant from the University of Sri Jayewardenepura, Grant No. ASP/01/RE/MED/2021/58.

### Conflicts of interest

There are no conflicts of interest.


## References


1. Yang L, Yang C, Pang X, Li D, Yang H, Zhang X, *et al.* Mechanoreceptors in diseased cervical intervertebral disc and vertigo. Spine (Phila Pa 1976) 2017;42:540-6.
2. Peng B, DePalma MJ. Cervical disc degeneration and neck pain. J Pain Res 2018;11:2853-7.
3. Kepler CK, Ponnappan RK, Tannoury CA, Risbud MV, Anderson DG. The molecular basis of intervertebral disc degeneration. Spine J 2013;13:318-30.
4. Li S, Huang C, Xiao J, Wu Y, Zhang Z, Zhou Y, *et al.* The potential role of cytokines in diabetic intervertebral disc degeneration. Aging Dis 2022;13:1323-35.
5. Perera RS, Dissanayake PH, Senarath U, Wijayaratne LS, Karunanayake AL, Dissanayake VH. Single nucleotide variants of candidate genes in aggrecan metabolic pathway are associated with lumbar disc degeneration and modic changes. PLoS One 2017;12:e0169835.
6. Wuertz K, Haglund L. Inflammatory mediators in intervertebral disk degeneration and discogenic pain. Global Spine J 2013;3:175-84.
7. Le Maitre CL, Freemont AJ, Hoyland JA. The role of interleukin-1 in the pathogenesis of human intervertebral disc

degeneration. Arthritis Res Ther 2005;7:R732-45.

8. Le Maitre CL, Hoyland JA, Freemont AJ. Catabolic cytokine expression in degenerate and herniated human intervertebral discs: IL-1beta and TNFalpha expression profile. Arthritis Res Ther 2007;9:R77.
9. Burke JG, Watson RW, McCormack D, Dowling FE, Walsh MG, Fitzpatrick JM. Intervertebral discs which cause low back pain secrete high levels of proinflammatory mediators. J Bone Joint Surg Br 2002;84:196-201.
10. Navone SE, Marfia G, Giannoni A, Beretta M, Guarnaccia L, Gualtierotti R, *et al.* Inflammatory mediators and signalling pathways controlling intervertebral disc degeneration. Histol Histopathol 2017;32:523-42.
11. Yin J, Huang Y, Gao G, Nong L, Xu N, Zhou D. Changes and significance of inflammatory cytokines in a rat model of cervical spondylosis. Exp Ther Med 2018;15:400-6.
12. Kang JD, Georgescu HI, McIntyre-Larkin L, Stefanovic-Racic M, Evans CH. Herniated cervical intervertebral discs spontaneously produce matrix metalloproteinases, nitric oxide, interleukin-6, and prostaglandin E2. Spine (Phila Pa 1976) 1995;20:2373-8.
13. Li H, Yin J, Huang Y, Xu N, Chen L, Nong L. Establishment of cervical dynamic and static imbalance models and preliminary study on the mechanism of cervical degeneration in rats. Innate Immun 2020;26:107-16.
14. Walraevens J, Liu B, Meersschaert J, Demaerel P, Delye H, Depreitere B, *et al.* Qualitative and quantitative assessment of degeneration of cervical intervertebral discs and facet joints. Eur Spine J 2009;18:358-69.
15. Cox J, Davidian C, Mior S. Neck pain in children: A retrospective case series. J Can Chiropr Assoc 2016;60:212-9.
16. Sarig Bahat H, Takasaki H, Chen X, Bet-Or Y, Treleaven J. Cervical kinematic training with and without interactive VR training for chronic neck pain – A randomized clinical trial. Man Ther 2015;20:68-78.
17. Perera RS, Dissanayake PH, Senarath U, Wijayaratne LS, Karunanayake AL, Dissanayake VH. Associations between disc space narrowing, anterior osteophytes and disability in chronic mechanical low back pain: A cross sectional study. BMC Musculoskelet Disord 2017;18:193.
18. Jensen MP, Chen C, Brugger AM. Interpretation of visual analog scale ratings and change scores: A reanalysis of two clinical trials of postoperative pain. J Pain 2003;4:407-14.
19. Lim JU, Lee JH, Kim JS, Hwang YI, Kim TH, Lim SY, *et al*. Comparison of World Health Organization and Asia-Pacific body mass index classifications in COPD patients. Int J Chron Obstruct Pulmon Dis 2017;12:2465-75.
20. Kim H, Hong JY, Lee J, Jeon WJ, Ha IH. IL-1β promotes disc degeneration and inflammation through direct injection of intervertebral disc in a rat lumbar disc herniation model. Spine J 2021;21:1031-41.
21. Suzuki S, Fujita N, Fujii T, Watanabe K, Yagi M, Tsuji T, *et al*. Potential involvement of the IL-6/JAK/STAT3 pathway in the pathogenesis of intervertebral disc degeneration. Spine (Phila Pa 1976) 2017;42:E817-24.
22. Guo Y, Li C, Shen B, Zhu Z, Chen X, Hu T, *et al.* Is There any relationship between Plasma IL-6 and TNF-α levels and lumbar disc degeneration? A retrospective single-center study. Dis Markers 2022;2022:6842130.
23. Lai A, Moon A, Purmessur D, Skovrlj B, Laudier DM, Winkelstein BA, *et al*. Annular puncture with tumor necrosis factor-alpha injection enhances painful behavior with disc degeneration *in vivo*. Spine J 2016;16:420-31.
24. Kraychete DC, Sakata RK, Issy AM, Bacellar O, Santos-Jesus R, Carvalho EM. Serum cytokine levels in patients with chronic low back pain due to herniated disc: Analytical cross-sectional study. Sao Paulo Med J 2010;128:259-62.
25. Yang H, Zhang Y, Sun G, Zhao D, Ma Y, Hao Y, *et al*. Correlation of inflammatory cytokines with radicular pain after lumbar intervertebral disc protrusion. Int J Clin Exp Med 2019;12:10380-6.
26. Jacobsen HE, Khan AN, Levine ME, Filippi CG, Chahine NO. Severity of intervertebral disc herniation regulates cytokine and chemokine levels in patients with chronic radicular back pain. Osteoarthritis Cartilage 2020;28:1341-50.
27. Lyu FJ, Cui H, Pan H, Mc Cheung K, Cao X, Iatridis JC, *et al.* Painful intervertebral disc degeneration and inflammation: From laboratory evidence to clinical interventions. Bone Res 2021;9:7.
28. Misailidou V, Malliou P, Beneka A, Karagiannidis A, Godolias G. Assessment of patients with neck pain: A review of definitions, selection criteria, and measurement tools. J Chiropr Med 2010;9:49-59.
29. Altun I. Cytokine profile in degenerated painful intervertebral disc: Variability with respect to duration of symptoms and type of disease. Spine J 2016;16:857-61.
30. Fay LY, Kuo CH, Chang HK, Yeh MY, Chang CC, Ko CC, *et al*. Comparative study of the cytokine profiles of serum and tissues from patients with the ossification of the posterior longitudinal ligament. Biomedicines 2023;11:2021.

Original Article

# Remazolam Combined with Sufentanil in the Treatment of HMGB1, Interleukin-6/10/17, Tumor Necrosis Factor in Patients Undergoing Thoracoscopic Surgery- α the Impact of Plasma Stress Response Indicators


## Abstract

**Objective:** This study explores the efficacy of remimazolam combined with sufentanil in managing anesthesia for patients undergoing thoracoscopic surgery. **Methods:** A simple random sampling method selected 178 patients from our hospital between May 2021 and May 2022. Patients were randomly divided into two groups: the control group (CG) received sufentanil alone, whereas the observation group (OG) received a combination of remimazolam and sufentanil. Pain mediators, inflammatory factors, and plasma stress response indicators were measured and compared preoperatively and at 1, 3, 12, 24, and 48 h postoperation. The occurrence of adverse reactions (ARs) postoperation was also monitored. **Results:** Out of 178 patients, two were excluded – one from the CG who underwent open surgery and one from the OG who voluntarily withdrew – resulting in 176 patients with a data recovery rate of 98.88%. Repeated measurement analysis of variance indicated significant differences in levels of prostaglandin E2, high mobility group proteins, interleukin-6/10/17, tumor necrosis factor α, adrenaline, norepinephrine, cortisol, and fasting blood glucose between groups and over time ($P < 0.05$). No significant differences in AR incidence were observed between the groups ($P > 0.05$). **Conclusion:** The combination of remimazolam and sufentanil effectively inhibits the release of pain mediators and inflammatory factors in patients undergoing thoracoscopic surgery, alleviates postoperative stress responses, and demonstrates acceptable safety.


**Keywords:** *Inflammatory response, plasma stress response, remazolam, sufentanil, thoracoscopic surgery*

**Meiling Jiang[1,2], Minghui Lun[1,2], Zeqing Huang[1,2]**

*[1]Department of Anesthesiology, Cancer Hospital of China Medical University, [2]Department of Anesthesiology, Liaoning Cancer Hospital and Institute, Shenyang, China*

## Introduction

With the boost of minimally invasive technology, thoracoscopic surgery, characterized by minimal trauma, fast recovery, and fewer complications, has gained clinical favor. Moreover, it has gradually replaced traditional thoracotomy as the preferred form of surgery for thoracic surgery and cardiac surgery.[1] However, chest surgery may require deep procedures such as tracheal traction and exposure and exposure of lung tissue. Therefore, in clinical practice, general anesthesia is administered to patients during thoracoscopic surgery to ensure the smooth progress of the surgery. Meanwhile, the selection of anesthetic drugs will directly affect the anesthesia and surgical effects. Sufentanil is a powerful opioid analgesic. This drug is not only used for inducing and maintaining general anesthesia in surgery and related procedures but is also a commonly used compound anesthesia and analgesic drug in clinical practice.[2] In the field of thoracoscopic surgery, existing anesthesia programs often rely on traditional drug combinations, such as the combination of propofol and midazolam. Although these drugs can effectively administer anesthesia, there are still potential side effects such as respiratory depression and hypotensive, which may affect the postoperative recovery and safety of patients.[3,4] Therefore, to find a safer and more effective anesthesia program has become an urgent problem. Ramidazolam, as a new benzodiazepine, has a very short action time and a good analgesic effect. In surgical anesthesia, ramidazolam provides effective sedation and reduces the risk of suppression of the respiratory and cardiovascular systems, especially for minimally invasive surgery and day surgery.



**How to cite this article:** Jiang M, Lun M, Huang Z. Remazolam combined with sufentanil in the treatment of HMGB1, interleukin-6/10/17, tumor necrosis factor in patients undergoing thoracoscopic surgery- α the impact of plasma stress response indicators. J Anat Soc India 2026;75:68-76.

**Article Info**

**Received:** 16 August 2024
**Revised:** 23 December 2024
**Accepted:** 13 January 2025
**Available online:** 27 March 2026

***Address for correspondence:***
*Dr. Zeqing Huang, Department of Anesthesiology, Cancer Hospital of China Medical University, Shenyang 110000, China. Department of Anesthesiology, Liaoning Cancer Hospital and Institute, Shenyang 110000, China. E-mail: huangzeqing 2023@126.com*

**Access this article online**

**Website:** https://journals.lww.com/joai

**DOI:** 10.4103/jasi.jasi_125_24

**Quick Response Code:**

In addition, it is used as a sedative during endoscopy to improve patient comfort and optimize the examination experience. At the same time, ramidazolam can also be used for sedation in intensive care units to help relieve stress response and promote patient recovery.[5,6] The use of remizolam in combination with sufentanil may significantly improve pain management and postoperative recovery in thoracoscopic surgery. Therefore, this study aims to explore the anesthetic effect of ramidazolam combined with sufentanil in patients undergoing thoracoscopic surgery and is expected to provide a new anesthesia strategy for clinical use to improve postoperative safety and comfort.

## Objects and Methods

### Object

From May 2021 to May 2022, our hospital admitted a total of 332 patients undergoing thoracoscopic surgery. According to the formula ($n = 2\sigma^2[Z_\alpha + Z_\beta] \div \delta^2$), the sample size should not be <178. The sample size of the study was calculated based on reports of similar studies in the primary reference literature and clinical experience to ensure sufficient statistical power to detect differences between the two groups. In terms of specific parameter selection, the standard deviation σ of the expected effect was derived from the pre-experimental results using surgery-related pain score data, whereas the minimum effect difference δ was determined based on clinical significance and effects reported in the relevant literature. In addition, to ensure the rationality of the sample size, the significance level was set at 0.05, and the efficiency was set at 80%, so as to ensure that statistical differences could be effectively detected in a small sample, and the total sample size was appropriately increased based on the sample loss estimate to improve the reliability of the results. All these considerations ensured the adequacy of the sample size of the study so that the results could truly reflect the actual impact of the combination of ramidazolam and sufentanil on patients undergoing thoracoscopic surgery.[7] Therefore, this study used a simple random sampling method to randomly select 178 patients from 325 patients undergoing thoracoscopic surgery as the study subjects. Moreover, it strictly follows the technical specifications for thoracoscopic surgery for all patients. Inclusion criteria: (1) Selective thoracoscopic surgery; (2) The American Society of Anesthesiologists (ASA) grading is I-II, with surgical tolerance; (3) Age ≥18 years old. Exclusion criteria: (1) accompanied by abnormal coagulation function; (2) Severe dysfunction of organs such as the heart, liver, and kidneys; (3) Accompanying pelvic adhesions or having large pelvic masses; (4) Merge advanced malignant tumors; (5) Diseases with severe abdominal or respiratory infections, bronchial asthma, and other chronic inflammatory reactions; (6) Umbilical dysplasia; and (7) There is an allergic reaction to the study drug or a history of long-term use of analgesics. Exclusion criteria: (1) Conversion to open surgery; (2) The patient voluntarily withdrew from the study. All patients are aware of the study and sign an informed consent form. According to the ethical principles of medical research on human subjects outlined in the Helsinki Declaration of the World Medical Assembly,[8] this study was approved by the Ethics Committee. The patients were randomly separated into two groups in a random number method, with 88 cases in the control group (CG) and 88 cases in the observation group (OG).

### Methods

After entering the operating room, both groups of patients immediately established venous access and underwent routine electroencephalogram and sign monitoring. On this basis, the CG patients were treated with 2～4 mg of midazolam (national drug approval number H20067040, Yichang Humanwell Pharmaceutical Co., Ltd., specification 2 mL: 2 mg) +3～4 μg/kg sufentanil (GYZZ H20054172, Yichang Humanwell Pharmaceutical Co., Ltd., specification 2 mL: 100 μg) +0.2 mg/kg etomidate (national drug approval number H32022379, Jiangsu Hengrui Pharmaceutical Co., Ltd., specification 10 mL: 20 mg) +0.15～0.20 mg/kg cisatracurium (national drug approval number H20060869, Jiangsu Hengrui Pharmaceutical Co., Ltd., specification 10 mg) for anesthesia induction, intravenous infusion, mechanical ventilation after tracheal intubation; then it uses 4～8 mg/kg/h propofol (national drug approval number H20030115, Sichuan Guorui Pharmaceutical Co., Ltd., specification 20 mL: 0.2 g) +0.1～0.3 μg/kg/h remifentanil (GYZZ H20030197, Yichang Humanwell Pharmaceutical Co., Ltd., specification 1 mg) +100 mL sufentanil (2.5 μg/kg) 0.9% sodium chloride injection combined with intravenous drip for maintenance anesthesia. On the basis of the CG patients, the OG patients were given an additional dose of remimazolam toluenesulfonate (national drug approval number H20190034, Jiangsu Hengrui Pharmaceutical Co., Ltd., specification 36 mg) at a rate of 12 mg/kg/h during anesthesia induction and 1～2 mg/kg/h during maintenance anesthesia. Both groups of patients received intermittent addition of cisatracurium during surgery.

### Outcome measures

5 mL of fasting venous blood was drawn from patients in preoperation, 1 h in postoperation, 3 h in postoperation, 12 h in postoperation, 24 h in post-operation, and 48 h in postoperation, and centrifugation was performed after natural precipitation 1 h (centrifugation speed 3500r/min, centrifugation time 15 min, and centrifugation radius 6.5 cm). After centrifugation, serum and plasma were separated and stored in a − 4°C refrigerator for future use. (1) Pain mediator: This study obtained appropriate amounts of blood samples after processing at various time points and used enzyme-linked immunosorbent assay (ELIA) to detect the levels of prostaglandin E2 (PGE2) and high mobility group box 1 (HMGB1). (2) Inflammatory factors: In this study, appropriate amounts

of blood samples were obtained after processing at various time points, and the levels of interleukin-6 (IL-6), IL-10, IL-17, and tumor necrosis factor α (TNF-α) were measured using ELIA. (3) Plasma stress response indicators: In this study, appropriate amounts of blood samples were obtained after processing at various time points, and the levels of adrenaline (A), norepinephrine (NA), cortisol (COR), and fasting blood glucose (FBG) were measured using ELIA. (4) adverse reaction (AR): The AR in patients participating in the experiment was recorded in detail after surgery.

### Statistics

Statistical Package for the Social Sciences (SPSS) 26.0 (International Business Machines Corporation, Armonk, New York, America) was selected for data processing and analysis. Kolmogorov–Smirnov test is used to verify whether the data are in line with the normal distribution, and the measurement data in line with the normal distribution are expressed by the mean ± standard deviation ( $\bar{x} \pm s$ ); Independent *t*-tests were conducted between groups, and paired *t*-tests were conducted within groups; It repeatedly measures data and performs repeated measurement variance analysis; The quantity of cases and percentage (*n* [%]) represent counting data, and $\chi^2$ Inspection. $P < 0.05$ indicates a statistically dramatic discrepancy.

### Data normality test

The study will obtain data for the normality test, and the test method is Shapiro–Wilk. If the $P \leq 0.05$, it indicates that the data does not conform to the normal distribution. If the $P > 0.05$, it indicates that the data conforms to the normal distribution [Table 1].

**Table 1: Data normality test**

| Variable | Group | Sample size (*n*) | *W* | *P* | Normality test results |
|---|---|---|---|---|---|
| PGE2 | CG | 88 | 0.932 | 0.123 | Normal distribution |
| | OG | | 0.948 | 0.274 | Normal distribution |
| HMGB1 | CG | | 0.911 | 0.065 | Normal distribution |
| | OG | | 0.930 | 0.115 | Normal distribution |
| IL-6 | CG | | 0.945 | 0.230 | Normal distribution |
| | OG | | 0.952 | 0.189 | Normal distribution |
| TNF-α | CG | | 0.923 | 0.042 | Normal distribution |
| | OG | | 0.940 | 0.097 | Normal distribution |

PGE2: Prostaglandin E2, HMGB1: High mobility group protein 1, IL-6: Interleukin-6, TNF-α: Tumor necrosis factor α, CG: Control group, OG: Observation group

**Table 2: Comparison of baseline data between patients participating in the experiment (*n* [%], [$\bar{x}$±*s*])**

| Project | CG (*n*=88) | OG (*n*=88) | $\chi^2$/*Z*/*t* | *P* |
|---|---|---|---|---|
| Gender | | | | |
| Male | 48 (54.55) | 45 (51.14) | 0.205 | 0.651 |
| Female | 40 (45.45) | 43 (48.86) | | |
| Age (years) | 54.80±4.73 | 55.07±4.69 | −0.384 | 0.701 |
| Body weight (kg) | 61.11±6.02 | 59.98±6.03 | 1.247 | 0.214 |
| Surgical anesthesia time (min) | 62.00±10.16 | 60.12±13.01 | 1.069 | 0.287 |
| ASA classification | | | | |
| Level I | 31 (35.23) | 26 (29.55) | −0.803 | 0.422 |
| Level II | 57 (64.77) | 62 (70.45) | | |
| Surgical type | | | | |
| Excision of mediastinal mass | 29 (32.95) | 35 (39.77) | 1.023 | 0.796 |
| Excision of benign lung masses | 27 (30.68) | 26 (29.55) | | |
| Pleural biopsy | 22 (25.00) | 19 (21.59) | | |
| Other | 10 (11.36) | 8 (9.09) | | |

ASA: American Association of Anesthesiologists, CG: Control group, OG: Observation group

## Results

### Comparison of baseline data between two groups of patients

Among 178 patients in this study, one patient in the CG underwent laparotomy due to the discovery of lymph nodes surrounding blood vessels during surgery; one patient in the OG voluntarily withdrew from the study due to their own reasons. All the above patients were excluded and 176 complete data were obtained, with a data recovery effective rate of 98.88%. There was no statistically dramatic discrepancy in baseline data such as gender, age, body mass, ASA grade, and surgical type between patients participating in the experiment ($P > 0.05$) [Table 2].

### Comparison of pain mediators between patients participating in the experiment

Overall analysis, there were discrepancies in PGE2 and HMGB1 levels between patients participating in the experiment in terms of intergroup, time, and interaction ($P < 0.05$). Compared between groups, the PGE2 and HMGB1 levels in the two groups of patients were dramatically lower at 1, 3, 12, 24, and 48 h in postoperation compared to the CG ($P < 0.05$). Compared within the group, both groups of patients indicated an upward trend in PGE2 from preoperative to postoperative 24 h, and a downward trend from postoperative 24 h to postoperative 48 h; Both groups of patients showed an upward trend in HMGB1 from preoperative to postoperative 1 h, and a downward trend from postoperative 1 h to postoperative 48 h. Moreover, there were statistically significant differences in PGE2 and HMGB1 levels between patients participating in the experiment at different time points ($P < 0.05$) [Table 3 and Figure 1].

### Comparison of inflammatory factors between patients participating in the experiment

Through the overall analysis, there were discrepancies in IL-6, IL-10, IL-17, and TNF-α between the two groups of patients in terms of intergroup, time, and interaction ($P < 0.05$). Through intergroup comparison, the

**Table 3: Comparison of pain mediator levels between patients participating in the experiment before and after surgery ($\bar{x}$±*s*)**

| Pain mediator | Detection time | CG (*n*=88) | OG (*n*=88) | *t* | *P* |
|---|---|---|---|---|---|
| PGE2 (ng·L$^{-1}$) | Preoperative | 107.41±10.89 | 107.85±11.16 | −0.265 | 0.791 |
| | Postoperative 1 h | 173.58±17.35* | 145.33±14.33* | 11.779 | <0.001 |
| | Postoperative 3 h | 201.81±16.84* | 168.28±15.03* | 13.935 | <0.001 |
| | Postoperative 12 h | 230.48±16.95* | 200.00±16.30* | 12.161 | <0.001 |
| | Postoperative 24 h | 270.96±14.49* | 225.32±17.59* | 18.787 | <0.001 |
| | Postoperative 48 h | 258.96±15.48* | 203.34±14.05* | 24.957 | <0.001 |
| HMGB1 (pg·L$^{-1}$) | Preoperative | 14.76±3.06 | 14.14±3.27 | 1.291 | 0.198 |
| | Postoperative 1 h | 22.17±3.34* | 20.00±3.32* | 4.323 | <0.001 |
| | Postoperative 3 h | 21.36±2.35* | 18.57±3.26* | 6.610 | <0.001 |
| | Postoperative 12 h | 20.23±3.18* | 17.05±2.59* | 7.277 | <0.001 |
| | Postoperative 24 h | 17.63±2.15* | 15.45±2.71* | 5.904 | <0.001 |
| | Postoperative 48 h | 16.35±2.46* | 14.52±3.25 | 4.221 | <0.001 |

*That compared with preoperative, $P$<0.05. PGE2: $F_{\text{Inter group}}/F_{\text{time}}/F_{\text{interactive}}$=1063.421/2693.666/90.688, $P_{\text{Inter group}}/P_{\text{time}}/P_{\text{interactive}}$=<0.001/<0.001/<0.001, HMGB1: $F_{\text{Inter group}}/F_{\text{time}}/F_{\text{interactive}}$=37.370/244.364/6.255, $P_{\text{Inter group}}/P_{\text{time}}/P_{\text{interactive}}$=<0.001/<0.001/<0.001.
PGE2: Prostaglandin E2, HMGB1: High mobility cluster protein 1, CG: Control group, OG: Observation group

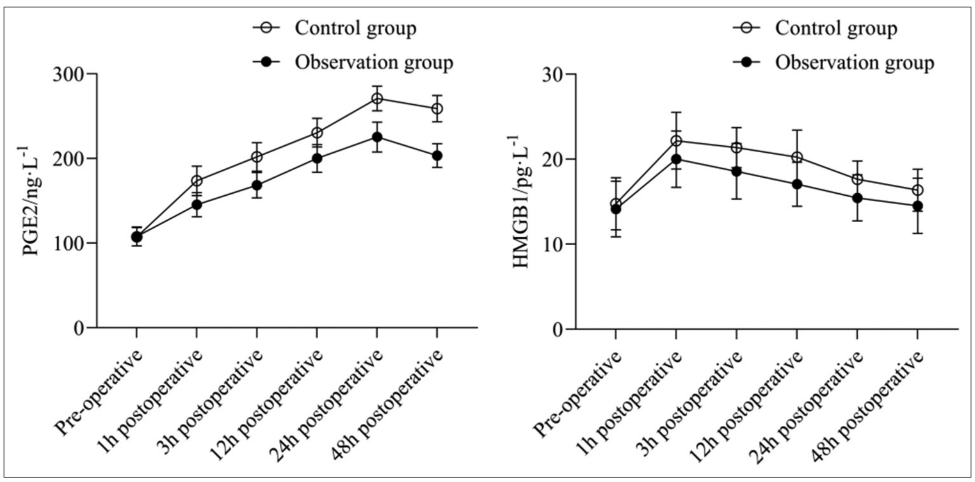


**Figure 1: Line chart of changes of pain media levels in patients of two groups before and after operation**

levels of IL-6, IL-10, IL-17, and TNF-α in the two groups of patients were lower than those in the CG at 1 h, 3 h, 12 h, 24 h, and 48 h in postoperation, with statistically significant differences ($P$ < 0.05). Compared within the group, IL-6, IL-10, and IL-17 in both groups showed an upward trend from preoperative to postoperative 24 h, and a downward trend from postoperative 24 h to postoperative 48 h; Both groups of patients showed an upward trend in TNF-α from preoperative to postoperative 12 h, and a downward trend from postoperative 12 h to postoperative 48 h. Moreover, statistically dramatic discrepancies exist in IL-6, IL-10, IL-17, and TNF-α between patients participating in the experimentat different time points ($P$ < 0.05) [Table 4 and Figure 2].

### Comparison of plasma stress response indicators between patients participating in the experiment

Through overall analysis, there were discrepancies in group, time, and interaction between patients participating in the experiment A, NA, COR, and FBG ($P$ < 0.05). Compared between groups, the A, NA, COR, and FBG levels of the two groups of patients at 1 h, 3 h, 12 h, 24 h, and 48 h in postoperation were lower than those of the CG, with statistically dramatic discrepancies ($P$ < 0.05). Through intragroup comparison, patients A, NA, COR, and FBG in both groups showed an upward trend from preoperative to postoperative 12 h, and a downward trend from postoperative 12 h to postoperative 48 h. Moreover, there were statistically significant differences between patients participating in the experiment at various time points A, NA, COR, and FBG ($P$ < 0.05) [Table 5 and Figure 3].

### Comparison of postoperative adverse reaction between patients participating in the experiment

There was no statistically dramatic discrepancy in the incidence of postoperative AR between patients participating in the experiment ($P$ > 0.05) [Table 6].

## Discussion

Effectively reducing surgical-related injuries and complications is the main reason why thoracoscopic

**Table 4: Comparison of inflammatory factors between patients participating in the experiment before and after surgery ($\bar{x}$±*s*)**

| Inflammatory factor | Detection time | CG (*n*=88) | OG (*n*=88) | *t* | *P* |
|---|---|---|---|---|---|
| IL-6 ($Ng \cdot L^{-1}$) | Preoperative | 3.94±0.80 | 4.03±0.91 | −0.716 | 0.475 |
| | Postoperative 1 h | 16.27±2.27* | 15.22±2.53* | 2.879 | 0.004 |
| | Postoperative 3 h | 18.85±3.41* | 17.61±2.86* | 2.604 | 0.010 |
| | Postoperative 12 h | 20.84±3.66* | 19.37±3.43* | 2.749 | 0.007 |
| | Postoperative 24 h | 31.75±5.34* | 30.04±5.95* | 2.008 | 0.046 |
| | Postoperative 48 h | 21.49±3.64* | 18.84±2.61* | 5.553 | <0.001 |
| IL-10 ($Ng \cdot L^{-1}$) | Preoperative | 4.60±0.96 | 4.44±1.03 | 1.087 | 0.278 |
| | Postoperative 1 h | 9.13±1.59* | 8.42±1.16* | 3.404 | 0.001 |
| | Postoperative 3 h | 10.98±1.91* | 10.04±1.49* | 3.646 | <0.001 |
| | Postoperative 12 h | 15.98±2.33* | 14.88±2.17* | 3.220 | 0.002 |
| | Postoperative 24 h | 17.42±2.14* | 16.37±2.00* | 3.348 | 0.001 |
| | Postoperative 48 h | 15.48±2.89* | 14.20±2.62* | 3.076 | 0.002 |
| IL-17 ($Ng \cdot L^{-1}$) | Preoperative | 5.45±1.13 | 5.37±1.13 | 0.474 | 0.636 |
| | Postoperative 1 h | 6.84±1.62* | 6.18±1.18* | 3.063 | 0.003 |
| | Postoperative 3 h | 8.40±1.76* | 7.68±1.65* | 2.799 | 0.006 |
| | Postoperative 12 h | 9.64±1.98* | 8.75±1.72* | 3.171 | 0.002 |
| | Postoperative 24 h | 11.32±3.12* | 10.41±1.91* | 2.326 | 0.021 |
| | Postoperative 48 h | 10.58±3.15* | 9.10±1.76* | 3.832 | <0.001 |
| TNF-α ($Ng \cdot L^{-1}$) | Preoperative | 4.51±1.17 | 4.45±1.33 | 0.341 | 0.733 |
| | Postoperative 1 h | 9.16±1.61* | 8.38±1.33* | 3.513 | 0.001 |
| | Postoperative 3 h | 10.61±1.95* | 9.82±1.78* | 2.796 | 0.006 |
| | Postoperative 12 h | 11.77±2.09* | 10.71±1.92* | 3.515 | 0.001 |
| | Postoperative 24 h | 11.39±2.17* | 10.32±1.88* | 3.494 | 0.001 |
| | Postoperative 48 h | 9.76±2.23* | 8.79±1.98* | 3.070 | 0.002 |

*That compared with preoperative, $P<0.05$., IL-6: $F_{\text{Inter group}}/F_{\text{time}}/F_{\text{interactive}}$=8.175/4991.381/72.967, $P_{\text{Inter group}}/P_{\text{time}}/P_{\text{interactive}}$=0.005/<0.001/<0.001, IL-10: $F_{\text{Inter group}}/F_{\text{time}}/F_{\text{interactive}}$=9.778/17272.678/17.546, $P_{\text{Inter group}}/P_{\text{time}}/P_{\text{interactive}}$=0.002/<0.001/<0.001, IL-17: $F_{\text{Inter group}}/F_{\text{time}}/F_{\text{interactive}}$=7.960/1158.447/72.410, $P_{\text{Inter group}}/P_{\text{time}}/P_{\text{interactive}}$=0.005/<0.001/<0.001, TNF-α: $F_{\text{Inter group}}/F_{\text{time}}/F_{\text{interactive}}$=8.682/7733.765/48.299, $P_{\text{Inter group}}/P_{\text{time}}/P_{\text{interactive}}$=0.004/<0.001/<0.001. IL-6: Interleukin-6, IL-10: Interleukin-10, IL-17: Interleukin-17, TNF-α: Tumor necrosis factor α, CG: Control group, OG: Observation group

surgery has become the first choice in clinical practice instead of thoracotomy. Meanwhile, the smooth progress of thoracic surgery is directly related to the effectiveness of anesthesia. At present, general anesthesia is chosen as the anesthesia treatment method for patients undergoing thoracoscopic surgery in clinical practice for two main reasons: (1) thoracoscopic surgery and traditional open surgery have the same requirements for anesthesia, and local anesthesia will not be used just because it is a minimally invasive surgery. Performing surgery in the chest can cause open pneumothorax, and during the surgery, it is essential to control and regulate the patient’s breathing through tracheal intubation. This method can not only prevent the occurrence of mediastinal oscillation but also achieve individual collapse of the lung tissue on the surgical side, thereby ensuring the exposure of the surgical field and creating conditions for the smooth progress of the surgery. Except for general anesthesia, other anesthesia methods cannot simultaneously meet the two effects of tracheal intubation and intraoperative analgesia; (2) Under nongeneral anesthesia, patients with autonomous consciousness may experience tension or anxiety and may experience pain intolerance or poor cooperation, resulting in the inability to perform surgery normally. General anesthesia can not only make patients unconscious and painless, but also avoid muscle tension and contraction, coughing, and other phenomena that can only occur during spontaneous breathing during the surgery process. This can effectively improve the safety factor of surgery.

For the selection of drugs for general anesthesia in thoracoscopic surgery, propofol and midazolam have always been the preferred choice in clinical practice. However, in long-term clinical practice, it has been found that propofol may cause AR, such as hypotension, respiratory acidosis, and systemic allergic reactions.[9] Although midazolam can enhance the anesthetic effect, its analgesic and sedative effects are average, and its value is more reflected in sleep induction.[10] Therefore, it is currently necessary to search for a new anesthetic to improve the effectiveness of anesthesia, analgesia, and sedation, providing guarantees for the implementation of thoracoscopic surgery. Remazolam is an improved version of midazolam, which increases the methyl propionate side chain on the basis of midazolam, allowing it to directly act on the γ-aminobutyric acid type A receptor. This significantly

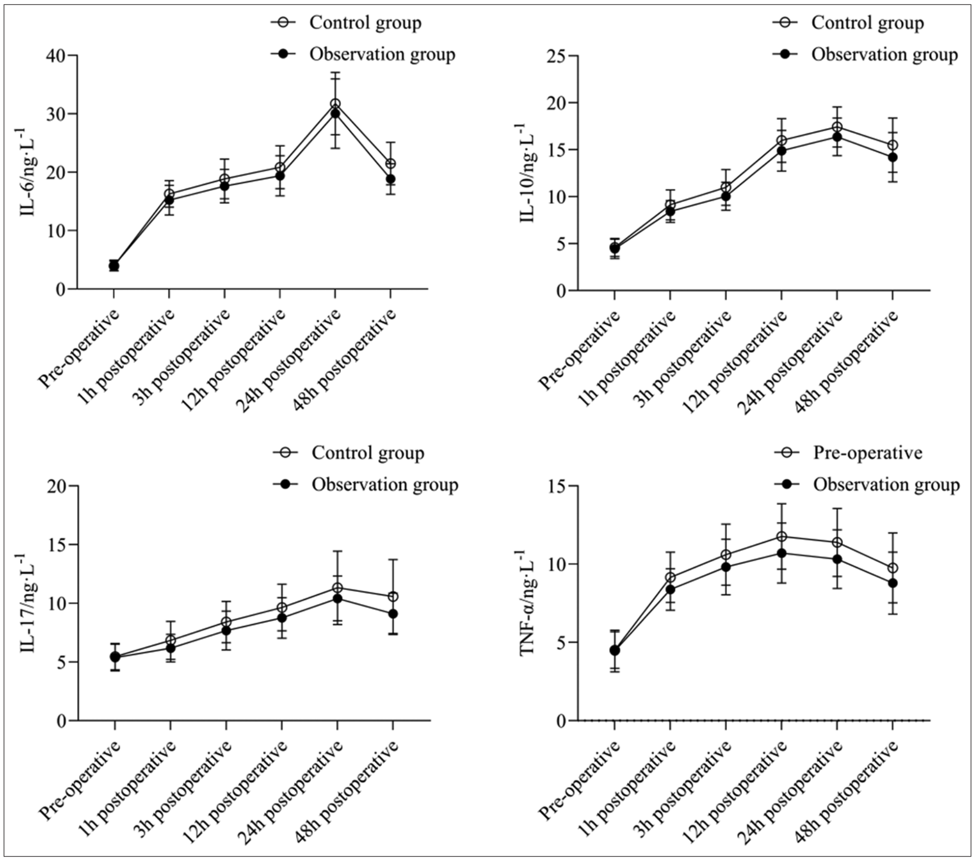


**Figure 2: Line chart of changes in inflammatory factor levels before and after surgery in two groups of patients**

improves the analgesic effect.[11,12] Studies have shown that ramidazolam during anesthesia induction is effective in reducing the release of postoperative pain mediators such as PGE2 and high mobility histone 1 (HMGB1), which are often increased during surgical trauma and inflammatory responses, leading to postoperative pain and inflammatory responses. The use of ramidazolam has also been shown to reduce the levels of inflammatory factors (such as IL-6, TNF-α), thereby slowing the postoperative stress response and improving the patient's recovery process. Combined with these mechanisms of action, ramidazolam not only provides good sedation but may also promote postoperative rehabilitation in laparoscopic patients by modulating physiological and pathological responses in the body. The levels of postoperative pain mediators PGE2 and HMGB1 were significantly increased in both groups. However, the former began to decline 12 h after surgery, whereas the latter began to decline 1 h after surgery. However, OG was lower than CG compared with each postoperative detection time index, suggesting that ramidazolam combined with sufentanil had a stronger inhibitory effect on pain mediators than sufentanil alone. This is no different from the research results of Zhang *et al*.[13] Ramazolam blocks the transmission of neurotransmitters through anesthesia, thereby reducing the release of pain mediators such as PGE2 and HMGB1. This can reduce the number of pain mediators acting on peripheral nerve endings, ultimately reducing the patient's pain perception. In addition, Sneyd[14] discovered that remazolam is a new ultra-short-acting benzodiazepine with a high affinity for the GABAA receptor. It acts rapidly on the GABAA receptor, promoting the opening of Cl-channels and resulting in an influx of Cl-ions, which causes hyperpolarization of neuronal cell membranes and consequently produces a sedative effect. Previous studies have pointed out that the trauma and pain caused by thoracoscopic surgery can activate the prostaglandin oxidase reductase in the body, triggering the inflammatory cascade reaction. Ultimately, it will lead to a large release of inflammatory factors. Figure 2 shows that IL-6, IL-10, IL-17, and TNF-α in both groups of patients continued to rise at least 12 h after surgery, which is consistent with previous studies. In addition, studies have shown through animal experiments[15] that benzodiazepine drugs can inhibit the inflammatory response of sepsis mice, which corresponds to the results in this study where the postoperative IL-6, IL-10, IL-17, and TNF-α levels in the OG were lower than those in the CG on average. Another study in this study showed that the levels of A, NA, COR, and FBG in both groups of patients showed an upward trend from preoperative to postoperative 12 h, and a downward trend from postoperative 12 h to postoperative 48 h; The A, NA, COR and FBG of patients participating in the experiment at 1 h, 3 h, 12 h, 24 h and 48 h in postoperation were lower than those in the CG,

**Table 5: Comparison of plasma stress response indicators between patients participating in the experiment before and after surgery ($\bar{x}\pm s$)**

| Serum stress response indicators | Detection time | CG (*n*=88) | OG (*n*=88) | *t* | *P* |
|---|---|---|---|---|---|
| Adrenaline (μg·L⁻¹) | Preoperative | 91.87±14.91 | 92.15±14.37 | −0.126 | 0.900 |
| | Postoperative 1 h | 102.58±18.20* | 97.15±13.49 | 2.247 | 0.026 |
| | Postoperative 3 h | 128.44±20.62* | 122.40±15.49* | 2.196 | 0.029 |
| | Postoperative 12 h | 139.22±23.21* | 131.04±18.03* | 2.612 | 0.010 |
| | Postoperative 24 h | 103.32±15.31* | 97.70±16.68* | 2.326 | 0.021 |
| | Postoperative 48 h | 96.59±14.59* | 88.86±16.37* | 3.304 | 0.001 |
| NA (μg·L⁻¹) | Preoperative | 345.20±20.22 | 347.69±26.29 | −0.703 | 0.483 |
| | Postoperative 1 h | 446.05±24.11* | 436.68±20.10* | 2.578 | 0.011 |
| | Postoperative 3 h | 497.41±33.25* | 484.89±23.01* | 2.905 | 0.004 |
| | Postoperative 12 h | 574.65±30.45* | 556.44±27.68* | 4.153 | <0.001 |
| | Postoperative 24 h | 399.34±25.60* | 386.96±29.87* | 2.953 | 0.004 |
| | Postoperative 48 h | 377.73±25.32 | 365.90±24.20 | 3.168 | 0.002 |
| COR (μg·L⁻¹) | Preoperative | 228.79±23.92 | 232.34±21.59 | −1.033 | 0.303 |
| | Postoperative 1 h | 267.70±22.16* | 260.08±25.14* | 2.132 | 0.034 |
| | Postoperative 3 h | 294.14±20.32* | 283.41±28.10* | 2.903 | 0.004 |
| | Postoperative 12 h | 318.82±32.08* | 294.56±26.45* | 5.472 | <0.001 |
| | Postoperative 24 h | 261.64±28.65* | 249.33±22.70* | 3.160 | 0.002 |
| | Postoperative 48 h | 239.15±22.20 | 227.75±18.11 | 3.733 | <0.001 |
| FBG (mmol·L⁻¹) | Preoperative | 4.97±1.10 | 4.92±0.95 | 0.375 | 0.708 |
| | Postoperative 1 h | 7.58±1.16* | 6.99±1.15* | 3.378 | 0.001 |
| | Postoperative 3 h | 8.67±1.21* | 7.76±1.55* | 4.333 | <0.001 |
| | Postoperative 12 h | 9.37±1.67* | 8.31±1.42* | 4.557 | <0.001 |
| | Postoperative 24 h | 6.43±1.20* | 6.04±1.14* | 2.215 | 0.028 |
| | Postoperative 48 h | 5.79±1.07* | 5.41±1.12* | 2.316 | 0.022 |

*That compared with preoperative, $P<0.05$. A: $F_{\text{Inter group}}/F_{\text{time}}/F_{\text{interactive}}$=4.689/2198.516/67.942, $P_{\text{Inter group}}/P_{\text{time}}/P_{\text{interactive}}$=0.032/<0.001/<0.001, NA: $F_{\text{Inter group}}/F_{\text{time}}/F_{\text{interactive}}$=6.910/59188.600/113.329, $P_{\text{Inter group}}/P_{\text{time}}/P_{\text{interactive}}$=0.009/<0.001/<0.001, COR: $F_{\text{Inter group}}/F_{\text{time}}/F_{\text{interactive}}$=8.235/5428.327/234.175, $P_{\text{Inter group}}/P_{\text{time}}/P_{\text{interactive}}$=0.005/<0.001/<0.001, FBG: $F_{\text{Inter group}}/F_{\text{time}}/F_{\text{interactive}}$=9.475/2941.279/42.634, $P_{\text{Inter group}}/P_{\text{time}}/P_{\text{interactive}}$=0.002/<0.001/<0.001. NA: Norepinephrine, COR: Cortisol, FBG: Fasting blood glucose, CG: Control group, OG: Observation group

which suggested that the combination of remimazolam and sufentanil could help reduce the stress reaction of patients undergoing thoracoscopic surgery. Lee *et al*.[16] found in their study that remazolam can effectively decrease the stress response before and after intubation in patients undergoing thoracic surgery, making circulation more stable, which is not different from the results of this study. In terms of the incidence of AR, there was no dramatic discrepancy in postoperative AR between patients participating in the experiment, indicating that the safety of remazolam is still good. Dai *et al*.[17] pointed out that as a safe and effective inducing sedative drug, ramazolam does not cause excessive AR in ASA I or II general anesthesia patients; Tang *et al*.[18] found that remidazolam used for general anesthesia in patients undergoing cardiac surgery can reduce hemodynamic fluctuations and surgical stress reactions caused by surgery compared to propofol, thereby reducing the risk of anesthesia related adverse events.

Regarding the regulation of pain mediators by ramidolam, similar to the findings of Zhang *et al*., this study showed that ramidolam significantly reduced the release of postoperative pain-related substance PGE2 in patients undergoing general anesthesia, suggesting its potential application in the field of postoperative analgesia. This effect of ramidazolam may be due to its optimization of GABA_A receptors, which in turn reduces the sensitivity of the central nervous system to pain signals compared to traditional anesthetic agents such as propofol.[19] This is consistent with the inhibitory effect of ramidazolam combined with sufentanil on the pain mediator HMGB1 observed in the study. In addition, with regard to changes in inflammatory factors, the results of the study showed that the application of ramidazolam effectively reduced the levels of IL-6, IL-10, and TNF-α, echoing Wan *et al*., which found that patients using ramidazolam had a significant reduction in postoperative inflammation, suggesting that the drug may work by inhibiting the inflammatory cascade.[20] This phenomenon provides an important basis for further clinical research on the use of ramidazolam to optimize anesthesia management and postoperative recovery of patients. Finally, with regard to the assessment of stress responses, the study found significantly lower plasma levels of epinephrine, NA, and COR after surgery than in the CG, suggesting that ramidazolam may play an important role in reducing anesthesia-related stress responses. This result is consistent with the study by Wan *et al*., which indicated

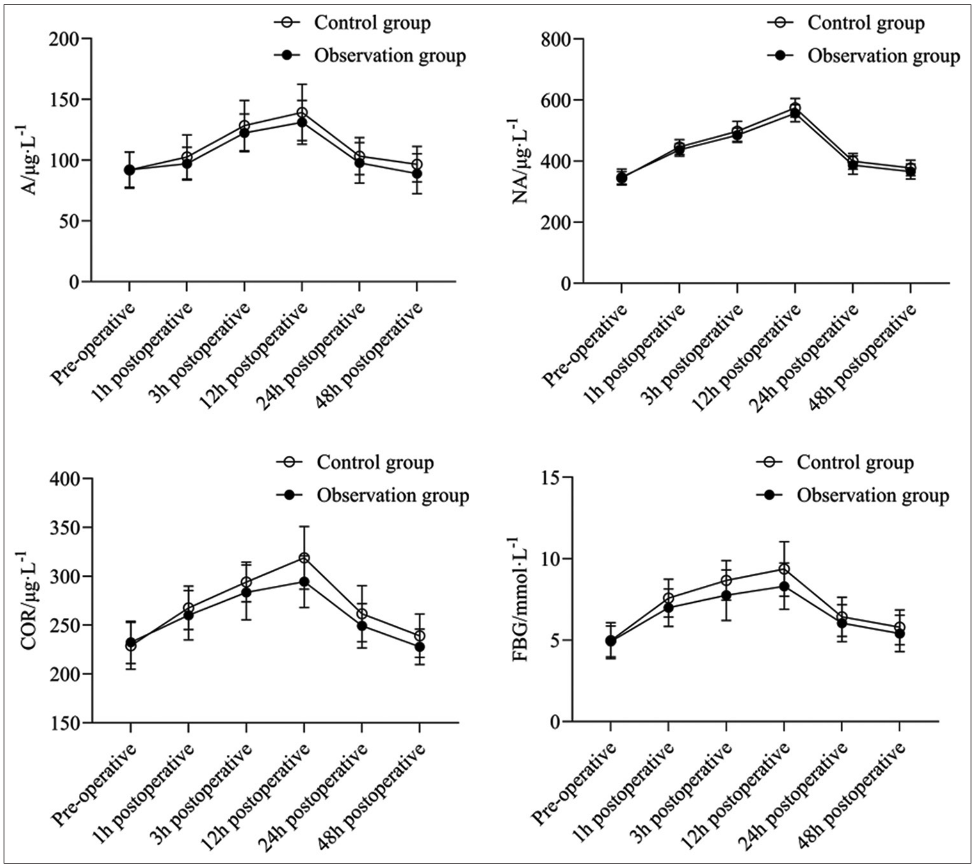


**Figure 3: Line chart of changes in plasma stress response index levels of patients in both groups before and after surgery**

**Table 6: Comparison of postoperative adverse reactions between two groups of patients *n* (%)**

| AR | CG (*n*=88) | OG (*n*=88) | $\chi^2$ | *P* |
|---|---|---|---|---|
| Nausea/vomiting | 2 (2.27) | 3 (3.41) | 0.097 | 0.755 |
| Dizziness/headache | 2 (2.27) | 1 (1.14) | | |
| Respiratory depression | 0 | 1 (1.14) | | |
| Drowsiness | 0 | 1 (1.14) | | |
| Hypoxemia | 1 (1.14) | 0 | | |
| Total occurrence | 5 (5.68) | 6 (6.82) | | |

CG: Control group, OG: Observation group, AR: Adverse reactions

that ramidazolam was effective in stabilizing hemodynamics during surgery and reducing the impact on the autonomic nervous system. Overall, these findings demonstrate the advantages of ramidazolam in improving the speed and comfort of postoperative rehabilitation of patients, and provide useful theoretical support for future clinical applications.[20] Through the in-depth discussion of the literature, the study can more comprehensively understand the mechanism of action of ramidazolam in laparoscopic anesthesia and its clinical application potential.

To sum up, remimazolam combined with sufentanil has a positive effect on inhibiting the release of pain mediators and inflammatory factors and reducing the stress response of patients undergoing thoracoscopic surgery. Moreover, it has high security.

## Conclusion

The combination of remazolam and sufentanil has shown considerable advantages in anesthesia management for thoracoscopic surgery. This anesthetic regimen effectively reduces pain mediators, leading to decreased postoperative pain perception. Additionally, the combination contributes to better hemodynamic stability and enhanced recovery and comfort post-surgery. Crucially, the safety profile of this anesthetic combination remains strong, with no significant differences in adverse reactions between groups, ensuring patient safety while improving anesthetic and analgesic efficacy. In conclusion, our study highlights the effectiveness of remazolam and sufentanil together for improved anesthesia in thoracoscopic procedures, with potential benefits for postoperative outcomes. Future research could explore the long-term effects of this combination on recovery and quality of life.

### Author contributions

Meiling Jiang: conceptualization, data curation, investigation, writing-original draft. Minghui Lun: methodology, validation, formal analysis and writing-review and editing. Zeqing Huang: formal analysis, investigation, methodology. All authors commented on previous versions of the manuscript. All authors read and approved the final manuscript.

### Ethics statement

This study was performed in line with the principles of the Declaration of Helsinki. Approval was granted by the Ethics Committee of Cancer Hospital of China Medical University and Liaoning Cancer Hospital and Institute. Consent to participate statement: Informed consent to participate in the study was obtained verbally from the participant.

### Availability of data and materials

The datasets used and/or analyzed during the current study available from the corresponding author on reasonable request.

### Financial support and sponsorship

Nil.

### Conflicts of interest

There are no conflicts of interest.

## References

1. Chen Z, Zhang Y, Yan Z, Dong J, Cai W, Ma Y, *et al.* Artificial intelligence assisted display in thoracic surgery: Development and possibilities. J Thorac Dis 2021;13:6994-7005.
2. Matsuura N, Igai H, Ohsawa F, Yazawa T, Kamiyoshihara M. Uniport versus multiport video-assisted thoracoscopic surgery for anatomical lung resection-which is less invasive? J Thorac Dis 2021;13:244-51.
3. Sridharan K, Sivaramakrishnan G. Comparison of fentanyl, remifentanil, sufentanil and alfentanil in combination with propofol for general anesthesia: A systematic review and meta-analysis of randomized controlled trials. Curr Clin Pharmacol 2019;14:116-24.
4. Wang M, Zhao X, Yin P, Bao X, Tang H, Kang X. Profile of remimazolam in anesthesiology: A narrative review of clinical research progress. Drug Des Devel Ther 2022;16:3431-44.
5. Kang S, Hu L, Zhou HM, Zhang L. Application of conscious sedation with afentanil combined with titrated infusion of remazolam in gastroscopy for obese patients. Asian J Surg 2024;47:3102-3.
6. Cao J, Luo XL, Lin Q. Remazolam combined with transversus abdominis plane block in gastrointestinal tumor surgery: Have we achieved better anesthetic effects? World J Gastrointest Oncol 2024;16:3368-71.
7. Tai Y, Shi J, Pan J, Hao A, Chang V. Augmented reality-based visual-haptic modeling for thoracoscopic surgery training systems. Virtual Real Intell Hardware 2021;3:274-86.
8. Shrestha B, Dunn L. The declaration of helsinki on medical research involving human subjects: A review of seventh revision. J Nepal Health Res Counc 2020;17:548-52.
9. Liu Y, Wang D, Chi W, Hu F. Study on the combination of remazolam besylate and sufentanil in elderly patients with percutaneous vertebroplasty. Biotechnol Genet Eng Rev 2024,40:1155-1163.
10. Conway A, Chang K, Mafeld S, Sutherland J. Midazolam for sedation before procedures in adults and children: A systematic review update. Syst Rev 2021;10:69.
11. Cardia L. Remimazolam: An ultrashort-acting intravenous anesthetic suitable for general anesthesia. Minerva Anestesiol 2021;87:1059-63.
12. Kim DK, Yoon SH, Kim JY, Oh CH, Jung JK, Kim J. Comparison of the effects of sufentanil and fentanyl intravenous patient controlled analgesia after lumbar fusion. J Korean Neurosurg Soc 2017;60:54-9.
13. Zhang H, Wu Z, Han N, Xu L, Xiong K. Dexmedetomidine pretreatment alleviates ischemia reperfusion injury-induced inflammatory reaction via inhibition of TLR-4/NF-KB signaling pathway. Trop J Pharm Res 2021;18:2031-5.
14. Sneyd JR, Rigby-Jones AE. Remimazolam for anaesthesia or sedation. Curr Opin Anaesthesiol 2020;33:506-11.
15. Xiao D, Zhang D, Xiang D, Liu QI, Liu Y, Lv L, *et al.* Effects of fentanyl, midazolam and their combination on immune function and mortality in mice with sepsis. Exp Ther Med 2015;9:1494-500.
16. Lee HJ, Kwack MH, Lee WJ. Red ginseng acidic polysaccharides promote the expression of acne-related inflammatory biomarkers in lipopolysaccharide-treated sebocytes and outer root sheath cells and cutibacterium acnes-injected mice. Ann Dermatol 2021;33:409-18.
17. Dai G, Pei L, Duan F, Liao M, Zhang Y, Zhu M, *et al.* Safety and efficacy of remimazolam compared with propofol in induction of general anesthesia. Minerva Anestesiol 2021;87:1073-9.
18. Tang F, Yi JM, Gong HY, Lu ZY, Chen J, Fang B, *et al.* Remimazolam benzenesulfonate anesthesia effectiveness in cardiac surgery patients under general anesthesia. World J Clin Cases 2021;9:10595-603.
19. Zhang X, Zhendong XU, Chen P, Xiong J, Pan Z. Effect of remimazolam on anesthetic efficacy of painless bronchoscopy in elderly patients. China Modern Doctor 2024;62:78-82.
20. Wan X, Gong H, Leng H, Zhang Y. Protective effect of remimazolam on neuronal cells from OGD/R induced damage: An *in vitro* study. Trop J Pharm Res 2024;23:537-42.

Original Article

# Anatomical Variations of the Temporal Bones and their Interrelationships


## Abstract

**Objective:** This study aims to investigate the prevalence of anatomical variations of the temporal bone (AVTBs) and to explore the interrelationships among these variations, which could have implications for diagnosis, surgical planning and outcomes in otologic surgeries. **Materials and Methods:** A retrospective analysis was conducted at a single-center hospital between November 2023 and March 2024, involving 260 patients aged 18–60 years who presented to the ENT outpatient clinic with various complaints. AVTBs were identified, and their prevalence was recorded based on the analysis of 520 temporal bones. Arterial, venous, and other anatomical variations were evaluated, and interrelationships of all variations were assessed statistically. **Results:** The most prevalent anatomical variations identified were Körner's septum (KS) (70%), low-lying tegmen tympani (LLT) (54%), and facial canal dehiscence (FCD) (55.8%). Significant correlations were found between tegmen tympani dehiscence and FCD ($P < 0.001$, $r = 0.39$). In addition, a strong correlation was observed between a large emissary vein and petrosquamous sinus ($r = 0.83$). In contrast, the correlations between superior semicircular canal dehiscence and KS were weak. LLT was found to be significantly different, with 40% in females than 20% in males ($P < 0.05$). **Conclusion:** AVTBs are common and exhibit some interrelationships that may impact surgical outcomes. Understanding these correlations is crucial for improving preoperative planning and reducing the risk of complications during otologic surgeries. Further research is needed to validate these findings and explore the clinical significance of these interrelationships.


**Keywords:** *Anatomical variation, facial nerve, mastoidectomy, temporal bone*

**Sari Neslihan, Çankal Fatih**[1]

*Department of ENT, Mardin Artuklu Üniversity Medical Faculty, Mardin, [1]Department of Anatomy, Faculty of Medicine, Ankara Medipol University, Ankara, Türkiye*

## Introduction

Anatomical variations of the temporal bone (AVTBs) involve shifts in the topography and morphology of normal anatomical structures. While many of these variations are benign, some may affect disease symptoms, clinical findings, and management, especially during surgical procedures.[1] Especially in mastoidectomy, we frequently encounter multiple AVTBs presenting significant challenges to the surgeon.[2] Mastoidectomy is the surgical procedure performed to treat chronic otitis media, cochlear implantation, endolymphatic sac surgery, and facial nerve surgery etc.[3] If the anatomical structures are not properly identified, there is a risk of damaging the sigmoid sinus posteriorly, the dura mater laterally, the posterior ear canal wall anteriorly, and the facial nerve, inferiorly leading to facial nerve injury, hearing loss, vertigo, cerebrospinal fluid leakage, the need for revision surgery, postoperative infection, and bleeding.[4] The goal of this investigation is to find out how common AVTBs and their relationships. Understanding these correlations helps to enhance surgical outcomes and minimize complications.

## Materials and Methods

This retrospective study was conducted at a single-center hospital between November 2023 and March 2024. A total of 260 patients presented to the ENT outpatient clinic with the following complaints: otalgia (12%), ear discharge (13%), vertigo (24%), tinnitus (26%), hearing loss (10%), headache (5%), prior surgery follow-up (5%), falls (2%), assault (1%), and others (2%). The study was conducted in accordance with the ethical principles stated in the Declaration of Helsinki and was approved by the local ethics committee for clinical research (2024/2-27). Institutional ethics committee approval was obtained prior to the start of the study.

Demographic, clinical, radiological, and photographic data were collected from chart reviews and the hospital's radiological repository. Medical records and computed

**Article Info**

**Received:** 02 September 2024
**Accepted:** 21 November 2025
**Available online:** 27 March 2026

***Address for correspondence:***
*Dr. Sari Neslihan, Department of ENT, Mardin Artuklu Üniversity Medical Faculty, Mardin, Türkiye.*
*E-mail: neslihansari@artuklu.edu.tr*

**Access this article online**

**Website:** https://journals.lww.com/joai

**DOI:** 10.4103/jasi.jasi_135_24

**Quick Response Code:**



**How to cite this article:** Neslihan S, Fatih Ç. Anatomical variations of the temporal bones and their interrelationships. J Anat Soc India 2026;75:77-83.

tomography (CT) images were reviewed retrospectively. Inclusion criteria included the technical suitability for CT performed after the diagnosis of ear pathology following otoscopic examination in the ENT outpatient clinic. Exclusion criteria encompassed ear pathologies that hindered visualization and/or erosion of bony landmarks and microanatomic features. Written informed consent was obtained from all patients meeting the inclusion criteria.

All patients underwent scanning using the same spiral CT scanner (Aquilion 16 CFX; Toshiba Medical Systems, Tokyo, Japan). The examination was performed in a supine, neutral position, parallel to the superior orbital–meatal line, without tilting of the chin. Scanning was performed from the beginning of the petrous pyramid to the mastoid. In each case, consecutive sections were obtained at 1-mm slice thickness in the axial plane. A 130 KV, 135 mAs, and 512 × 512 matrix were used. To assess bone structures, the "bone algorithm" was applied. No contrast agent was administered. Digital imaging and communications in medicine images were visualized using dedicated image processing software to generate three-dimensional volumetric images on axial, coronal, and sagittal planes. Images were analyzed by a single experienced radiologist on two separate occasions and ENT surgeon performing otologic surgery.

Arterial, venous, and other variations were analyzed. The diagnosed vascular anomalies and variants were evaluated based on the following criteria:

**Arterial variations**

- Aberrant internal carotid artery (aICA): Refers to the displacement of the internal carotid artery (ICA) through the middle ear[5,6]
- Lateral ICA (LICA) or dehiscent ICA: Involves a bony wall of the petrous ICA that is dehiscent with or without protrusion into the middle ear[5,6]
- Persistent stapedial artery (PSA): Diagnosed when the foramen spinosum is absent and an artery running parallel to the promontory through the stapes footplate is present.[5,6]

**Venous variations**

- High Jugular Bulb (HJB) [Figure 1a and b]: The jugular bulb extends above the inferior border of the round window or reaches the level of the basal turn of the cochlea within 2 mm of the internal auditory canal (IAC)[7]
- Jugular bulb dehiscence (JBD): Diagnosis involves observing the absence of hyperdense bony septa between the tympanic cavity and the jugular bulb[8]
- Anterior sigmoid sinus (ASS) [Figure 2]: A protrusive type of sigmoid sinus located anteriorly, with reduced distance between Henle's spine and the sigmoid sinus[5]
- Lateral sigmoid sinus(LSS): A protrusive type of sigmoid sinus placed laterally, with reduced distance between the sigmoid sinus and mastoid cortex[5]
- Prominent sigmoid sinus (pSS): Sigmoid sinus that is prominent compared to the opposite side[5]
- Sigmoid sinus dehiscence (SSD): A condition where there is a dehiscence in the bone separating the sigmoid sinus from the middle ear[9]
- Large emissary vein (LEV): Emissary veins with a diameter greater than 5 mm[10]
- Petrosquamous sinus (PSS): An embryologic emissary vein running along the petrosquamosal fissure.[11]

**Other variations**

- Körner's septum (KS) is a thin bony wall that separates the antrum petrosum from the mastoid antrum[12] [Figure 3]. Cochlear cleft (CC) is a radiographic curvilinear hypodensity area anterior to the oval window on CT.[13] The distance between the temporal meninges and the upper edge of the petrous bone in the case of low-lying tegmen tympani (LLT) should be sloping intermediate and high, not flat.[14] Tegmen dehiscence (TTD) can be observed through HRCT of the temporal bone as a revelation of TTD.[15] Facial canal dehiscence (FCD) exhibits a dehiscent mastoid segment of the facial nerve bony canal by a prominent or HJB[5] [Figure 4]. Superior semicircular canal dehiscence (SSCD) can be visualized through CT scan, demonstrating dehiscence in the bone over the superior semicircular canal.[16] Foramen of Huschke (FH), a developmental anomaly, is found in the anteroinferior segment of the bony external auditory meatus, situated posteromedial to the temporomandibular joint.[17]

For statistical analysis, the SPSS 26.0 trial version for Windows (IBM Corp., Armonk, NY, USA) was used. In descriptive statistics, the number, percentage for categorical variables, and mean, standard deviation, minimum, and maximum for numerical variables were given. Kolmogorov–Smirnov test was used to examine the normality of quantitative data. 'The role of gender on the prevalence of anatomic variations of the temporal bone was analyzed by the Chi-square test. Correlation analysis was

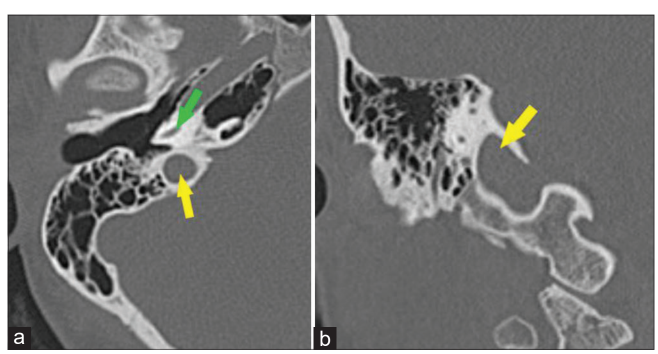


**Figure 1: (a) Axial CT image of the temporal bone, high riding jugular bulb(HJB) is seen. (yellow arrow: jugular bulb, green arrow: cochlear basal turn). (b) Coronal CT image of HJB (yellow arrow: jugular bulb)**

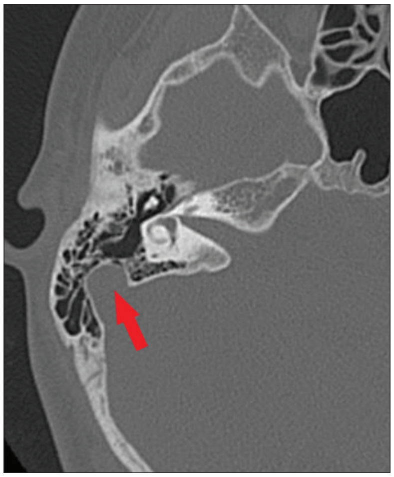

Figure 2: Axial CT image of temporal bone shows the significant anterior location of the sigmoid sinus (red arrow: sigmoid sinus)

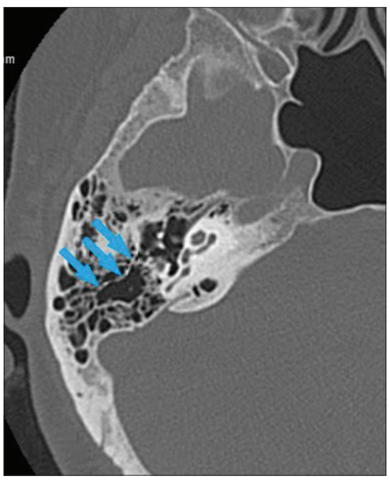

Figure 3: Körner's septum in temporal computed tomography taken in axial plane (blue arrow: Körner's septum)

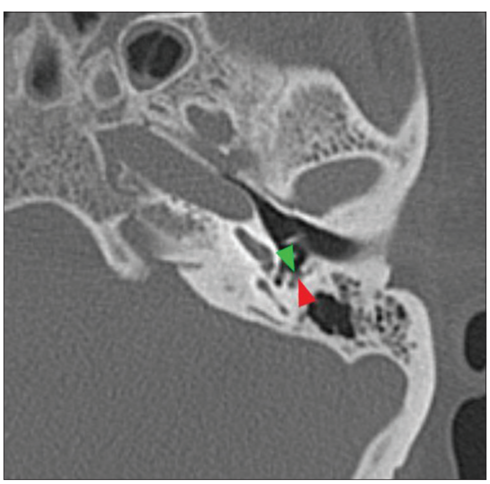

Figure 4: Anterior dehiscence in the proximal part of the mastoid segment of the facial canal on temporal computed tomography taken in the axial plane (red arrowhead: facial canal, green arrowhead: dehiscence)

made among the temporal bone variations. The level of statistical significance was set to $P < 0.05$.

## Results

Out of the 520 temporal bone CT scans analyzed from 260 patients, 132 (50.8%) were male and 128 (49.2%) were female, with a mean age of 37.5 years (standard deviation = 11.5). The most prevalent anatomical variations identified were KS (70%), LLT (54%), and FCD (55.8%). In addition, other notable variations included HJB (14%), SSD (20%), and TTD (32.6%) [Graph 1].

The comparison of parameters by gender revealed that LLT was found to be significantly different, with 40% in females and 20% in males [$P < 0.05$; Table 1].

Correlation analysis revealed a strong and significant association between LEV and PSS ($r = 0.83$, $P = 0.000$), and between JBD and LSS ($r = 0.61$, $P = 0.000$). Other significant associations were found between FCD and TTD ($r = 0.378$, $P < 0.001$), between pSS and SSD ($r = 0.400$, $P = 0.000$), between ASS and SSD ($r = 0.285$, $P = 0.000$), between ASS and pSS ($r = 0.197$, $P = 0.001$), and between LSS and pSS ($r = 0.206$, $P = 0.001$). Additional weak correlations included the relationships between LEV and SSD ($r = 0.136$, $P = 0.029$), LEV and HJB ($r = 0.18$, $P = 0.004$), pSS and JBD ($r = 0.127$, $P = 0.000$), SSD and JBD ($r = 0.148$, $P = 0.017$), LLT and pSS ($r = –0.124$,

**Table 1: Comparison of temporal bone anatomical variations between genders**

| Anatomical variation | Female *n* (%) | Male *n* (%) | *P* |
|---|---|---|---|
| LICA | 11(4.3%) | 8 (3.1%) | 0.81 |
| PSA | 0 (0%) | 3 (1.2%) | 0.86 |
| ASS | 49 (18.8%) | 49(18.8%) | 0.63 |
| LSS | 4(1.6%) | 8(3.1%) | 0.37 |
| pSS | 24 (9.3%) | 23(8.9%) | 0.22 |
| SSD | 41 (15.8%) | 44 (16.9%) | 0.34 |
| KS | 109 (41.9%) | 123 (47.4%) | 0.09 |
| HJB | 20(7.7%) | 31 (11.9%) | 0.31 |
| JBD | 15(5.7%) | 20 (7.7%) | 0.18 |
| JBDv | 3(1.2%) | 8(3.1%) | 0.23 |
| CC | 17 (6.5%) | 19 (7.4%) | 0.27 |
| LLT | 104 (40%) | 53(20.3%) | 0.00* |
| TTD | 67 (25.7%) | 63(24.3%) | 0.62 |
| FCD | 92(35.4%) | 92(35.4%) | 0.98 |
| SSCD | 7 (2.6%) | 8 (3.1%) | 0.42 |
| LEV | 3 (1.2%) | 3 (1.2%) | 0.71 |
| FH | 12 (4.6%) | 15 (5.8%) | 0.55 |
| PSS | 3(1.2%) | 4(1.6%) | 0.65 |

LICA: Lateral Internal Carotid artery, PSA: Persistent Stapedial Artery, ASS: Anterior Sigmoid Sinus, LSS: Lateral Sigmoid Sinus, pSS: Prominent Sigmoid Sinus, SSD: Sigmoid Sinus Dehiscence,KS: Körner Septum, HJB: High Jugular Bulb, JBD: Jugular Bulb Dehiscence, JBDv: Jugular Bulb Diverticulum,CC: Cochlear Cleft, LLT:Low-lying tegmen tympani,TTD: Tegmen Dehiscence,FCD: Facial Canal Dehiscence,SSCD: Superior Semicircular Canal Dehiscence, LEV: Large Emissary Vein, FH: Foramen of Huschke, PSS: Petrosquamous Sinus. *indicates statistical significance ($P<0.05$)

| | | LICA | PSA | ASS | LSS | pSS | SSD | KS | HJB | JBD | JBDv | CC | LLT | TTD | FCD | SSCD | LEV | FH | PSS |
|---|---|---|---|---|---|---|---|---|---|---|---|---|---|---|---|---|---|---|---|
| LICA | r | 1 | | | | | | | | | | | | | | | | | |
| | p | | | | | | | | | | | | | | | | | | |
| PSA | r | -0.029 | 1 | | | | | | | | | | | | | | | | |
| | p | 0.64 | | | | | | | | | | | | | | | | | |
| ASS | r | 0.054 | -0.074 | 1 | | | | | | | | | | | | | | | |
| | p | 0.386 | 0.236 | | | | | | | | | | | | | | | | |
| LSS | r | -0.057 | 0.056 | 0.019 | 1 | | | | | | | | | | | | | | |
| | p | 0.363 | 0.369 | 0.764 | | | | | | | | | | | | | | | |
| pSS | r | 0.04 | -0.046 | .197** | .206** | 1 | | | | | | | | | | | | | |
| | p | 0.517 | 0.463 | 0.001 | 0.001 | | | | | | | | | | | | | | |
| SSD | r | 0.005 | -0.007 | .285** | .189** | .400** | 1 | | | | | | | | | | | | |
| | p | 0.941 | 0.906 | 0 | 0.002 | 0 | | | | | | | | | | | | | |
| KS | r | -0.057 | 0.106 | 0.036 | -0.066 | -0.044 | -0.049 | 1 | | | | | | | | | | | |
| | p | 0.362 | 0.089 | 0.559 | 0.288 | 0.477 | 0.43 | | | | | | | | | | | | |
| HJB | r | 0.062 | -0.048 | -0.071 | 0.006 | 0.034 | -0.116 | 0.046 | 1 | | | | | | | | | | |
| | p | 0.318 | 0.446 | 0.256 | 0.928 | 0.58 | 0.063 | 0.462 | | | | | | | | | | | |
| JBD | r | -0.06 | 0.017 | 0.071 | .609** | .127* | .148* | -0.038 | 0.023 | 1 | | | | | | | | | |
| | p | 0.332 | 0.785 | 0.251 | 0 | 0.041 | 0.017 | 0.547 | 0.708 | | | | | | | | | | |
| JBDv | r | 0.034 | -0.022 | 0 | -0.044 | -0.088 | -0.098 | 0.023 | 0.042 | -0.074 | 1 | | | | | | | | |
| | p | 0.584 | 0.718 | 0.995 | 0.483 | 0.157 | 0.113 | 0.707 | 0.504 | 0.236 | | | | | | | | | |
| CC | r | -0.106 | -0.042 | 0.018 | -0.004 | 0.031 | -0.011 | 0.028 | -0.032 | -0.01 | -0.054 | 1 | | | | | | | |
| | p | 0.088 | 0.495 | 0.773 | 0.953 | 0.621 | 0.863 | 0.656 | 0.602 | 0.873 | 0.388 | | | | | | | | |
| LLT | r | -0.075 | 0.075 | 0.009 | 0.027 | -.124* | -0.069 | -0.069 | -0.001 | 0.003 | -0.001 | 0.089 | 1 | | | | | | |
| | p | 0.226 | 0.228 | 0.879 | 0.665 | 0.046 | 0.27 | 0.265 | 0.99 | 0.964 | 0.991 | 0.151 | | | | | | | |
| TTD | r | 0.066 | -0.094 | 0.004 | 0.048 | 0.041 | -0.073 | -0.05 | 0.002 | 0.061 | 0.061 | -0.002 | 0.066 | 1 | | | | | |
| | p | 0.292 | 0.129 | 0.952 | 0.444 | 0.512 | 0.238 | 0.42 | 0.976 | 0.325 | 0.329 | 0.978 | 0.292 | | | | | | |
| FCD | r | -0.06 | -.125* | -0.105 | -0.046 | -0.01 | 0.087 | -0.097 | -0.014 | -0.012 | 0.028 | -0.028 | 0.083 | .378** | 1 | | | | |
| | p | 0.336 | 0.044 | 0.092 | 0.46 | 0.868 | 0.161 | 0.119 | 0.828 | 0.848 | 0.653 | 0.656 | 0.183 | 0 | | | | | |
| SSCD | r | -0.061 | -0.024 | -0.041 | -0.047 | -0.059 | -0.057 | 0.069 | -0.008 | 0.028 | -0.047 | -0.089 | -0.015 | 0.03 | 0.02 | 1 | | | |
| | p | 0.329 | 0.696 | 0.507 | 0.448 | 0.344 | 0.357 | 0.268 | 0.892 | 0.659 | 0.452 | 0.155 | 0.812 | 0.626 | 0.748 | | | | |
| LEV | r | -0.041 | -0.016 | 0.033 | -0.032 | 0.113 | .136* | 0.092 | .180** | -0.007 | .126* | -0.059 | -0.046 | -0.08 | -0.047 | -0.034 | 1 | | |
| | p | 0.514 | 0.794 | 0.599 | 0.612 | 0.07 | 0.029 | 0.139 | 0.004 | 0.909 | 0.042 | 0.342 | 0.462 | 0.2 | 0.453 | 0.586 | | | |
| FH | r | 0.061 | -0.035 | 0.041 | -0.068 | 0.046 | 0.035 | -0.021 | 0.034 | 0.006 | .124* | -.127* | 0.031 | 0.032 | 0.064 | -0.073 | 0.033 | 1 | |
| | p | 0.329 | 0.575 | 0.512 | 0.275 | 0.457 | 0.579 | 0.735 | 0.582 | 0.929 | 0.046 | 0.04 | 0.614 | 0.612 | 0.305 | 0.242 | 0.596 | | |
| PSS | r | -0.043 | -0.017 | 0.006 | -0.033 | 0.107 | 0.094 | .130* | 0.104 | -0.011 | 0.019 | -0.062 | -0.042 | -0.036 | -0.029 | 0.024 | .832** | -0.024 | 1 |
| | p | 0.491 | 0.783 | 0.917 | 0.593 | 0.085 | 0.131 | 0.037 | 0.095 | 0.865 | 0.761 | 0.316 | 0.495 | 0.561 | 0.646 | 0.696 | 0 | 0.695 | |

**Figure 5: Correlation analysis of anatomic variations of temporal bone**

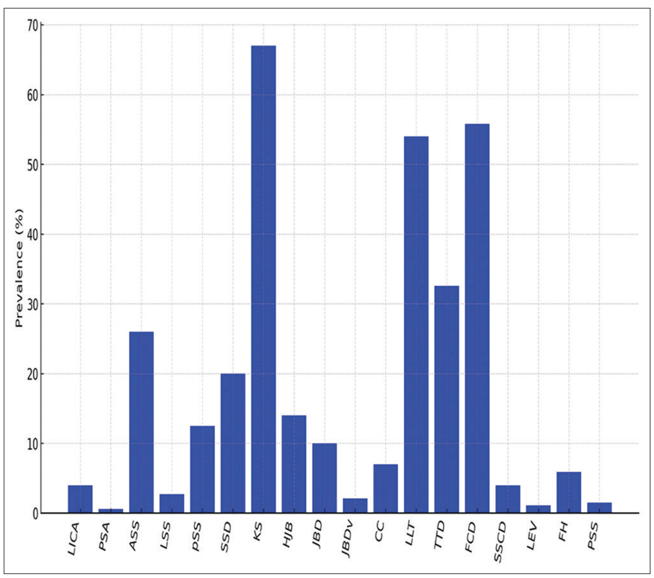


**Graph 1: Prevalence of Temporal Bone Anatomical Variations**

$P$ = 0.046), and FH and JBDv ($r$ = 0.124, $P$ = 0.046). More details are presented in Figure 5.

## Discussion

The findings of this study emphasize the prevalence and significance of AVTBs in clinical and surgical contexts. Arterial variations of the temporal bone, namely aICA, LICA, and PSA, are rare or nil.[6] They carry a high risk of iatrogenic catastrophic bleeding during medical interventions. Usually, the ICA travels through the temporal bone on the anteromedial part of the hypotimpanum, with a thin layer of bone covering it. On the other hand, congenital ossification failure can cause dehiscence or gap in approximately 1% of cases on its course. An aberrant lateral course in the temporal bone passing through and occupying the middle ear cavity causes danger in ear surgeries.[2,19,20] PSA is generally causes intractable bleeding in stapes surgery.[6,18]

Of the venous variation, ASS, LSS, LEV, and HJB bleeding and long operation time in mastoidectomies.[5] Furthermore, LEV causes the spread of infection from the neck to the sigmoid sinus and the cavernous sinus.[8,18] It is the persistence of a residual vein draining into the sigmoid sinus.[5,10] Turbulence in normally located veins and the enlargement or abnormal location of veins near the conductive auditory pathway causes pulsatile tinnitus.[19] They are pathologic abnormalities in the lateral sinus (trans verse sinus stenosis and sigmoid sinus wall anomalies), dilated emissary veins (mastoid emissary vein, petrosquamous vein), and pathologic abnormalities of the jugular vein and bulb (HJB, JBD, and JBDv).[20] Although the prevalence of HJB is found to be 14% in our study, In study of Atmaca *et al*., HJB is the most common venous variation in the temporal bone with 15.2%. Prevalence levels in our study and the literature are given in Table 2. The broad variability in prevalence rates noted in the literature can be attributed to both geographical variation and genetics[8] [Table 2]. JBD entity is the superior and medial extension of the JB into the bone of the posterior wall of the IAC. Although most cases are asymptomatic, the jugular bulb diverticulum presents with tinnitus, vertigo, hearing loss, and recurrent facial nerve palsy

**Table 2: Incidence of temporal bone anatomical variations according to various studies**

| | Our study (%) | Literature (%) |
|---|---|---|
| aICA | 0% | <1% Koesling *et al*[6] |
| LICA | 4% | 2-3.4%Koesling *et al*[6], Bozec *et al*[5] |
| PSA | 0.60% | 0.2-0.48% Goderie *et al*[18] |
| ASS | 26% | 34% Karaca *et al*[2] |
| LSS | 2.70% | 8.33% Bozec *et al*[5] |
| pSS | 12.50% | 15.58% Bozec *et al*[5] |
| SSD | 20% | 25-30% Ravichandran *et al*[9] |
| KS | 67% | 0.5-74% Karaca *et al*[2] |
| HJB | 14% | 6-21% Bozec *et al*[5] |
| JBD | 10% | 1-9.5% Bozec *et al*[5] |
| | | 6% Koesling *et al*[6] |
| | | 32% Karaca *et al*[2] |
| JBDv | 2.10% | 4% Bozec *et al*[5] |
| CC | 7% | 15-26%(children) Caldwell *et al*[13] |
| LLT | 54% | 35% Makki *et al*[14] |
| TTD | 32.60% | 15-34% Kuo *et al*[15] |
| FCD | 55.80% | 55.1% Kalaiarasi *et al*[24] |
| SSCD | 4% | 0.5-74% Karaca *et al*[2] |
| LEV | 1.10% | 6% (prominent)Koesling *et al*[6] |
| FH | 5.90% | 4-7 % Tozoglu *et al*[17] |
| PSS | 1.50% | 6.88% Bozec *et al*[5] |

aICA: Aberrant Internal Carotid artery, LICA: Lateral Internal Carotid artery, PSA: Persistent Stapedial Artery, ASS: Anterior Sigmoid Sinus, LSS: Lateral Sigmoid Sinus, pSS: Prominent Sigmoid Sinus, SSD: Sigmoid Sinus Dehiscence,KS: Körner Septum, HJB: High Jugular Bulb, JBD: Jugular Bulb Dehiscence, JBDv: Jugular Bulb Diverticulum,CC: Cochlear Cleft, LLT:Low-lying tegmen tympani,TTD: Tegmen Dehiscence, FCD: Facial Canal Dehiscence,SSCD: Superior Semicircular Canal Dehiscence,LEV: Large Emissary Vein, FH: Foramen of Huschke,PSS: Petrosquamous Sinus

due to compression to the petrous apex.[21] A HJB with or without a diverticulum influences the approach in acoustic neurinoma surgery. JB diverticulum can progress in size. When a dehiscent JB protrudes into the middle ear, it can be confused with a glomus tumor by otoscopy. Bleeding complications during middle ear procedures have been reported in such cases.[22] The bony covering over the jugular bulb forms the posteromedial part of the floor of the tympanic cavity. On otoscopy, a bluish mass in the posteroinferior aspect of the middle ear behind the tympanic membrane can be seen when the bony covering of the jugular bulb is dehiscent, and this may lead to complications even in simple procedures such as myringotomy or during the elevation of the tympanomeatal flap because the wall of the jugular bulb is very thin.[8]

Embryologically, the cranial nerves, cochlea, and vestibular apparatus arise from neuroectoderm. Everything else in temporal bone, including the ossicles, arises from ectoderm.[23] The relationship of the facial nerve in the temporal bone is determined by embryological closure of the otic capsule sulcus to form fallopian canal. By the 5th month of gestation, the bone begins to cover the nerve, but the facial nerve is not completely enclosed by bone even at birth. Postnatally, the ossification process continues. This is the reason why children are affected by facial nerve palsy secondary to acute otitis media due to higher incidence of dehiscent facial canal in the middle ear.[24] Moreover, development of the intracerebral veins and their extracranial drainage is complex in humans but have common origion. Venous sinuses are underdeveloped during early fetal life and maintain their small caliber until 2 years after birth. Variations in the course of the sigmoid sinus appear to arise during the 8th and 9th months of fetal life and are influenced by the development of the cerebellum.[25] This explains the strong correlation between a LEV and the PSS underscores the importance of vascular variations in surgical planning supporting common embryologic and pathological mechanism. Surgeons should be particularly vigilant when dealing with patients exhibiting these vascular variations, as failure to recognize and appropriately manage these structures could lead to severe intraoperative complications.

The high incidence of variations such as KS, LLT, and FCD highlights the complexity of temporal bone anatomy and the importance of careful preoperative planning [Graph 1]. During mastoidectomy, LLT and TTD cause dural tears, cerebrospinal fluid leaks, and brain herniation. KS, a structure that creates a false antrum base in mastoidectomy, can be mistaken for the finding of an antrum. This misunderstanding can lead to injury to the facial nerve lying under the antrum base. Clinically, KS is considered a factor in the development of chronic diseases of the ear, like chronic otitis media, especially attic retraction pockets, and cholesteatoma. The presence of KS can complicate mastoidectomy procedures, potentially leading to these chronic ear diseases. There is also an association between tympanosclerosis and KS.[12] The prevalence of KS is high, as indicated in Tables 2 and Graph 1. The significant correlation between FCD and TTD suggests a potential shared developmental or pathological mechanism as stated above. This relationship may have crucial implications during mastoidectomy or other ear surgeries where inadvertent damage to the facial nerve or dura could lead to severe complications. Therefore, preoperative identification of these variations is essential to mitigate risks such as facial nerve injury, cerebrospinal fluid leakage, and postoperative infections.

SSCD is a rare clinical condition with a dehiscence in the bone overlying the superior semicircular canal, presenting with complex and varied symptoms, including pressure- or sound-induced vertigo, hyperacusis to bone-conducted sounds, and pulsatile tinnitus.[16] Among the labyrinthine variants, CC is a complex condition that is often observed in children. If it persists into adulthood, it can be mistaken for fissula antefenestram or pathology related to the otic capsule. This condition is characterized by incomplete enchondral ossification containing marrow with fat lobules.[13]

In terms of gender differences, the study found that LLT was significantly more common in females than in males, which may have implications for sex-specific considerations in surgical approaches. In a study by Sever *et al*., in which they study risk groups in ear surgeries, females were found to have more LLT and placed in high risk group.[26] This finding highlights the importance of considering patient demographics in the evaluation of AVTBs, as these factors may influence both the prevalence of variations and the risk of associated complications.

In conclusion, AVTBs are common and often exhibit significant interrelationships that can impact surgical outcomes. Recognizing these variations and understanding their correlations are critical for improving preoperative planning and reducing the risk of complications in otologic surgeries. The study's findings underscore the need for further research to validate these results and explore the clinical significance of these interrelationships, potentially leading to more tailored and safer surgical approaches in the future.

### Limitations and future directions

Despite the strengths of this study, including a large sample size and detailed analysis of multiple anatomical variations, there are limitations that should be acknowledged. The retrospective and single-centered nature of the study may limit the generalizability of the findings. Moreover, correlation does not imply causation; therefore, prospective and multicenter studies are needed to confirm these findings and explore the underlying mechanisms behind these correlations.

Future research should also focus on the clinical outcomes associated with these anatomical variations, particularly in relation to facial nerve function postsurgery. Understanding how these variations affect long-term surgical outcomes will be crucial in refining surgical techniques and improving patient care.

## Conclusion

This study emphasizes the critical role of identifying AVTB in reducing the risk of facial nerve injury during otologic surgeries. The strong correlations observed between certain variations, such as FCD with TTD, LEV with PSS. They highlight the importance of thorough preoperative imaging and careful surgical planning. By recognizing these interrelationships, surgeons can better anticipate potential challenges and optimize surgical outcomes. The findings also underscore the importance of further research to validate these associations and to explore the clinical significance of less common variations.

### Acknowledgment

We thank the hospital staff in Radiology and ENT in Pursaklar Government Hospital, Ankara, Türkiye, for their kind cooperation and timely help.

### Financial support and sponsorship

Nil.

### Conflicts of interest

There are no conflicts of interest.

## References

1. Visvanathan V, Morrissey MS. Anatomical variations of the temporal bone on high-resolution computed tomography imaging: How common are they? J Laryngol Otol 2015;129:634-7.
2. Karaca CT, Toros SZ, Noseri HK. Analysis of anatomic variations in temporal bone by radiology. J Int Adv Otol 2012;8:239-43.
3. Tames HL, Padula M, Sarpi MO, Gomes RL, Toyama C, Murakoshi RW, *et al.* Postoperative ımaging of the temporal bone. Radiographics 2021;41:858-75.
4. Kennedy KL, Lin JW. Mastoidectomy. In: StatPearls; 2024. Available from: https://www.ncbi.nlm.nih.gov/books/NBK559153/. [Last accessed on 2024 Jun 27, Last updated on 2023 May 29].
5. Bożek P, Kluczewska E, Misiołek M, Ścierski W, Lisowska G. The prevalence of persistent petrosquamosal sinus and other temporal bone anatomical variations on high-resolution temporal bone computed tomography. Med Sci Monit 2016;22:4177-85.
6. Koesling S, Kunkel P, Schul T. Vascular anomalies, sutures and small canals of the temporal bone on axial CT. Eur J Radiol 2005;54:335-43.
7. Dong C, Zhao PF, Yang JG, Liu ZH, Wang ZC. Incidence of vascular anomalies and variants associated with unilateral venous pulsatile tinnitus in 242 patients based on dual-phase contrast-enhanced computed tomography. Chin Med J (Engl) 2015;128:581-5.
8. Atmaca S, Elmali M, Kucuk H. High and dehiscent jugular bulb: Clear and present danger during middle ear surgery. Surg Radiol Anat 2014;36:369-74.
9. Ravichandran AP, Su Y, Yacoub HA. A treatable cause of pulsatile tinnitus: A case of sigmoid sinus dehiscence. Cureus 2023;15:e35577.
10. Lee SH, Kim SS, Sung KY, Nam EC. Pulsatile tinnitus caused by a dilated mastoid emissary vein. J Korean Med Sci 2013;28:628-30.
11. Liu Z, Chen C, Wang Z, Gong S, Xian J, Liang X. Petrosquamosal sinus in the temporal bone as a cause of pulsatile tinnitus: a radiological detection. Clin Imaging 2013;37:561-63.
12. Wojciechowski T, Skadorwa T, Drożdż A, Ciszek B, Szopiński K. The radioanatomical assessment of the Körner's septum. Surg Radiol Anat 2019;41:669-73.
13. Chadwell JB, Halsted MJ, Choo DI, Greinwald JH, Benton C. The cochlear cleft. AJNR Am J Neuroradiol 2004;25:21-4.
14. Makki FM, Amoodi HA, van Wijhe RG, Bance M. Anatomic analysis of the mastoid tegmen: Slopes and tegmen shape variances. Otol Neurotol 2011;32:581-8.
15. Kuo CY, Wang CH, Feng HM, Chen HC. Conductive hearing loss as the initial manifestation of spontaneous herniation of epitympanic meningocele. J Int Adv Otol 2014;10:91-3.
16. Ward BK, van de Berg R, van Rompaey V, Bisdorff A, Hullar TE, Welgampola MS, *et al.* Superior semicircular canal dehiscence syndrome: Diagnostic criteria consensus document of the committee for the classification of vestibular disorders of the Bárány Society. J Vestib Res 2021;31:131-41.
17. Tozoglu U, Caglayan F, Harorli A. Foramen tympanicum or foramen of Huschke: Anatomical cone beam CT study. Dentomaxillofac Radiol 2012;41:294-7.

18. Goderie TP, Alkhateeb WH, Smit CF, Hensen EF. Surgical management of a persistent stapedial artery: A review. Otol Neurotol 2017;38:788-91.
19. Ahmad R, Ali I, Naikoo GM, Choo NA, Jan F. Giant mastoid emissary vein: Source of profuse bleeding during mastoid surgery. Indian J Otolaryngol Head Neck Surg 2011;63:102-3.
20. Trivelato FP, Araújo JF, Dos Santos Silva R, Rezende MT, Ulhôa AC, Castro GD. Endovascular treatment of pulsatile tinnitus associated with transverse sigmoid sinus aneurysms and jugular bulb anomalies. Interv Neuroradiol 2015;21:548-51.
21. Alkhamis F, Alhajri K, Aljaafari D, Alhashim A, Alsamarah A, Sharydah A, *et al*. Recurrent Facial Palsy Due to High Jugular Bulb Dehiscence. J Multidiscip Healthc 2021;14:359-62.
22. Abdalkader M, Nguyen TN, Norbash AM, Raz E, Shapiro M, Lenck S, *et al*. State of the Art: Venous Causes of Pulsatile Tinnitus and Diagnostic Considerations Guiding Endovascular Therapy. Radiology 2021;300:2-16.
23. Dublin AB, Al-Dhahir MA. Anatomy, head and neck, temporal region. In: StatPearls; 2024. Available from: https://www.ncbi.nlm.nih.gov/books/NBK482497/. [Last accessed on 2024 Jun 27, Last updated on 2023 Jun 05].
24. Kalaiarasi R, Kiran AS, Vijayakumar C, Venkataramanan R, Manusrut M, Prabhu R. Anatomical features of ıntratemporal course of facial nerve and its variations. Cureus 2018;10:e3085.
25. Kiritsi O, Noussios G, Tsitas K, Chouridis P, Lappas D, Natsis K. Anatomical variants of the emissary veins: Unilateral aplasia of both the sigmoid sinus and the internal jugular vein and development of the petrosquamosal sinus. A rare case report. Folia Morphol (Warsz) 2011;70:305-8.
26. Sever SN, Çetin H, Çalıskan S, Akkasoglu S. Anatomical and clinical evaluation of tympanic tegmen and mastoid bone with multidetector computed tomography. Int J Morphol 2023;41:937-43.

Review Article

# Anatomical Differences in the Cranial Cavity and their Impact on Neurological Health: A Systematic Review

**Mohammad Rehan Asad, Sonika Sharma[1], Sanjeev Kumar Jain[1], Suraj Prakash[1], Vishram Singh[2], Riyaz Ahamed Shaik[3]**

*Department of Basic Medical Sciences, College of Medicine, Majmaah University, [3]Department of Family and Community Medicine, Majmaah University, Al Majma'ah, Saudi Arabia, [1]Department of Anatomy, TMMC and RC, Teerthanker Mahaveer University, Moradabad, Uttar Pradesh, [2]Department of Anatomy, KMC, MAHE, Mangalore, Karnataka, India*

## Abstract

The cranial cavity exhibits significant anatomical diversity, with consequences for neurological function through the modification of intracranial pressure, cerebral perfusion, and neurovascular interactions. Cranial structural diversity has been linked to the pathophysiological processes of neurodevelopmental disorders, cerebrovascular disease, and neurodegenerative disease. The extent to which these anatomical diversities influence neurological health is uncertain. This systematic review was undertaken to combine the existing evidence on cranial cavity variations and their association with neurological outcomes. A comprehensive search of seven databases was conducted to identify cross-sectional studies, case-cohort studies (retrospective and prospective designs), and clinical trials that have investigated cranial cavity morphometry and its neurological importance. Quantitative data on cranial cavity measurements and their relationship with measures of neurological well-being provided by studies were utilized. Potential for bias was assessed using the Joanna Briggs Institute systematic review checklist. Synthesis of data was a systematic analysis of variables such as cranial volume, skull base angulation, cortical thickness, ventricular size, and related neurological parameters. The findings indicated significant interindividual and condition-dependent variation in cranial cavity structure. Cranial volume ranged from 950 to 1200 $cm^3$, with deviations in the cases of craniosynostosis and Chiari malformation. Skull base angles varied between 124° and 134°, with alterations associated with osteogenesis imperfecta and platybasia. Ventricular enlargement was associated with cognitive impairment, with affected individuals exhibiting a 2.3% greater ventricular occupancy compared with controls ($P < 0.01$). Cortical thickness reductions were significant in neuropsychiatric disorders, with thinning observed at rates of up to 50% relative to controls ($P < 0.05$). Gray-to-white matter ratio had profound predictive value for neurological outcome, with a threshold range of 1.17–1.27 exhibiting a sensitivity of 85% and specificity of 90%. Preservation of cerebral perfusion pressure above 70 mmHg was associated with favorable survival, though not statistically significant ($P = 0.08$). Overall risk of bias was low-to-moderate throughout the included studies. Anatomical variations in the structure of the cranial cavity demonstrated quantifiable correlations with neurological well-being, specifically with respect to cerebrovascular surgery, intracranial pressure, and mental function. They highlighted the need for the incorporation of cranial morphometric assessment into neurological evaluation to enhance diagnostic and prognostic strategies. Longitudinal studies and sophisticated imaging techniques should be the focus of future studies to establish causal relationships between anatomical variation and neurological disease.

**Keywords:** *Brain volume, cerebral perfusion, cranial cavity shape, intracranial pressure, morphometric analysis, neuroanatomy, neurological function*

**Article Info**

**Received:** 09 April 2025
**Revised:** 18 August 2025
**Accepted:** 19 August 2025
**Available online:** 27 March 2026

***Address for correspondence:***
*Dr. Sonika Sharma, Department of Anatomy, TMMC and RC, Teerthanker Mahaveer University, Moradabad, Uttar Pradesh, India. E-mail: sonikaanatomy.medical@tmu.ac.in*

**Access this article online**

**Website:** https://journals.lww.com/joai

**DOI:** 10.4103/jasi.jasi_75_25

**Quick Response Code:**

## Introduction

The cranial vault, a highly evolved and complex osseous complex, not only encloses and safeguards the brain but also plays a role in the dynamic modulation of intracranial pressures and neurological functions.[1] The anatomical organization of the vault is a result of the subtle interplay between genetic, developmental, and environmental influences, resulting in a significant degree of variability among various individuals and populations.[2] Cranial variability has been linked with a variety of neurological disorders, including neurodevelopmental disabilities, cerebrovascular abnormalities, and neurodegenerative diseases.[3] These variabilities exist in varying dimensions, including cranial cavity volume, skull base angulation, cerebral cortex thickness, and ventricular size, all of which have significant physiological and biomechanical implications for brain function.[4]



**How to cite this article:** Asad MR, Sharma S, Jain SK, Prakash S, Singh V, Shaik RA. Anatomical differences in the cranial cavity and their impact on neurological health: A systematic review. J Anat Soc India 2026;75:84-91.

 

The cranial vault remodels during development because of the dynamic interaction between bone adaptation and neural growth.[5] Abnormality of the process, congenital, acquired, or age-related, influences intracranial compliance, reduces cerebrospinal fluid (CSF) dynamics, and modifies cerebral perfusion pressure (CPP) and thus predisposes the patient to neurological impairments.[6] Craniosynostosis is an example of the outcome of premature suture closure, causing compensatory skull shape changes and the risk of intracranial hypertension in spite of preservation of cranial volume.[7] Similarly, changes in the shape of the skull base, as in Chiari malformation, have been associated with compromised CSF flow dynamics and subsequent neurovascular complications.[8] The change of cranial structures over time also illustrates the complex interdependence between cranial anatomy and neurological well-being.

Cortical tissue atrophy that develops in neurodegenerative diseases, such as Alzheimer's disease, is characteristically associated with the enlargement of cerebral ventricles, which is considered a compensatory change in response to the loss of white and gray matter.[9] Asymmetrical morphometric features within the cranial compartment, especially in areas related to cognitive functions and motor control, have been identified in neuropsychiatric diseases like schizophrenia, in which abnormal maturation and cortical thinning is associated with alterations in functional connectivity and cognitive impairment.[10] Current evidence also points to an emerging interrelationship between skeletal mineral density and cerebral well-being, indicating that bone mineral density (BMD) loss is associated with an increase in white matter lesions and cognitive impairment in the elderly.[11,12]

Given the complex interrelation between neurological function and cranial anatomy, there is a need to perform an extensive review of the literature in order to determine the specific influence of anatomical variation within the cranial cavity on neurological health. Through such a review, evidence from primary studies examining variation in cranial architecture and consequent physiological and pathological effects will be critically examined and synthesized.

## Materials and Methods

### Population, Exposure, Comparison, Outcome, Study Design protocol and Preferred Reporting Items for Systematic Reviews and Meta-Analyses adherence

The Population, Exposure, Comparison, Outcome, and Study Design framework for the systematic review was constructed in line with the Preferred Reporting Items for Systematic Reviews and Meta-Analyses guidelines[13] to ensure methodological quality and transparency. The population (P) was participants of varying ages who exhibited documented anatomical variations in the cranial cavity regardless of any underlying neurological condition. The exposure (E) was morphological variation in cranial cavity parameters, such as but not limited to cranial cavity volume, skull base angulation, cortical thickness, ventricular dimensions, foramen magnum morphology, and morphometric asymmetry. The comparator (C) was normative cranial anatomical data, where present, or comparative analysis between varying anatomical subgroups. The outcomes (O) were measures of neurological health such as intracranial pressure, CPP, cognitive function, cerebrovascular dynamics, and neuroimaging biomarkers related to neurodevelopmental, neurodegenerative, or cerebrovascular disorders. The study design (S) was cross-sectional studies, case–cohort studies (prospective and retrospective), and clinical trials to allow overall examination of the interrelation between cranial cavity anatomy and neurological health outcomes.

### Inclusion and exclusion criteria

Inclusion was original research papers that examined cranial cavity anatomy and its relation to neurological health outcomes. Research had to have at least one measurable cranial morphometric variable and an associated neurological variable, for example, intracranial pressure, cortical atrophy, or cognitive impairment. Human studies of any gender or age were included. English-language studies with clearly described methodologies published in peer-reviewed journals were included.

Research articles were excluded from consideration if they did not contain primary data or were set as narrative reviews, commentaries, expert opinion, or conference abstracts. Case series or case reports involving <10 patients were ignored for the reason of limited generalizability of findings. Studies exclusively on cranial trauma, infectious origin, or neoplastic diseases were excluded, as these are specific pathological processes and might not reflect intrinsic anatomical differences. Those articles that did not have complete data on cranial morphometry or whose full-text versions were not accessible were not considered for inclusion.

### Database search methodology

A systematic and comprehensive review of the evidence was conducted using seven electronic databases, including PubMed, Scopus, Web of Science, Embase, Cochrane Library, CINAHL, and PsycINFO. The search strategy utilized medical subject headings terms and Boolean operators to yield an effective identification of relevant studies. The search terms were modified to each database to maximize sensitivity and specificity. Boolean operators such as AND, OR, and NOT were utilized to limit the focus of the searches.

### Data extraction process

A systematic data extraction protocol was developed to facilitate proper acquisition of study characteristics and outcome measures. Data were independently extracted by two reviewers from a predetermined template, and a third reviewer resolved any discrepancies. The data that were extracted included a range of study characteristics (e.g., author, year, study design, sample size, location, and follow-up duration), cranial cavity measurements (e.g., cranial volume, skull base angulation, foramen magnum dimensions, cortical thickness, ventricular volume, and indices of asymmetry), neurological outcomes (which included intracranial pressure, CPP, cognitive assessment, and neuroimaging biomarkers), and measures of methodological quality. Where there was more than one outcome measure, those with the highest level of rigorous statistical analysis were utilized. The studies were classified by methodological design to allow comparative evaluation.

### Bias evaluation framework

Risk of bias in the systematic review was assessed using the Joanna Briggs Institute (JBI) Critical Appraisal Checklist for Systematic Reviews,[14] thus ensuring methodological rigour and transparency.

## Results

One hundred and sixty four records were found by database searching with no additional records from registers [Figure 1]. Before screening, 43 duplicate records were removed, leaving 121 unique records for subsequent assessment. At the screening level, a total of 121 records were screened, and no records were excluded at this level. An attempt was made to retrieve the full text of all 121 reports, but 39 reports were not available, thus reducing the number of available full-text articles to be assessed to 82. The screening phase of the eligibility assessment resulted in the exclusion of 74 studies, comprising 25 reviews and 49 irrelevant articles, thus resulting in the inclusion of 8 primary studies[15-22] in the systematic review.

### Bias assessment observations

The JBI checklist evaluation of bias indicated that the studies included within this review were largely at low-to-moderate risk of bias, thus confirming an acceptable level of methodological quality [Figure 2]. The inclusion criteria were clearly defined in most of the studies; however, some were at moderate risk due to less detailed eligibility criteria specification.[16,19,21] The conduct of the literature search was largely robust, with most studies conducting thorough searches; however, some were at moderate risk due to restricted search scope or the danger of excluding relevant sources.[15,18,20]

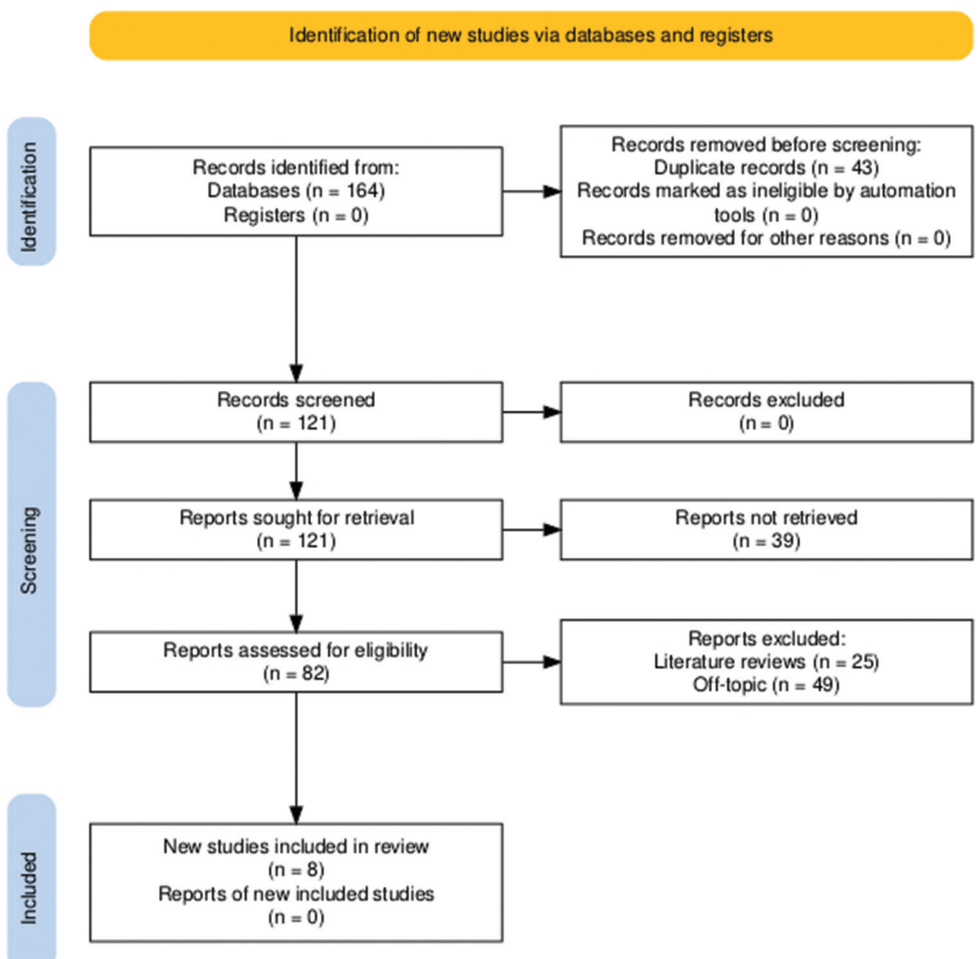


**Figure 1: PRISMA study selection process for the review**

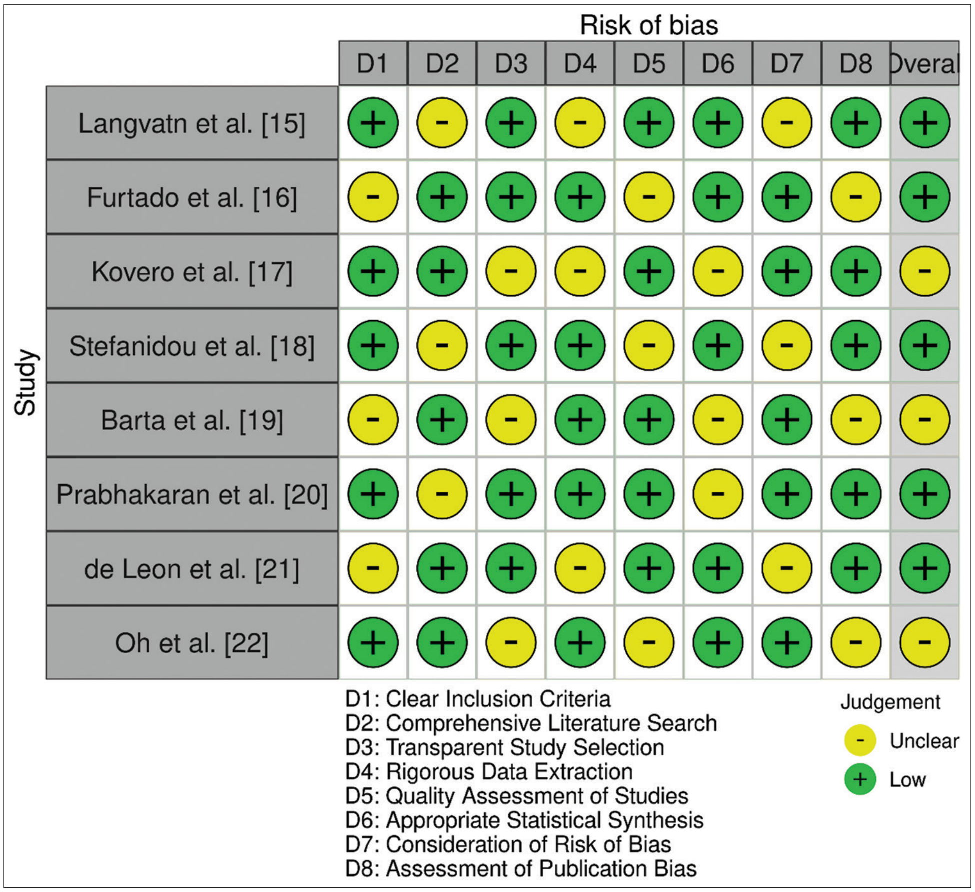


**Figure 2: Bias assessment observations for the review**

The clarity of the study selection was well documented to a great extent; however, some studies did not state clear details concerning the selection process, causing a moderate risk in some instances.[17,19,22] Data extraction was done with care in most studies; however, some had a moderate risk due to inconsistencies in standardizing data collection procedures.[15,17,21] The quality assessment of the included studies was done effectively to a great extent; however, some studies had a moderate risk because of improper study validity and reliability assessment.[16,18,22]

Statistical synthesis methods were considered appropriate for most of the studies reviewed; a subgroup, however, had a moderate risk according to potential limitations in statistical power or data harmonization.[17,19,20] Bias between individual studies' risk assessment was heterogeneous, with a moderate risk defined where confounding variables were not adequately controlled.[15,18,21] Publication bias was also assessed in most of the studies, but a moderate risk was indicated in some where inadequate discussions were given for selective reporting or missing data.[16,19,22]

### Demographic features

The studies incorporated in this systematic review were conducted in various geographic locations [Table 1], such as Norway,[15] India,[16] Finland,[17] the United States,[18-21] and South Korea.[22] The applied study design varied from being a variety of study types, with a prevailing majority of cross-sectional case–control studies,[15-19,21] and involvement of retrospective[22] and randomized controlled trials (RCTs).[20] The sample sizes also varied considerably, from small cohorts of 17 patients in an RCT to treat severe traumatic brain injury[20] to the whole cohort study of 1905 participants from a population-based registry.[18] The ages of the participants also had extreme variation, with some studies conducted among pediatric populations[15,16,20] and others among middle-aged or older populations.[18,19,21,22] While the male-to-female ratio was not consistently reported in the studies incorporated, where reported, distribution ranged from nearly equal numbers[18,22] to unstated numbers in pediatric samples.[15-17,19-21] The follow-up periods were mostly missing in cross-sectional studies,[15-19,21] while retrospective studies and RCTs had longer observation periods, such as measurement at 1 year following injury in severe traumatic brain injury[20] and observation to hospital discharge in prognosis studies.[22]

### Cranial morphology and intracranial parameters

The cranial cavity volume was found to possess high individual variation and under variable conditions from as low as 950–1000 $cm^3$ in patients with craniosynostosis[15] and approaching 1200 $cm^3$ in control pediatric subjects.[16]

**Table 1: Technical characteristics and key findings assessed across the included studies**

| Author ID | Location | Study design | Sample size | Mean age (years) | Male: female ratio | Conclusion (key findings) |
|---|---|---|---|---|---|---|
| Langvatn *et al*.[15] | Norway | Cross-sectional (case-control) | 31 | 2.2 (patients), 2.5 (controls) | NR | Reduced ICV did not correlate with raised ICP; intracranial HTN in craniosynostosis is not caused by volume alone |
| Furtado *et al*.[16] | India | Retrospective (case-control) | 42 | NR (children) | NR | Foramen magnum area in Chiari children was normal; irregular FM shape due to developmental anomalies - individualized assessment is needed |
| Kovero *et al*.[17] | Finland | Cross-sectional (case-control) | 162 | NR (mixed ages) | NR | OI patients show skull base flattening increasing with severity; prior thresholds for "platybasia" were met by some controls, indicating need for revised diagnostic criteria |
| Stefanidou *et al*.[18] | USA | Cross-sectional (cohort analysis) | 1905 | 66±9 | 870:1035 | Higher BMD was associated with less white matter lesion burden and better cognitive performance in older adults, suggesting a link between bone health and brain aging |
| Barta *et al*.[19] | USA | Cross-sectional (case-control) | 60 | 39±11 (patients) versus 36±10 (controls) | NR | Schizophrenia patients showed reversed planum temporale asymmetry (right larger than left) with significantly thinned right PT gray matter (~50% of control thickness), despite normal total brain volume |
| Prabhakaran *et al*.[20] | USA | RCT (pilot, severe TBI) | 17 | NR (15 m–15 years range) | NR | CPP-targeted therapy (maintain CPP~70 mmHg) was feasible and safe in pediatric TBI; showed a trend toward more unimpaired survivors compared to ICP-focused therapy, though not statistically significant |
| George *et al*.[21] | USA | Cross-sectional (case-control) | 64 | >60 (all subjects) | NR | Alzheimer's patients had enlarged ventricles (~7.5% of cranial volume) versus controls (~5.2%); ventricular size correlated with cognitive impairment severity |
| Oh *et al*.[22] | South Korea | Retrospective (prognostic) | 86 | 56.1±15.5 | 56:30:00 | Gray/white matter attenuation ratio on CT was an effective predictor of poor neurological outcome after cardiac arrest; optimal GWR cutoff ≈1.17-1.27 for 100% specificity |

ICV: Intracranial volume, HTN: Hypertension, ICP: Intracranial pressure, FM=foramen magnum, BMD=Bone mineral density, CPP: Cerebral perfusion pressure, RCT: Randomized controlled trial, TBI: Traumatic brain injury, CT: Computed tomography, GWR: Gray-white matter ratio

Measured where feasible, skull base angles were seen to possess the greatest variation, governed by pathological and developmental factors, with mean values averaging around 129.8°C ± 5.5°C in osteogenesis imperfecta patients, with progressive flattening of the skull base with greater disease severity.[17] Intracranial pressure was seen to be exceedingly high, with mean values ranging up to 17.1 ± 5.6 mmHg in patients with craniosynostosis; however, no intracranial volume correlation was determined.[15] In pediatric brain injury due to trauma, intracranial pressure was managed actively at below 20 mmHg in order to permit CPP maintenance.[20]

## Cortical and ventricular morphology

Cortical thickness measurements demonstrated remarkable decreases in neurodevelopmental and neuropsychiatric disorders, with planum temporale gray matter showing a decrease nearing 50% of control levels in schizophrenic patients.[19] This was also seen with a reversal of cortical asymmetry in this same anatomical region, differing from the normal left-dominant morphology.[19] Ventricular volume in neurodegenerative disorders showed marked enlargement, as Alzheimer's disease patients had considerably larger ventricular occupancy (7.5% of total intracranial volume) compared to healthy subjects (5.2%),[21] thus further validating the known correlation between progressive cortical atrophy and ventricular enlargement in dementia-related disorders.

## Foramen magnum anatomy and cerebrovascular physiology

Foramen magnum measurements were in normal ranges among pediatric patients with Chiari malformation, and this shows that congenital variation in CSF dynamics is not necessarily associated with stenotic structural pathology alone, but more with atypical posterior fossa morphologies.[16] CPP monitoring in traumatic brain injury was improved in situations where levels were maintained above 70 mmHg compared to 50 mmHg, tending toward improved survival and reduced neurological deficits.[20] Statistical significance was not, however, achieved, and this emphasizes the necessity for stronger, rigorous validation.

### Neuroimaging biomarkers and bone mineral density

Gray-to-white matter ratio (GWR) is a significant neuroimaging biomarker for cardiac arrest patient prognosis, and the best specificity cut-offs are postulated to fall in the 1.17–1.27 range, although these may be influenced by scanner selection.[22] Reduced GWR values have been found to correspond significantly with undesirable neurological outcomes and therefore with substantial utility in the early risk stratification of hypoxic–ischemic brain damage.[22] Morphometric measurements, especially on skull base examination, indicate historic diagnostic criteria for platybasia will be called into question as asymptomatic control subjects yielded historic threshold levels.[17] BMD measurements have suggested a likely neuroprotective advantage, such that high BMD subjects yield reduced burden of white matter lesion and improved cognition, especially among elderly subjects.[18] Such a finding indicates the correlation of skeletal and neurological health, and the role of systemic metabolic drivers on neurodegeneration will be required to further investigate.

## Discussion

The results of this systematic review emphasized the significant influence of cranial shape on neurological health outcomes. Quantifiable correlations between cranial volume, skull base angle, and cortical thickness and cerebrovascular control, intracranial pressure variability, and cognitive function were demonstrated. The association between ventricular enlargement and cognitive impairment emphasized the contribution of structural brain measurements to the pathogenesis of neurodegenerative disease.

The prognostic value of the ratio of gray matter to white matter with respect to neurological outcome predicted its potential value to the stratification of the management of postcardiac arrest and cerebrovascular disease. Translational value was emphasized by the usefulness of the application of standard morphometric measures to the practice of clinical neurology, with particular reference to circumstances in which differences in cranial anatomy may be used as a marker of disease in the very earliest stages. Use of high-resolution magnetic resonance imaging and computer-based volumetric measurement has the potential to increase the sensitivity of diagnostic evaluation. Future studies will have to utilize longitudinal study designs in order to determine the causal relationships of cranial shape to neurological outcome.

The complex interaction between cranial cavity anatomy and nervous system health is regulated by a complex interaction between genetic, developmental, and biomechanical controls that modulate intracranial mechanics and cerebrovascular integrity.[23] The cranial vault is a rigid container for the brain, and cranial shape change influences intracranial pressure regulation, cerebral perfusion, and neurophysiological homeostasis. Cranial anatomy morphometric abnormalities have been linked to a wide variety of neurological disorders, such as neurodevelopmental disorders, cerebrovascular disease, and neurodegenerative disorders, and underscore the functional importance of cranial architecture beyond structure containment.[24]

One of the major concerns of cranial morphometry is the interaction of skull base angulation and CSF kinematics. The skull base with intricate articular relationships of the sphenoid, occipital, and temporal bones is remodeled after birth, which changes the pathway of neural and vascular channels.[25] Malalignment of the skull base angle has been found to correlate with impaired CSF flow patterns, e.g., Chiari malformation, wherein an obliquely placed skull base changes the volume of the posterior fossa and also the position of the brainstem.[26] Such a change leads to patient susceptibility to neurological deficit secondary to increased CSF turbulence and resistance to drainage, thereby once again affirming the functional importance of skull base parameters to neurological health.

But yet another influence on cranial morphology is the interaction between cortical thinning and ventricular enlargement, which has been implicated in both neurodevelopmental and neurodegenerative illness. Cortical thinning has been found in psychiatric illnesses such as schizophrenia, where abnormal neurodevelopment is linked with abnormal patterns of gyrification and cortical atrophy.[27] Ventricular enlargement, on the other hand, is commonly found in neurodegenerative illness, where brain tissue loss leads to compensatory dilatation of the CSF spaces, a process which has classically been referred to as hydrocephalus ex vacuo.[28] The interaction between the influences means that cranial morphometry is not an invariant parameter but one that is reconstituted on a continuous basis by both the processes of physiological aging and illness.

From a hemodynamic perspective, CPP and GWR have been the primary predictors of neurological function. Biomechanical limitations are imposed on cerebral blood flow by the cranial cavity, with perfusion efficiency modified by alterations in intracranial compliance.[29] Reduced GWR has been linked with hypoxic–ischemic injury following cerebral insults such as traumatic brain injury or cardiac arrest, where impaired perfusion withholds oxygenation from the neuronal tissue.[30] This would suggest that cranial morphometry could be predictive in the risk patient identification for cerebrovascular dysfunction, and further investigation of its combination with clinical decision models would be justified.

Improvements in neuroimaging technology, especially high-resolution magnetic resonance imaging and computerized volumetric analysis, have greatly improved the accuracy of cranial morphometric measurement. Machine learning algorithms have increasingly been utilized to quantify cranial shape variation and predict the course of disease from morphometric measurements.[31] This computational model strategy presents an intriguing target for the development of the diagnostic and prognostic value of cranial cavity analysis to offer individualized risk stratification and early intervention planning. Longitudinal analyses must be the target of future research to further define the pattern of cranial morphometric change across the life stages and disease states.[32]

### Limitations

This systematic review was limited by several factors. The studies included were heterogeneous with respect to their design, most importantly imaging modalities and assessment criteria that could have resulted in inconsistency of the cranial parameters reported. Utilization of cross-sectional data is limited, making causal inferences on the relationship between anatomical variation and neurological outcomes. Sample sizes of the included studies were heterogeneous, with some of them having low statistical power, which could have impacted the effect size estimates. Exclusion of studies published in non-English languages could have resulted in publication bias, thus limiting the generalizability of the findings. Furthermore, heterogeneity of the study populations, including age, sex distribution, and comorbidities, could have influenced cranial morphometric variations, thus requiring a careful interpretation of the findings.

## Conclusion

The findings obtained through this review provide key insight into the anatomical and physiological associations in the cranial cavity and their bearing on neurological health. The variability of research methods and patient groups highlights the importance of standardization in cranial morphometric and neuroimaging measurements, particularly in instances of inherent anatomical variability, as in craniosynostosis, Chiari malformation, and osteogenesis imperfecta. The application of CPP monitoring protocols to the management of traumatic brain injury and the prognostic value of the GWR in post-cardiac arrest patients similarly highlight the clinical relevance of these measures in the determination of therapeutic interventions. Moreover, the association of BMD with cognitive resilience provides potential areas for inter-disciplinary research to examine the metabolic underpinnings of neurodegeneration. Taken together, these studies highlight the importance of holistic, multimodal assessments incorporating anatomical, functional, and biochemical markers to enable greater insight into the complex interdependencies underpinning neurological outcomes.

### Financial support and sponsorship

The authors extend their appreciation to the Deanship of Post graduate Studies and Scientific Research at Majmaah University for funding this research work through the project number R-2025-1978.

### Conflicts of interest

There are no conflicts of interest.

## References

1. Leak RK, Clark RN, Abbas M, Xu F, Brodsky JL, Chen J, *et al.* Current insights and assumptions on α-synuclein in Lewy body disease. Acta Neuropathol 2024;148:18.
2. Reardon T, Turnow M, Elston S, Brown NJ, Koller GM, Sharma S, *et al*. Surgical management of petrous apex cholesteatomas in the pediatric population: A systematic review. Surg Neurol Int 2022;13:494.
3. Lee S, Kim S, Sunwoo JS. Otogenic *Enterobacter cloacae* meningitis complicated with pneumocephalus. Encephalitis 2023;3:125-8.
4. McGillion-Moore J, Sampath P, Wong ET. Methylphenidate reversal of executive dysfunction in a patient with bi-frontal lobe glioblastoma. R I Med J (2013) 2023;106:7-10.
5. Albuck AL, Techabunyart DB, Cardona JJ, Chaiyamoon A, Tsang P, Iwanaga J, *et al*. Review of the caroticotympanic nerves: Anatomy, function and pathology. Anat Histol Embryol 2023;52:823-6.
6. Iwanaga J. The alveolar canals and foramina in the first edition of terminologia Oroanatomica: A preview. Anat Sci Int 2024;99:461-8.
7. Chaiyamoon A, Boontem P, Samrid R, Cardona JJ, Khanthiyong B, Yurasakpong L, *et al*. An anatomical study of the nasal foramina. Surg Radiol Anat 2024;46:1495-500.
8. Fillingham P, Rane Levendovszky S, Andre J, Parsey C, Bindschadler M, Friedman S, *et al*. Patient-specific computational fluid dynamic simulation of cerebrospinal fluid flow in the intracranial space. Brain Res 2022;1790:147962.
9. Mano T, Tatsumi S, Fujimura S, Hotta N, Kido A. Isolated bilateral hypoglossal nerve paralysis following an atlanto-occipital dislocation: A case report. Front Neurol 2022;13:965717.
10. Aicher ML, Bisch-Karatas J, Maurer A, Wagner F, Wartenberg M, Zimmerli S. Rare case of a chronic rhinocerebral mucormycosis. Med Mycol Case Rep 2024;44:100648.
11. Kobayashi Y, Kamijima S, Okumura G, Morizumi T, Nagamatsu K, Shimizu Y, *et al*. Cavernous sinus swelling and abducens nerve paresis due to intracranial hypotension. Intern Med 2022;61:3111-3.
12. Kantaputra PN, Angkurawaranon S, Khwanngern K, Ngamphiw C, Intachai W, Adisornkanj P, *et al*. Clinical and genetic studies of the first monozygotic twins with Pfeiffer syndrome. Genes (Basel) 2022;13:1850.
13. Page MJ, Moher D, Bossuyt PM, Boutron I, Hoffmann TC, Mulrow CD, *et al.* PRISMA 2020 explanation and elaboration: Updated guidance and exemplars for reporting systematic reviews. BMJ 2021;372:n160.
14. Porritt K, Gomersall J, Lockwood C. JBI's systematic reviews: Study selection and critical appraisal. Am J Nurs 2014;114:47-52.

15. Langvatn EA, Frič R, Due-Tønnessen BJ, Eide PK. Intracranial volume versus static and pulsatile intracranial pressure values in children with craniosynostosis. J Neurosurg Pediatr 2019;24:66-74.
16. Furtado SV, Thakre DJ, Venkatesh PK, Reddy K, Hegde AS. Morphometric analysis of foramen magnum dimensions and intracranial volume in pediatric Chiari I malformation. Acta Neurochir (Wien) 2010;152:221-7.
17. Kovero O, Pynnönen S, Kuurila-Svahn K, Kaitila I, Waltimo-Sirén J. Skull base abnormalities in osteogenesis imperfecta: A cephalometric evaluation of 54 patients and 108 control volunteers. J Neurosurg 2006;105:361-70.
18. Stefanidou M, O'Donnell A, Himali JJ, DeCarli C, Satizabal C, Beiser AS, *et al.* Bone mineral density measurements and association with brain structure and cognitive function: The Framingham offspring cohort. Alzheimer Dis Assoc Disord 2021;35:291-7.
19. Barta PE, Pearlson GD, Brill LB 2nd, Royall R, McGilchrist IK, Pulver AE, *et al.* Planum temporale asymmetry reversal in schizophrenia: Replication and relationship to Gray matter abnormalities. Am J Psychiatry 1997;154:661-7.
20. Prabhakaran P, Reddy AT, Oakes WJ, King WD, Winkler MK, Givens TG. A pilot trial comparing cerebral perfusion pressure-targeted therapy to intracranial pressure-targeted therapy in children with severe traumatic brain injury. J Neurosurg 2004;100:454-9.
21. George AE, de Leon MJ, Rosenbloom S, Ferris SH, Gentes C, Emmerich M, *et al.* Ventricular volume and cognitive deficit: A computed tomographic study. Radiology 1983;149:493-8.
22. Oh JH, Choi SP, Zhu JH, Kim SH, Park KN, Youn CS, *et al.* Differences in the Gray-to-white matter ratio according to different computed tomography scanners for outcome prediction in post-cardiac arrest patients receiving target temperature management. PLoS One 2021;16:e0258480.
23. Abdallah A, Çınar İ, Güler Abdallah B. Long-term surgical outcome of Chiari type-I malformation-related syringomyelia: An experience of tertiary referral hospital. Neurol Res 2022;44:299-310.
24. Lara-Olivas JA, Sangrador-Deitos MV, Marian-Magaña R, Padilla-Leal KE, Soto-Hernández JL, Gomez-Amador JL. Endoscopic endonasal resection of a *Drechslera hawaiiensis* sphenoid fungal ball. Surg Neurol Int 2023;14:321.
25. Neugebauer F, Antonakakis M, Unnwongse K, Parpaley Y, Wellmer J, Rampp S, *et al.* Validating EEG, MEG and combined MEG and EEG beamforming for an estimation of the epileptogenic zone in focal cortical dysplasia. Brain Sci 2022;12:114.
26. Li P, Dai L, Yuan K, Song C, Cheng Y, Jing Y, *et al.* Necrotizing pneumonia and purulent meningitis caused by bloodstream infection of CA-MRSA in a child: A rare case report. Front Pediatr 2022;10:1045774.
27. Hamed M, Potthoff AL, Layer JP, Koch D, Borger V, Heimann M, *et al.* Benchmarking safety indicators of surgical treatment of brain metastases combined with intraoperative radiotherapy: Results of prospective observational study with comparative matched-pair analysis. Cancers (Basel) 2022;14:1515.
28. Silva MI, Santos P, Viegas D, Miranda M, Montes V, Pita F, *et al.* Neurolymphomatosis as primary presentation of extra-nodal NK/T-cell lymphoma, nasal type. Neurol Sci 2024;45:4003-6.
29. Han XC, Liu RX, Lin X, He JY, Bu H. Clinical observation of 8 cases with central nervous system anaerobic infection diagnosed by metagenomic next-generation sequencing of cerebrospinal fluid. Zhonghua Yi Xue Za Zhi 2022;102:1533-6.
30. Fukushima K, Takazono T, Ashizawa N, Hara S, Kitaoka K, Ideguchi R, *et al*. A case of Lemierre's syndrome with double vision as the first symptom. J Infect Chemother 2022;28:286-9.
31. Agyemang K, Gómez Rodríguez R, Rocha Marussi VH, Marte Arias SA, Feliciano Vilcahuaman Paitań A, Campos Filho JM, *et al.* Case report: Delayed outflow obstruction of a DVA: A rare complication of brainstem cavernoma surgery. Front Neurol 2023;14:1073366.
32. Li X, Liu HZ, Pang LY, Wen X, Sun SZ. A retrospective study of recurrent bacterial meningitis in children: Etiology, clinical course, and treatment. Comput Math Methods Med 2022;2022:3681871.

JASI

# Laparoscopic Repair of Diaphragmatic Hernia: A Report of Two Adult Cases


## Abstract

The protrusion of abdominal contents into the thoracic cavity through a defect in the diaphragm is known as a diaphragmatic hernia. It can be either congenital or acquired with congenital cases often diagnosed prenatally and repaired shortly after birth. Diagnosing an adult diaphragmatic hernia can be difficult because the condition may stay asymptomatic or exhibit unusual and unrelated symptoms. Acquired diaphragmatic hernias are more common in adults, with trauma, both blunt and penetrating, as the primary cause. High clinical suspicion is essential, and prompt radiological investigation is crucial for accurate diagnosis. Early diagnosis and appropriate surgical intervention are essential for optimal outcomes. In the present article, two cases of adult diaphragmatic hernias are described. The first case presented with herniation of small gut loops into the left hemithorax in a 29-year-old woman. The second case was with a giant diaphragmatic hernia containing the spleen, stomach, small gut, and large gut loops and a part of the liver masquerading as tension pneumothorax in a 30-year-old woman (Gastrospleenothorax). Both cases were diagnosed and managed successfully via laparoscopic repair. This report, along with a review of the literature, highlights the unusual presentation of diaphragmatic hernias in adults and demonstrates the feasibility of laparoscopic repair.


**Keywords:** *Adult, diaphragmatic hernia, laparoscopy, surgery*


**Jibreel Yousuf, Mubashir A. Shah, Hira Ateeq[1], Yaqoob Hassan**

*Department of General and Minimal Invasive Surgery, SKIMS, Srinagar, Jammu and Kashmir, [1]Department of Surgery, Aligarh Muslim University, Aligarh, Uttar Pradesh, India*


## Introduction

The protrusion of abdominal contents into the thoracic cavity through a diaphragm defect is known as a diaphragmatic hernia. It may be acquired or congenital. Congenital diaphragmatic hernia is an idiopathic malformation that usually presents in the newborn period and occurs in 1–5 neonates every 1000 live births.[1] The most common presentation is respiratory distress, which is often in association with underlying pulmonary hypoplasia secondary to compression caused by the herniated viscera on the affected side, and may even progress to pulmonary hypertension. However, although rare but congenital diaphragmatic hernia can present at later stages of life as well and may present as mild respiratory distress or incidental detection at a routine examination.

A diaphragmatic hernia may also be acquired. Acquired diaphragmatic hernia usually occurs secondary to blunt or penetrating trauma to the thoraco-abdominal region,[2] resulting in increased pleuroperitoneal pressure that causes an anatomical defect at the weak fusion sites of the diaphragm and subsequent upward protrusion of the abdominal contents.[3] Bulging of the abdominal contents into the thoracic cavity leads to symptoms such as chest pain and dyspnea, whereas gastrointestinal symptoms may also be present secondary to herniating of stomach and bowel loops into the thoracic cavity. Other than trauma, iatrogenic injury to the diaphragm can also lead to an acquired diaphragmatic defect, leading to hernia. Examples include surgical procedures involving resection of the liver, urological procedures or adrenal gland tumors.[4] Although very rare, there have been reports of spontaneous diaphragmatic hernias in the absence of any trauma or iatrogenic injury.[5]

The clinical diagnosis of diaphragmatic hernia is highly challenging because of the heterogeneous spectrum of symptoms.[6] Hence, the diagnosis is confirmed using various radiological methods, among which computed tomography (CT)



**How to cite this article:** Yousuf J, Shah MA, Ateeq H, Hassan Y. Laparoscopic repair of diaphragmatic hernia: A report of two adult cases. J Anat Soc India 2026;75:92-7.

**Article Info**

**Received:** 12 January 2026
**Revised:** 03 February 2026
**Accepted:** 09 February 2026
**Available online:** 27 March 2026

***Address for correspondence:***
*Dr. Yaqoob Hassan,*
*Senior Resident Hostel, SKIMS Soura, Srinagar, Jammu and Kashmir, India.*
*E-mail: dryaqoobwani@gmail.com*

**Access this article online**

**Website:** https://journals.lww.com/joai

**DOI:** 10.4103/jasi.jasi_5_26

**Quick Response Code:**

is the preferred method due to its high sensitivity and specificity.[7] This article discusses the clinical presentation, diagnosis, and management of diaphragmatic hernia in adults, while also contributing two additional cases to the existing literature. Our case series highlights the atypical, delayed presentation, and challenges in the diagnosis and management of diaphragmatic hernia in adults. A brief literature review of the condition in this context is also included.

## Materials and Methods

The patients of adult diaphragmatic hernia encountered over the period of 1 year in our Department of General and Minimally Invasive Surgery, SKIMS, were managed and reported. The medical records of the patients included demographic characteristics, clinical presentation, and radiological parameters, were collected. Further, the preoperative workup, operative methods, postoperative status, and the conditions on follow-up were recorded, analyzed, and reported.

## Case Reports

### Case 1

A 29-year-old female, P3 L3, BM1 = 23.3, with no known co-morbidity, presented to a peripheral emergency surgical facility with a 1-week history of abdominal pain along with nausea and vomiting. The patient also reported respiratory distress and a history of a respiratory tract infection 2 weeks prior, which was associated with a severe cough. At the peripheral center, the patient underwent a chest radiograph, which was misinterpreted as showing a left-sided pneumothorax, following which an intercostal chest tube (ICT) was inserted into the left hemithorax [Figure 1]. No abdominal pathology was suspected at that time, and the abdominal symptoms were attributed to gastritis. An abdominal ultrasound performed at the peripheral center was inconclusive, likely due to bowel gas and lack of suspicion for a diaphragmatic pathology.

Following the chest tube (ICT) insertion, the complaints of respiratory distress persisted along with worsening abdominal pain and vomiting. She was, therefore, referred to our tertiary care center for further evaluation and management. The patient was subjected to thorough physical and clinical examination, which revealed decreased breath sounds in the left hemithorax. Abdominal examination showed mild distension with epigastric tenderness. There was no prior history of trauma, surgery, or similar complaints. Baseline investigations, including complete blood count, renal and liver function tests, and serum electrolytes, were within normal limits. In view of recurrent vomiting and abdominal distension, a 16-Fr Ryle's tube was inserted for gastric decompression and to alleviate the symptoms.

A repeat chest radiograph obtained after Ryle's tube placement revealed the tube coiled within the left hemithorax, with its tip projecting above the level of the diaphragm, strongly raising suspicion of a left-sided diaphragmatic hernia. The stomach was noted to be herniated into the thoracic cavity along with small bowel loops, explaining the abnormal course of the nasogastric tube. Subsequently, a contrast-enhanced CT of the chest and abdomen was performed, which confirmed a left-sided diaphragmatic defect with herniation of the stomach and small bowel loops into the left hemithorax, causing compression of the adjacent lung parenchyma. Based on these findings, a preoperative diagnosis of left-sided acquired diaphragmatic hernia was made [Figure 1].

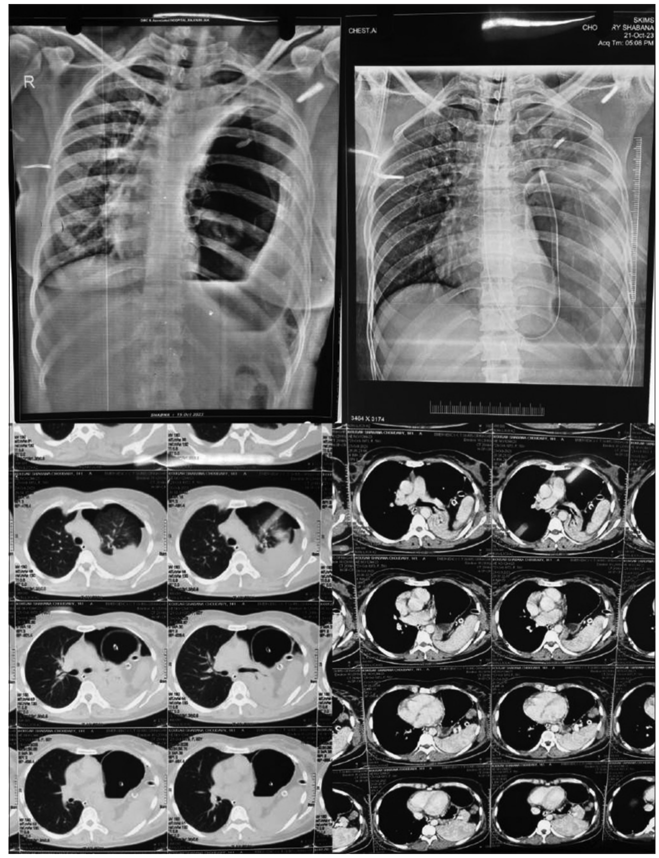


**Figure 1: Case 1 - Preoperative imaging**

The patient was scheduled for laparoscopic repair. Intraoperatively, a defect of 7 cm × 4 cm was identified along the posterior-lateral margin of the left hemidiaphragm, through which the stomach and multiple small bowel loops had herniated into the thoracic cavity [Figure 2]. The herniated contents were reduced into the abdominal cavity, and the defect was primarily repaired using interrupted Prolene mattress sutures [Figure 2]. The postoperative period was uneventful, and the patient was discharged on the 3rd postoperative day. The patient is currently doing well and is on regular follow-up.

### Case 2

A 35-year-old married female, P1 L1, presented with a 2-month history of respiratory distress, for which she had sought multiple consultations at peripheral outpatient departments and in a private set-up. Unfortunately, she was initially diagnosed with an upper respiratory tract infection and treated accordingly, but her symptoms persisted. Eventually, she was referred to a tertiary care center, where a chest radiograph [Figure 3] revealed multiple air–fluid levels in the left hemithorax, with collapsed left lung parenchyma. Detailed surgical, medical, obstetric, personal, and family histories were recorded, which were not significant. Upon clinical examination, her temperature was 99.8°F, BMI = 23.1, respiratory rate 20 breaths/min, her blood pressure (BP) was 120/70 mm Hg, her pulse rate was 88 bpm, and her saturation was 93% at room air. A CT scan of the patient's chest and abdomen showed a large diaphragmatic defect on the left side, along with a herniation of the contents of the abdomen into the left hemithorax (Gastrospleenothorax) [Figure 3]. In addition, the CT scan showed intestinal loops and a protrusion of the left liver lobe into the left hemithorax.

After obtaining informed written consent, the patient was planned for laparoscopic repair of the diaphragmatic defect. Intraoperatively, a massive diaphragmatic defect approximately 13 cm × 11 cm in size was identified on the left side. Only a thin rim of diaphragmatic tissue along the posteriorio-medial margin of the left hemithorax was found. Along with the stomach, small and large gut loops, the spleen and the left lobe of the liver were also found to have herniated into the left hemithorax [Figure 4]. The herniated contents were meticulously reduced, and the defect was closed using a 15 cm × 30 cm mesh [Figure 4].

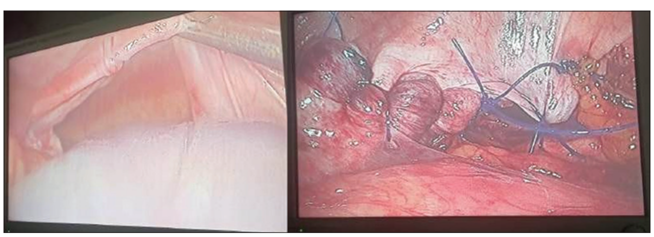

**Figure 2: Case 1 - Intra-operative photographs**

Postoperatively, a chest radiograph confirmed a fully inflated left lung [Figure 5]. On the fourth surgical day, the patient was discharged in satisfactory condition after an uncomplicated recovery.

**Procedure details**

Under general anesthesia, the procedures were carried out in a supine, leg-split (French position). A 10 mm 30° telescope and two 5 mm working ports were employed. The operating table was in left-up and reverse Trendelenburg position, the operating surgeon stood between the legs, the scrub nurse and assistant were on the right, and the monitor was on the head end. Diaphragmatic hernia was diagnosed and verified by diagnostic laparoscopy. Direct vision was used to design the other two ports, one on either side of the main port.

In Case 1, the jejunal and ileal loops had herniated through the diaphragmatic defect. In Case 2, the herniated contents included the stomach, small and large intestines, spleen, and part of the left lobe of the liver. There were no ischemic alterations in the colon or other herniated contents, nor were there any indications of incarceration, blockage, or strangulation. However, Case 2 showed a notable collapse of the left lung [Figure 6].

The herniated contents were reduced using atraumatic laparoscopic graspers. The defects measured 7 cm × 4 cm in CASE-1 and 13 cm × 11 cm in Case 2. Multiple small adhesions in Case 2 were meticulously dissected using cold scissors, and free edges of hernial defect were demarcated. The spleen was pulled down gradually with steady traction, the chest cavity was visualized, and any reactionary fluid was aspirated.

In Case 1, a 26F chest tube drain was inserted into the left pleural cavity, and the defect was repaired with interrupted mattress 1-0 prolene sutures. In Case 2, a 26F tube drain was positioned in the left subphrenic area, and the defect was repaired with 15 cm × 30 cm mesh.

The pneumoperitoneum was deflated following the final laparoscopic examination, and the working ports were

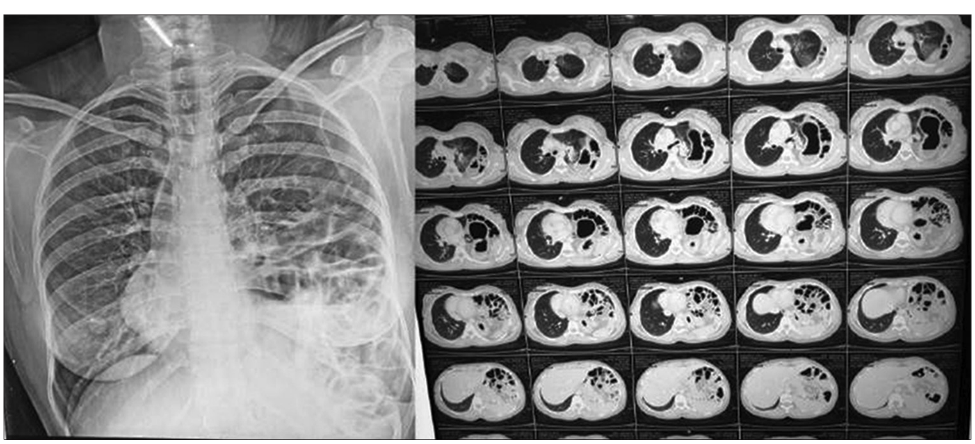

**Figure 3: Case 2 - Pre-operative imaging**

withdrawn under vision. A 2-0 Vicryl suture was used to close the 10 mm port. After extubation, both patients were moved to the high-dependency section of our surgical wards for careful observation for the first 24 h following surgery. In both cases, oral liquids were initiated 24 h later. The drains were removed 72 h after the operation and after normal check radiograph. Postoperatively, antibiotics were continued for 48 h in both cases.

Case 1 was discharged on the 3rd postoperative day and Case 2 on the 4th postoperative day. Both patients are doing well and are enrolled in our outpatient department for routine follow-up.

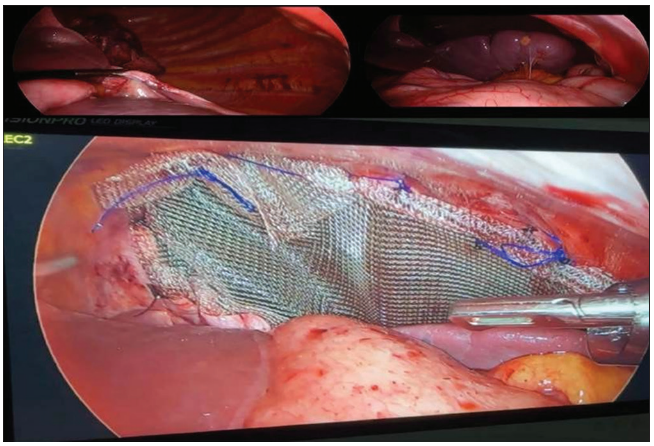

**Figure 4: Case 2 - Intraoperative photographs**

## Discussion

Diaphragmatic hernia in adults can occur secondary to trauma or could result from a delayed congenital type presentation, which is extremely rare with an incidence of 0.17%–6%.[8] Traumatic diaphragmatic hernia (TDH) is commonly associated with other abdominal and thoracic organs, along with musculoskeletal injuries. It occurs in 17% of thoraco-abdominal penetrating injuries and 0.8%–6% of blunt trauma cases.[9,10]

Symptomatic congenital diaphragmatic hernias (CDH) in adults are exceedingly uncommon and are usually identified inadvertently during the evaluation of nonspecific symptoms. There is limited literature on the presentation and management of CDH in adults. In neonates and infants, CDH commonly present with cyanosis and respiratory distress, whereas in adults, symptoms may include chest pain, difficulty in breathing, abdominal discomfort, and, in some cases, visceral incarceration and intestinal obstruction.[11]

Due to the potential for serious complications, early diagnosis and prompt surgical intervention of diaphragmatic hernia becomes mandatory and is the only mainstay of treatment of affected individuals. However, diagnosing this condition remains challenging due to its subtle and nonspecific symptoms. Emergency residents and clinicians must maintain a high index of suspicion, particularly in patients with a history of thoraco-abdominal trauma who

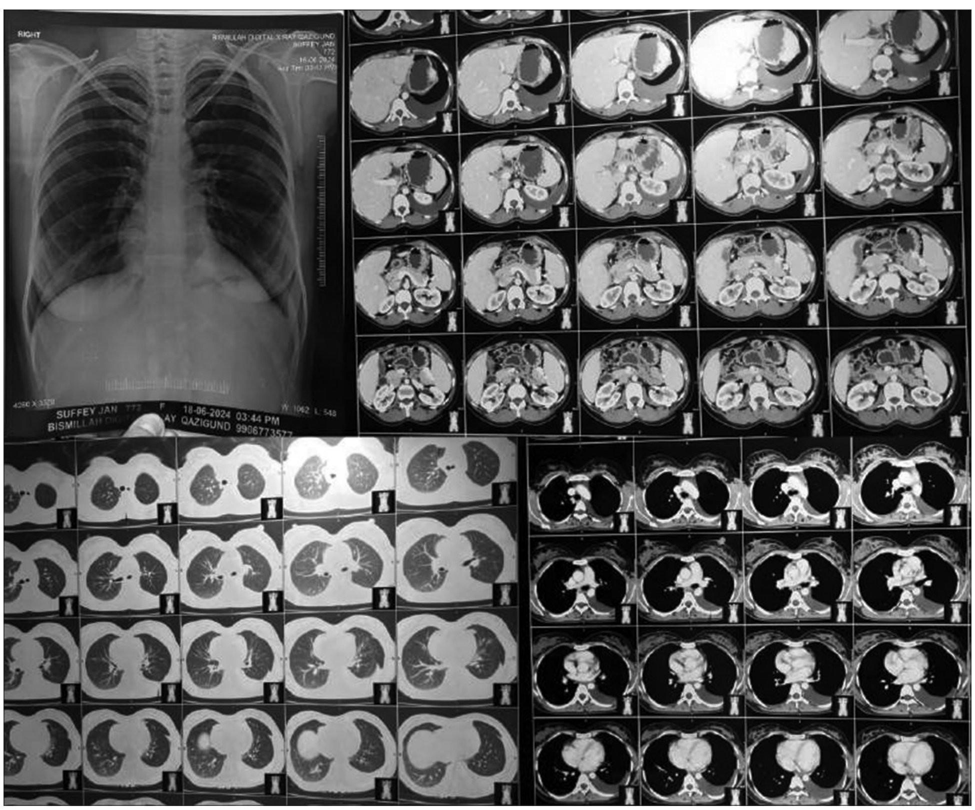

**Figure 5: Case 2 - Postoperative imaging**

present with respiratory distress, vomiting, and abdominal pain.

Radiological imaging remains the primary modality for evaluating the thoracic cavity and diaphragm, and it is the best initial diagnostic test. Chest radiographs may reveal air–fluid levels, gas-filled loops, and contralateral shifting of the mediastinum. Although 75%–95% of chest radiographs show abnormalities, they are only diagnostic in 25%–50% of cases when intrathoracic bowel is visible, typically on the left side.[12,13] In some cases, diaphragmatic hernias may mimic lung consolidation or masquerade as a pneumothorax.[14,15]

In our study, the patient was initially misdiagnosed as tension pneumothorax and consequently, underwent the left intercostal thoracostomy tube drainage. Emergency surgical residents must be proficient in differentiating between tension gastrothorax, tension pneumothorax, and tension bullae, as these conditions share similar clinical manifestations and radiographic features. The clinical diagnosis in the acute setting can be particularly challenging, as all these conditions present with respiratory distress, chest pain, and tachycardia. Tension pneumothorax may also be associated with rib fractures and subcutaneous emphysema in trauma cases. Contrast-enhanced CT is the most effective and useful imaging modality for distinguishing between these clinical scenarios. While standard CT has a sensitivity of 61%–73% for diagnosing traumatic diaphragmatic rupture,[16] it remains limited in the detection of diaphragmatic injury. In our study, both patients were subjected to CT scans for definitive diagnosis, evaluation of the hernia contents, and to guide the appropriate treatment plan.

Surgery is the principal intervention for both symptomatic and asymptomatic diaphragmatic hernia in adult patients. Standard surgical options include transabdominal and transthoracic approaches, with both open and minimally invasive techniques available. In acute trauma settings, the transabdominal approach is generally preferred, as it allows for the identification of the concomitant intra-abdominal injuries and allows easier reduction of the hernial contents. Besides providing excellent visualization for repair, minimally invasive approaches are associated with lesser postoperative pain, shorter hospital stay, better cosmosis, and comparable recurrence rates.[17-19] The diaphragmatic defect can be closed using nonabsorbable interrupted mattress sutures or in case of large defects, a mesh can be used to achieve a tension-free repair. In our case series of adult diaphragmatic hernias, two patients underwent laparoscopic repair. Adhering to fundamental concepts of a customized strategy based on patient and hernial features, careful lysis of adhesions, and precise reduction of herniated contents, together with the judicious application of synthetic mesh when necessary, yields outstanding outcomes. The decision between open versus minimally invasive approaches depends on factors such as the condition of the patient, the size and site of the hernia, and the experience of the surgeon.

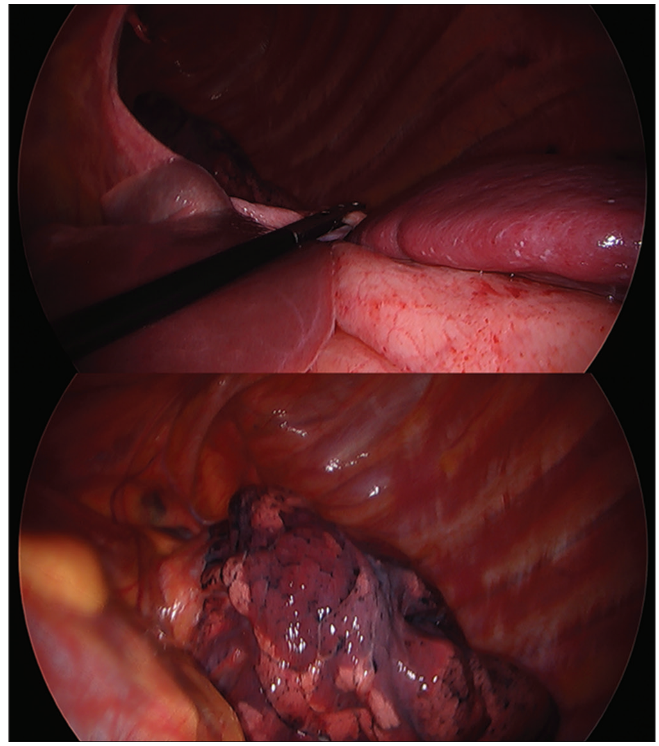

**Figure 6: Intra-operative image of Case No. 2 showing big diaphragmatic hernia and ipsilateral collapsed lung**

## Conclusion

Diagnosing an adult diaphragmatic hernia can be challenging because it may show up with atypical and unrelated symptoms or stay asymptomatic. Accurate diagnosis requires a high level of clinical suspicion and quick radiological testing. Laparoscopy and thoracoscopy are minimally invasive procedures that have essentially replaced traditional methods like thoracotomy or laparotomy. For the treatment of adult traumatic and non-TDHs, laparoscopy in particular is an acceptable, safe, and efficient method.

### Declaration of patient consent

The authors certify that they have obtained all appropriate patient consent forms. In the form, the patients have given their consent for their images and other clinical information to be reported in the journal. The patients understand that their names and initials will not be published, and due efforts will be made to conceal their identity, but anonymity cannot be guaranteed.


### Financial support and sponsorship

Nil.


### Conflicts of interest

There are no conflicts of interest.

## References

1. Gallot D, Boda C, Ughetto S, Perthus I, Robert-Gnansia E, Francannet C, *et al.* Prenatal detection and outcome of congenital diaphragmatic hernia: A French registry-based study. Ultrasound Obstet Gynecol 2007;29:276-83.
2. Zaidi ZA, Tebha SS, Sethar SS, Mishra S. Incidental finding of right-sided idiopathic spontaneous acquired diaphragmatic hernia. Cureus 2021;13:e15793.
3. Testini M, Girardi A, Isernia RM, De Palma A, Catalano G, Pezzolla A, *et al.* Emergency surgery due to diaphragmatic hernia: Case series and review. World J Emerg Surg 2017;12:23.
4. Cortes M, Tapuria N, Khorsandi SE, Ibars EP, Vilca-Melendez H, Rela M, *et al.* Diaphragmatic hernia after liver transplantation in children: Case series and review of the literature. Liver Transpl 2014;20:1429-35.
5. Katukuri GR, Madireddi J, Agarwal S, Kareem H, Devasia T. Delayed diagnosis of left-sided diaphragmatic hernia in an elderly adult with no history of trauma. J Clin Diagn Res 2016;10:D04-5.
6. Abbas A, Rana W, Liaqat H, Shuaib N. Pervasiveness and distribution of congenital malformations in newborns in tertiary care hospital. Int J Adv Biotechnol Res 2018;9:133-8.
7. Lodhia JV, Appiah S, Tcherveniakov P, Krysiak P. Diaphragmatic hernia masquerading as a pulmonary metastasis. Ann R Coll Surg Engl 2015;97:e27-9.
8. Mullins ME, Stein J, Saini SS, Mueller PR. Prevalence of incidental Bochdalek's hernia in a large adult population. AJR Am J Roentgenol 2001;177:363-6.
9. Okada M, Adachi H, Kamesaki M, Mikami M, Ookura Y, Yamakawa J, *et al.* Traumatic diaphragmatic injury: Experience from a tertiary emergency medical center. Gen Thorac Cardiovasc Surg 2012;60:649-54.
10. Gao JM, Du DY, Li H, Liu CP, Liang SY, Xiao Q, *et al.* Traumatic diaphragmatic rupture with combined thoracoabdominal injuries: Difference between penetrating and blunt injuries. Chin J Traumatol 2015;18:21-6.
11. Alam A, Chander BN. Adult Bochdalek hernia. Med J Armed Forces India 2005;61:284-6.
12. Groskin SA. Selected topics in chest trauma. Radiology 1992;183:605-17.
13. Kearney PA, Rouhana SW, Burney RE. Blunt rupture of the diaphragm: Mechanism, diagnosis, and treatment. Ann Emerg Med 1989;18:1326-30.
14. Lin ST, Moss DM, Henderson SO. A case of Morgagni hernia presenting as pneumonia. J Emerg Med 1997;15:297-301.
15. Mattei P, Wiebke E, Lipsett P. Tension pneumothorax as a presentation of traumatic diaphragmatic hernia. South Med J 1992;85:847-50.
16. Aoki AA, Mock CN, Talner LB. Traumatic rupture of the right hemidiaphragm in an automobile accident victim. AJR Am J Roentgenol 1998;171:386.
17. Palanivelu C, Rangarajan M, Senthilkumar R, Madankumar MV. Laparoscopic surgery for giant adult bochdalek diaphragmatic hernia: Combined suturing and polypropylene mesh repair. J Coll Physicians Surg Pak 2007;17:502-4.
18. Young MC, Saddoughi SA, Aho JM, Harmsen WS, Allen MS, Blackmon SH, *et al.* Comparison of laparoscopic versus open surgical management of morgagni hernia. Ann Thorac Surg 2019;107:257-61.
19. Rather Ajaz A, Hassan Yaqoob, Rather Sanan Ajaz . Laparoscopic management of acquired diaphragmatic hernia. J Indian Med Assoc 2021;119:55-8

JASI

# Anomalous Median Nerve Innervation of the Adductor Pollicis: A Cadaveric Observation

**Mayur Bhagvanjibhai Baraiya, Vaibhavi Dipakbhai Bhatti, Kintukumar Vyas[1]**

*Department of Anatomy, GMERS Medical College, [1]Department of Anatomy, Medical College, Vadodara, Gujarat, India*

## Abstract

The adductor pollicis is classically supplied by the deep branch of the ulnar nerve. Rarely, anomalous innervation by the median nerve has been reported, with potential implications for carpal tunnel surgery, nerve repair, and anatomical teaching. A descriptive cadaveric prevalence report was conducted on 60 upper limb specimens from 30 cadavers over three academic years. Specimens with prior trauma, surgery, or deformity were excluded. Standard palmar incisions were made, the flexor retinaculum divided, and muscular branches of the median nerve traced following *Cunningham's Manual of Practical Anatomy*. Observations were documented and photographed. Ethical clearance was obtained from the institutional review board, and all procedures complied with body donation regulations. Median nerve supply to the adductor pollicis was identified in one specimen (1.67%), confined to the left side. All other specimens demonstrated the classical ulnar innervation. The anomalous branch originated within the carpal tunnel. Median nerve contribution to the adductor pollicis represents a rare anatomical variation. Although observed in only one specimen, awareness of such anomalies is important for surgical safety in carpal tunnel release and nerve repair, and for educational emphasis on variability in peripheral nerve supply. Ontogenetic and phylogenetic perspectives suggest that such variations may reflect persistence of early developmental branches or ancestral innervation patterns.

**Keywords:** *Adductor pollicis, anatomical variation, cadaveric study, carpal tunnel, median nerve*

## Introduction

The adductor pollicis muscle is classically supplied by the deep branch of the ulnar nerve.[1,2] This innervation pattern is well established in anatomical texts and clinical practice. Rarely, however, anomalous supply from the median nerve has been reported. Such a finding carries clinical importance, as it may influence the presentation of nerve injuries, alter outcomes of carpal tunnel release surgeries, and complicate nerve repair procedures.[3-8]

Although the median nerve typically passes through the carpal tunnel to supply most of the thenar muscles and the lateral two lumbricals, occasional deviations in its branching pattern have been described.[9-13] In these rare instances, the median nerve may contribute to muscles usually innervated by the ulnar nerve, including the adductor pollicis. Recognition of this anomaly is not only relevant to surgeons but also essential in anatomical education, as it underscores the variability of peripheral nerve supply beyond classical textbook descriptions.[14,15]

Therefore, the present descriptive cadaveric prevalence report was undertaken to examine the branching pattern of the median nerve within the carpal tunnel, with particular emphasis on its anomalous supply to the adductor pollicis muscle. In our series, a single specimen demonstrated this rare variation, which, though observed only once, highlights its cautious clinical relevance and educational importance.

## Materials and Methods

### Study design

This work represents a cadaveric case report of an anatomical variation, identified during routine academic dissections.

### Study setting

The study was conducted in the department of anatomy.

### Sample size

A total of 60 upper limb specimens from 30 human cadavers were dissected over



**How to cite this article:** Baraiya MB, Bhatti VD, Vyas K. Anomalous median nerve innervation of the adductor pollicis: A cadaveric observation. J Anat Soc India 2026;75:98-101.

**Article Info**

**Received:** 04 January 2026
**Revised:** 30 January 2026
**Accepted:** 03 February 2026
**Available online:** 27 March 2026

***Address for correspondence:***
*Dr. Mayur Bhagvanjibhai Baraiya, Department of Anatomy, GMERS Medical College, Gotri, Vadodara, Gujarat, India. E-mail: mayurbaraiya0760@gmail.com*

**Access this article online**

**Website:** https://journals.lww.com/joai

**DOI:** 10.4103/jasi.jasi_2_26

**Quick Response Code:**

three academic years. Each year, 10 cadavers were used for academic dissection, yielding 20 upper limbs annually. In total, 30 right and 30 left upper limbs were examined.

**Inclusion criteria**

- Upper limb specimens of human cadavers with no previous surgeries in the hand region.

**Exclusion criteria**

- Specimens with evidence of trauma, fractures, surgical procedures, pathologies, or congenital deformities.

**Ethical considerations**

Ethical clearance was obtained from the institutional review board for publication of the findings.

**Method of data collection**

Gross dissection was performed following the guidelines of *Cunningham's Manual of Practical Anatomy*.[16]

- In the palmar region, a transverse incision was made at the palmar crease of the wrist
- From its midpoint, an incision was extended along the medial border of the thenar eminence to the tip of the thumb
- A longitudinal incision was made from the midpoint of the proximal wrist crease to the tip of the middle finger
- A transverse incision was placed at the root of the fingers.

Skin flaps were reflected, exposing the palmar aponeurosis, which was divided at the distal border of the flexor retinaculum and reflected distally. The superficial palmar arch was removed. The flexor retinaculum was divided at the midline, avoiding damage to underlying structures. Thenar muscles and lumbricals were identified.

The muscular branches of the median nerve in the hand were traced and examined for anomalous supply to the adductor pollicis muscle. Each specimen was numbered, observations were recorded, and photographs were captured to document the dissection findings and any observed variation.

## Results

Out of a total of 60 upper limb specimens dissected, the adductor pollicis muscle received anomalous innervation from the median nerve in a single specimen (1/60; 1.67%), observed on the left side [Figure 1]. In all other specimens, the classical supply from the deep branch of the ulnar nerve was noted. The anomalous branch originated within the carpal tunnel region.

This rare variation was documented photographically and recorded in detail. No bilateral occurrence was observed. Given that the finding was limited to one specimen, the percentage value should be interpreted with caution.

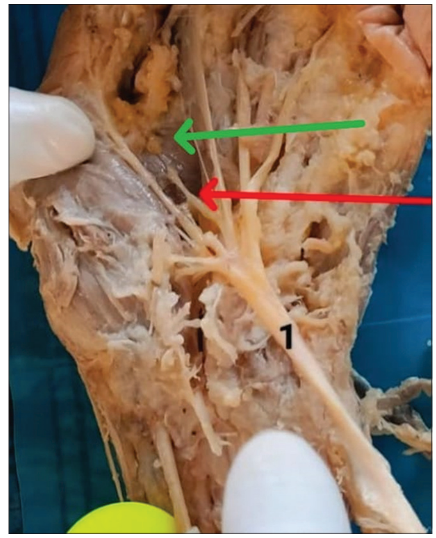


**Figure 1: Dissection showing the median nerve branch supplying the adductor pollicis muscle**

## Discussion

The present descriptive cadaveric prevalence report (2025) observed anomalous innervation of the adductor pollicis muscle by the median nerve in 1 out of 60 specimens (1.67%) [Table 1], while all other specimens demonstrated the classical supply from the deep branch of the ulnar nerve.[3,6,7] This finding highlights the rarity of the median nerve contribution to the adductor pollicis.

A comparison with previous cadaveric studies is summarized in Table 2, which demonstrates the incidence of median nerve supply across different series. Both the present study and earlier reports confirm the dominance of the ulnar nerve in supplying the adductor pollicis, while acknowledging rare contributions from the median nerve.[1-3] The discrepancy in incidence (ranging from 1.67% to 6.67%, and isolated case reports of complete median supply) underscore the variability of innervation patterns, which may be influenced by developmental factors or population-specific differences.

From a clinical perspective, recognition of such anomalous innervation is relevant. Carpal tunnel release surgeries may encounter unexpected branches of the median nerve, nerve repair procedures may be complicated by atypical supply patterns, and the diagnosis of nerve injuries may be confounded by nonclassical presentations.[12-14,17,18] These considerations emphasize the importance of integrating knowledge of rare variations into surgical planning and clinical teaching.

Ontogenetically, the variation can be explained by the embryological development of peripheral nerves. During limb bud formation, motor axons from the brachial plexus grow under mesenchymal guidance. Persistence of an early median nerve branch, or failure of regression during remodeling, may result in anomalous supply to the adductor

**Table 1: Frequency of median nerve supply to the adductor Pollicis in 60 cadaveric upper limb specimens**

| Total specimens examined | Side observed | Variation (median nerve supply to adductor Pollicis) | Frequency (%) |
|---|---|---|---|
| 60 upper limb specimens | Left side | 1 specimen | 1/60 (1.67) |

**Table 2: Incidence of median nerve supply to the adductor pollicis in cadaveric studies**

| Study | Year | *n* (specimens) | Ulnar nerve supply (%) | Median nerve supply (%) |
|---|---|---|---|---|
| Present descriptive cadaveric report | 2025 | 60 | 98.33 | 1.67 |
| Elsabeh *et al*.[3] | 2005 | 30 | 93.33 | 6.67 |
| Chaudhary and Bharti (case report)[1] | 2019 | 1 | - | 100 (single specimen) |
| Encarnacion *et al*. (cadaveric study)[2] | 2022 | 40 | 95 | 5 |

pollicis or accessory branches within the carpal tunnel. This mechanism has been described in developmental anatomy texts.[19,20]

Phylogenetically, such a variation may represent persistence of ancestral innervation patterns observed in primates. Comparative studies have shown differences in intrinsic hand muscle innervation across species, suggesting evolutionary remodeling of nerve supply. Diogo, Wood, and Haines provide evidence that the adductor pollicis and related muscles have undergone shifts in innervation during primate evolution, which may occasionally persist in humans as rare variants.[21,22]

Educationally, this finding emphasizes the importance of teaching anatomical variations alongside classical descriptions. Awareness of such rare innervation patterns enhances the preparedness of medical students and surgeons to deal with unexpected findings in clinical practice.

The limitations of this study include its restriction to cadaveric specimens, which may not fully represent live anatomical variations, the single-event observation, the single-center design, and the absence of direct embryological correlation within the present work. Nevertheless, the identification of even a single anomalous case reinforces the need for vigilance in both clinical and educational contexts.

In summary, the present descriptive cadaveric prevalence report reinforces the dominance of the ulnar nerve in supplying the adductor pollicis muscle while acknowledging rare contributions from the median nerve. Recognition of such variations is important for surgical safety, accurate diagnosis, and comprehensive anatomical education.

## Conclusion

The present descriptive cadaveric prevalence report reinforces the classical understanding that the adductor pollicis muscle is predominantly supplied by the ulnar nerve, with only rare contributions from the median nerve. In our series of 60 upper limb specimens, anomalous innervation by the median nerve was observed in a single specimen (1.67%), confined to the left side.[3,6,7] Although infrequent, such variations may have clinical relevance, as they can influence the presentation of nerve injuries, affect outcomes of carpal tunnel release surgeries, and complicate nerve repair or reconstructive procedures. From an educational perspective, the study highlights the importance of emphasizing anatomical variability alongside classical descriptions, thereby preparing students and clinicians to recognize and manage unexpected findings in practice.[12-14,18,19]

Ontogenetically, persistence of early median nerve branches during embryological development may explain such anomalies, while phylogenetic evidence suggests they may represent ancestral innervation patterns occasionally persisting in humans.[20-22]

In conclusion, while the ulnar nerve remains the dominant supplier of the adductor pollicis, awareness of rare median nerve contributions is important for surgical safety, accurate diagnosis, and comprehensive anatomical education.

**Acknowledgments**

We acknowledge the support of the Anatomy Department staff and technical team during dissections.

**Financial support and sponsorship**

Nil.

**Conflicts of interest**

There are no conflicts of interest.

## References

1. Chaudhary S, Bharti R. A rare variant innervation of adductor pollicis muscle from median nerve in an adult cadaver: A case report. Int J Curr Adv Res 2019;8:205325.
2. Encarnacion M, Nurmukhametov R, Barrientos RE, Melchenko D, Goncharov E, Bernard E, *et al.* Anatomical variations of the median nerve: A cadaveric study. Neurol Int 2022;14:664-72.
3. Elsabeh S, Mokhtar Z, Hassan A, Biram D. Anatomical study of the arterial and nerve supply of the thenar muscles. Egypt J Anat 2005;28:11522.
4. Lanz U. Anatomical variations of the median nerve in the carpal tunnel. J Hand Surg Am 1977;2:44-53.
5. Al Qattan MM. Variations in the course of the thenar motor branch of the median nerve and their relationship to carpal tunnel release. J Hand Surg Br 1996;21:68993.

6. Mitchell R, Chesney A, Seal S, McKnight L, Thoma A. Anatomical variations of the carpal tunnel structures. Can J Plast Surg 2009;17:e3-7.
7. Demircay E, Civelek E, Cansever T, Kabatas S, Yilmaz C. Anatomic variations of the median nerve in the carpal tunnel: A brief review of the literature. Turk Neurosurg 2011;21:388-96.
8. Akio M. Variations and anomalies of the branching of the median nerve observed on carpal tunnel release. J Jpn Soc Surg Hand 1998;15:4526.
9. Canter HI, Asku AE, Safak T, Kecik A. Duplication of median nerve proximal to carpal tunnel. Int J Surg 2007;9:13.
10. Olave E, Prates JC, Sol MD, Sarmento A, Gabriell C. Distribution pattern of the muscular branch of the median nerve in the thenar region. J Anat 1995;186:4416.
11. Olave E, Prates JC, Gabrielli C, Pardi P. Morphometric studies of the muscular branch of the median nerve. J Anat 1996;189:445-9.
12. Pushpalatha M, Jayanthi KS. Accessory thenar branches of median nerve in hand. Anat Karnataka 2007;3:813.
13. Vashishtha K. Variations of median nerve in carpal tunnel and its distribution in hand. J Anat Soc India 2011;60:1938.
14. Dogan NU, Uysal II, Seker M. The communication between the ulnar and median nerves in upper limb. Neuroanatomy 2009;8:159.
15. Poisel S. Origin and course of the muscular branch of the common palmar digital nerve I (median nerve). Chir Praxis. 1974;18:471-4.
16. Cunningham DJ, Romanes GJ. Cunningham's Manual of Practical Anatomy. Upper Limb and Lower Limb. 15th ed., Vol. II. Oxford: Oxford University Press; 2017.
17. Mizia E, Klimek-Piotrowska W, Walocha J, Rutowski R, Wojtala R. The median nerve in the carpal tunnel. Folia Morphol (Warsz) 2011;70:41-6.
18. Moore KL, Persaud TV, Torchia MG. The Developing Human: Clinically Oriented Embryology. 11th ed. Philadelphia: Elsevier; 2020.
19. Standring S, editor. Gray's Anatomy: The Anatomical Basis of Clinical Practice. 42nd ed. London: Elsevier; 2021.
20. Sadler TW. Langman's Medical Embryology. 15th ed. Philadelphia: Wolters Kluwer; 2024.
21. Diogo R, Wood B. Comparative Anatomy and Phylogeny of Primate Muscles and Human Evolution. Boca Raton: CRC Press; 2012.
22. Haines RW. The anatomy of the hand in primates. J Anat 1955;89:115.

Case Report

# An Unusual Midline Venous Collateral along the Median Umbilical Fold: Computed Tomography Findings of a Retropubic Venous Plexus Variant


## Abstract

We describe a previously unreported venous anatomical variation identified on contrast-enhanced abdominal computed tomography performed for evaluation of abdominal pain in a young male. Imaging demonstrated a 3-mm enhancing venous collateral originating from the lower retropubic (vesical) venous plexus, traversing the retzius space, and ascending cranially along the median umbilical fold toward the umbilicus, with small tributaries connecting to the anterior abdominal wall veins. No associated pelvic venous congestion, mass lesion, or urachal abnormality was identified. This rare variant highlights that venous structures arising from the retropubic venous plexus may course superiorly along the median umbilical fold – an area where veins are not typically expected – underscoring the importance of recognizing this anatomy to avoid imaging misinterpretation and to prevent inadvertent vascular injury during retropubic, suprapubic, or ventral midline surgical procedures.


**Keywords:** *Computed tomography, median umbilical fold, retropubic venous plexus, retzius space, venous variant*

**Vedat Yaman**

*Department of Radiology, Idil State Hospital, Sirnak, Türkiye*

## Introduction

With the widespread use of multidetector computed tomography (CT), incidental vascular variants are increasingly recognized during routine abdominal and pelvic imaging. While many venous variations are well documented, unusual collateral pathways in the anterior pelvic extraperitoneal space remain poorly characterized.

The space of Retzius is traditionally regarded as a relatively avascular midline compartment, typically containing only fat, loose connective tissue, and the median umbilical ligament, a fibrous remnant of the urachus. Venous structures are therefore not routinely expected along the median umbilical fold, and midline tubular structures in this location are commonly presumed to represent urachal remnants or fibrotic bands.[1,2]

Here, we report a previously unrecognized venous anatomical variant in which a midline venous collateral arises from the retropubic venous plexus, traverses the retzius space, and ascends superiorly along the median umbilical fold. To our knowledge, this variation has not been previously described and carries important implications for radiologic interpretation and abdominopelvic surgical procedures.

## Case Report

A 30-year-old male underwent contrast-enhanced abdominal CT for abdominal pain. An incidental 3-mm enhancing midline venous collateral was identified. The vessel originated within the lower retropubic venous network and ascended cranially in a straight midline course, precisely following the trajectory of the median umbilical fold toward the umbilicus [Figure 1]. The vessel enhanced uniformly with contrast, confirming its venous nature. Several small tributaries connected this collateral to the superficial anterior abdominal wall veins. The inferior vena cava, iliac veins, renal veins, and hepatic veins were patent. There was no evidence of mass effect, inflammation, or prior surgical alteration of the region. The patient was asymptomatic regarding this finding.

## Discussion

Herein, we report a previously undescribed venous variant arising from the retropubic



**How to cite this article:** Yaman V. An unusual midline venous collateral along the median umbilical fold: Computed tomography findings of a retropubic venous plexus variant. J Anat Soc India 2026;75:102-4.

**Article Info**

**Received:** 06 January 2026
**Revised:** 17 February 2026
**Accepted:** 18 February 2026
**Available online:** 27 March 2026

***Address for correspondence:***
*Dr. Vedat Yaman, Department of Radiology, Idil Devlet Hastanesi, 73000 Idil, Sirnak, Türkiye.
E-mail: drvedatyaman@gmail.com*

**Access this article online**

**Website:** https://journals.lww.com/joai

**DOI:** 10.4103/jasi.jasi_3_26

**Quick Response Code:**

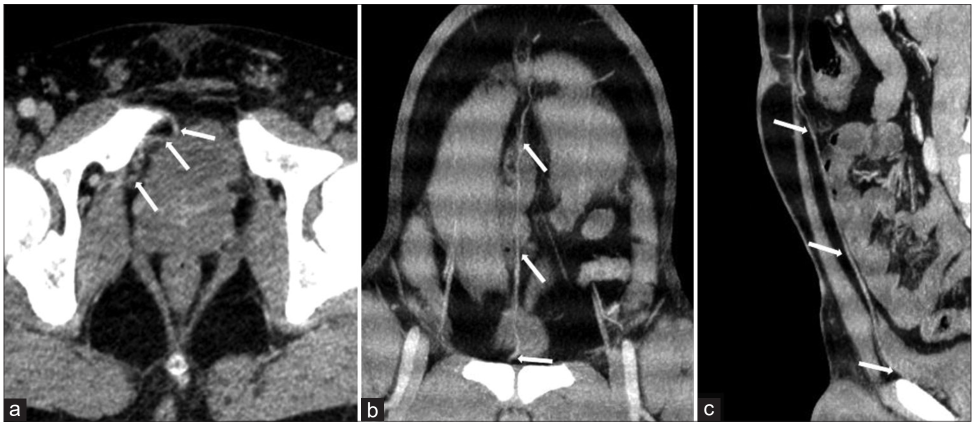


**Figure 1: Axial (a), coronal (b), and sagittal (c) contrast-enhanced abdominal computed tomography images demonstrate the retropubic venous plexus (a, arrows) and its superiorly ascending midline collateral vein extending along the median umbilical fold (b and c, arrows)**

venous plexus, characterized by a distinct midline collateral ascending along the median umbilical fold toward the umbilicus. To the best of our knowledge, such a continuous cranial midline course from the retropubic venous plexus has not been previously documented.

The space of Retzius (retropubic space) is an anatomically significant potential space situated between the pubic symphysis anteriorly and the urinary bladder posteriorly. It is bordered superiorly by the transversalis fascia – which continues cranially toward the umbilicus — and posteriorly by the parietal peritoneum. Inferior borders include the anterior urethra, pubocervical fascia, and bladder neck, whereas the lateral boundaries are formed by the pubic rami and obturator internus muscles.[2] Although the median umbilical ligament is considered the only consistent midline structure within the retzius space, some studies have indicated that small venous branches from the surrounding pelvic plexuses may extend into this region. Cadaveric observations have described fine tributaries arising from the vesical, prostatic, and obturator venous systems that can course anteriorly toward the pubic region and enter the anterior extraperitoneal compartment.[3] Intraoperative findings have similarly shown that superficial preprostatic veins may traverse the retropubic fat, with a small-caliber midline vein identified in most of the patients.[4] These findings show that small venous branches may be seen in the Retzius space; however, our case demonstrates a previously undescribed pattern in which a midline venous collateral ascends superiorly from the Retzius space along the median umbilical fold.

The venous drainage of the bladder is organized into three interconnected plexuses: Submucosal, intramuscular, and external. The external plexus, or vesical plexus, is well developed in areas lacking peritoneal covering and envelops the lower bladder and the base of the prostate. It is particularly dense around the bladder neck, where it continues as the prostatic venous plexus, and at the bladder base, where it surrounds the seminal vesicles and terminal ureters. The prostatic venous plexus, situated behind the lower pubic symphysis and adjacent pubic ligaments, receives the deep dorsal vein of the penis and maintains direct communication with the vesical plexus. Together, these venous networks form a continuous anterior pelvic venous system from which small tributaries may extend into the Retzius space.[3]

During early embryogenesis, venous drainage of the body is provided by the paired anterior and posterior cardinal veins, which empty into the common cardinal veins and subsequently the sinus venosus. From the 5th week of development onward, the posterior cardinal veins largely regress, with only their most caudal portions persisting to form the common iliac veins and the sacral segment of the inferior vena cava. As development progresses, the posterior cardinal system is replaced by the subcardinal and supracardinal veins, which contribute to the definitive abdominal and pelvic venous architecture.[5] Because the vesical and prostatic venous plexuses ultimately drain into the iliac venous system, their embryological origin is closely linked to the remodeling of these posterior cardinal-derived venous channels. Variations in the regression, persistence, or anastomosis of these primitive venous pathways may result in atypical pelvic venous connections or collateral channels. Such embryological variability provides a plausible developmental basis for unusual venous extensions arising from the retropubic venous plexus and traversing the Retzius space, as observed in the present case.

If not carefully evaluated, this venous collateral may be misinterpreted as a prominent median umbilical ligament, particularly on routine axial imaging, where its continuity and enhancement pattern may be overlooked.[1] Accurate identification, therefore, requires attention to its contrast opacification, venous connections in the lower retropubic region, and the small tributaries that join it along its cranial course.

In radical retropubic prostatectomy, awareness of such a venous variant is clinically important, as it may help reduce unexpected bleeding by allowing surgeons to anticipate and carefully manage midline venous structures during retropubic dissection.[6] Beyond prostatectomy, the presence of a midline venous collateral may also complicate suprapubic surgical or interventional procedures, urachal excision, or ventral midline incisions by increasing the risk of inadvertent vascular injury. Furthermore, an anomalous venous pathway of this type could potentially redirect the venous drainage of various prostatic conditions toward atypical midline or supravesical locations, altering expected patterns of disease spread or congestion.

## Conclusion

This case describes a previously unreported midline venous collateral arising from the retropubic venous plexus and ascending along the median umbilical fold. This finding expands the spectrum of known pelvic venous variations. Recognition of this rare anatomical configuration is important to avoid imaging misinterpretation and to prevent inadvertent vascular injury during retropubic and suprapubic surgical procedures.

### Declaration of patient consent

The authors certify that they have obtained all appropriate patient consent forms. In the form, the patient has given his consent for his images and other clinical information to be reported in the journal. The patient understands that his name and initials will not be published and due efforts will be made to conceal identity, but anonymity cannot be guaranteed.

### Financial support and sponsorship

Nil.

### Conflicts of interest

There are no conflicts of interest.

## References

1. Buddha S, Menias CO, Katabathina VS. Imaging of urachal anomalies. Abdom Radiol (NY) 2019;44:3978-89.
2. Patel J, Sasson A, Simpson WL Jr., Wilck E. The anatomy and pathology of the space of Retzius. Clin Imaging 2024;110:110137.
3. Shehata R. Venous drainage of the urinary bladder. Acta Anat (Basel) 1979;105:61-4.
4. Myers RP. Anatomical variation of the superficial preprostatic veins with respect to radical retropubic prostatectomy. J Urol 1991;145:992-3.
5. Knipp BS, Knechtges P, Gest TR, Wakefield TW. Inferior vena cava: Embryology and anomalies. In: Aortic Aneurysms. New Jersey: Humana Press; 2009. p. 289-307.
6. Herranz Amo F. Radical retropubic prostatectomy: Control of Santorini's venous plexus. Actas Urol Esp (Engl Ed) 2020;44:417-22.

Case Report

# An Anatomical Surprise during Cancer Follow-up: The Atypical Origin of the Left Common Carotid Artery


## Abstract

Variations in aortic arch branching may have important clinical implications. One significant variant is the left common carotid artery (LCCA) arising from the brachiocephalic trunk (BT) rather than directly from the aortic arch. A 20-year-old female, previously treated for osteoblastic osteosarcoma, underwent routine follow-up magnetic resonance angiography. Imaging demonstrated the LCCA originating from the BT. Although typically asymptomatic, this variant is a clinically significant pattern that can complicate surgical or endovascular procedures, particularly carotid stenting. Preoperative recognition is essential for safe vascular interventions.


**Keywords:** *Aortic arch variations, common carotid artery, magnetic resonance angiography*


**Ayse Gamze Ozcan, Busra Pirinc, Betul Sevindik, Emine Uysal[1]**

*Departments of Anatomy and [1]Radiology, Faculty of Medicine, Selcuk University, Konya, Turkey*


## Introduction

The aortic arch normally branches into three great vessels: the brachiocephalic trunk (BT) on the right, the left common carotid artery (LCCA) in the middle, and the left subclavian artery on the left. These large vessels supply blood to the head and upper extremities.[1] The most commonly observed aortic arch pattern is the "normal" configuration described above and represents the majority of the general population. Large series and meta-analyses in the literature report a prevalence of 80.9% for the normal arch.[1] A significant variation is the LCCA, which originates from the BT rather than directly from the aortic arch.[2] In today's world, where vascular surgery and interventional procedures are becoming increasingly common, it is of great importance to be aware of these variations preoperatively to avoid complications.[3] In this article, we report this clinically important anatomic variation of LCCA in a young patient, which was discovered incidentally by magnetic resonance angiography (MRA), and discuss the place of this variation in the literature and its clinical significance.

## Case Report

The patient, a 20-year-old female, presented with pain in the right hemithorax. Imaging studies revealed a lytic lesion at the level of the 5th rib, and the patient underwent surgery at the thoracic surgery clinic. Histopathologic examination of the resected material confirmed the diagnosis of osteoblastic osteosarcoma. During follow-up, the possibility of recurrent metastasis was considered due to a suspicious appearance on chest imaging, and further evaluation was planned.

MRA of the thoracic aorta was performed to detect possible metastatic lesions and to evaluate vascular structures. Imaging was performed with a 1.5 Tesla MRI machine using a 3D contrast-enhanced MRA sequence with contrast. The MRA examination revealed that the diameters of the ascending aorta, arch aorta, and descending aorta were within normal limits, and the lumens were patent. The branching pattern of the arch aorta was classified as classic type. However, a significant anatomical variation was identified in the origin of the great vessels: the LCCA did not originate as an independent third branch from the aortic arch, as is typically observed, but instead originated from the BT. The LCCA was observed to originate proximally from the BT. The BT made its normal bifurcation more distally [Figure 1]. The described vascular variation was noted as an important incidental finding. The case is presented to highlight the clinical significance of the anatomical variation.



**How to cite this article:** Ozcan AG, Pirinc B, Sevindik B, Uysal E. An anatomical surprise during cancer follow-up: The atypical origin of the left common carotid artery. J Anat Soc India 2026;75:105-6.

**Article Info**

**Received:** 29 September 2025
**Revised:** 26 January 2026
**Accepted:** 30 January 2026
**Available online:** 27 March 2026

***Address for correspondence:***
*Dr. Ayse Gamze Ozcan, Department of Anatomy, Faculty of Medicine, Selcuk University, Konya, Turkey.*
*E-mail: draysegamzeozcan@gmail.com, ayse.ozcan@selcuk.edu.tr*

**Access this article online**
**Website:** https://journals.lww.com/joai
**DOI:** 10.4103/jasi.jasi_151_25
**Quick Response Code:**

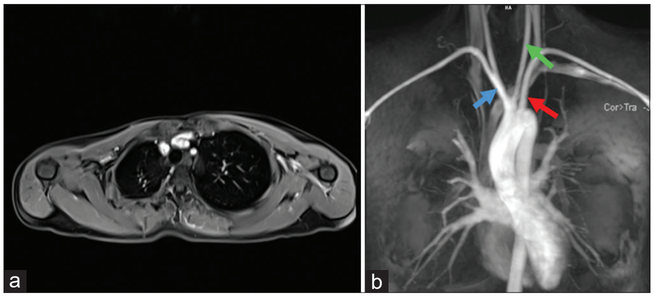

**Figure 1: (a) Axial magnetic resonance angiography (MRA) image showing the left common carotid artery (LCCA) originating from the brachiocephalic trunk (BT); (b) Coronal MRA image showing the BT (blue arrow), LCCA (green arrow), and left subclavian artery (red arrow)**

## Discussion

In the presence of aortic arch variations, a comprehensive understanding of vascular anatomy is essential in clinical practice. In patients scheduled to undergo surgical or endovascular intervention, meticulous scrutiny of preoperative imaging and discernment of variations are paramount to avert complications. Shaw *et al*. reported that an aortic arch configuration, characterized by the LCCA originating from the BT, is associated with greater technical difficulty and higher procedural risk during carotid artery stenting compared with the standard aortic arch configuration. Alternative intervention strategies should be considered for patients with this variation. For instance, a straighter access can be achieved by approaching through the radial artery instead of the femoral artery. Furthermore, new methods such as transcarotid arterial revascularization can be preferred in suitable patients. These approaches have the potential to enhance procedural safety by mitigating the angular disadvantages associated with variations.[4] It is imperative to acknowledge the significance of arch variations during surgical interventions. For instance, if the anomalous origin of the LCCA is not taken into consideration during arch surgery, it may result in accidental ligation or damage to this vessel.[5] Aortic arch variations are predominantly detected incidentally and do not manifest clinical symptoms in isolation. Our case was also asymptomatic and was incidentally detected during an underlying oncological disease follow-up. As indicated in the extant literature, a significant proportion of patients with this variation are identified during imaging for unrelated indications or during cadaver dissections.[3] Previous studies have shown a higher prevalence of this anatomical variation in patients with thoracic aortic aneurysm or dissection, suggesting that it may not be entirely benign. Altered origin of the LCCA from the BT may modify aortic arch hemodynamics by changing carotid angulation and reducing the number of arch branches, thereby predisposing to aneurysm formation or dissection.[1,5] In conclusion, based on the presented case and the existing literature, recognition of the LCCA originating from the BT is essential, given its important clinical implications.

### Declaration of patient consent

The authors certify that they have obtained all appropriate patient consent forms. In the form, the patient has given his consent for his images and other clinical information to be reported in the journal. The patient understands that his name and initials will not be published and due efforts will be made to conceal his identity, but anonymity cannot be guaranteed.


### Financial support and sponsorship

Nil.

### Conflicts of interest

There are no conflicts of interest.


## References


1. Popieluszko P, Henry BM, Sanna B, Hsieh WC, Saganiak K, Pękala PA, *et al*. A systematic review and meta-analysis of variations in branching patterns of the adult aortic arch. J Vasc Surg 2018;68:298-306.e10.
2. Murray A, Meguid EA. Anatomical variation in the branching pattern of the aortic arch: A literature review. Ir J Med Sci 2023;192:1807-17.
3. Bae SB, Kang EJ, Choo KS, Lee J, Kim SH, Lim KJ, *et al.* Aortic arch variants and anomalies: Embryology, imaging findings, and clinical considerations. J Cardiovasc Imaging 2022;30:231-62.
4. Shaw JA, Gravereaux EC, Eisenhauer AC. Carotid stenting in the bovine arch. Catheter Cardiovasc Interv 2003;60:566-9.
5. Mylonas SN, Barkans A, Ante M, Wippermann J, Böckler D, Brunkwall JS. Prevalence of bovine aortic arch variant in patients with aortic dissection and its implications in the outcome of patients with acute type B Aortic Dissection. Eur J Vasc Endovasc Surg 2018;55:385-91.

Case Report

# Quadricuspid Pulmonary Valve with Main Pulmonary Artery Aneurysm Causing Ostial Left Main Coronary Artery Compression: A Coronary Computed Tomography Angiography

**Muhammed Tekinhatun, Fatih Cihan, Hasan Emre, Muhammed Akif Deniz**

*Department of Radiology, Dicle University Hospital, Diyarbakır, Turkey*

## Abstract

A 37-year-old woman with a history of surgically repaired atrial septal defect presented with long-standing exertional chest pain and dyspnea. Laboratory tests and electrocardiography were normal, and transthoracic echocardiography showed valvular regurgitation and elevated pulmonary pressures, but limited assessment of left ventricular function. Coronary computed tomography angiography (CCTA) revealed a quadricuspid pulmonary valve (QPV), pulmonary artery aneurysm measuring 45.5 mm, and ostial compression of the left main coronary artery (LMCA), reducing the luminal diameter to 2.3 mm. This is the first report linking pulmonary artery aneurysm and LMCA compression to an underlying QPV, emphasizing the diagnostic value of CCTA.

**Keywords:** *Aneurysm, computed tomography angiography, left main coronary artery, pulmonary hypertension, quadricuspid pulmonary valve*

## Introduction

The quadricuspid pulmonary valve (QPV) is an exceptionally rare congenital anomaly increasingly recognized with advanced cardiac imaging. Although frequently asymptomatic, it may be associated with valvular dysfunction and contribute to right-sided volume overload. In patients with pulmonary hypertension, progressive enlargement of the main pulmonary artery can, in rare circumstances, produce external compression of the left main coronary artery (LMCA). This unusual mechanism may result in angina or even myocardial ischemia in the absence of atherosclerotic disease. Coronary computed tomography angiography (CCTA) plays a key role in detecting such congenital valve anomalies and in delineating the anatomical basis of coronary compression.

## Case Report

A 37-year-old woman with a history of surgically repaired atrial septal defect was referred for evaluation of long-standing exertional chest pain and dyspnea. She had undergone surgical closure of the atrial septal defect in 2004 and remained intermittently symptomatic thereafter, reporting recurrent chest pain and occasional dyspnea during cardiology follow-up. On admission, vital signs were stable, with blood pressure 120/75 mmHg, heart rate 78 beats per minute, and oxygen saturation 98% on room air. Laboratory tests, including cardiac troponin, complete blood count, and basic biochemistry, were within normal limits. Electrocardiography showed sinus rhythm without ischemic ST-T changes.

Transthoracic echocardiography revealed reduced left ventricular systolic function, with an ejection fraction measured at 48%. Mild mitral and tricuspid regurgitation were present, along with severe pulmonary regurgitation. The estimated systolic pulmonary artery pressure was 37 mmHg, and the main pulmonary artery measured 28 mm in diameter (pulmonary artery-to-aorta ratio – 0.76).

Electrocardiography-gated CCTA demonstrated a QPV and aneurysmal dilatation of the pulmonary arteries. The main pulmonary artery measured 45.5 mm, while the right and left pulmonary arteries measured 30.5 mm and 35.5 mm, respectively. The enlarged pulmonary trunk produced crescent-shaped extrinsic compression at the ostium of the LMCA,



**How to cite this article:** Tekinhatun M, Cihan F, Emre H, Deniz MA. Quadricuspid pulmonary valve with main pulmonary artery aneurysm causing ostial left main coronary artery compression: A coronary computed tomography angiography. J Anat Soc India 2026;75:107-9.

**Article Info**

**Received:** 23 December 2025
**Revised:** 05 February 2026
**Accepted:** 09 February 2026
**Available online:** 27 March 2026

***Address for correspondence:***
*Dr. Muhammed Akif Deniz, Department of Radiology, Dicle University Hospital, Diyarbakır, Turkey.*
*E-mail: makifdeniz@yahoo.com*

**Access this article online**

**Website:** https://journals.lww.com/joai

**DOI:** 10.4103/jasi.jasi_204_25

**Quick Response Code:**

reducing the minimal luminal diameter to 2.3 mm compared with 6.5 mm in the poststenotic segment. No significant atherosclerotic plaque was identified. The left coronary system was dominant, and the right coronary artery was hypoplastic.

The patient was managed conservatively with close clinical and imaging follow-up, as she remained hemodynamically stable and did not meet criteria for immediate surgical intervention.

## Discussion

QPV is an exceedingly rare congenital malformation, with only a limited number of cases described in the literature.[1-3] Both the pulmonary and aortic valves share a common embryological origin. By the 4th week of gestation, bulbar ridges form in the cephalad portion of the truncus arteriosus, and the semilunar valves develop from mesenchymal outgrowths arising from these ridges. Abnormal proliferation or disruption during this process may result in cusp formation anomalies, leading to rare conditions such as a QPV. Although usually isolated, QPV may occasionally coexist with other congenital heart defects, including patent ductus arteriosus and atrioventricular septal defects.[4] The patient had undergone surgical closure of an atrial septal defect approximately 18 years prior to the current presentation. Long-standing atrial septal defect may result in chronic right-sided volume overload, potentially leading to pulmonary hypertension and subsequent dilatation of the pulmonary artery. In this case, although the previously corrected atrial septal defect may have contributed to pulmonary artery dilatation, its relatively early surgical repair is likely to have limited its long-term hemodynamic impact. Therefore, the coexistence of a QPV suggests that abnormal valve morphology may have played a contributory role in the development and progression of the pulmonary artery aneurysm.

According to the Hurwitz and Roberts classification, the QPV observed in our case corresponds to Hurwitz Type B, characterized by three similarly sized cusps and one smaller accessory cusp [Figure 1]. Although often asymptomatic, it may be associated with valvular dysfunction and contribute to right-sided volume overload. In our patient, QPV was identified by CCTA in the context of severe pulmonary regurgitation and pulmonary artery aneurysm.[5]

Pulmonary artery aneurysm is an uncommon but recognized consequence of pulmonary hypertension and chronic volume overload. When the main pulmonary artery exceeds 40 mm in diameter, it is generally considered aneurysmal.[6-9] In rare circumstances, such aneurysmal dilatation can externally compress the ostial LMCA, leading to angina or even myocardial ischemia despite the absence of atherosclerotic disease.[6-8] In our patient, the main pulmonary artery measured 45.5 mm, producing

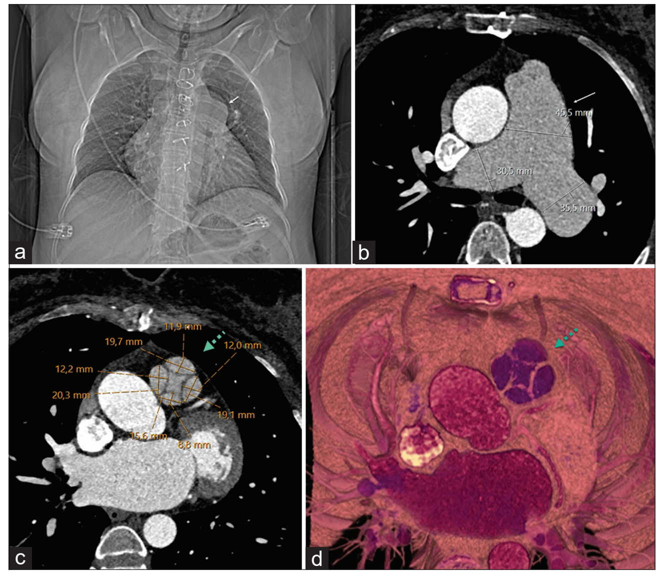


**Figure 1: (a) Scout view showing dilatation of the main pulmonary artery (white arrow). (b) Coronary computed tomography angiography (CCTA) with electrocardiogram-gating demonstrating aneurysmal enlargement of the main pulmonary artery extending into the left pulmonary artery (white arrow). (c) Reformatted CCTA image demonstrating a quadricuspid pulmonary valve with three similarly sized cusps and one smaller accessory cusp (Hurwitz Type B), highlighted by a dashed green arrow. (d) Three-dimensional reconstruction confirming the quadricuspid pulmonary valve morphology (dashed green arrow)**

crescent-shaped compression of the LMCA ostium and reducing the luminal diameter to 2.3 mm [Figure 2].

Multimodality imaging was essential in establishing the diagnosis. Transthoracic echocardiography demonstrated ventricular dysfunction, valvular regurgitation, and elevated pulmonary pressures but did not identify the quadricuspid morphology of the pulmonary valve. This limitation is consistent with previous reports showing that QPV may be difficult to diagnose by echocardiography alone.[4,10]

## Conclusion

This case highlights the exceptionally rare coexistence of a QPV, main pulmonary artery aneurysm, and ostial LMCA compression. It emphasizes that pulmonary artery dilatation secondary to congenital valve anomalies may represent an uncommon but clinically significant mechanism of myocardial ischemia in the absence of atherosclerotic disease. CCTA proved essential in providing a comprehensive anatomical assessment, allowing simultaneous evaluation of valve morphology, pulmonary artery aneurysm, and the mechanism of coronary compression. Awareness of this rare association may facilitate accurate diagnosis and appropriate management in patients with pulmonary hypertension and atypical chest pain.

### Declaration of patient consent

The authors certify that they have obtained all appropriate patient consent forms. In the form, the patient has given her consent for her images and other clinical information to be

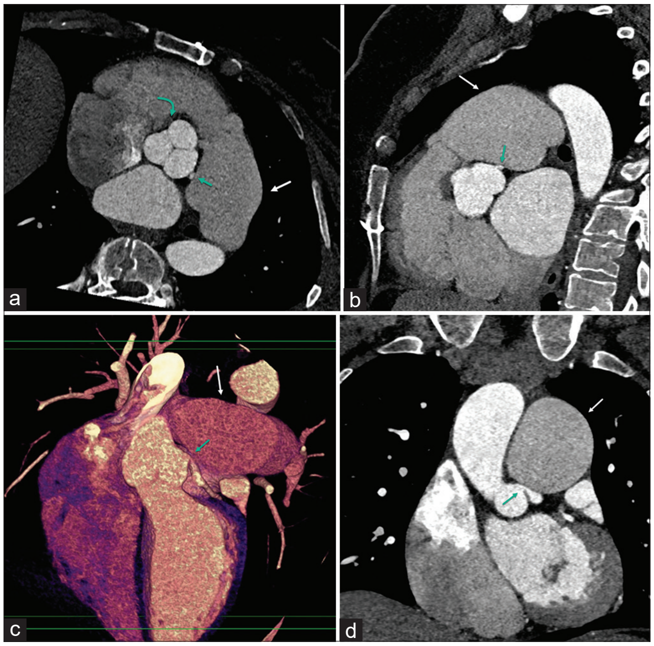


**Figure 2: (a) Reformatted image showing the tricuspid aortic valve (curved green arrow) and the left main coronary artery (green arrow) compressed between the dilated aorta and pulmonary artery. (b) Sagittal reformatted image demonstrating the pulmonary artery aneurysm (white arrow) and the compressed left main coronary artery (green arrow). (c) Three-dimensional reconstruction illustrating the pulmonary artery aneurysm (white arrow) and extrinsic left main coronary artery (LMCA) compression (green arrow). (d) Coronal reformatted image further confirming pulmonary artery aneurysm (white arrow) with LMCA compression (green arrow)**

reported in the journal. The patient understand that her name and initial will not be published and due efforts will be made to conceal her identity, but anonymity cannot be guaranteed.

**Financial support and sponsorship**

Nil.

**Conflicts of interest**

There are no conflicts of interest.

## References

1. Miyake T, Inoue T, Mushiake S. Quadricuspid pulmonary valve: Case report and the comparison with quadricuspid aortic valve. Curr Cardiol Rev 2023;19:e220322202505.
2. Li W, Zhang Y, Cui X, Ji Q. Quadricuspid pulmonary valve with pulmonary hypertension: A case report. Eur Heart J Case Rep 2024;8:ytae408.
3. Tekinhatun M. Quadricuspid pulmonary valve: A rare cause of pulmonary artery aneurysm. Pediatr Pulmonol 2024;59:2664-6.
4. Fernández-Armenta J, Villagómez D, Fernández-Vivancos C, Vázquez R, Pastor L. Quadricuspid pulmonary valve identified by transthoracic echocardiography. Echocardiography 2009;26:288-90.
5. Hurwitz LE, Roberts WC. Quadricuspid semilunar valve. Am J Cardiol 1973;31:623-6.
6. Choi YJ, Kim U, Lee JS, Park WJ, Lee SH, Park JS, *et al*. A case of extrinsic compression of the left main coronary artery secondary to pulmonary artery dilatation. J Korean Med Sci 2013;28:1543-8.
7. Goswami S, Deora S, Kaushik A. Two cases of left main coronary artery compression by dilated pulmonary artery. IHJ Cardiovasc Case Rep 2022;6:115-7.
8. Galiè N, Saia F, Palazzini M, Manes A, Russo V, Bacchi Reggiani ML, *et al.* Left main coronary artery compression in patients with pulmonary arterial hypertension and angina. J Am Coll Cardiol 2017;69:2808-17.
9. Theodoropoulos P, Ziganshin BA, Tranquilli M, Elefteriades JA. Pulmonary artery aneurysms: Four case reports and literature review. Int J Angiol 2013;22:143-8.
10. Barrios L, Delcroix M, Dymarkowski S, Bennett J, Adriaenssens T. Left main coronary artery compression in pulmonary hypertension: Value of multimodality imaging in diagnosis and treatment. J Invasive Cardiol 2022;34:E892.

# Revolutionizing Anatomy Education in Simulated Virtual Labs through Immersive Three-dimensional Projection Technologies to Tackle Overcrowding and Conceptual Confusion

Sir,

Simulated virtual labs (SVLs) serve as transformative platforms in anatomy education that provides dynamic and interactive platforms for understanding complex human anatomical structures. Although SVLs are used as advance platform, overcrowding in SVLs session is a challenge for students for visual access that ultimately reduces the understanding of anatomical structures and decreased student involvement. In SVLs, anatomical content basically explained using two-dimensional displays or basic three-dimensional (3D) digital screens so that only few students are able to understand or engage with the mannequin models and rest students faces a challenge due to obstructed lines of sight, reduced visibility from multiple angles, and the inability to participate in hands-on practice and limits the detail conceptual understanding during practical assessments.[1] The integration of high-resolution, immersive 3D visualization, and spatial projection technology is one of the innovative solutions to overcome these challenges. This innovative approach includes advanced techniques, such as 3D holographic displays, stereoscopic 3D projectors, and volumetric projection methods has the ability to visualize the anatomical structures in the high-resolution scale. These advanced techniques allow models to be projected into space so that students can study the models in 3D projection from different angles and easily accessible for all students. Such immersive visualization techniques enhance spatial orientation and allow for more accurate internalization of anatomical relationships.[2,3]

Implementation of these high-resolution 3D projection techniques in SVLs provides academic and pedagogical advantages. Mainly, it ensures equitable visual access for all students, regardless of their physical position within the learning environment. Furthermore, it supports multisensory learning by integrating visual, spatial, and kinesthetic inputs, which has been demonstrated to enhance retention and understanding in anatomical education. This innovative approach has the ability to study and interact with anatomically accurate projections of virtual mannequins improves the precision of psychomotor skills during practical exercises and assessments.[3]

In addition, this approach combines with developing competency-based medical education, which can be useful for the development of observable and measurable competencies. These approaches support students to increase the acquisition of complex skills at higher levels of Miller's Pyramid, such as "show how" and "perform," particularly when integrated with guided simulations and feedback mechanisms. Furthermore, this approach can provide the long-term academic benefits such as enhanced conceptual clarity, improved skill acquisition, and accurate learning environments that offers strong justification for integration into modern anatomy education.[4] However, adoption of this innovative approach of 3D projection technologies accompanied by challenges that includes financial investment, equipment maintenance, sufficient infrastructure, and the proper training. Moreover, there remains a need for rigorous, evidence-based assessment of learning outcomes to ensure that virtual modalities match or surpass the efficacy of conventional methods.[3,5]

In conclusion, the integration of immersive 3D projection technologies in SVLs for anatomy education can be a beneficial platform for more interactive, accessible, and effective learning. These technologies have the potential to augment and revolutionize the teaching and learning of human anatomy in the advance way. Continued interdisciplinary collaboration, institutional investment, and pedagogical research are essential for transformative potential.

**Financial support and sponsorship**

Nil.

**Conflicts of interest**

There are no conflicts of interest.

**Ankit K. Badge, Nandkishor J. Bankar, Ujwal Gajbe[1], Tanishka Pandey[1]**

*Departments of Microbiology and [1]Anatomy, Datta Meghe Medical College, Datta Meghe Institute of Higher Education and Research (DU), Nagpur, Maharashtra, India*

***Address for correspondence:***
*Dr. Nandkishor J. Bankar,*
*Professor and Head, Department of Microbiology, Datta Meghe Medical College, Datta Meghe Institute of Higher Education and Research (DU), Nagpur - 441 110, Maharashtra, India.*
*E-mail: drbankarnj28@gmail.com*

## References

1. Al-Hor M, Almahdi H, Al-Theyab M, Mustafa AG, Seed Ahmed M, Zaqout S. Exploring student perceptions on virtual reality in anatomy education: Insights on enjoyment, effectiveness, and preferences. BMC Med Educ 2024;24:1405.
2. Rojas GM, Gálvez M, Vega Potler N, Craddock RC, Margulies DS, Castellanos FX, *et al.* Stereoscopic three-dimensional visualization applied to multimodal brain images: Clinical applications and a functional connectivity atlas. Front Neurosci 2014;8:328.

 

3. Wang J, Li W, Dun A, Zhong N, Ye Z. 3D visualization technology for Learning human anatomy among medical students and residents: A meta- and regression analysis. BMC Med Educ 2024;24:461.
4. Williams BW, Byrne PD, Welindt D, Williams MV. Miller's pyramid and core competency assessment: A study in relationship construct validity. J Contin Educ Health Prof 2016;36:295-9.
5. Cook M, Lischer-Katz Z, Hall N, Hardesty J, Johnson J, McDonald R, *et al*. Challenges and strategies for educational virtual reality: Results of an expert-led forum on 3D/VR technologies across academic institutions. ITAL 2019;38:25-48.



**Article Info**

**Received:** 16 May 2025
**Revised:** 02 February 2026
**Accepted:** 04 February 2026
**Available online:** 27 March 2026

| Access this article online | |
|---|---|
| Quick Response Code: | **Website:** https://journals.lww.com/joai |
| | **DOI:** 10.4103/jasi.jasi_90_25 |

**How to cite this article:** Badge AK, Bankar NJ, Gajbe U, Pandey T. Revolutionizing anatomy education in simulated virtual labs through immersive three-dimensional projection technologies to tackle overcrowding and conceptual confusion. J Anat Soc India 2026;75:110-1.

## The Editorial Process

A manuscript will be reviewed for possible publication with the understanding that it is being submitted to Journal of the Anatomical Society of India alone at that point in time and has not been published anywhere, simultaneously submitted, or already accepted for publication elsewhere. The journal expects that authors would authorize one of them to correspond with the Journal for all matters related to the manuscript. All manuscripts received are duly acknowledged. On submission, editors review all submitted manuscripts initially for suitability for formal review. Manuscripts with insufficient originality, serious scientific or technical flaws, or lack of a significant message are rejected before proceeding for formal peer-review. Manuscripts that are unlikely to be of interest to the Journal of the Anatomical Society of India readers are also liable to be rejected at this stage itself.

Manuscripts that are found suitable for publication in Journal of the Anatomical Society of India are sent to two or more expert reviewers. During submission, the contributor is requested to provide names of two or three qualified reviewers who have had experience in the subject of the submitted manuscript, but this is not mandatory. The reviewers should not be affiliated with the same institutes as the contributor/s. However, the selection of these reviewers is at the sole discretion of the editor. The journal follows a double-blind review process, wherein the reviewers and authors are unaware of each other's identity. Every manuscript is also assigned to a member of the editorial team, who based on the comments from the reviewers takes a final decision on the manuscript. The comments and suggestions (acceptance/ rejection/ amendments in manuscript) received from reviewers are conveyed to the corresponding author. If required, the author is requested to provide a point by point response to reviewers' comments and submit a revised version of the manuscript. This process is repeated till reviewers and editors are satisfied with the manuscript.

Manuscripts accepted for publication are copy edited for grammar, punctuation, print style, and format. Page proofs are sent to the corresponding author. The corresponding author is expected to return the corrected proofs within three days. It may not be possible to incorporate corrections received after that period. The whole process of submission of the manuscript to final decision and sending and receiving proofs is completed online. To achieve faster and greater dissemination of knowledge and information, the journal publishes articles online as 'Ahead of Print' immediately on acceptance.

## Clinical trial registry

Journal of the Anatomical Society of India favors registration of clinical trials and is a signatory to the Statement on publishing clinical trials in Indian biomedical journals. Journal of the Anatomical Society of India would publish clinical trials that have been registered with a clinical trial registry that allows free online access to public. Registration in the following trial registers is acceptable: http://www.ctri.in/; http://www.actr.org.au/; http://www.clinicaltrials.gov/; http://isrctn.org/; http://www.trialregister.nl/trialreg/index.asp; and http://www.umin.ac.jp/ctr. This is applicable to clinical trials that have begun enrollment of subjects in or after June 2008. Clinical trials that have commenced enrollment of subjects prior to June 2008 would be considered for publication in Journal of the Anatomical Society of India only if they have been registered retrospectively with clinical trial registry that allows unhindered online access to public without charging any fees.

## Authorship Criteria

Authorship credit should be based only on substantial contributions to each of the three components mentioned below:

1. Concept and design of study or acquisition of data or analysis and interpretation of data;
2. Drafting the article or revising it critically for important intellectual content; and
3. Final approval of the version to be published.

Participation solely in the acquisition of funding or the collection of data does not justify authorship. General supervision of the research group is not sufficient for authorship. Each contributor should have participated sufficiently in the work to take public responsibility for appropriate portions of the content of the manuscript. *The order of naming the contributors should be based on the relative contribution of the contributor towards the study and writing the manuscript. Once submitted the order cannot be changed without written consent of all the contributors*. Addition and deletion of names of authors, change in name of corresponding author is not permitted. The journal prescribes a maximum number of authors for manuscripts depending upon the type of manuscript, its scope and number of institutions involved (vide infra). The authors should provide a justification, if the number of authors exceeds these limits.

The Journal recommends Orcid registration for all authors and mention Orcid ID at the time of article submission.

## Contribution Details

Contributors should provide a description of contributions made by each of them towards the manuscript. Description should be divided in following categories, as applicable: concept, design, definition of intellectual content, literature search, clinical studies, experimental studies, data acquisition, data analysis, statistical analysis, manuscript preparation, manuscript editing and manuscript review. One or more author should take responsibility for the integrity of the work as a whole from inception to published article and should be designated as 'guarantor'.

## Conflicts of Interest/ Competing Interests

All authors must disclose any and all conflicts of interest they may have with publication of the manuscript or an institution or product that is mentioned in the manuscript and/or is important to the outcome of the study presented. Authors should also disclose conflict of interest with products that compete with those mentioned in their manuscript.

## Anti-Plagiarism Policy:

The Journal of Anatomical Society of India follows strict anti-plagiarism policy and use commercially available Plagiarism Checking software. Before submission of their manuscript, authors can subject their manuscript to the plagiarism checking software available in their Institute or free softwares and submit a Similarity Index report obtained. The Journal of Anatomical Society of India allows manuscripts with similarity index as recommended by the Governing Bodies from time to time. Manuscripts with higher similarity index shall be returned to authors for modifications and revisions.

## Generative AI Policy:

Authors must declare the use of AI and AI assisted technologies in writing the manuscript (Large Language Models) or creation of images / graphics (ChatGPT, Gemini, Deep Seek etc) and collection and analysis of data in Methods or Acknowledgment section of the article. They must disclose the specific AI tool used and for what purpose used. Authors are fully responsible for the content of their manuscript,even those parts produced by an AI tool, and are thus liable for any breach of publication ethics. Authors are directed to refer to the Ethical BestPractices in Scholarly Publishing for Lippincott's policy on generative AI.

## Submission of Manuscripts

All manuscripts must be submitted on-line through the website https://review.jow.medknow.com/jasi. First time users will have to register at this site. Registration is free but mandatory. Registered authors can keep track of their articles after logging into the site using their user name and password.

- If you experience any problems, please contact the editorial office by e-mail at editor@jasi.org.in

The submitted manuscripts that are not as per the "Instructions to Authors" would be returned to the authors for technical correction, before they undergo editorial/ peer-review. **Generally, the manuscript should be submitted in the form of two separate files:**

**[1] Title Page/First Page File/covering letter:**

This file should provide

1. The type of manuscript (original article, case report, review article, Letter to editor, Images, etc.) title of the manuscript, running title, names of all authors/ contributors (with their highest academic degrees, designation and affiliations) and name(s) of department(s) and/ or institution(s) to which the work should be credited, . All information which can reveal your identity should be here. Use text/rtf/doc files. Do not zip the files.
2. The total number of pages, total number of photographs and word counts separately for abstract and for the text (excluding the references, tables and abstract), word counts for introduction + discussion in case of an original article;
3. Source(s) of support in the form of grants, equipment, drugs, or all of these;
4. Acknowledgement, if any. One or more statements should specify 1) contributions that need acknowledging but do not justify authorship, such as general support by a departmental chair; 2) acknowledgments of technical help; 3) acknowledgments of financial and material support, which should specify the nature of the support. and 4) **Studies based on cadavers should acknowledge the donor and family members for donating the body for educational and research purposes**. This should be included in the title page of the manuscript and not in the main article file.
5. If the manuscript was presented as part at a meeting, the organization, place, and exact date on which it was read. A full statement to the editor about all submissions and previous reports that might be regarded as redundant publication of the same or very similar work. Any such work should be referred to specifically, and referenced in the new paper. Copies of such material should be included with the submitted paper, to help the editor decide how to handle the matter.
6. Registration number in case of a clinical trial and where it is registered (name of the registry and its URL)
7. Conflicts of Interest of each author/ contributor. A statement of financial or other relationships that might lead to a conflict of interest, if that information is not included in the manuscript itself or in an authors' form
8. Criteria for inclusion in the authors'/ contributors' list
9. A statement that the manuscript has been read and approved by all the authors, that the requirements for authorship as stated earlier in this document have been met, and that each author believes that the manuscript represents honest work, if that information is not provided in another form (see below); and
10. The name, address, e-mail, and telephone number of the corresponding author, who is responsible for communicating with the other authors about revisions and final approval of the proofs, if that information is not included on the manuscript itself.

**[2] Blinded Article file:** The main text of the article, beginning from Abstract till References (including tables) should be in this file. The file must not contain any mention of the authors' names or initials or the institution at which the study was done or acknowledgements. Page headers/ running title can include the title but not the authors' names. **Manuscripts not in compliance with the Journal's**

**blinding policy will be returned to the corresponding author**. Use rtf/doc files. Do not zip the files. **Limit the file size to 1 MB.** Do not incorporate images in the file. If file size is large, graphs can be submitted as images separately without incorporating them in the article file to reduce the size of the file. The pages should be numbered consecutively, beginning with the first page of the blinded article file.

**[3] Images:** Submit good quality color images. **Each image should be less than 2 MB in size.** Size of the image can be reduced by decreasing the actual height and width of the images (keep up to 1600 x 1200 pixels or 5-6 inches). Images can be submitted as jpeg files. Do not zip the files. **Legends for the figures/images should be included at the end of the article file.**

**Digital Copyright Agreement in the Manuscript Submission System:** The copyright process is now digital to streamline manuscript submissions. Please follow these guidelines fora smooth submission process:

The submitting author must ensure that all co-authors, with their correct email addresses [mandatory],are added in the 'Authors and Institutions' section during the third step of online submission.

After submission, all co-authors will receive an email with a link to provide their digital copyrightconsent. Please ensure all co-authors complete this process within seven days of submission.

The submitting author can track the copyright status of their co-authors in the 'ManuscriptInformation' page by clicking the manuscript ID on their dashboard.

Do not upload scanned copies of signed copyright forms during submission.

Manuscript review will proceed only after all co-authors have submitted their digital copyright consent.

## Preparation of Manuscripts

'Manuscripts must follow the latest ICMJE Recommendations for the Conduct, Reporting, Editing, and Publication of Scholarly Work in Medical Journals (www.icmje.org).' The specific requirement of Journal of the Anatomical Society of India are summarized below. Before submitting a manuscript, contributors are requested to check for the latest instructions available. Instructions are also available from the website of the journal (www.jasi.org.in) and from the manuscript submission site https://review.jow.medknow.com/jasi.

Journal of the Anatomical Society of India accepts manuscripts written in American English.

## Copies of any permission(s)

It is the responsibility of authors/ contributors to obtain permissions for reproducing any copyrighted material. A copy of the permission obtained must accompany the manuscript. Copies of any and all published articles or other manuscripts in preparation or submitted elsewhere that are related to the manuscript must also accompany the manuscript.

## Types of Manuscripts

### Original articles:

These include randomized controlled trials, intervention studies, studies of screening and diagnostic test, outcome studies, cost effectiveness analyses, case-control series, and surveys with high response rate. The text of original articles amounting to up to 3000 words (excluding Abstract, references and Tables) should be divided into sections with the headings Abstract, Key-words, Introduction, Material and Methods, Results, Discussion Limitations of the study (if any) and Conclusion, References, Tables and Figure legends.

An abstract should be in a **structured format** under following heads: **Introduction, Material and Methods, Results,** and **Discussion and Conclusion.** The Journal encourages authors to submit Highlights / Key Points of their article separately in 4-5 bullet points to motivate the readers. **Additionally, Illustrated Abstracts / Graphic Abstracts along with Highlights/Key Points can also be submitted. The Journal shall accept Videos (MP4 format- up to 4) of educational value as supplement to their article**. Size of each video should not exceed 30 MB and they will be published as Supplementary Files available only online. Videos shall not be embedded within the article.

**Introduction:** State the purpose and summarize the rationale for the study or observation.

**Material and Methods:** It should include and describe the following aspects:

***Ethics:*** When reporting studies on human beings, indicate whether the procedures followed were in accordance with the ethical standards of the responsible committee on human experimentation (institutional or regional) and with the Helsinki Declaration of 1975, as revised in 2000 (available at http://www.wma.net/e/policy/17-c_e.html). For prospective studies involving human participants, authors are expected to mention about approval of (regional/ national/ institutional or independent Ethics Committee or Review Board, obtaining informed consent from adult research participants and obtaining assent for children aged over 7 years participating in the trial. The age beyond which assent would be required could vary as per regional and/ or national guidelines. Ensure confidentiality of subjects by desisting from mentioning participants' names, initials or hospital numbers, especially in illustrative material. When reporting experiments on animals, indicate whether the institution's or a national research council's guide for, or any national law on the care and use of laboratory animals was followed. Evidence for approval by a local Ethics Committee (for both human as well as animal studies) must be supplied by the authors on demand. Animal experimental procedures should be as humane as possible and the details of anesthetics and analgesics used should be clearly stated. The ethical standards of experiments must be in accordance with the guidelines provided by the CPCSEA and World Medical Association Declaration of Helsinki on Ethical Principles for Medical Research Involving Humans for studies involving experimental animals and human beings, respectively). The journal will not consider any paper which is ethically unacceptable. A statement on ethics committee permission and ethical practices must be included in all research articles under the 'Materials and Methods' section.

**Study design:**

Selection and Description of Participants: Describe your selection of the observational or experimental participants (patients or laboratory animals, including controls) clearly, including eligibility and exclusion criteria and a description of the source population. *Technical information*: Identify the methods, apparatus (give the manufacturer›s name and address in parentheses), and procedures in sufficient detail to allow other workers to reproduce the results. Give references to established methods, including statistical methods (see below); provide references and brief descriptions for methods that have been published but are not well known; describe new or substantially modified methods, give reasons for using them, and evaluate their limitations. Identify precisely all drugs and chemicals used, including generic name(s), dose(s), and route(s) of administration.

Reports of randomized clinical trials should present information on all major study elements, including the protocol, assignment of interventions (methods of randomization, concealment of allocation to treatment groups), and the method of masking (blinding), based on the CONSORT Statement (http://www.consort-statement.org).

**Reporting Guidelines for Specific Study Designs**

| Initiative | Type of Study | Source |
|---|---|---|
| CONSORT | Randomized controlled trials | http://www.consort-statement.org |
| STARD | Studies of diagnostic accuracy | http://www.consort-statement.org/stardstatement.htm |
| QUOROM | Systematic reviews and meta-analyses | http://www.consort- statement.org/Initiatives/MOOSE/moose.pdf statement.org/Initiatives/MOOSE/moose.pdf |
| STROBE | Observational studies in epidemiology | http://www.strobe-statement.org |
| MOOSE | Meta-analyses of observational studies in epidemiology | http://www.consort- statement.org/Initiatives/MOOSE/moose.pdf |
| CARE | Case Reports | https://www.care-statement.org/checklist |

*Statistics*: Whenever possible quantify findings and present them with appropriate indicators of measurement error or uncertainty (such as confidence intervals). Authors should report losses to observation (such as, dropouts from a clinical trial). When data are summarized in the Results section, specify the statistical methods used to analyze them. Avoid non-technical uses of technical terms in statistics, such as 'random' (which implies a randomizing device), 'normal', 'significant', 'correlations', and 'sample'. Define statistical terms, abbreviations, and most symbols. Specify the computer software used. Use upper italics (*P* 0.048). For all *P* values include the exact value and not less than 0.05 or 0.001. Mean differences in continuous variables, proportions in categorical variables and relative risks including odds ratios and hazard ratios should be accompanied by their confidence intervals.

**Results:** Present your results in a logical sequence in the text, tables, and illustrations, giving the main or most important findings first. Do not repeat in the text all the data in the tables or illustrations; emphasize or summarize only important observations. Extra- or supplementary materials and technical detail can be placed in an appendix where it will be accessible but will not interrupt the flow of the text; alternatively, it can be published only in the electronic version of the journal.

When data are summarized in the Results section, give numeric results not only as derivatives (for example, percentages) but also as the absolute numbers from which the derivatives were calculated, and specify the statistical methods used to analyze them. Restrict tables and figures to those needed to explain the argument of the paper and to assess its support. Use graphs as an alternative to tables with many entries; do not duplicate data in graphs and tables. Where scientifically appropriate, analyses of the data by variables such as age and sex should be included.

**Discussion:** Include summary of *key findings* (primary outcome measures, secondary outcome measures, results as they relate to a prior hypothesis); *Strengths and limitations* of the study (study question, study design, data collection, analysis and interpretation); *Interpretation and implications* in the context of the totality of evidence (is there a systematic review to refer to, if not, could one be reasonably done here and now?, what this study adds to the available evidence, effects on patient care and health policy, possible mechanisms); *Controversies* raised by this study; and *Future research directions* (for this particular research collaboration, underlying mechanisms, clinical research).

Do not repeat in detail data or other material given in the Introduction or the Results section. In particular, contributors should avoid making statements on economic benefits and costs unless their manuscript includes economic data and analyses. Avoid claiming priority and alluding to work that has not been completed. New hypotheses may be stated if needed, however they should be clearly labeled as such. About 30 references can be included. These articles generally should not have more than six authors.

**Review Articles:**

These are comprehensive review articles (Narrative / Literature review, Systematic review, Scoping Review, Systematic review with Meta-analysis, Umbrella Review) on topics related to various fields of Anatomy. The entire manuscript should not exceed 5000 words with no more than 100 references and 'Number of authors should be justified based on the nature and scope of the study. Following types of articles can be submitted under this category:

• Newer techniques of dissection and histology

• New methodology in Medical Education

• Review of a current concept

• CME type Review Article with MCQ

• Recent advances in Developmental biology, Neurobiology, Genetics.

Authors can submit any kind of review article which will be considered for publication on merit basis. Editor can also invite suitable review articles from the experts in a particular field.

**Case reports:**

New, interesting and rare cases can be reported. They should be unique, describing a great diagnostic or therapeutic challenge and providing a learning point for the readers. Cases with clinical significance or implications will be given priority. These communications could be of up to 1000 words (excluding Abstract and references) and should have the following headings: Abstract (unstructured), Key-words, Introduction, Case report, Discussion and Conclusion, Reference, Tables and Legends in that order.

The manuscript could be of up to 1000 words (excluding references and abstract) and could be supported with up to 10 references. Case Reports could be authored by up to four authors.

**Clinical Anatomy Case study** with a brief note on the given case supported by images, photographs followed by MCQs available in Google form to be answered and submitted. This is for the benefit of postgraduates and undergraduates.

**Letter to the Editor:**

These should be short and decisive observations. They should preferably be related to articles previously published in the Journal or views expressed in the journal. They should not be preliminary observations that need a later paper for validation. The letter could have up to 500 words and 5 references. It could be generally authored by not more than four authors.

**Book Review:** This consists of a critical appraisal of selected books on Anatomy. Potential authors or publishers may submit books, as well as a list of suggested reviewers, to the editorial office. The author/publisher has to pay INR 10,000 per book review.

**Other:**

Editorial, Guest Editorial, Commentary, Brief Communication and Opinion are solicited by the editorial board.

**References**

References should be *numbered* consecutively in the order in which they are first mentioned in the text (not in alphabetic order). Identify references *in text*, tables, and legends by Arabic numerals in superscript with square bracket after the punctuation *marks. References cited only* in tables or figure legends should be numbered in accordance with the sequence established by the first identification in the text of the particular table or figure. Use the style of the examples below, which are based on the formats used by the NLM *in Index Medicus*. The titles of journals *should be abbreviated* according to the style used in Index Medicus. Use complete name of the journal for non-indexed journals. Avoid using abstracts as references. Information from manuscripts submitted but not accepted should be cited in the text as "unpublished observations" with written permission from the source. Avoid citing a "personal communication" unless it provides essential information not available from a public source, in which case the name of the person and date of communication should be cited in parentheses in the text. The commonly cited types of references are shown here, for other types of references such as newspaper items please refer to ICMJE Guidelines (http://www.icmje.org or http://www.nlm.nih.gov/bsd/uniform_requirements.html).

**Articles in Journals**

1. Standard journal article (for up to six authors): Sawal A, Chaudhary KB, Dang B, Bokariya P. Comparative study of oocyte quality in young and advanced-aged women. J Anat Soc India. 2025; 74:338-342.
2. Standard journal article (for more than six authors): List the first six contributors followed by *et al*.

Prabhu LV, Murlimanju BV, Yadav S, Rao YL, Vadagaonkar R, Pai MM, et al. Morphology and topography of fossa ovalis, limbus fossa ovalis, and probe patency of foramen ovale in formalin-fixed hearts. J Anat Soc India. 2025; 74: 332-337.

3. Volume with supplement: Otranto D, Capelli G, Genchi C: Changing distribution patterns of canine vector borne diseases in Italy: leishmaniosis vs. dirofilariosis. Parasites & Vectors 2009; Suppl 1:S2.

**Books and Other Monographs**

1. Personal author(s): Sadler TW. Langman's Medical Embryology, 13th Edn. Wolters Kluwer, New Delhi 2016.
2. Editor(s), compiler(s) as author: Garcia LS, Filarial Nematodes In: Garcia LS (editor) Diagnostic Medical Parasitology ASM press Washington DC 2007: pp 319-356.

3. Chapter in a book: Bhullar JS. Large Intestine. In Gray's Anatomy. The Anatomical Basis of Clinical Practice. 42 Edn. Standring S. (ed) Elsevier, 2021.

**Electronic Sources as reference**

Journal article on the Internet: Ahluwalia N, Nassereddin A, Arbor TC, Futterman B. Anatomy, Abdomen and Pelvis: Celiac Trunk. 2024 Jan 30. In: StatPearls [Internet]. Treasure Island (FL): StatPearls Publishing; 2025

**Tables**

- Tables should be self-explanatory and should not duplicate textual material.
- Tables with more than 10 columns and 25 rows are not acceptable.
- Number tables, in Arabic numerals, consecutively in the order of their first citation in the text and supply a brief title for each.
- Place explanatory matter in footnotes, not in the heading.
- Explain in footnotes all non-standard abbreviations that are used in each table.
- Obtain permission for all fully borrowed, adapted, and modified tables and provide a credit line in the footnote.
- For footnotes use the following symbols, in this sequence: *, †, ‡, §, ||,¶ , **, ††, ‡‡
- Tables with their legends should be provided at the end of the text after the references. The tables along with their number should be cited at the relevant place in the text

**Illustrations (Figures)**

- Upload the images in JPEG format. The file size should be within 1024 kb in size while uploading.
- Figures should be numbered consecutively according to the order in which they have been first cited in the text.
- Labels, numbers, and symbols should be clear and of uniform size. The lettering for figures should be large enough to be legible after reduction to fit the width of a printed column.
- Symbols, arrows, or letters used in photomicrographs should contrast with the background and should be marked neatly with transfer type or by tissue overlay and not by pen.
- Titles and detailed explanations belong in the legends for illustrations not on the illustrations themselves.
- When graphs, scatter-grams or histograms are submitted the numerical data on which they are based should also be supplied.
- The photographs and figures should be trimmed to remove all the unwanted areas.
- If photographs of individuals are used, their pictures must be accompanied by written permission to use the photograph.
- If a figure has been published elsewhere, acknowledge the original source and submit written permission from the copyright holder to reproduce the material. A credit line should appear in the legend for such figures.
- Legends for illustrations: Type or print out legends (maximum 40 words, excluding the credit line) for illustrations using double spacing, with Arabic numerals corresponding to the illustrations. When symbols, arrows, numbers, or letters are used to identify parts of the illustrations, identify and explain each one in the legend. Explain the internal scale (magnification) and identify the method of staining in photomicrographs.
- Final figures for print production: Send sharp, glossy, color photographs, with height of 4 inches and width of 6 inches at the time of submitting the revised manuscript. If digital images are the only source of images, ensure that the image has minimum resolution of 300 dpi or 1800 x 1600 pixels in TIFF format.
- The Journal reserves the right to crop, rotate, reduce, or enlarge the photographs to an acceptable size.

## Protection of Patients' Rights to Privacy

Identifying information should not be published in written descriptions, photographs, sonograms, CT scans, etc., and pedigrees unless the information is essential for scientific purposes and the patient (or parent or guardian, wherever applicable) gives informed consent for publication. Authors should remove patients' names from figures unless they have obtained informed consent from the patients. The journal abides by ICMJE guidelines:

1. Authors, not the journals nor the publisher, need to obtain the patient consent form before the publication and have the form properly archived. The consent forms are not to be uploaded with the cover letter or sent through email to editorial or publisher offices.
2. If the manuscript contains patient images that preclude anonymity, or a description that has obvious indication to the identity of the patient, a statement about obtaining informed patient consent should be indicated in the manuscript.

## Sending a revised manuscript

The revised version of the manuscript should be submitted online in a manner similar to that used for submission of the manuscript for the first time. However, there is no need to submit the "First Page" or "Covering Letter" file while submitting a revised version. When submitting a revised manuscript, contributors are requested to include, the 'referees' remarks along with point to point clarification at the beginning in the revised file itself. In addition, **they are expected to mark the changes as underlined or colored text in the article.**

## Reprints and proofs

Journal provides no free printed reprints. Authors can purchase reprints, payment for which should be done at the time of submitting the proofs.

## Publication schedule

The journal publishes articles on its website immediately on acceptance and follows a ‘continuous publication’ schedule. Articles are compiled in issues for ‘print on demand’ quarterly.

## Copyrights



## Checklist

**Covering letter**

- Signed by all contributors
- Previous publication / presentations mentioned
- Source of funding mentioned
- Conflicts of interest disclosed

**Authors**

- Last name and given name provided along with Middle name initials (where applicable)
- Author for correspondence, with e-mail address provided
- Number of contributors restricted as per the instructions
- Identity not revealed in paper except title page (e.g. name of the institute in Methods, citing previous study as ‘our study’, names on figure labels, name of institute in photographs, etc.)

**Presentation and format**

- Double spacing
- Margins 2.5 cm from all four sides
- Page numbers included at bottom
- Title page contains all the desired information
- Running title provided (not more than 50 characters)
- Abstract page contains the full title of the manuscript
- Abstract provided (structured abstract of 250 words for original articles, unstructured abstracts of about 150 words for all other manuscripts excluding letters to the Editor)
- Key words provided (three or more Provide MeSH (Medical Subject Heading) terms as Key Words. Key Words arranged in alphabetical order is preferable.)
- 'Introduction should be concise and focused
- Headings in title case (not ALL CAPITALS)
- The references cited in the text should be after punctuation marks, in superscript with square bracket.
- References according to the journal’s instructions, punctuation marks checked
- Send the article file without ‘Track Changes’

**Language and grammar**

- Uniformly **American English**
- Write the full term for each abbreviation at its first use in the title, abstract, keywords and text separately unless it is a standard unit of measure. Numerals from 1 to 10 spelt out
- Numerals at the beginning of the sentence spelt out
- Check the manuscript for spelling, grammar and punctuation errors
- If a brand name is cited, supply the manufacturer’s name and address (city and state/country).
- Species names should be in italics

**Tables and figures**

- No repetition of data in tables and graphs and in text
- Actual numbers from which graphs drawn, provided
- Figures necessary and of good quality (colour)
- Table and figure numbers in Arabic letters (not Roman)
- Labels pasted on back of the photographs (no names written)
- Figure legends provided (not more than 40 words)
- Patients’ privacy maintained (if not permission taken)
- Credit note for borrowed figures/tables provided
- Write the full term for each abbreviation used in the table as a footnote

**Dos & Don'ts:** Do not use abbreviations in the Title of the article.

- Do not use any reference in the abstract.
- A separate list of abbreviations used can be submitted after conclusion in the main article file.
- Do not begin a paragraph with a numeral; spell the numeral
- Usage of terms like " tertiary care hospital with name of city", in the title should be avoided.

# Journal of
# The Anatomical Society of India

## Salient Features :

- Publishes research articles related to all aspects of Anatomy and Allied medical/surgical sciences.
- Publishes Articles with Videos, Clinical Anatomy Cases, CME-type Review, Original / Review articles with Illustrated / Graphic Abstracts & Highlights / Key points with Abstracts
- Pre-Publication Peer Review and Post-Publication Peer Review
- Online Manuscript Submission System
- Selection of articles on the basis of MRS system
- Eminent academicians across the globe as the Editorial board members
- Electronic Table of Contents alerts
- Available in both online and print form.

**The journal is registered with the following abstracting partners:**
Baidu Scholar, CNKI (China National Knowledge Infrastructure), EBSCO Publishing's Electronic Databases, Ex Libris – Primo Central, Google Scholar, Hinari, Infotrieve, Netherlands ISSN center, ProQuest, TdNet, Wanfang Data

**The journal is indexed with, or included in, the following:**
SCOPUS, Science Citation Index Expanded, IndMed, MedInd, Scimago Journal Ranking, Emerging Sources Citation Index.

Impact Factor® as reported in the 2025 Journal Citation Reports® (Clarivate Analytics, 2026): 0.2

Editorial Office:
**Prof. C.S. Ramesh Babu,** Editor-in-Chief, JASI
309, Block-B, Canopy Calyx Apartments, Coffee Board Layout,
Hebbal-Kempapura, Bengaluru-560024. India
Email: editorjasi@gmail.com
(O) | Website: www.asiindia.in

The journal is owned and run by The Anatomical Society of India